Methods in Molecular Biology 1274

Springer Protocols

Ann Van Schepdael *Editor*

Microchip Capillary Electrophoresis Protocols

Humana Press

METHODS IN MOLECULAR BIOLOGY

Series Editor
John M. Walker
School of Life and Medical Sciences
University of Hertfordshire
Hatfield, Hertfordshire, AL10 9AB, UK

For further volumes:
http://www.springer.com/series/7651

Microchip Capillary Electrophoresis Protocols

Edited by

Ann Van Schepdael

Pharmaceutical Analysis, KU Leuven, Leuven, Belgium

Humana Press

Editor
Ann Van Schepdael
Pharmaceutical Analysis
KU Leuven
Leuven, Belgium

ISSN 1064-3745 ISSN 1940-6029 (electronic)
Methods in Molecular Biology
ISBN 978-1-4939-2352-6 ISBN 978-1-4939-2353-3 (eBook)
DOI 10.1007/978-1-4939-2353-3

Library of Congress Control Number: 2015931079

Springer New York Heidelberg Dordrecht London

Cover illustration: Cover image courtesy of Bart Heleven

Printed on acid-free paper

Humana Press is a brand of Springer
Springer Science+Business Media LLC New York is part of Springer Science+Business Media (www.springer.com)

Preface

Microchip capillary electrophoresis (MCE) has evolved from capillary electrophoresis through further miniaturization, providing improvements in speed and sample requirements as well as the possibility to perform more complex and highly integrated analyses. MCE may be well investigated in the scientific literature, yet it is a rapidly maturing technique, and detailed validated protocols are not widely described yet. This book is intended to be a working guide to the operation of microchip capillary electrophoresis.

It explains step by step how to fabricate and operate microchips in electrophoresis as well as electrochromatography mode. It addresses some small molecule as well as biomolecule applications. Furthermore, various detection modes as well as sample preparation approaches are described. In analogy with capillary electrophoresis, MCE also knows a large variety of application fields such as drug development, environmental analysis, biomedical and clinical analysis, and food analysis.

The notes incorporated in each chapter represent valuable remarks from the authors on the described protocol. These allow the readership gain more insight into the explained procedures and may prevent time loss encountered by troubleshooting when performing a poorly explained experimental procedure.

All biological scientists applying bioanalytical separation techniques will benefit from the protocols described in this book.

Leuven, Belgium *Ann Van Schepdael*

Contents

Contributors

Vojtech Adam • *Faculty of Agronomy, Department of Chemistry and Biochemistry, Mendel University, Brno, Czech Republic, EU; Central European Institute of Technology, Brno University of Technology, Brno, Czech Republic, EU*

Dario Anselmetti • *Faculty of Physics, Experimental Biophysics and Applied Nanoscience, Bielefeld University, Bielefeld, Germany*

Róbert Bodor • *Faculty of Natural Sciences, Department of Analytical Chemistry, Comenius University in Bratislava, Bratislava, Slovak Republic*

Keri A. Brown • *Manchester Institute of Biotechnology, Faculty of Life Sciences, University of Manchester, Manchester, Lancashire, UK*

Terence A. Brown • *Manchester Institute of Biotechnology, Faculty of Life Sciences, University of Manchester, Manchester, Lancashire, UK*

Deirdre Cabooter • *Department of Pharmaceutical and Pharmacological Sciences, Pharmaceutical Analysis, KU Leuven, Leuven, Belgium*

Bing Chen • *College of Chemistry and Chemical Engineering, Lingnan Normal University, Zhanjiang, The People's Republic of China*

Yi Chen • *Key Laboratory of Analytical Chemistry for Living Biosystems, Institute of Chemistry, Chinese Academy of Sciences, Beijing, The People's Republic of China*

G. Cretier • *Institut des Sciences Analytiques, UMR 5280 (CNRS/Université Lyon 1/ ENS Lyon), Université de Lyon, Villeurbanne, France*

B. Delacourt • *Department of Micro and Nanotechnology, Technical University of Denmark, Kongens Lyngby, Denmark*

Wim de Malsche • *Department of Micro and Nanotechnology, Vrije Universiteit Brussel, Brussels, Belgium*

K. Faure • *Institut des Sciences Analytiques, UMR 5280 (CNRS/Université Lyon 1/ENS Lyon), Université de Lyon, Villeurbanne, France*

Frantisek Foret • *Institute of Analytical Chemistry, v. v. i., Czech Academy of Sciences, Brno, Czech Republic*

Ying Sing Fung • *Department of Chemistry, The University of Hong Kong, Hong Kong, Hong Kong Special Administrative Region*

Yuanming Guo • *Key Lab of Mariculture and Enhancement of Zhejiang Province, Marine Fishery Institute of Zhejiang Province, Zhoushan, China*

András Guttman • *Horváth Laboratory of Bioseparation Sciences, University of Debrecen, Debrecen, Hungary; Institute of Analytical Chemistry, v. v. i., Czech Academy of Sciences, Brno, Czech Republic; MTA-PE Translational Glycomics Group, University of Pannonia, Veszprem, Hungary*

Stephen J. Haswell • *Department of Chemistry, University of Hull, Kingston Upon Hull, Humberside, UK*

Stijn Hendrickx • *Department of Pharmaceutical and Pharmacological Sciences, Pharmaceutical Analysis, KU Leuven, Leuven, Belgium*

Can Hu • *Key Laboratory of Analytical Chemistry for Living Biosystems, Institute of Chemistry, Chinese Academy of Sciences, Beijing, The People's Republic of China*

Hongmei Hu • *Key Lab of Mariculture and Enhancement of Zhejiang Province, Marine Fishery Institute of Zhejiang Province, Zhoushan, China*
Henrik Jensen • *Faculty of Pharmaceutical Sciences, University of Copenhagen, Copenhagen, Denmark*
Seong Ho Kang • *Department of Applied Chemistry, College of Applied Science, Kyung Hee University, Yongin-si, Gyeonggi-do, Republic of Korea*
Rene Kizek • *Faculty of Agronomy, Department of Chemistry and Biochemistry, Mendel University, Brno, Czech Republic, EU; Central European Institute of Technology, Brno University of Technology, Brno, Czech Republic, EU*
Pavel Kopel • *Faculty of Agronomy, Department of Chemistry and Biochemistry, Mendel University, Brno, Czech Republic, EU; Central European Institute of Technology, Brno University of Technology, Brno, Czech Republic, EU*
Jana Krenkova • *Institute of Analytical Chemistry, v. v. i., Czech Academy of Sciences, Brno, Czech Republic*
Sona Krizkova • *Faculty of Agronomy, Department of Chemistry and Biochemistry, Mendel University, Brno, Czech Republic, EU; Central European Institute of Technology, Brno University of Technology, Brno, Czech Republic, EU*
J.P. Kutter • *Department of Micro and Nanotechnology, Technical University of Denmark, Kongens Lyngby, Denmark; Department of Pharmacy, University of Copenhagen, Universitetsparken 2, Copenhagen, Denmark*
Y. Ladner • *Institut des Sciences Analytiques, UMR 5280 (CNRS/Université Lyon 1/ENS Lyon), Université de Lyon, Villeurbanne, France*
Seungah Lee • *Department of Applied Chemistry, College of Applied Science, Kyung Hee University, Yongin-si, Gyeonggi-do, Republic of Korea*
Kaicheng Li • *Department of Physics, Kenyon College, Gambier, OH, USA*
Tiejun Li • *Key Lab of Mariculture and Enhancement of Zhejiang Province, University Marine Fishery Institute of Zhejiang Province, Zhoushan, China*
Tao Liao • *Key Laboratory of Analytical Chemistry for Living Biosystems, Institute of Chemistry, Chinese Academy of Sciences, Beijing, The People's Republic of China*
Marián Masár • *Faculty of Natural Sciences, Department of Analytical Chemistry, Comenius University in Bratislava, Bratislava, Slovak Republic*
K.B. Mogensen • *Department of Micro and Nanotechnology, Technical University of Denmark, Kongens Lyngby, Denmark*
Maria F. Mora • *NASA Jet Propulsion Laboratory, California Institute of Technology, Pasadena, CA, USA*
He Nan • *Department of Chemistry, Graduate School, Kyung Hee University, Yongin-si, Gyeonggi-do, Republic of Korea*
Hoai Viet Nguyen • *Faculty of Agronomy, Department of Chemistry and Biochemistry, Mendel University, Brno, Czech Republic, EU*
Jan Partyka • *Institute of Analytical Chemistry, v. v. i., Czech Academy of Sciences, Brno, Czech Republic*
Stig Pedersen-Bjergaard • *Faculty of Pharmaceutical Sciences, University of Copenhagen, Copenhagen, Denmark*
Nickolaj J. Petersen • *Faculty of Pharmaceutical Sciences, University of Copenhagen, Copenhagen, Denmark*
Qiaosheng Pu • *College of Chemistry and Chemical Engineering, Lanzhou University, Lanzhou, Gansu, People's Republic of China*

Jan Regtmeier • *Faculty of Physics, Experimental Biophysics and Applied Nanoscience, Bielefeld University, Bielefeld, Germany*
Kirsty J. Shaw • *Faculty of Science and Engineering, Manchester Metropolitan University, Manchester, UK*
Maja Stanisavljevic • *Faculty of Agronomy, Department of Chemistry and Biochemistry, Mendel University, Brno, Czech Republic, EU*
Amanda M. Stockton • *NASA Jet Propulsion Laboratory, California Institute of Technology, Pasadena, CA, USA*
Ákos Szekrényes • *Horváth Laboratory of Bioseparation Sciences, University of Debrecen, Debrecen, Hungary*
Peter Troška • *Faculty of Natural Sciences, Department of Analytical Chemistry, Comenius University in Bratislava, Bratislava, Slovak Republic*
Marketa Vaculovicova • *Faculty of Agronomy, Department of Chemistry and Biochemistry, Mendel University, Brno, Czech Republic, EU; Central European Institute of Technology, Brno University of Technology, Brno, Czech Republic, EU*
Csaba Varadi • *Horváth Laboratory of Bioseparation Sciences, University of Debrecen, Debrecen, Hungary*
Martina Viefhues • *Faculty of Physics, Experimental Biophysics and Applied Nanoscience, Bielefeld University, Bielefeld, Germany*
Zhiping Wang • *Singapore Institute of Manufacturing Technology, Singapore, Singapore*
Xuan Wei • *College of Chemistry and Chemical Engineering, Lanzhou University, Lanzhou, Gansu, People's Republic of China*
Peter A. Willis • *NASA Jet Propulsion Laboratory, California Institute of Technology, Pasadena, CA, USA*
Ruige Wu • *Singapore Institute of Manufacturing Technology, Singapore*
Peng Zhang • *Department of Chemistry, Graduate School, Kyung Hee University, Yongin-si, Gyeonggi-do, Republic of Korea*

Part I

Overview

Chapter 1

An Overview of the Use of Microchips in Electrophoretic Separation Techniques: Fabrication, Separation Modes, Sample Preparation Opportunities, and On-Chip Detection

Stijn Hendrickx, Wim de Malsche, and Deirdre Cabooter

Abstract

This chapter is intended as a basic introduction to microchip-based capillary electrophoresis to set the scene for newcomers and give pointers to reference material.

An outline of some commonly used setups and key concepts is given, many of which are explored in greater depth in later chapters.

Key words Microchip capillary electrophoresis, Fabrication, Separation modes, Sample preparation, On-chip detection

1 Introduction

1.1 What Is Capillary Electrophoresis?

Capillary electrophoresis (CE) is a well-established analytical technique that allows rapid and highly efficient separations of charged analytes in minute sample volumes [1, 2]. CE is a separation technique which is driven by an electric potential difference applied across a narrow-bore capillary or microchip channel (usually smaller than 100 μm I.D.) filled with a (typically aqueous) electrolyte solution. A sample mixture of different compounds in solution is introduced into the capillary as a relatively narrow zone. When a potential difference is applied across the capillary, bulk flow of the solution is generated by a process referred to as electroosmotic flow (EOF). Analytes, introduced at one end of the capillary, are driven toward the detector with a velocity that is proportional to the EOF and their charge/mass ratio. Separation is then based on differences in electrophoretic mobility of the analyte ions [1]. The EOF leads to a flat velocity profile, in contrast with the parabolic flow arising from mechanical pumping as encountered in liquid chromatography. The flat velocity profile or "plug flow" results in a decrease in band broadening and hence higher plate numbers [1].

Ann Van Schepdael (ed.), *Microchip Capillary Electrophoresis Protocols*, Methods in Molecular Biology, vol. 1274,
DOI 10.1007/978-1-4939-2353-3_1,

After the introduction of CE by Hjertén in 1967 [3], Jorgensen and Lukacs developed it into the modern technique which is used nowadays. They demonstrated that high separation efficiencies (more than 400,000 plates) could be obtained by applying field strengths of up to 30 kV in narrow capillaries [4–6]. The small I.D. of the capillaries (20–100 μm) ensured an efficient dissipation of the heat generated by the high voltages.

Since then, CE has been applied for the separation of a wide range of different analytes: from inorganic to organic ions, achiral to chiral compounds, neutral molecules, biopolymers such as peptides, proteins, DNA and RNA molecules or their fragments, and even viruses and bacterial cells [7–13].

Capillary electrophoresis has since long been regarded as an alternative to more traditional separation techniques such as gel electrophoresis (GE) and liquid chromatography (LC). CE has a number of advantages over both of them, such as speed, flexibility, ease of automation, portability, sample and reagent requirements, and cost, but also a number of disadvantages such as lack of reproducibility and lower sensitivity.

1.2 Microchip Electrophoresis

The implementation of electrophoresis in flat planar microchips was initiated some 20 years ago by Harrison, Manz, and Widmer [14–16]. Capillary channels were fabricated in planar glass substrates using micromachining techniques, and separation in the channels was obtained using electrophoresis [14]. More than 100,000 theoretical plates could be obtained under optimized conditions [16, 17], comparable to results attainable in fused silica capillaries. The application of microchips for the separation of analytes by electrophoresis has the important advantage that heat dissipation is much better in microchips than in capillaries of the same dimensions. This allows the application of higher electrical fields in much shorter separation channels, resulting in much faster separations.

Manz et al. moreover demonstrated the possibility to couple injectors and detectors onto a miniaturized separation device using microlithography techniques and hence introduced the concept of a "miniaturized total chemical analysis system" (μTAS), also referred to as lab-on-a-chip [14]. The term "lab-on-a-chip" embodies the idea of a small, low-cost, completely self-contained, portable device with advanced chemical analysis capability, low reagent consumption, and low power requirements.

Miniaturization of the electrophoretic process onto microchips permits very complex and highly integrated analyses, as micromachining techniques allow manufacturing microchannel systems with integrated injection and detection capabilities with minimal dead volumes. Additionally, due to the simplicity of the required instrumentation for CE, which requires no moving parts, miniaturization is rather straightforward. Consequently, microchip electrophoresis (MCE) has the potential to combine most of the

advantages of CE (sample handling capabilities, fast analysis time, custom design, and small sample requirements) with the advantage of portability, while maintaining similar analytical performance as standard benchtop instrumentation. Additional advantages of MCE devices include the possibility to use a wide variety of well-established separation techniques and control the entire system electronically [18].

Today, MCE devices have become well-accepted, multidimensional, analytical platforms in biomedical, pharmaceutical, environmental, and forensic sciences [19–22]. In the last decade, there has been a steep rise in the number of applications of MCE which has resulted in the development of a number of commercial products by Agilent, Hitachi, and Shimadzu [23–25]. To achieve advanced performance and allow for specific applications, surface modification methods for the microchannels have been developed [26–28]. In the past years, new microfabrication methods [29, 30], injection schemes [31, 32], channel geometries [33–35], separation modes, and detection techniques [36–38] have been introduced for MCE.

While MCE is seen as a viable (and often superior) alternative to CE, it can be considered as a complementary analytical technique to LC for the analysis of nonvolatile compounds [39].

1.3 Fabrication of Microchips

The rising interest in MCE research in the past decade has been a direct consequence of recent developments in micromachining techniques, such as those based on common semiconductor processing techniques. These improved techniques have made it possible to integrate multiple functions such as sampling, sample processing, and separation in a single microchip device using complex fluidic circuits, enabling high-throughput bioanalyses without additional connectors [40]. Although considerable progress has been made toward this goal, nearly all chips reported to date still require some external ancillary equipment such as pumps, valves, detectors, and power supplies. This introduction gives a short overview of the materials and techniques most commonly used for MCE production.

1.3.1 Microchip Materials

In the early stage of CE microchip development, glass and quartz substrates were mainly used as chip material because of their optical transparency, excellent electroosmotic flow characteristics, and similar chemistry as the fused silica capillaries used in traditional CE [14]. However, the time-consuming and labor-intensive fabrication process and necessity for costly equipment and clean rooms have shifted the focus to polymer-based chips [41]. These are cheaper and require only relatively simple fabrication infrastructure and technologies. Various polymers, each with their own specific advantages and drawbacks, such as poly(dimethylsiloxane) (PDMS), poly(methyl methacrylate) (PMMA), polycarbonate (PC), polyethylene terephthalate (PET), polyester, cyclo-olefin polymer

(COP), and SU-8 have been used in MCE applications. PDMS is the most commonly used material due to its high flexibility and optical transparency. The biggest disadvantage, however, is the low separation efficiency it yields [42]. To overcome this, hybrid PDMS/glass microchips are usually employed. In recent years, paper- and polyester-toner (PT) substrates have emerged as simple, versatile, lightweight, and low-cost promising platforms for the production of disposable devices for MCE [43, 44]. Channels are usually used as such, but can be coated to prevent surface adsorption of peptides and proteins and avoid irreproducible results.

1.3.2 Micromachining Techniques

For the production of glass microfluidic chips, standard photolithographic technologies are mostly used, in combination with wet chemical etching and a bonding step. After the application of a photoresist layer, a photomask with the intended channel layout is placed between the chip and the light source. Next, the photomask is exposed to UV light to either dissolve or cross-link the photoresist layer. Subsequently, the glass can be etched according to the produced pattern by a solution containing hydrofluoric acid. After removal of the layers, fluidic access holes for microfluidic connections can be drilled or powder-blasted into the chip. After an extensive cleaning step, the chip can be bonded at high temperature [45]. An example of a basic lithography procedure is given in Fig. 1.

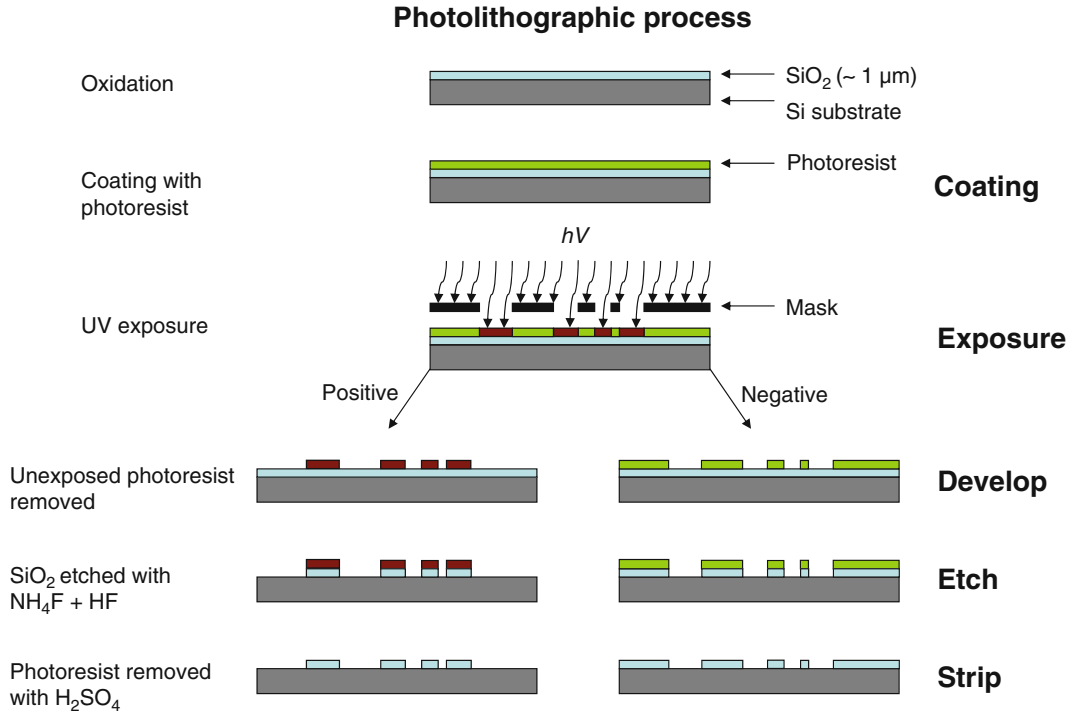

Fig. 1 Schematic representation of the different steps in the lithographic process. Process steps include coating, exposure, development, oxide etching, and resist stripping

In the last decade, chips based on polymer materials have gained much more interest because of some inherent advantages. The cost is lower, fabrication often requires less stringent conditions and subsequently less expensive facilities such as a clean room and other specialized equipment, and the design of complex and highly diverse microchannel structures is much easier on these polymeric substrates [40, 46]. It should, however, be stressed that when the definition of micron-sized structures is targeted before applying a bonding step (which is the case for most techniques), the time spent in the clean room is the price-determining factor and the substrate price becomes negligible.

Polymer chips can be produced using various microfabrication techniques such as injection molding [47], laser ablation [48], hot embossing [49], casting [50], and imprinting [51]. Recently, some new exciting techniques have emerged, such as in situ polymerization of methyl methacrylate (MMA) for the fabrication of fiber electrophoresis microchips [52]; optofluidic maskless lithography (OFML), an in situ photopolymerization technique used to fabricate microstructures (such as microparticles) within a fluidic channel using computer-controlled two-dimensional spatial light modulators [53]; and substrate modification and replication by thermoforming (SMART), wherein heated and hence softened thermoplastic polymer films or plates are shaped by three-dimensional stretching [54]. In the past few years, the fabrication of hybrid glass/quartz–polymer microchips has also become fairly established. Leakage and blockage have proven to be the major challenges when fabricating microfluidic chips combining different materials [55]. It requires fabrication techniques for perfect bonding between different materials, such as oxygen plasma bonding [55, 56], as well as a clean room environment (which is often not available).

1.4 Microchip Electrophoresis Modes

Different modes of capillary electrophoretic separations can be performed using standard CE instrumentation. The most important capillary electroseparation modes include capillary zone electrophoresis (CZE), capillary gel electrophoresis (CGE), micellar electrokinetic capillary chromatography (MEKC), capillary electrochromatography (CEC), capillary isoelectric focusing (CIEF), and capillary isotachophoresis (CITP) [1, 57]. Depending on the type of analytes, the same separation modes can be used on a microfluidic chip. Small molecules are usually analyzed with CZE, CEC, or MEKC in glass/silica microchips. Larger molecules such as DNA are separated using CGE, while for larger proteins CGE, CIEF, and CZE are preferred [19].

1.4.1 CZE

Capillary zone electrophoresis is the simplest, most universal, and most frequently used CE mode. Many compounds can be separated rapidly and easily. The separation in CZE is based on differences in the electrophoretic mobility, which result in different velocities of migration of ionic species in the electrophoretic buffer

contained in the capillary or microchannel. The separation mechanism is mainly based on differences in solute size and charge (charge/mass ratio) at a specific pH. The charge/mass ratio of many ions can be changed by adjusting the pH of the buffer medium to affect their ionization and hence their migration time. There are many examples of CZE applied in microchips [58–61]. The technique is often also combined with MS [62–65].

1.4.2 CEC

In CEC, the separation column is packed with a chromatographic packing which can retain analytes, similar to LC techniques. The mobile phase, consisting of aqueous buffer and organic modifier, is in contact with both the silica wall and the particle surfaces. The separation mechanism can hence be seen as a combination of two techniques: liquid chromatography and capillary electrophoresis. Due to the presence of the packed bed in the microchannel, the flow is less plug like than for other electrophoretic techniques. This effect becomes more pronounced at increasing ratios of double layer thickness and average particle spacing. To provide sufficient interaction surface, the use of support structures is, however, vital. In recent chip-based work, ordered pillar arrays in fused silica [66] were used to provide more surface area, while providing higher efficiency than a disordered (packed) column. The use of a foil-shaped pillar allowed for minimization of dispersion and impedance simultaneously, an optimization which is not possible in pressure-driven chromatography.

The nature of the mobile phase makes coupling to MS easier than for other CE techniques. Separation in CEC has been obtained with different separation modes, using reversed-phase, cationic, or anionic ion-exchange stationary phases [67]. CEC is regularly used in MCE for the analysis of small, neutral molecules or enantiomers which are difficult to analyze by other electrophoretic methods [19, 68, 69].

1.4.3 MEKC

In MEKC, the analytes are separated by differential partitioning between micelles (which form a pseudo-stationary phase) and a surrounding aqueous buffer solution (mobile phase). Micelles form in solution when a surfactant is added to the mobile phase in a concentration which surpasses its critical micelle concentration (CMC). This technique provides a way to resolve neutral molecules as well as charged molecules using CE. The most commonly used surfactant in MEKC is sodium dodecyl sulfate (SDS). Chip MEKC has been used for the separation of amino acids [70, 71], flavonoids [72], alkaloids [73], narcotic drugs [74], explosives [75], pesticides [76], and many more.

1.4.4 CGE

The main separation mechanism in capillary gel electrophoresis is based on differences in solute size as analytes migrate through the pores of a gel-filled column. Separation takes place based on

"molecular sieving." The gel, which is formed by polymers such as polyacrylamide and SDS, must be thermally stable and have an appropriate range of pore sizes to be a suitable electrophoretic medium. The technique is not very suitable for neutral molecules, since EOF is suppressed in this mode of separation, preventing migration of neutral molecules. Microchips for CGE can be obtained by introducing the gel into the microchannel via capillary action [77] and have been used for rapid DNA and DNA fragment separations [78, 79], but also for allergens [80] and proteins [81].

1.4.5 CIEF

Microchip isoelectric focusing is a strong tool for protein analysis [19]. In IEF analytes are separated based on their isoelectric point. Protein samples are introduced in the separation channel together with a solution which forms a pH gradient along the channel. Under the influence of an applied electrical field, charged proteins will migrate through the medium until they reside in a pH region were they become electrically neutral and therefore stop migrating. Eventually, a steady state is reached. After focusing, the zones can be mobilized from the separation channel by pressurized flow [1]. Recent developments of this technique and various applications in protein and peptide analysis in microchips are described in a detailed review [82].

1.5 Sample Preparation Opportunities

One of the goals of microfluidics research is to incorporate sample preprocessing and analysis platforms onto the same device. The concept of a "lab-on-a-chip" is an attractive idea, but considerable effort is still required to make it feasible for most analyses. With this concept in mind, many scientists have tried to miniaturize and implement sample preparation onto microfluidic devices. In this way, sample preparation steps such as extraction, desalting, preconcentration, and modification of analytes have been incorporated in microchips.

1.5.1 Sample Cleanup and Pre-concentration of Analytes

Low detection limits for small molecules are a major problem in MCE due to the small channel dimensions. Therefore, online concentration before MCE is an important step of sample preparation. Various methods have been described in literature for sample cleanup and pre-concentration of analytes on a microfluidic chip. On-chip pre-concentration techniques can generally be classified into two major categories: static and dynamic methods [83]. Static techniques entail (1) solvent extraction techniques that concentrate analytes in aqueous solution in an organic solvent via phase transfer and dissolution [84, 85], (2) surface-binding techniques that trap analytes via adsorption or binding [86–89], and (3) porous membrane or nanochannel techniques which stack analytes through filtering or exclusion enrichment [90, 91].

Dynamic techniques do not require physical barriers or structures to retain analytes and can be subdivided into techniques that

concentrate analytes (1) through velocity differences across the boundary between sample and running buffer and (2) based on the focusing effect. Field-amplified sample stacking (FASS) [92], field-amplified sample injection (FASI) [92, 93], isotachophoresis (ITP) [61], transient ITP (tITP) [94], sweeping [95], and dynamic pH junction [96] are all examples of dynamic pre-concentration based on velocity differences.

Dynamic pre-concentration methods based on focusing entail that the net velocity of the analytes approaches zero somewhere in the channel. Focusing can, for example, be obtained via (1) isoelectric focusing (IEF) [97], (2) temperature gradient focusing (TGF) [98], and (3) electric field gradient focusing (EFGF) [99].

1.5.2 Other Integrated Sample Preprocessing Platforms

Other sample preprocessing techniques such as mixing, sample labeling, and metabolite generation have been used on microfluidic devices as well. An example is reported by Ma et al. [100] describing an integrated solgel-based bioreactor in a microfluidic device for the generation of drug metabolites. The group of Wu et al. [101] reported on the implementation of a microfluidic platform for sampling and mixing small volumes of blood to aid in quantitative positron emission tomography (PET) studies of mice.

Laser-induced fluorescence (LIF) is the primary detection tool for MCE. Therefore, on-chip labeling before the electrophoretic separation is often required as most analytes are nonfluorescent. A high number of on-chip labeling strategies have been presented, both pre-column and post-column. Pre-column labeling is preferred because reaction time and other conditions do not affect band broadening during separation. The two most common labeling methods are fluorescent covalent labeling and affinity labeling [102, 103].

The use of selective analytical techniques, such as immunoassays and other analyte immobilization techniques, diminishes the need for extensive sample cleanup and preprocessing because they allow for direct determination of biofluids. These selective techniques are therefore very interesting to be incorporated in microchips [104–106].

1.6 On-Chip Detection

1.6.1 Optical Detection

Laser-induced fluorescence (LIF) detection is the most widely used optical detection mode for microchip analysis [107–109]. LIF can easily be adapted to the dimensions of microchips and has superior selectivity and sensitivity compared to other common detectors. The main disadvantage of LIF is the requirement of pre- or post-column derivatization with a fluorophore. At the moment, most lasers are also significantly larger in scale than microchips and not portable and disposable [41]. Microchip LIF detection has been widely employed for DNA analysis, because of its high throughput and sensitivity [110], and for immunoassays and enzymatic reactions [111]. Although MCE-LIF systems have proven very useful

for the analysis of large compounds such as DNA and proteins, they are not the first choice for detection of small molecules.

UV absorption and deep UV-induced fluorescence can be suitable for aromatic compounds [112]. UV detection has a wide application range, but is usually limited because of its poor sensitivity due to the short optical path length across the separation channel. As a result, several means to increase the path length on a CE microchip have been investigated, such as the fabrication of U-cells and optical waveguides to increase the channel depth [113]. The use of a capillary expansion (bubble cell) at the detection zone has also been employed to enhance detection sensitivity, without significantly compromising separation efficiency [114].

1.6.2 Electrochemical Detection

Due to the high cost of classical UV instrumentation and the need for analyte derivatization in the case of LIF detection, significant effort has been dedicated to the development of alternative detection modes for MCE. Electrochemical detection (EC) has raised a lot of interest as possible online detection mode for MCE. Advantages of EC include good sensitivity, ease of miniaturization, low cost, and low power requirements. EC detection has been widely used for detection of small molecules in MCE [21, 72, 115].

The most frequently used EC detector for MCE is the amperometric detector (AD). It is mainly employed to monitor electroactive analytes. The AD has a high sensitivity and performance, but generally suffers from interferences caused by the CE separation voltage. Examples include the development of a miniaturized MCE device for the simultaneous measurement of lactate and glucose [116] and an MCE-AD system for the analysis of uric acid in urine [117]. A second electrochemical detection method is conductivity detection, which can be seen as the most universal quantification method in CE and MCE. There are two modes of conductivity detection, one where the electrodes are in direct contact with the buffer solution and the so-called contactless conductivity detection [118]. Capacitively coupled contactless conductivity detection (C^4D) is used today for the analysis of small ions [119] as well as for complex biochemical analytes [120]. C^4D is composed of two radial electrodes placed around the capillary or two planar electrodes placed in the end of the microchip channel. The main advantages of the contactless mode over the contact mode are the greatly decreased background noise and the avoidance of bubble creation [18]. Potentiometric detection is a third electrochemical detection method which is, however, seldom used for MCE.

1.6.3 MS and NMR Detection

The combination of mass spectrometry (MS) with MCE combines high separation efficiency with a highly sensitive detection method. MCE-MS has been successfully used for the analysis of biogenic compounds such as peptides, proteins, amino acids, sugars, metabolites, and pharmaceutical compounds [121–123]. ESI is the

preferred ionization mode for MCE-MS, due to the simple structure which is easily implemented on a microchip and its suitability to ionize analytes dissolved in a liquid phase. Typical MCE-ESI-MS interfaces comprise microsprayers similar to CE-ESI-MS interfaces, tapered capillary spray tips inserted in a separation channel, and monolithically fabricated spray tip structures [124–126].

When the high separation efficiency of CE is combined with NMR, it can lead to unique analytical possibilities. The great strength of NMR spectroscopy lies in its capability to provide molecular information on samples in a nondestructive way and at atomic resolution. For these reasons, the technique is often used for the identification of small molecules, to study structure and reaction dynamics, and to probe intermolecular interactions. The poor sensitivity of NMR, however, is a major drawback in combination with MCE. There are a few examples of MCE devices with integrated NMR detection [127].

References

1. Li SFY (1992) Capillary electrophoresis: principles, practice and applications. Elsevier, Amsterdam
2. Landers JP (2008) Handbook of capillary and microchip electrophoresis and associated microtechniques. CRC, Boca Raton
3. Hjertén S (1967) Free zone electrophoresis. Chromatogr Rev 9:122–219
4. Jorgensen JW, Lukacs KD (1981) Zone electrophoresis in open-tubular glass capillaries. Anal Chem 53:1298–1302
5. Jorgensen JW, Lukacs KD (1981) High resolution separations based on electrophoresis and electroosmosis. J Chromatogr 218:209–216
6. Jorgensen JW, Lukacs KD (1981) Zone electrophoresis in open-tubular glass capillaries: preliminary data on performance. J High Resolut Chromatogr 4:230–231
7. Fercher G, Haller A, Smetana W et al (2010) Ceramic capillary electrophoresis chip for the measurement of inorganic ions in water samples. Analyst 135:965–970
8. Lamalle C, Marini RDA, Debrus B et al (2012) Development of a generic micellar electrokinetic chromatography method for the separation of 15 antimalarial drugs as a tool to detect medicine counterfeiting. Electrophoresis 33:1669–1678
9. Wu R, Wang Z, Zhao W et al (2013) Multidimension microchip-capillary electrophoresis device for determination of functional proteins in infant milk formula. J Chromatogr A 1304:220–226
10. Hopwood A, Hurth C, Yang J et al (2010) Integrated microfluidic system for rapid forensic DNA analysis: sample collection to DNA profile. Anal Chem 82:6991–6999
11. Vaculovicova M, Smerkova K, Sedlacek J et al (2013) Integrated chip electrophoresis and magnetic particle isolation used for detection of hepatitis B virus oligonucleotides. Electrophoresis 34:1548–1554
12. Jung JH, Kim GY, Seo TS (2011) An integrated passive micromixer-magnetic separation-capillary electrophoresis microdevice for rapid and multiplex pathogen detection at the single-cell level. Lab Chip 11:3465–3470
13. Xu CX, Yin XF (2011) Continuous cell introduction and rapid dynamic lysis for high-throughput single-cell analysis on microfluidic chips with hydrodynamic focusing. J Chromatogr A 1218:726–732
14. Harrison DJ, Fluri K, Seiler K et al (1993) Micromachining a miniaturized capillary electrophoresis-based chemical analysis system on a chip. Science 261:895–897
15. Harrison DJ, Manz A, Fan Z et al (1992) Capillary electrophoresis and sample injection systems integrated on a planar glass chip. Anal Chem 64:1926–1932
16. Seiler K, Harrison DJ, Manz A (1993) Planar glass chips for capillary electrophoresis: repetitive sample injection, quantitation, and separation efficiency. Anal Chem 65:1481–1488
17. Effenhauser CS, Manz A, Widmer HM (1993) Glass chips for high-speed capillary electrophoresis separation with submicrometer plate heights. Anal Chem 65:2637–2642
18. Felhofer JL, Blanes L, Garcia CD (2010) Recent developments in instrumentation for

capillary electrophoresis and microchip-capillary electrophoresis. Electrophoresis 31: 2469–2486

19. Wu D, Qin J, Lin B (2008) Electrophoretic separations on microfluidic chips. J Chromatogr A 1184:542–559
20. Kraly JR, Holcomb RE, Guan Q et al (2009) Microfluidic applications in metabolomics and metabolic profiling. Anal Chim Acta 653:23–35
21. Chen G, Lin Y, Wang J (2006) Monitoring environmental pollutants by microchip capillary electrophoresis with electrochemical detection. Talanta 68:497–503
22. Verpoorte E (2002) Microfluidic chips for clinical and forensic analysis. Electrophoresis 23:677–712
23. Nuchtavorn N, Smejkal P, Breadmore MC et al (2013) Exploring chip-capillary electrophoresis-laser-induced fluorescence field-deployable platform flexibility: separations of fluorescent dyes by chip-based non-aqueous capillary electrophoresis. J Chromatogr A 1286:216–221
24. Fouad M, Jabasini M, Kaji N et al (2008) Microchip analysis of plant glucosinolates. Electrophoresis 29:2280–2287
25. Miyado T, Wakida S, Aizawa H et al (2008) High-throughput assay of nitric oxide metabolites in human plasma without deproteinization by lab-on-a-chip electrophoresis using a zwitterionic additive. J Chromatogr A 1206: 41–44
26. Schulze M, Belder D (2011) Poly(ethylene glycol)-coated microfluidic devices for chip electrophoresis. Electrophoresis 33:370–378
27. Liang RP, Meng XY, Liu CM et al (2011) PDMS microchip coated with polydopamine/gold nanoparticles hybrid for efficient electrophoresis separation of amino acids. Electrophoresis 32:3331–3340
28. Alvarez-Martos I, Fernàndez-Abedul MT, Anillo A et al (2012) Poly (acrylic acid) microchannel modification for the enhanced resolution of catecholamines microchip electrophoresis with electrochemical detection. Anal Chim Acta 724:136–143
29. Chen Y, Duan H, Zhang L et al (2008) Fabrication of PMMA CE microchips by infrared-assisted polymerization. Electrophoresis 29:4922–4927
30. Huang FC, Chen YF, Lee GB (2007) CE chips fabricated by injection molding and polyethylene/thermoplastic elastomer film packaging methods. Electrophoresis 28:1130–1137
31. Ito T, Inoue A, Sato K et al (2005) Autonomous polymer loading and sample injection for microchip electrophoresis. Anal Chem 77:4759–4764
32. Lee NY, Yamada M, Seki M (2005) Control-free air vent system for ultra-low volume sample injection on a microfabricated device. Anal Sci 21:465–468
33. Ono K, Kaneda S, Fujii T (2013) Single-step CE for miniaturized and easy-to-use system. Electrophoresis 34:903–910
34. Chen Y, Choi JY, Choi SJ et al (2010) Sample stacking capillary electrophoretic microdevice for highly sensitive mini Y short tandem repeat genotyping. Electrophoresis 31:2974–2980
35. Zhang Y, Park S, Yang S et al (2010) An all-in-one microfluidic device for parallel DNA extraction and gene analysis. Biomed Microdevices 12:1043–1049
36. Hsiung SK, Lee CH, Lee GB (2008) Microcapillary electrophoresis chips utilizing controllable micro-lens structures and buried optical fibers for on-line optical detection. Electrophoresis 29:1866–1873
37. Castaño-Álvarez M, Fernández-la-Villa A, Pozo-Ayuso DF et al (2009) Multiple-point electrochemical detection for a dual-channel hybrid PDMS-glass microchip electrophoresis device. Electrophoresis 30:3372–3380
38. Wu D, Wu J, Zhu YH et al (2010) An electrically heated Au electrode for electrochemical detection in microchip system. Electroanalysis 22:1217–1222
39. Breadmore MC (2012) Capillary and microchip electrophoresis: challenging the common conceptions. J Chromatogr A 1221:42–55
40. Sia SK, Whitesides GM (2003) Microfluidic devices fabricated in poly(dimethylsiloxane) for biological studies. Electrophoresis 24: 3563–3576
41. Shang F, Guihen E, Glennon JD (2012) Recent advances in miniaturisation – the role of microchip electrophoresis in clinical analysis. Electrophoresis 33:105–116
42. Kitagawa F, Otsuka K (2011) Recent progress in microchip electrophoresis-mass spectrometry. J Pharm Biomed Anal 55:668–678
43. Coltro WK, de Jesus DP, da Silva JA et al (2010) Toner and paper-based fabrication techniques for microfluidic applications. Electrophoresis 31:2487–2498
44. Gabriel EF, do Lago CL, Gobbi AL et al (2013) Characterization of microchip electrophoresis devices fabricated by direct-printing process with colored toner. Electrophoresis 34:2169–2176
45. Baker CA, Roper MG (2010) A continuous-flow, microfluidic fraction collection device. J Chromatogr A 1217:4743–4748
46. Tay ET, Law WS, Li SF et al (2009) Microchip capillary electrophoresis. Methods Mol Biol 509:159–168

47. Nickcevic I, Lee SH, Piruska A et al (2007) Characterization and performance of injection molded poly(methylmethacrylate) microchips for capillary electrophoresis. J Chromatogr A 1154:444–453
48. Yap YC, Guijt RM, Dickson TC et al (2013) Stainless steel pinholes for fast fabrication of high-performance microchip electrophoresis devices by CO2 laser ablation. Anal Chem 85:10051–10056
49. Kricka LJ, Fortina P, Panaro NJ et al (2002) Fabrication of plastic microchips by hot embossing. Lab Chip 2:1–4
50. Liu C, Cui D, Cai H et al (2006) A rigid poly(dimethylsiloxane) sandwich electrophoresis microchip based on thin-casting method. Electrophoresis 27:2917–2923
51. Sun X, Peeni BA, Yang W et al (2007) Rapid prototyping of poly(methyl methacrylate) microfluidic systems using solvent imprinting and bonding. J Chromatogr A 1162:162–166
52. Chen Z, Zhang L, Chen G (2007) Fabrication and performance of fiber electrophoresis microchips. Electrophoresis 28:2466–2473
53. Martinsson H, Sandstrom T, Bleeker AJ et al (2005) Current status of optical maskless lithography. J Microlithogr. doi:10.1117/1.1862649
54. Truckenmüller R, Giselbrecht S, van Blitterswijk CA et al (2008) Flexible fluidic microchips based on thermoformed and locally modified thin polymer films. Lab Chip 8:1570–1579
55. Shameli SM, Elbuken C, Ou J et al (2011) Fully integrated PDMS/SU-8/quartz microfluidic chip with a novel macroporous poly dimethylsiloxane (PDMS) membrane for isoelectric focusing of proteins using whole-channel imaging detection. Electrophoresis 32:333–339
56. Beh CW, Zhou W, Wang TH (2012) PDMS-glass bonding using grafted polymeric adhesive – alternative process flow for compatibility with patterned biological molecules. Lab Chip 12:4120–4127
57. Krikku P, Grass B, Hokkanen A et al (2004) Isotachophoresis of beta-blockers in a capillary and on a poly(methyl methacrylate) chip. Electrophoresis 25:1687–1694
58. Jacobson SC, Hergenroder R, Koutny LB et al (1994) High-speed separations on a microchip. Anal Chem 66:1114–1118
59. Jacobson SC, Culbertson CT, Daler JE et al (1998) Microchip structures for submillisecond electrophoresis. Anal Chem 70:3476–3480
60. Grass B, Hergenröder R, Neyer A et al (2002) Determination of selenoamino acids by coupling of isotachophoresis/capillary zone electrophoresis on a PMMA-microchip. J Sep Sci 25:135–140
61. Weiller BH, Ceriotti L, Shibata T et al (2002) Analysis of lipoproteins by capillary zone electrophoresis in microfluidic devices: assay development and surface roughness measurements. Anal Chem 74:1702–1711
62. Mao X, Wang K, Du Y et al (2003) Analysis of chicken and turkey ovalbumins by microchip electrophoresis combined with exoglycosidase digestion. Electrophoresis 24:3273–3278
63. Mao X, Chu IK, Lin B (2006) A sheath-flow nanoelectrospray interface of microchip electrophoresis MS for glycoprotein and glycopeptide analysis. Electrophoresis 27:5059–5067
64. Wang Z, Wang W, Wang W et al (2011) Separation and determination of β-casomorphins by using glass microfluidic chip electrophoresis together with laser-induced fluorescence detection. J Sep Sci 34:196–201
65. Atalay Y, Verboven P, Vermeir S et al (2009) Modeling and optimization of a multi-enzyme electrokinetically driven multiplexed microchip for simultaneous detection of sugars. Microfluid Nanofluid 7:393–406
66. Sukas S, De Malsche W, Desmet G et al (2012) Performance evaluation of different design alternatives for microfabricated non-porous fused silica pillar columns for capillary electrochromatography. Anal Chem 84: 9996–10004
67. Kasicka V (2012) Recent developments in CE and CEC of peptides (2009-2011). Electrophoresis 33:48–73
68. Jemere AB, Martinez D, Finot M et al (2009) Capillary electrochromatography with packed bead beds in microfluidic devices. Electrophoresis 30:4237–4244
69. Ladner Y, Crétier G, Faure K (2012) Electrochromatography on acrylate-based monolith in cyclic olefin copolymer microchip: a cost-effective and easy-to-use technology. Electrophoresis 33:3087–3094
70. Culbertson CT, Jacobson SC, Ramsey JM (2000) Microchip devices for high-efficiency separations. Anal Chem 72:5814–5819
71. Skelley AM, Scherer JR, Aubrey AD et al (2005) Development and evaluation of a microdevice for amino acid biomarker detection and analysis on Mars. Proc Natl Acad Sci U S A 102:1041–1046
72. Hompesch RW, García CD, Weiss DJ et al (2005) Analysis of natural flavonoids by microchip-micellar electrokinetic chromatography with pulsed amperometric detection. Analyst 130:694–700

73. Newman CI, Giordano BC, Copper CL et al (2008) Microchip micellar electrokinetic chromatography separation of alkaloids with UV-absorbance spectral detection. Electrophoresis 29:803–810
74. Du Y, Wang E (2008) Separation and detection of narcotic drugs on a microchip using micellar electrokinetic chromatography and electrochemiluminescence. Electrophoresis 20:643–647
75. Wallenborg SR, Bailey CG (2000) Separation and detection of explosives on a microchip using micellar electrokinetic chromatography and indirect laser-induced fluorescence. Anal Chem 72:1872–1878
76. Smirnova A, Shimura K, Hibara A et al (2008) Pesticide analysis by MEKC on a microchip with hydrodynamic injection from organic extract. J Sep Sci 31:904–908
77. Hong JW, Hosokawa K, Fujii T et al (2001) Microfabricated polymer chip for capillary gel electrophoresis. Biotechnol Prog 17:958–962
78. Oh D, Cheong IC, Lee HG et al (2010) Fast microchip electrophoresis using field strength gradients for single nucleotide polymorphism identification of cattle breeds. Bull Korean Chem Soc 31:1902–1906
79. Liu D, Ou Z, Xu M et al (2008) Simplified transient isotachophoresis/capillary gel electrophoresis method for highly sensitive analysis of polymerase chain reaction samples on a microchip with laser-induced fluorescence detection. J Chromatogr A 1214:165–170
80. Coisson JD, Cereti E, Garino C et al (2010) Microchip capillary electrophoresis (Lab-on-chip®) improves detection of celery (Apium graveolens L.) and sesame (Sesamum indicum L.) in foods. Food Res Int 43:1237–1243
81. Okada H, Kaji N, Tokeshi M et al (2008) Highly sensitive double-fluorescent dye staining on microchip electrophoresis for analysis of milk proteins. Electrophoresis 29:2533–2538
82. Shimura K (2009) Recent advances in IEF in capillary tubes and microchips. Electrophoresis 30:11–28
83. Sueyoshi K, Kitagawa F, Otsuka K (2008) Recent progress of online sample preconcentration techniques in microchip electrophoresis. J Sep Sci 31:2650–2666
84. Wägli P, Chang YC, Homsy A et al (2013) Microfluidic droplet-based liquid-liquid extraction and on-chip IR spectroscopy detection of cocaine in human saliva. Anal Chem 85:7558–7565
85. Petersen NJ, Jensen H, Hansen SH et al (2010) On-chip electro membrane extraction. Microfluid Nanofluid 9:881–888
86. Yu C, Davey MH, Svec F et al (2001) Monolithic porous polymer for on-chip solid-phase extraction and preconcentration prepared by photoinitiated in situ polymerization within a microfluidic device. Anal Chem 73:5088–5096
87. Yang Y, Li C, Lee KH et al (2005) Coupling on-chip solid-phase extraction to electrospray mass spectrometry through an integrated electrospray tip. Electrophoresis 26:3622–3630
88. Ramsey JD, Collins GE (2005) Integrated microfluidic device for solid-phase extraction coupled to micellar electrokinetic chromatography separation. Anal Chem 77:6664–6670
89. Svobodova Z, Mohamadi MR, Jankovicova B et al (2012) Development of a magnetic immunosorbent for on-chip preconcentration of amyloid β isoforms: representatives of Alzheimer's disease biomarkers. Biomicrofluidics 6:24126–2412612
90. Hoeman KW, Lange JJ, Roman GT et al (2009) Electrokinetic trapping using titania nanoporous membranes fabricated using sol-gel chemistry on microfluidic devices. Electrophoresis 30:3160–3167
91. Lee JH, Cosgrove BD, Lauffenburger DA (2009) Microfluidic concentration-enhanced cellular kinase activity assay. J Am Chem Soc 131:10340–10341
92. Guan Q, Henry CS (2009) Improving MCE with electrochemical detection using a bubble cell and sample stacking techniques. Electrophoresis 30:3339–3346
93. Zhang Y, Ping G, Zhu B et al (2007) Enhanced electrophoretic resolution of monosulfate glycosaminoglycan disaccharide isomers on poly(methylmethacrylate) chips. Electrophoresis 28:414–421
94. Wang J, Zhang Y, Okamoto Y et al (2011) Online transient isotachophoresis concentration by the pseudo-terminating electrolyte buffer for the separation of DNA-aptamer and its thrombin complex in poly(methyl methacrylate) microchip. Analyst 136:1142–1147
95. Pan Q, Zhao M, Liu S (2009) Combination of on-chip field amplification and bovine serum albumin sweeping for ultrasensitive detection of green fluorescent protein. Anal Chem 81:5333–5341
96. Ptolemy AS, Britz-McKibbin P (2008) New advances in on-line sample preconcentration by capillary electrophoresis using dynamic pH junction. Analyst 133:1643–1648
97. Herr AE, Molho JI, Drouvalakis KA et al (2003) On-chip coupling of isoelectric focusing and free solution electrophoresis for multidimensional separations. Anal Chem 75: 1180–1187

98. Balss KM, Ross D, Begley HC et al (2004) DNA hybridization assays using temperature gradient focusing and peptide nucleic acids. J Am Chem Soc 126:13474–13479
99. Kelly RT, Woolley AT (2005) Electric field gradient focusing. J Sep Sci 28:1985–1993
100. Ma B, Zhang G, Qin J et al (2009) Characterization of drug metabolites and cytotoxicity assay simultaneously using an integrated microfluidic device. Lab Chip 9:232–238
101. Wu HM, Sui G, Lee CC et al (2007) In vivo quantitation of glucose metabolism in mice using small-animal PET and a microfluidic device. J Nucl Med 48:837–845
102. Ro KW, Lim K, Kim H et al (2002) Poly(dimethylsiloxane) microchip for precolumn reaction and micellar electrokinetic chromatography of biogenic amines. Electrophoresis 23:1129–1137
103. Bromberg A, Mathies RA (2003) Homogeneous immunoassay for detection of TNT and its analogues on a microfabricated capillary electrophoresis chip. Anal Chem 75:1188–1195
104. Ye F, Liu J, Huang Y et al (2013) Competitive immunoassay of progesterone by microchip electrophoresis with chemiluminescence detection. J Chromatogr B 936:74–79
105. Kim AR, Kim JY, Choi K et al (2013) On-chip immunoassay of a cardiac biomarker in serum using a polyester-toner microchip. Talanta 109:20–25
106. Cheng SB, Skinner CD, Taylor J et al (2001) Development of a multichannel microfluidic analysis system employing affinity capillary electrophoresis for immunoassay. J Anal Chem 73:1472–1479
107. Li HF, Lin JM, Su RG et al (2004) A compactly integrated laser-induced fluorescence detector for microchip electrophoresis. Electrophoresis 25:1907–1915
108. Schulze P, Ludwig M, Kohler F et al (2005) Deep UV laser-induced fluorescence detection of unlabeled drugs and proteins in microchip electrophoresis. Anal Chem 77: 1325–1329
109. Johnson ME, Landers JP (2004) Fundamentals and practice for ultrasensitive laser-induced fluorescence detection in microanalytical systems. Electrophoresis 25: 3513–3527
110. Young KC, Lien HM, Lin CC et al (2002) Microchip and capillary electrophoresis for quantitative analysis of hepatitis C virus based on RT-competitive PCR. Talanta 56: 323–330
111. Huang Y, Zhao S, Shi M et al (2011) Competitive immunoassay of phenobarbital by microchip electrophoresis with laser induced fluorescence detection. Anal Chim Acta 694:162–166
112. Ma B, Zhou X, Wang G et al (2006) Integrated isotachophoretic preconcentration with zone electrophoresis separation on a quartz microchip for UV detection of flavonoids. Electrophoresis 27:4904–4909
113. Gustafsson O, Mogensen KB, Ohlsson PD et al (2008) An electrochromatography chip with integrated waveguide for UV absorbance detection. J Micromech Microeng 18:055021–055027
114. Lu Q, Copper CL, Collins GE (2006) Ultraviolet absorbance detection of colchicine and related alkaloids on a capillary electrophoresis microchip. Anal Chim Acta 572:205–211
115. Lee HL, Chen SC (2004) Microchip capillary electrophoresis with electrochemical detector for precolumn enzymatic analysis of glucose, creatinine, uric acid and ascorbic acid in urine and serum. Talanta 64:750–757
116. Wang J, Chatrathi MP, Collins GE (2007) Simultaneous microchip enzymatic measurements of blood lactate and glucose. Anal Chim Acta 585:11–16
117. Fanguy JC, Henry CS (2002) The analysis of uric acid in urine using microchip capillary electrophoresis with electrochemical detection. Electrophoresis 23:767–773
118. Alves Brito-Neto JG, Fracassi da Silva JA, Blanes L et al (2005) Understanding capacitively coupled contactless conductivity detection in capillary and microchip electrophoresis. Part 1. Fundamentals. Electroanalysis 17:1198–1206
119. Kubáň P, Hauser PC (2005) Application of an external contactless conductivity detector for the analysis of beverages by microchip capillary electrophoresis. Electrophoresis 26:3169–3178
120. Abad-Villar EM, Kubáň P, Hauser PC (2005) Determination of biochemical species on electrophoresis chips with an external contactless conductivity detector. Electrophoresis 26:3609–3614
121. Tachibana Y, Otsuka K, Terabe S et al (2004) Effects of the length and modification of the separation channel on microchip electrophoresis-mass spectrometry for analysis of bioactive compounds. J Chromatogr A 1025:287–296
122. Mechref Y (2011) Analysis of glycans derived from glycoconjugates by capillary electrophoresis-mass spectrometry. Electrophoresis 32: 3467–3481

123. Fritzsche S, Hoffmann P, Belder D (2010) Chip electrophoresis with mass spectrometric detection in record speed. Lab Chip 10: 1227–1230
124. Shinohara H, Suzuki T, Kitagawa F et al (2008) Polymer microchip integrated with nano-electrospray tip for electrophoresis-mass spectrometry. Sens Actuat B 132:368–373
125. Tachibana Y, Otsuka K, Terabe S et al (2003) Robust and simple interface for microchip electrophoresis-mass spectrometry. J Chromatogr A 1011:181–192
126. Kameoka J, Orth R, Ilic B et al (2002) An electrospray ionization source for integration with microfluidics. Anal Chem 74: 5897–5901
127. Trumbull JD, Glasgow IK, Beebe DJ et al (2000) Integrating microfabricated fluidic systems and NMR spectroscopy. IEEE Trans Biomed Eng 47:3–7

Part II

Microchip Capillary Electrophoresis of Small Molecules

Chapter 2

Microchip Electrophoresis for Fast and Interference-Free Determination of Trace Amounts of Glyphosate and Glufosinate Residues in Agricultural Products

Xuan Wei and Qiaosheng Pu

Abstract

Fast screening of herbicide residues is becoming important to ensure food safety, but traditional chromatographic methods may not be suitable for rapid on-site analysis of samples with complicated matrices. Here, we describe a method for rapid and sensitive determination of glyphosate (GLYP) and glufosinate (GLUF) residues in agricultural products by electrophoresis on disposable microchips with laser-induced fluorescence detection. With this method, quantitative analysis of trace amounts of GLYP and GLUF can be achieved with relatively simple sample preparation.

Key words Microchip electrophoresis, Glyphosate, Glufosinate, Laser-induced fluorescence, Agricultural products

1 Introduction

Glyphosate (GLYP) and glufosinate (GLUF) are widely used herbicides due to their excellent performance and low toxicity. However, excessive use of these compounds may cause high levels of residue in agricultural products and increase the possibility to be transferred into foods. Although they are considered as low toxic, there is some research indicating the potential threat [1]. Actually, regulations on the residual levels of these compounds have been established: the Environment Protection Agency (EPA) of USA sets the maximum residue level (MRL) of GLYP at 0.7 μg/mL in drinking water [2], while the Food and Agriculture Organization (FAO) regulates the upper limits of GLYP and GLUF as 0.1–5.0 mg/kg and 0.05 mg/kg in many crops [3]. Therefore, rapid, simple, and efficient analysis methods for these two compounds are highly necessary.

Ann Van Schepdael (ed.), *Microchip Capillary Electrophoresis Protocols*, Methods in Molecular Biology, vol. 1274,
DOI 10.1007/978-1-4939-2353-3_2,

Due to their unique structure, both GLYP and GLUF are devoid of chromophores and have poor volatility and good solubility in water. Analysis with the traditional techniques such as gas chromatography (GC), high-performance liquid chromatography (HPLC), and capillary electrophoresis (CE) frequently involves tedious sample preparation and derivatization [4–6].

Microchip electrophoresis (MCE) has the advantages of increased speed and reduced sample consumption [7–9]. With disposable plastic microchips, MCE can be a very efficient and economical technique for rapid analysis. Meanwhile, due to its excellent optical transparency and low autofluorescence [10], cyclic olefin copolymer (COC) has been widely used as a substrate of microchips for the analysis of both small molecules [11, 12] and macromolecules including proteins [13, 14] and nucleic acids [15]. Although surface treatment is frequently necessary for MCE with plastic microchips, we have proven that with the presence of water-soluble polymers acting as multifunctional additives, highly efficient separation could be achieved for samples with complicated matrices [16, 17].

Here, a fast, interference-free detection of GLYP and GLUF with MCE is described. After derivatization of these two herbicides with fluorescein isothiocyanate (FITC) at an elevated temperature in a short period of time, trace amounts of GLYP and GLUF could be separated quickly in borate buffer containing hydroxypropyl cellulose (HPC). Because of the negative charge on the fluorescein moiety of FITC and the suppressed electroosmotic flow (EOF) caused by HPC [18, 19], these analytes migrate anodically, ahead of the components of the sample matrices that may interfere with the analysis in other techniques, such as amino acids, small amino sugars, and proteins. Therefore, sample pretreatment can be simplified; it involves only water extraction and protein precipitation with acetonitrile. With the advantages of simple sample preparation, accelerated derivatization, rapid separation, and high sensitivity provided by the laser-induced fluorescence (LIF) detection, the proposed method can be a competent candidate for the rapid on-site screening of residues of GLYP and GLUF in agricultural products or foods. The detailed investigation and validation of the method have been reported elsewhere [20].

2 Materials

2.1 Solutions

1. Borax stock solution (100 mmol/L): weigh 9.572 g sodium tetraborate decahydrate and dissolve it in approximately 100 mL of distilled water in a glass beaker (*see* **Note 1**). Quantitatively transfer the solution to a 250 mL volumetric flask and adjust the liquid level to the mark with distilled water. Borax solutions of lower concentrations can be prepared by proper dilution of the stock solution with distilled water.

2. GLYP standard stock solution (1.69 mg/mL): accurately weigh 16.9 mg GLYP (*see* **Note 2**) and dissolve it in about 3 mL of distilled water. Quantitatively transfer the solution into a 10 mL volumetric flask and adjust the liquid level to the mark with distilled water.
3. GLUF standard stock solution (1.81 mg/mL): weigh 18.1 mg GLUF and prepare the solution following the same procedure as for GLYP.

   Both GLYP and GLUF stock solutions should be stored at 4 °C and re-prepared every 30 days.
4. Separation buffer: 10 mmol/L borax solution, 2 % HPC at pH 9.0. Add 10 g HPC to 500 mL 10 mmol/L borax solution in a glass beaker (*see* **Note 3**), stirring until all solids dissolve. Adjust the pH to 9.0 with 1.0 mol/L HCl. Filter the solution through a 0.45 μm membrane before use (*see* **Note 4**).
5. FITC solution: 20 mM fluorescein isothiocyanate, 1 % (v/v) pyridine, acetone. Dissolve 1.5 mg of FITC in 200 μL acetone containing 1 % (v/v) pyridine (*see* **Note 5**).
6. Sodium tetraborate buffer: 15 mmol/L sodium tetraborate, pH 9.2.

3 Methods

3.1 Sample Preparation

1. River water: filter the water sample through a 0.45 μm membrane and directly use the filtrate for the derivatization.
2. Soybean:
   (a) Grind the soybean into powder. Accurately weigh 2 g of grinded soybean powder and put it in a 10 mL polypropylene centrifuge tube containing 6.00 mL of distilled water, making sure all powder is soaked in water (*see* **Note 6**).
   (b) Sonicate the mixture for 5 min and then centrifuge at 390 × *g* for 3 min (*see* **Note 7**).
   (c) Take 1.00 mL of the supernatant to a 5 mL plastic microcentrifuge tube with an airtight lid, add 1.00 mL of acetonitrile, and vortex the tube for 1 min to precipitate proteins (*see* **Note 8**).
   (d) Close the lid and centrifuge the solution at 290 × *g* for 5 min. Use the supernatant for the derivatization.
3. Broccoli:
   (a) Accurately weigh 10 g of broccoli, homogenize it with 100 mL distilled water, and transfer the mixture to a 250 mL beaker.
   (b) Sonicate the mixture for 10 min, and vacuum filter through a Büchner funnel.

(c) Wash the precipitate twice with 30 mL distilled water each.

(d) Quantitatively transfer the filtrate into a 250 mL volumetric flask and adjust the liquid level to the mark with distilled water. Use this solution for the derivatization.

3.2 Derivatization Procedure

1. Mix 20.0 μL of FITC solution, 30.0 μL of sample solution (supernatant in the centrifuge tube for the soybean sample or the solution in the volumetric flask for the broccoli sample), and 100 μL of sodium tetraborate buffer in a 0.5 mL microcentrifuge tube wrapped with aluminum foil (*see* **Note 9**).
2. Vortex the mixture for 30 s.
3. Put the tube in a water bath at 55 °C for 20 min.
4. Filter the solution through a 0.45 μm membrane with a dry syringe filter head (*see* **Note 10**).

3.3 Microchip Electrophoresis

1. Check the microchip (*see* **Note 11**) under a microscope to make sure there are no visible particles in any of the channels (*see* **Note 12**).
2. Rinse the microchip channel with ethanol (filtered with a 0.45 μm membrane) for 1 min with the aid of a syringe connected to a reservoir of the microchip.
3. Mount the microchip onto the stage of the LIF detector (*see* **Note 13**); ensure all channels are filled with ethanol.
4. Remove the ethanol from the *Buffer* reservoir (*see* Fig. 1 for the reservoir definition) and quickly fill this reservoir with 100 μL of separation buffer.
5. Fill the reservoirs *Sample* and *Sample Waste* exactly as described in **step 4**.
6. Apply a vacuum using a syringe or an air pump at the *Buffer Waste* reservoir to fill all channels with the separation buffer (*see* **Note 14**).
7. Replace all reservoirs with 100 μL separation buffer.
8. Insert platinum electrodes to each reservoir and set the voltage for the *Buffer Waste* to 0 V and the other three reservoirs to 500 V (*see* **Note 15**). Sequentially switch on the voltage

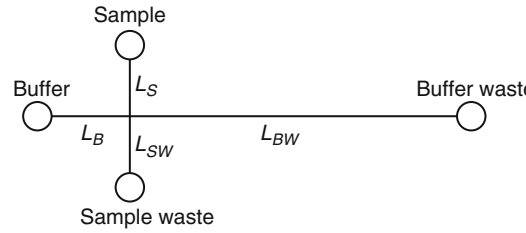

Fig. 1 Schematic diagram of microchannels on a disposable microchip

between the three reservoirs and the *Buffer Waste* reservoir, check the currents, and make sure the currents are stable. If no current or unstable currents are observed, repeat steps 1–7 (*see* **Note 16**).

9. Replace the *Sample* reservoir with standard or sample solutions (100 μL).
10. Perform the pinched injection and separation following the voltage program listed in Table 1 (*see* **Note 17**). A typical electropherogram is shown in Fig. 2. Normally 3–5 cycles of injection–separation should be performed for each standard or sample (*see* **Note 18**).

Table 1
Voltage program for microchip-based electrophoresis

Phase	Voltage at each reservoir (V)[a]			
	Sample	Sample waste	Buffer	Buffer waste
Injection	0 (−250)[b]	$250L_S+290L_{SW}$ (290)	$250L_S-20L_B$ (−20)	$250L_S-20L_{BW}$ (−20)
Separation	$550L_B+125L_S$ (125)	$550L_B+125L_{SW}$ (125)	0 (−550)	$550L_B+300L_{BW}$ (300)

[a]L_S, L_{SW}, L_B, and L_{BW} are distances (in cm) from the cross point to the *Sample*, *Sample Waste*, *Buffer*, and *Buffer Waste* reservoirs (to the inner edges of the drilled holes), respectively. *See* Fig. 1 for the position of reservoirs
[b]Electric field strength (V/cm) in the microchannel connected to the reservoir

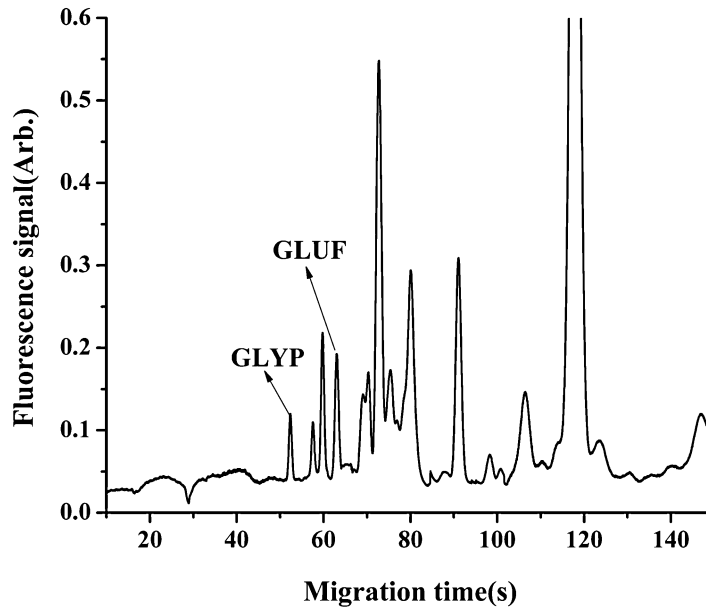

Fig. 2 Electropherogram of a soybean sample spiked with 0.100 μg/g of GLYP and 0.100 μg/g of GLUF. The effective separation length, 3.5 cm

11. Prepare the calibration curves of peak areas of both GLYP and GLUF vs. concentrations, and calculate the concentration of analytes in the derivatized sample solutions with the regression equations of the calibration curves.
12. Calculate the contents of GLYP and GLUF in the original samples through correction of the dilution in the sample preparation and derivatization process.

4 Notes

1. To accelerate dissolution, an ultrasonic bath or elevated temperature may be used. Wait until the solution has cooled to room temperature before transferring the solution into the volumetric flask.
2. GLYP and GLUF may absorb moisture, so they should be stored in airtight vessels.
3. Vigorous stirring is normally necessary to dissolve HPC.
4. Avoid using vacuum filtration, since large numbers of bubbles may be produced. Syringe filtration is recommended.
5. This solution should be freshly prepared. Pyridine is toxic; handle it in a hood or a well-ventilated space.
6. 10 g of sample may be used to avoid inhomogeneity of the sample, with proportional increase of the volume of water and extraction time in the following two steps.
7. The supernatant may be turbid. Longer centrifugation times may be necessary for larger volumes of filtrate.
8. This step can be skipped if the supernatant from the former step is clear.
9. The tube should be wrapped with aluminum foil to avoid light-induced degradation of FITC and its derivatives.
10. Dilution with separation buffer may be necessary for herbicide standards.
11. Commercial plastic microchips made of COC or other materials may be used. Disposable COC microchips can be fabricated by the following procedure:
    (a) COC annealing:
    Cut the original COC plate (Topas 8007, 1.0 mm thick) into small pieces with a size of 6×2 cm. Sandwich each COC piece between two microscope slides (2.5 cm wide, 7.5 cm long, and 2.0 mm thick) and clamp them with six small binder clips (19 mm) along two long sides of the microscope slides. Each microchip needs two pieces of COC; prepare two of such assemblies according to the number of microchips needed. Put the assemblies in an

oven at 150 °C for 30 min. After that, take the assemblies out of the oven and let them cool down naturally. When they have cooled down to room temperature, remove the binder clips and take the COC pieces out.

(b) Wire embossing:
For embossing each COC slide, stretch two copper wires (diameter of 80 μm) on a clean microscope slide, to form the necessary cross pattern of the microchannels (*see* Fig. 1). Fix the ends of the wires at the backside of the microscope slide with Scotch tape to ensure the wires are straight. Put a piece of annealed COC on the top of the patterned copper wires and cover the COC with another microscope slide. Clamp the slide assembly with six small binder clips in the same way as for COC annealing. Prepare such assemblies as many as needed. Put the assemblies into an oven at 140 °C for 25 min to embed the wires into the COC slides. Take them out of the oven and let them cool down naturally. Detach the COC pieces together with embedded copper wires from the microscope slides.

(c) Wire etching and hole drilling:
Put the COC pieces with copper wires into a bath of concentrated HNO_3 in a hood for 15 min to etch copper wires away (*Caution*: Concentrated HNO_3 is very corrosive and may give off toxic fume. Wear goggles and gloves and handle it in a well-ventilated hood). Rinse the COC pieces thoroughly with water. Drill four holes (3 mm) at the appropriate positions (*see* Fig. 1).

(d) Thermal bonding:
Check the COC pieces with embossed microchannels and drilled holes under a stereomicroscope, and remove any debris at the ends of microchannels with a needle. Clean the slides with ethanol in an ultrasonic bath for 5 min. Cover the microchannel COC piece with another piece of clean annealed COC. Sandwich them between two microscope slides with six binder clips, as for annealing and wire embossing. Put it in an oven at 120 °C for 10 min to thermally bond the microchip.

(e) Reservoir adhesion:
Glue four pieces of plastic tubes (i.d. ~6 mm, height of ~10 mm) as the reservoirs using COC dissolved in toluene. Seal the chip edge with dissolved COC too and let them dry in a hood. Store the prepared microchips in sealed vessels to avoid contamination.

12. Small particles can be flushed away with ethanol.
13. Any fluorescence detector that matches the excitation and emission of FITC derivatives may be used for the detection.

An economical LIF detector can be assembled in an epifluorescence format with the following parts (*see* Fig. 1A of ref. 20). All parts may be replaced with equivalents from other vendors: an MBL-III-473 diode-pumped solid-state blue laser (473 nm, Changchun New Industries Optoelectronics Tech Co., Ltd., Changchun, China), a filter set including a dichroic mirror (505 nm) and a long-pass filter (520 nm) (both from Shenyang HB Optical Technology Co., Ltd., Shenyang, China), a microscope objective (20×, Beijing 7-Star Optical Instruments Co., Ltd., Beijing, China), and a photomultiplier tube (PMT) (CR105-01, Beijing Hamamatsu Photon Techniques Inc. Co., Ltd.).

14. Fully draining the reservoir may produce air bubbles inside the microchannels; do not fully drain any of the reservoirs in this step.
15. Any multichannel high-voltage power supply may be used. The power supply can be assembled with four DC–DC modules (DWP303-1 AC, Dongwen High-Voltage Power Supply, Tianjin, China, or similar modules from other venders may be used). The module can produce an output of 0–3,000 V DC with 0–5 V control signal. Connect four digital-to-analog channels of one or two data acquisition cards (e.g., two USB-6008, National Instruments, Austin, TX, USA) to the DC–DC modules. Use a computer program to control the output of the modules in order to perform the *Injection* and *Separation* steps of microchip electrophoresis.
16. The microchip should be replaced if occurring current problems cannot be solved after repeating **steps 1–7**.
17. Considering the possible variation of the lengths of the microchannels from the reservoirs to the cross point, equations are given in Table 1 instead of voltage values.
18. To ensure good repeatability, separation buffer should be replaced every 6–8 injection–separation cycles.

Acknowledgment

This work is supported by the Natural Science Foundation of China (No. 21175062).

References

1. George J, Prasad S, Mahmood Z et al (2010) Studies on glyphosate-induced carcinogenicity in mouse skin: a proteomic approach. J Proteomics 73:951–964
2. US Environmental Protection Agency (EPA) (2003) National primary drinking water regulations. http://www.epa.gov/safewater/consumer/pdf/mcl.pdf. Accessed 21 Dec 2014
3. Food and Agriculture Organization (FAO) and World Health Organization (WHO) (2006) Joint FAO/WHO food standards programme. http://www.codexalimentarius.net/download/report/655/al29_24e.pdf. Accessed 21 Dec 2014
4. Tseng S-H, Lo Y-W, Chang P-C et al (2004) Simultaneous quantification of glyphosate,

glufosinate, and their major metabolites in rice and soybean sprouts by gas chromatography with pulsed flame photometric detector. J Agric Food Chem 52:4057–4063

5. Khrolenko MV, Wieczorek PP (2005) Determination of glyphosate and its metabolite aminomethylphosphonic acid in fruit juices using supported-liquid membrane preconcentration method with high-performance liquid chromatography and UV detection after derivatization with *p*-toluenesulphonyl chloride. J Chromatogr A 1093:111–117
6. Corbera M, Hidalgo M, Salvadó V et al (2005) Determination of glyphosate and aminomethylphosphonic acid in natural water using the capillary electrophoresis combined with enrichment step. Anal Chim Acta 540:3–7
7. Yang W, Sun X, Wang H-Y et al (2009) Integrated microfluidic device for serum biomarker quantitation using either standard addition or a calibration curve. Anal Chem 81:8230–8235
8. Dittrich PS, Tachikawa K, Manz A (2006) Micro total analysis systems. Latest advancements and trends. Anal Chem 78:3887
9. Wang H, Chen J, Zhu L et al (2006) Continuous flow thermal cycler microchip for DNA cycle sequencing. Anal Chem 78:6223–6231
10. Nunes PS, Ohlsson PD, Ordeig O et al (2010) Cyclic olefin polymers: emerging materials for lab-on-a-chip applications. Microfluid Nanofluid 9:145–161
11. Park J, Lee D, Kim W et al (2007) Fully packed capillary electrochromatographic microchip with self-assembly colloidal silica beads. Anal Chem 79:3214–3219
12. Faure K, Albert M, Dugas V et al (2008) Development of an acrylate monolith in a cyclo-olefin copolymer microfluidic device for chip electrochromatography separation. Electrophoresis 29:4948–4955
13. Zhang J, Das C, Fan ZH (2008) Dynamic coating for protein separation in cyclic olefin copolymer microfluidic devices. Microfluid Nanofluid 5:327–335
14. Luna-Vera F, Ferguson JD, Alvarez JC (2011) Real time detection of lysozyme by pulsed streaming potentials using polyclonal antibodies immobilized on a renewable nonfouling surface inside plastic microfluidic channels. Anal Chem 83:2012–2019
15. Lin R, Burns MA (2005) Surface-modified polyolefin microfluidic devices for liquid handling. J Micromech Microeng 15:2156
16. Li R, Wang L, Gao X et al (2013) Rapid separation and sensitive determination of banned aromatic amines with plastic microchip electrophoresis. J Hazard Mater 248–249: 268–275
17. Wang L, Wu J, Wang Q et al (2012) Rapid and sensitive determination of sulfonamide residues in milk and chicken muscle by microfluidic chip electrophoresis. J Agric Food Chem 60:1613–1618
18. Kelly RT, Pan T, Woolley AT (2005) Phase-changing sacrificial materials for solvent bonding of high-performance polymeric capillary electrophoresis microchips. Anal Chem 77: 3536–3541
19. Das C, Zhang J, Denslow ND et al (2007) Integration of isoelectric focusing with multichannel gel electrophoresis by using microfluidic pseudo-valves. Lab Chip 7:1806–1812
20. Wei X, Gao X, Zhao L et al (2013) Fast and interference-free determination of glyphosate and glufosinate residues through electrophoresis in disposable microfluidic chips. J Chromatogr A 1281:148–154

Chapter 3

Microchip Capillary Electrophoresis of Nitrite and Nitrate in Cerebrospinal Fluid

Marián Masár, Róbert Bodor, and Peter Troška

Abstract

Microchip capillary electrophoresis (MCE) is a relatively new analytical method requiring only small sample amounts, which is very favorable for the analysis of volume-limited biofluids. The practical use of MCE in bioanalysis is still restricted in terms of requirements for simplifying and/or concentrating sample pretreatment techniques. Here, we describe an MCE method for trace analysis of nitrite and nitrate, indicators of various neurological diseases, in cerebrospinal fluid (CSF). The complex CSF samples were simplified by solid-phase microextraction prior to an online combination of isotachophoresis with capillary zone electrophoresis performed on a microchip with coupled channels and a high-volume sample injection channel (9.9 μL). The method is suitable for rapid (total analysis time lasted 20 min), reproducible (0.6–2.4 % RSD for migration time), and sensitive (3–9 nM limits of detection) determinations of nitrite and nitrate in 15–50 times diluted CSF samples.

Key words Nitrite and nitrate, Cerebrospinal fluid, Microchip capillary electrophoresis, Microchip with coupled channels, Isotachophoresis, Capillary zone electrophoresis, Contact conductivity detection, Solid-phase microextraction

1 Introduction

Nitrite and nitrate represent the major oxidation products of nitric oxide (NO), an important cell signaling molecule and biological mediator in various physiological functions [1]. Considering the relatively short half-life of NO in biofluids [2], nitrite and nitrate are to be used as indicators of its formation [3]. An excess production of NO is associated with various diseases, e.g., cluster headache [4], multiple sclerosis [5], bacterial meningitis [6], or Parkinson's disease [7]. Hence the determination of nitrite and nitrate in cerebrospinal fluid (CSF) is useful for monitoring of the NO generation within the central nervous system and for early diagnosis of such neurological diseases.

Ann Van Schepdael (ed.), *Microchip Capillary Electrophoresis Protocols*, Methods in Molecular Biology, vol. 1274,
DOI 10.1007/978-1-4939-2353-3_3,

Although different separation methods based on chromatography and capillary electrophoresis (CE) have been developed for the determination of nitrite and nitrate in various biofluids, an appropriate sample pretreatment technique eliminating interferences of complex biomatrices has to be used to achieve adequate concentration limits. Microchip capillary electrophoresis (MCE), which is considered as a miniaturized version of CE, has benefits in terms of high speed, high separation efficiency in small channels, high throughput, reduced consumption of solvents and toxic waste, easy automation, and low running costs [8]. On the other hand, the use of MCE in the analysis of complex biosamples is limited, mainly due to the problems resulting from downscaling [9].

Short separation channels on the microchip require the injection of relatively simplified samples; otherwise, separation capacity could be critical. In the same way, reduced i.d. of the microchip channels puts heavy demands on sensitive detection techniques [8]. Detectability of the analyte in capillary zone electrophoresis (CZE), the most widely used (M)CE technique, can be enhanced by increasing the sample pulse length. The high sample injection volume requires a suitable concentration technique prior to the CZE separation; otherwise, the injection dispersion contributes significantly to the total peak dispersion [10]. A loss of the resolution of the analyte, e.g., due to electromigration dispersion of the matrix constituent, is another factor that may prevent an increase of the sample injection volume.

In biofluids, the analytes of interest are often present at low concentrations, while potential interfering constituents are the major components. For example, only (sub-) μM concentrations of nitrite and nitrate are observed in CSF, while chloride, which is a typical macroconstituent, is present at 100,000 times higher concentration. Only a few papers have been published on the MCE separation and determination of nitrite and nitrate in various biofluids, e.g., in blood plasma [11], blood serum [12, 13], saliva [12], and CSF [14]. Considering the limiting factors of MCE mentioned above, its use for bioanalysis is limited without simplifying the sample and/or concentrating the analytes by a pretreatment technique.

Isotachophoresis (ITP) is a highly efficient concentration technique [15]. In a single channel microchip, ITP itself cannot solve the problem with interference of chloride present in the sample at high concentration. ITP-CZE employed on a microchip with coupled channels provides concentration and, at the same time, effective sample cleanup by electrophoretically removing chloride in the first separation channel [10]. On the other hand, a very high concentration of chloride often results in an incomplete resolution of analytes in ITP due to its limited separation capacity, and a negative bias into the CZE determination is introduced [16]. The use of a suitable pretreatment technique prior to the ITP-CZE analysis

is therefore necessary. Micro-solid-phase extraction (mSPE) based on silver-form resin that specifically retains chloride [17] is a good alternative in this respect.

The present text describes an MCE method for the determination of trace concentrations of nitrite and nitrate in CSF [14]. A large volume (9.9 μL) of mSPE-treated CSF sample was injected on the microchip with coupled channels. Online ITP-CZE separations were monitored by contact conductivity detectors. MSPE using sulfonated polystyrene-divinylbenzene cation-exchange resin in a silver form significantly reduced the concentration of chloride in the sample. The mSPE-ITP-CZE method is reproducible (0.6–2.4 % RSD for migration time) and sensitive (3–9 nM limits of detection). The time of analysis including both pretreatment steps does not exceed 20 min.

2 Materials

2.1 Instruments and Components

1. MCE analyzer with the electrolyte (*see* **Note 1**) and electronic units (*see* **Note 2**), a computerized MCE system.
2. IonChip™ 3.0 poly(methyl methacrylate) microchip with coupled channels (Merck, Darmstadt, Germany) and integrated conductivity sensors (*see* Fig. 1). For production details, *see* ref. 18.
3. MicroITP, ver. 2.4, data acquisition and analysis software (Merck) for Microsoft Windows XP/7. The software is used to control the MCE electronic unit and to perform data acquisition and analysis. A data acquisition rate of 25 points per second is used.
4. pH meter with combined glass electrode (*see* **Note 3**).
5. Test tube shaker for sample homogenization.
6. Ultrasonic bath for degassing the electrolyte solutions.
7. Small laboratory centrifuge (10,000 rpm; 5,600 rcf).
8. SPE microcolumn with 0.5 mL sulfonated polystyrene-divinylbenzene cation-exchange resin in a silver form (Alltech, Grace Davison Discovery Sciences, Deerfield, USA).
9. 0.5 mL Spin-X® centrifuge tube filter (Corning, Amsterdam, the Netherlands) with 0.45 μm cellulose acetate membrane.
10. 10 mL syringe PP/PE without needle, Luer tip.
11. Digital burette with 0.01 mL resolution.
12. Disposable syringe membrane filters of 0.8 μm pore size.
13. Single channel mechanical pipettes with a variable volume (1–10, 10–100, 100–1,000 μL) and adequate tips.

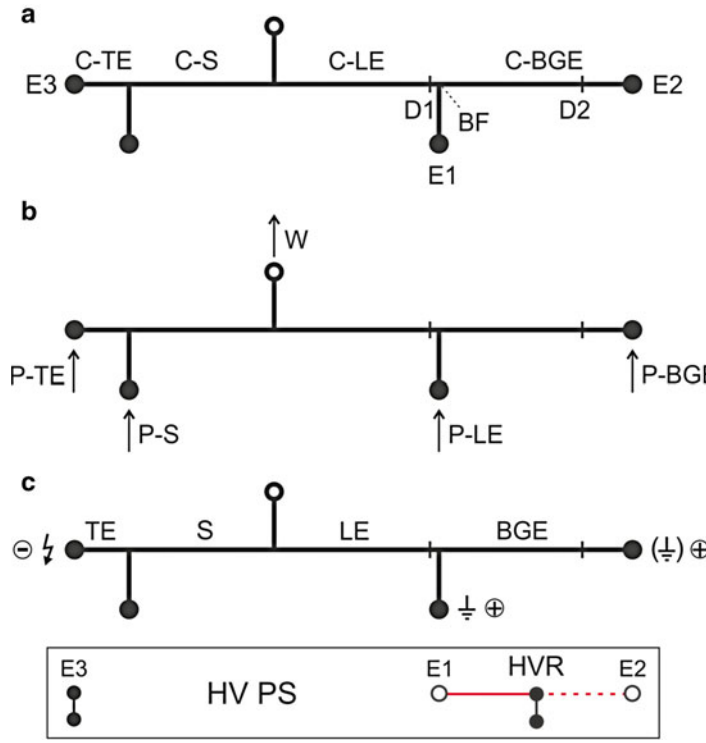

Fig. 1 A scheme of the microchip for the ITP-CZE separations. (**a**) Arrangement of the channels and the contact conductivity detection sensors on the microchip. (**b**) Inlets to the microchip channels for filling the background (BGE), leading (LE) and terminating electrolyte (TE), and sample (S) solutions using peristaltic micropumps (P-BGE, P-LE, P-TE, P-S) and the outlet (W) from all channels. (**c**) Initial configuration of the electrolyte and sample solutions in the ITP-CZE run. C-TE, TE channel (0.8 μL); C-S, sample injection channel (9.9 μL); C-LE, the first (LE) separation channel (4.5 μL, 59 mm separation path) with Pt conductivity sensor (D1); C-BGE, the second (BGE) separation channel (4.3 μL, 56 mm separation path) with Pt conductivity sensor (D2); E1, E2, driving electrodes for the first and the second separation channels, respectively; E3, the driving electrode connected to a high-voltage pole of high-voltage power supply (HVPS); HVR, a high-voltage relay switching the direction of the driving current between E3–E1 or E3–E2; BF, bifurcation section of the coupled channels

2.2 Reagents and Stock Solutions

Prepare all the solutions using fresh ultrapure water (UPW) with resistivity 18 MΩ.cm at 25 °C and analytical grade reagents.

1. A stock solution of 100 mM HCl for preparation of the leading electrolyte (LE): Use potentiometric titration with NaOH for determination of the HCl concentration purified by isothermal distillation (ca. 7 M). Calculate the volume of purified HCl needed for preparation of 500 mL stock solution. Prepare the solution and determine the concentration. When the concentration is different from 100 mM, adjust the concentration by UPW or by concentrated purified HCl. Determine again

the concentration and repeat adjusting until a 100 ± 1 mM value is obtained in three repeated runs. Fill the bottle of the digital burette (*see* **item 11** of Subheading 2.1) with the solution and store at room temperature.

2. A stock solution of 1 M formic acid for preparation of the terminating electrolyte (TE): Pipette 381 µL of concentrated formic acid (99 %, 1.22 g/mL, 26.2 M) into a 10 mL volumetric flask filled with ca. 5 mL of UPW. Dilute with UPW to a volume of 10 mL, mix well, and store in a closed bottle at 4 °C.
3. A stock solution of 1 M acetic acid for preparation of the background electrolyte (BGE): Pipette 578 µL of concentrated acetic acid (99 %, 1.05 g/mL, 17.3 M) into a 10 mL volumetric flask filled with ca. 5 mL of UPW. Dilute with UPW to a volume of 10 mL, mix well, and store in a closed bottle at 4 °C.
4. A stock solution of 1 % electroosmotic flow suppressor solution (methyl hydroxyethyl cellulose 30,000, MHEC): Add 2 g of MHEC into a 250 mL glass beaker filled with 200 mL of UPW and stir with a magnetic stirrer until dissolved. Store the solution in a closed bottle at 4 °C.
5. A stock solution of 10 mg/L nitrite for calibration: Pipette 250 µL of 1,000 mg/L nitrite solution (CertiPUR®, Merck Millipore) into a 25 mL volumetric flask and add UPW to reach the level of the etched line. Mix well (alternatively homogenize in ultrasonic bath) and store at 4 °C. The stock solution can be stored for a month.
6. A stock solution of 10 mg/L nitrate stock solution for calibration: Pipette 250 µL of 1,000 mg/L nitrate solution (CertiPUR®, Merck Millipore) into a 25 mL volumetric flask and add UPW to reach the level of the etched line. Mix well (alternatively homogenize in ultrasonic bath) and store at 4 °C. The stock solution can be stored for a month.
7. A stock solution of 1 % detergent for microchip maintenance: Pipette 0.5 mL of Extran® MA 02 (Merck Millipore) into a 50 mL volumetric flask and add UPW to reach the level of the etched line. Mix well and store at 4 °C. The stock solution can be stored for 3 months.

3 Methods

3.1 Preparation of ITP-CZE Electrolyte Solutions (See Note 4)

1. LE: Dispense 5.00 mL of HCl (*see* **item 1** of Subheading 2.2) from a digital burette into a 50 mL volumetric flask filled with ca. 20 mL of UPW. Add 98.0 mg β-alanine (BALA) (*see* **Note 5**), 5 mL of 1 % MHEC (*see* **item 4** of Subheading 2.2 and **Note 6**), and dilute to a volume of 50 mL. Homogenize and degas the solution in an ultrasonic bath, and measure the pH (3.6 ± 0.05) (*see* **Note 7**).

2. TE: Pipette 500 µL of formic acid (*see* **item 2** of Subheading 2.2) into a 50 mL volumetric flask filled with ca. 20 mL of UPW. Add 89.1 mg BALA (*see* **Note 5**), 5 mL of 1 % MHEC (*see* **item 4** of Subheading 2.2 and **Note 6**), and dilute to a volume of 50 mL. Homogenize and degas the solution in an ultrasonic bath, and measure the pH (3.9 ± 0.05) (*see* **Note 7**).
3. BGE: Pipette 500 µL of acetic acid (*see* **item 3** of Subheading 2.2) into a 50 mL volumetric flask filled with ca. 20 mL of UPW. Add 10.7 mg BALA (*see* **Note 5**), 3.356 g DDAPS (*see* **Note 8**), 5 mL of 1 % MHEC (*see* **item 4** of Subheading 2.2 and **Note 6**), and dilute to a volume of 50 mL. Homogenize and degas the solution in an ultrasonic bath, and measure the pH (3.8 ± 0.05) (*see* **Note 7**).

3.2 Preparation of Calibration Solutions

1. Fill 2 mL microcentrifuge tube with stock solution of 10 mg/L nitrite (*see* **item 5** of Subheading 2.2).
2. Fill 2 mL microcentrifuge tube with stock solution of 10 mg/L nitrate (*see* **item 6** of Subheading 2.2).
3. Prepare 1 mL of mixed standard solution (MSS) by pipetting 10 µL of nitrite and 20 µL of nitrate stock solutions (*see* **steps 1** and **2**) into 2 mL microcentrifuge tube and add 970 µL of UPW. Mix well and 1 day process only.
4. Prepare calibration solutions of nitrite (1, 2.5, 5, 10, 25 µg/L) and nitrate (2, 5, 10, 20, 50 µg/L) from the MSS (*see* **step 3**) and TE (*see* **step 2** of Subheading 3.1):
   (a) 1 µg/L nitrite and 2 µg/L nitrate calibration solution: Pipette 10 µL of MSS, 750 µL of TE, and 240 µL of UPW into a 2 mL microcentrifuge tube.
   (b) 2.5 µg/L nitrite and 5 µg/L nitrate calibration solution: Pipette 25 µL of MSS, 750 µL of TE, and 225 µL of UPW into a 2 mL microcentrifuge tube.
   (c) 5 µg/L nitrite and 10 µg/L nitrate calibration solution: Pipette 50 µL of MSS, 750 µL of TE, and 200 µL of UPW into a 2 mL microcentrifuge tube.
   (d) 10 µg/L nitrite and 20 µg/L nitrate calibration solution: Pipette 100 µL of MSS, 750 µL of TE, and 150 µL of UPW into a 2 mL microcentrifuge tube.
   (e) 25 µg/L nitrite and 50 µg/L nitrate calibration solution: Pipette 250 µL of MSS and 750 µL of TE into a 2 mL microcentrifuge tube.

3.3 MSPE Pretreatment of CSF Samples

1. Attach a 10 mL syringe filled with UPW to the SPE microcolumn (*see* **item 8** of Subheading 2.1) and pass the UPW through the device. Repeat the rinsing procedure three times and remove the UPW from the device (with air purge).

2. Open the device using pliers and collect resin (ca. 450 mg) into a 1.5 mL microcentrifuge tube. Cover the microcentrifuge tube with aluminum foil and store at 4 °C for a max of 5 days.
3. Weigh 150 mg of wet resin into a 1.5 mL microcentrifuge tube; add 200 μL TE solution (*see* **step 2** of Subheading 3.1) and 50 μL CSF sample (*see* **Note 9**). Shake for 2 min using test tube shaker.
4. Transfer the mixture quantitatively to the centrifuge tube filter (*see* **item 9** of Subheading 2.1) inserted in a 2 mL microcentrifuge tube. Carry out the filtration in a microcentrifuge (*see* **item 7** of Subheading 2.1) at 10,000 rpm (5,600 rcf) for 2 min.
5. Dilute the filtrate with TE solution (*see* **step 2** of Subheading 3.1) prior to ITP-CZE analysis. The total dilution factor should be 15–50, depending on the analyte concentration in the CSF sample. Dilution of CSF in **step 3** (five times) should be taken into account.

3.4 ITP-CZE Running Protocol

The procedure to perform ITP-CZE separations on the microchip is summarized in Table 1.

1. Fill four vials with UPW and insert the inlet capillaries connected to the peristaltic micropumps into the vials.
2. Wash the microchip channels using the peristaltic micropumps controlled by MicroITP software (*see* Procedure 1 of Table 1). This cleaning procedure should be applied prior to the first run of the day.
3. Filter the electrolyte solutions (*see* Subheading 3.1) using disposable syringe filters (*see* **item 12** of Subheading 2.1) into the vials (*see* **Note 10**).

Table 1
Microchip procedures

	Inlet vial					
Procedure	**BGE**	**LE**	**TE**	**Sample**	**Time (s)**	**Note**
1. Wash	UPW	UPW	UPW	UPW	300	
2. Fill	BGE	LE	TE	S	150	*See* Table 2
3. Separation	BGE[a]	LE[a]	TE[a]	S[a]	600	*See* Table 3
4. Wash	BGE[a]	LE[a]	TE[a]	UPW	25	
5. Clean	DET	DET	DET	DET	300	
6. Wash	UPW	UPW	UPW	UPW	600	

[a]Peristaltic micropumps turned off
UPW ultrapure water, *DET* detergent. For other abbreviations, *see* Fig. 1

4. Replace the UPW vials at the inlet capillaries with the vials containing electrolytes and sample solutions (TE used in a blank run, calibration solution, CSF treated by mSPE).
5. Enter the "Filling method" in MicroITP software (*see* Table 2).
6. Enter the "Running method" in MicroITP software (*see* Table 3).
7. Set the number of repetitions you need to perform in MicroITP software and start the run (*see* **Note 11**).
8. Replace the sample vial with UPW vial and wash the sample channel (*see* Procedure 4 of Table 1). This procedure should be used between each sample.
9. Replace the UPW vial with the next sample vial and repeat the procedure from **step 7**.
10. Clean and wash the microchip channels (*see* Procedures 5 and 6 of Table 1) after the last run of the day.

Table 2
Filling method

Step	Pump turned on	Time (s)	Rpm
1	P-BGE, P-LE, P-TE, P-S	25	20
2	P-BGE, P-LE, P-TE	10	10
3	P-BGE	20	5
4	P-LE	20	5
5	P-TE	20	5
6	P-S	25	5

Each step was followed by 5 s relaxation time (pumps turned off) for complete standstill of hydrodynamic flow
Rpm rotations per minute. For other abbreviations, *see* Fig. 1

Table 3
Running method

Step	Time (s)	Current (μA)	Reference level (mV)	Current direction	Data acquisition
1	500	20	50	E3 → E1	–
2	10	20	–	E3 → E1	D1
3	150	20	–	E3 → E2	D2

Reference level is the value of the resistance at which the zone boundary is to be "recognized" and the next step of the method starts automatically (*see* Fig 2a). For abbreviations, *see* Fig. 1

3.5 Data Analysis

1. Evaluation of electropherogram of a blank sample: Measure the areas under the peaks in the migration position of nitrite and nitrate. The positions of the peaks should be clear according to Fig. 2b or identify the peaks by overlapping the electropherograms of blank and calibration samples (*see* **Note 12**).
2. Evaluation of electropherogram of a calibration sample: Measure the areas under the nitrite and nitrate peaks. Subtract the peak areas measured in the blank sample.
3. Construct the calibration curves from corrected peak areas of nitrite and nitrate. Use concentration on X and corrected peak area on Y axis, respectively. Calculate slope, intercept, and correlation coefficient.

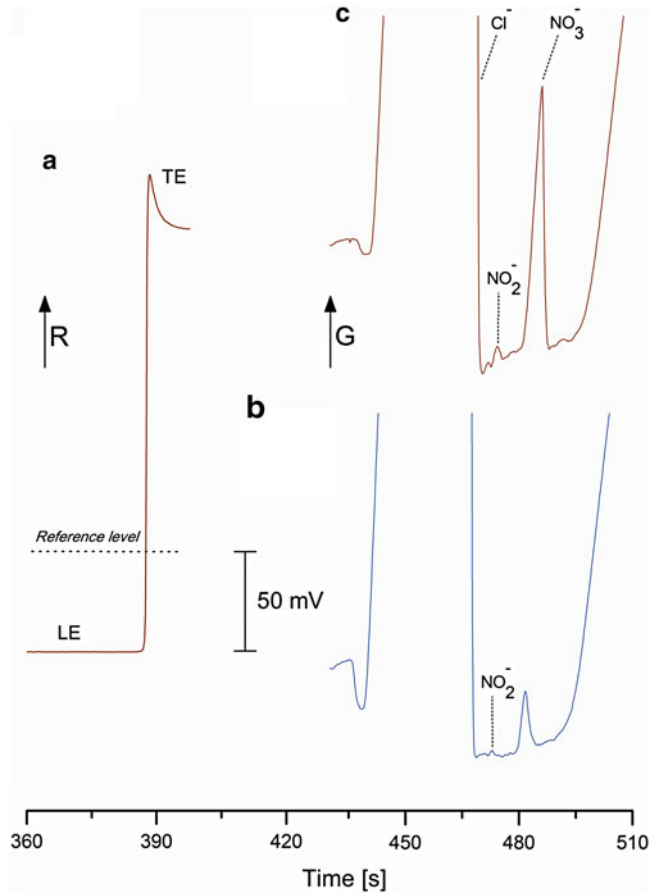

Fig. 2 MSPE-ITP-CZE analysis of CSF sample with identified nitrite and nitrate on the microchip. (**a**) ITP and (**b**), (**c**) CZE stages of the separation. Injected sample: (**a**, **c**), 50 times diluted CSF sample, and (**b**), TE (a blank run). For experimental conditions, *see* Subheading 3.4. For sample pretreatment, *see* Subheading 3.3. *R* resistance, *G* conductivity

4. Evaluation of electropherogram of a CSF sample: A typical electropherogram from ITP-CZE separation is shown in Fig. 2c. Identify the nitrite and nitrate peaks by overlapping the electropherograms of CSF and calibration samples, when the position is not clear (*see* **Note 12**). Measure the areas under the peaks of nitrite and nitrate and subtract the peak areas measured in the blank sample. Calculate the concentration of nitrite and nitrate in the CSF sample using the calibration curves (*see* **step 3**). The total sample dilution factor should be taken into account in the calculation (*see* **step 5** of Subheading 3.3).

4 Notes

1. An electrolyte unit consists of microchip holder, four peristaltic micropumps, and three membrane driving electrodes (E1-E3). Mutual connections of these devices and their connections to the inlets of the microchip channels are made by plastic capillaries of 500 μm i.d. The micropump rollers automatically close the corresponding inlet to the microchip channel when the solution pumping is stopped. The excess of the solutions pumped through the microchip channels in the preparation of the run is trapped into a waste container connected to a permanently opened outlet of the microchip. The membrane driving electrodes are used to eliminate disturbances due to the bubble formation during the separation [10].
2. The high-voltage power supply (max 50 μA and 7 kV) of the electronic unit delivers the driving voltage of a required polarity to the electrodes (E1–E3) placed between the inlets of the corresponding microchip channels and the micropumps. Here, the driving electrode E3 is permanently connected to the high-voltage pole (negative) of the power supply, while the driving electrodes E1 and E2 (the counter electrodes for the separation channels) are connected to its positive pole via a high-voltage relay. Such connections of the electrodes allow to transport the separated constituents either to the electrode E1 or E2. The electronic unit includes the measuring electronics of the AC contact conductivity detectors. The measuring electronics is galvanically decoupled from the platinum conductivity sensors on the microchip by transformers [19]. The electronic unit also drives the peristaltic pumps in the preparation of the run and interfaces the MCE analyzer to a PC.
3. A two-point calibration of pH meter should be used (pH 4 and 7).
4. The electrolyte solutions can be stored at 4 °C for a week. Filter the solutions by disposable syringe nylon membrane filter of 0.8 μm pore size before use.

5. Use β-alanine of highest purity (≥99 %) with a content of chloride and sulfate ≤50 mg/kg.
6. A graduated plastic syringe should be used to measure the volume of viscous solution.
7. Use only a small volume (10 mL) of electrolyte for pH measurement. Do not pour back the used electrolyte into the original stock.
8. Zwitterionic surfactant (3-(*N*,*N*-dimethyldodecylammonio) propanesulfonate, DDAPS) should be purified on a C8 column with particle size of 25–40 μm using UPW and methanol.
9. Collection of CSF should only be performed by experienced personnel under aseptic conditions. CSF samples can be stored frozen (≤−60.0 °C) indefinitely. Prior to analysis, melt the samples at laboratory temperature and homogenize using test tube shaker. Use gloves when working with CSF sample.
10. Discard the first part of the filtrate (ca. 0.5 mL). One vial (20 mL) filled with the electrolyte solution should be used for ca. 20 runs.
11. The ITP-CZE runs are performed with the same sample (*see* Procedures 2 and 3 of Table 1).
12. When the peak identification is performed by overlapping the electropherograms, you should shift them in order to match the rear part of the chloride zone in the same position.

Acknowledgments

This work was supported by the Slovak Grant Agency for Science (VEGA 1/1149/12) and by the Slovak Research and Development Agency (APVV-0259-12). Cerebrospinal fluid samples were provided by Prof. Turčáni (first neurological clinic of Medical Faculty and University Hospital, Comenius University in Bratislava). The financial support of Merck (Darmstadt, Germany) is also acknowledged.

References

1. Esplugues JV (2002) NO as a signalling molecule in the nervous system. Br J Pharmacol 135:1079–1095
2. Kelm M (1999) Nitric oxide metabolism and breakdown. Biochim Biophys Acta 1411: 273–289
3. Feelisch M, Stamler JS (1996) Measurements of NO-related activities – which assay for which purpose. In: Feelisch M, Stamler J (eds) Methods in nitric oxide research. Wiley, Chichester, pp 303–309
4. Steinberg A, Wiklund NP, Brundin L et al (2010) Levels of nitric oxide metabolites in cerebrospinal fluid in cluster headache. Cephalalgia 30:696–702
5. Danilov AI, Andersson M, Bavand N et al (2003) Nitric oxide metabolite determinations reveal continuous inflammation in multiple sclerosis. J Neuroimmunol 136:112–118
6. Murawska-Ciałowicz E, Szychowska Z, Trebusiewicz B (2000) Nitric oxide production during bacterial and viral meningitis in children. Int J Clin Lab Res 30:127–131
7. Kuiper MA, Visser JJ, Bergmans PLM et al (1994) Decreased cerebrospinal fluid nitrate levels in Parkinson's disease, Alzheimer's

disease and multiple system atrophy patients. J Neurol Sci 121:46–49

8. Henry CS (2006) Microchip capillary electrophoresis: methods and protocols. Humana, Totowa
9. Manz A, Eijkel JCT (2001) Miniaturization and chip technology. What can we expect? Pure Appl Chem 73:1555–1561
10. Kaniansky D, Masár M, Bodor R et al (2003) Electrophoretic separations on chips with hydrodynamically closed separation systems. Electrophoresis 24:2208–2277
11. Miyado T, Wakida S-i, Aizawa H et al (2008) High-throughput assay of nitric oxide metabolites in human plasma without deproteinization by lab-on-a-chip electrophoresis using a zwitterionic additive. J Chromatogr A 1206: 41–44
12. Miyado T, Tanaka Y, Nagai H et al (2004) Simultaneous determination of nitrate and nitrite in biological fluids by capillary electrophoresis and preliminary study on their determination by microchip capillary electrophoresis. J Chromatogr A 1051:185–191
13. Miyado T, Tanaka Y, Nagai H et al (2006) High-throughput nitric oxide assay in biological fluids using microchip capillary electrophoresis. J Chromatogr A 1109:174–178
14. Troška P, Chudoba R, Danč L et al (2013) Determination of nitrite and nitrate in cerebrospinal fluid by microchip electrophoresis with microsolid phase extraction pre-treatment. J Chromatogr B 930:41–47
15. Foret F, Křivánková L, Boček P (1993) Capillary zone electrophoresis. VCH, Weinheim
16. Bodor R, Kaniansky D, Masár M et al (2003) Determination of bromate in drinking water by zone electrophoresis-isotachophoresis on a column-coupling chip with conductivity detection. Electrophoresis 23:3630–3637
17. Boudko DY, Cooper BY, Harvey WR et al (2002) High-resolution microanalysis of nitrite and nitrate in neuronal tissues by capillary electrophoresis with conductivity detection. J Chromatogr B 774:97–104
18. Grass B, Neyer A, Jöhnck M et al (2001) A new PMMA-microchip device for isotachophoresis with integrated conductivity detector. Sensor Actuator B Chem 72:249–258
19. Everaerts FM, Beckers JL, Verheggen TPEM (1976) Isotachophoresis: theory, instrumentation and applications. Elsevier, Amsterdam

Chapter 4

Analysis of Thiols by Microchip Capillary Electrophoresis for In Situ Planetary Investigations

Maria F. Mora, Amanda M. Stockton, and Peter A. Willis

Abstract

Microchip capillary electrophoresis with laser-induced fluorescence detection (μCE-LIF) enables sensitive analyses of a wide range of analytes employing small volumes of sample and reagent (nL to μL) on an instrument platform with minimal mass, volume, and power requirements. This technique has been used previously in the analysis of amino acids and other organic molecules of interest in the fields of astrobiology and planetary science. Here, we present a protocol for the analysis of thiols using μCE-LIF. This protocol utilizes Pacific Blue C5-maleimide for fluorescent derivatization of thiols, enabling limits of detection in the low nM range (1.4–15 nM). Separations are conducted in micellar electrokinetic chromatography mode with 25 mM sodium dodecyl sulfate in 15 mM tetraborate, pH 9.2. This method allows analysis of 12 thiols in less than 2 min following a labeling step of 2 h. A step-by-step protocol, including tips on microchip capillary electrophoresis, is described here.

Key words Thiols, Microchip capillary electrophoresis, Laser-induced fluorescence, Pacific Blue C5-maleimide

1 Introduction

Thiols play an essential role in a wide range of biological processes, including protein folding, regulation of enzyme activity, defense against oxidation, and redox signaling. As such, they have been proposed as a potential biosignature in the search for extraterrestrial life [1, 2]. The study of this class of compounds could also provide insight into chemical and geological processes occurring on extraterrestrial bodies with known sulfur-enriched environments, including Mars, Europa, and Titan. For example, the discovery of thiols on Saturn's largest moon, Titan, could provide an indication that oxidized sulfates from the interior mix with the reduced carbon on Titan's surface, thus potentially serving as evidence for cryovolcanic activity [3].

Ann Van Schepdael (ed.), *Microchip Capillary Electrophoresis Protocols*, Methods in Molecular Biology, vol. 1274,
DOI 10.1007/978-1-4939-2353-3_4, © Springer Science+Business Media New York 2015

The analysis of thiols is an area of active interest due to their importance in medicinal, biological, industrial, and environmental studies. Multiple separation methods, including gas chromatography (GC), liquid chromatography (LC), and capillary electrophoresis (CE), have been implemented for selective and sensitive analysis of thiols [4]. These separation methods have been coupled to electrochemical [5–7], optical [8, 9], and mass spectrometric (MS) detection [10]. Microchip capillary electrophoresis (μCE) coupled to laser-induced fluorescence (LIF) detection enables fast and sensitive analysis of a broad range of compounds employing reduced volumes of sample and reagents. This technique is particularly attractive for spaceflight applications due to its inherent miniaturization which allows for the development of portable instruments with low mass, volume, and power requirements [11, 12]. Portable, miniaturized μCE-LIF instruments have been demonstrated for potential field use in the analysis of species ranging from larger biopolymers to small organic molecules [13, 14]. Protocols have been developed for analysis of amines, amino acids, aldehydes, ketones, and carboxylic acids [12].

In this chapter, a protocol employing fluorescent derivatization is described for the analysis of thiols via μCE-LIF [15]. Thiols are derivatized for LIF detection with a 405 nm excitation source using the commercial fluorescent probe Pacific Blue C5-maleimide. A micellar electrokinetic chromatography (MEKC) method is utilized for separation using sodium dodecyl sulfate (SDS) as the surfactant. The separation conditions can be tuned for analysis of species at low concentration or for optimal resolution for samples of greater complexity. For spaceflight applications, this protocol could readily be added to the organic chemical analytical suite of μCE-LIF instrumentation currently under development for in situ deployment (e.g., the Chemical Laptop [16]). The protocol was previously validated by analyzing thiols in a complex real sample from the geothermal pools at Hot Creek Gorge near Mammoth Lake, California [15]. Detailed information about the optimization of the protocol and the results from the analysis of geothermal pools is described in ref. 15 (Fig. 1).

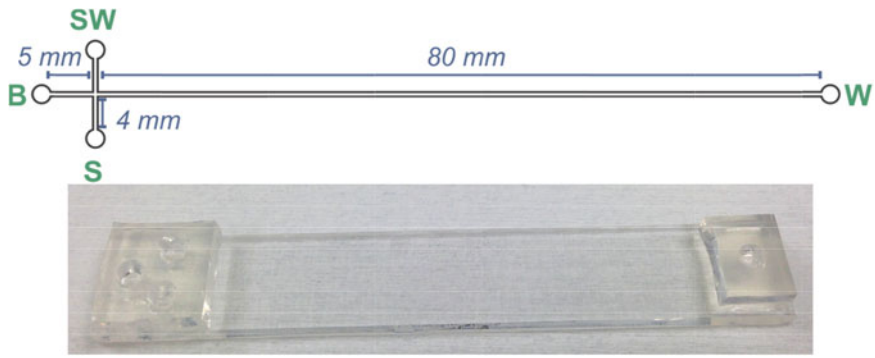

Fig. 1 *Top:* Dimensions of the commercial microchips (Micralyne MC-BF4-SC) employed to develop the protocol described here and nomenclature of the CE reservoirs (*S* sample, *SW* sample waste, *B* buffer, and *W* waste). *Bottom*: photograph of a microchip with PDMS gaskets on top

2 Materials

Prepare all solutions using ultrapure water (18 MΩ.cm at 25 °C) and analytical grade reagents. Prepare and store all reagents at room temperature (unless indicated otherwise). The pH was adjusted using either 1 M NaOH or 1 M HCl and measured using a glass electrode and a digital pH meter. Thiols were purchased from Sigma-Aldrich (St. Louis, MO): 2-mercaptoethanol (ME), 2-propanethiol (2PT), 1-propanethiol (1PT), 1-butanethiol (BT), 1-pentanethiol (PeT), 1-hexanethiol (HT), 1-heptanethiol (HpT), 1-octanethiol (OT), 3-methyl-2-butanethiol (MBT), cyclohexanethiol (CHT), methyl 3-mercaptopropionate (MMP), and butyl 3-mercaptopropionate (BMP). Pacific Blue C5-maleimide (PBM) was purchased from Invitrogen (Carlsbad, CA). All experiments were performed at room temperature.

2.1 Solutions

1. Separation buffer: 15 mM sodium tetraborate ($Na_2B_4O_7 \cdot 10\,H_2O$) pH 9.2, 25 mM sodium dodecyl sulfate (SDS) (*see* **Note 1**).
2. Labeling buffer: 25 mM SDS, 25 mM phosphate pH 7 (*see* **Note 1**).
3. Dilution buffer: 50 mM SDS, 50 mM phosphate pH 7. This solution is used to dilute samples for labeling so that the final concentration is the same as that used to label standards (*see* **Note 1**).
4. Stock dye: Dissolve 1 mg Pacific Blue C5-maleimide in DMF to obtain a 20 mM solution. This solution must be kept at −20 °C when not in use (*see* **Note 1**).
5. Thiol standards: Prepare thiol standards in DMF (10 mM each thiol) and store at −20 °C when not in use (*see* **Note 1**).

2.2 Special Equipment

1. High-voltage power supply for electrophoresis capable of supplying a 6,000 V differential, fitted with platinum wire electrodes (e.g., LabSmith HVS448 model # 6000D).
2. Laser-induced fluorescence detection system with 405 nm excitation laser (e.g., a Nikon Eclipse TE2000-U inverted microscope system with a 405 nm Melles Griot diode laser and a Photometrics Cascade 650 CCD camera).
3. Glass microdevice (8 cm long channel intersected with a 1 cm cross channel approximately 5 mm from one end) fitted with PDMS gaskets punched with 3 mm diameter wells. Microdevices should be checked for defects prior to use, as even relatively small defects can lead to irreproducible data and poor resolution.

3 Methods

3.1 Labeling Reaction

1. Label standard solutions of each thiol (10–20 μM each) with PBM in labeling buffer and allow the reaction to proceed for 1.5–2 h in sealed vials at room temperature. Use a molar ratio in excess of 2:1 [PBM]:$[thiol]_{total}$ to assure completion of the labeling reaction.

3.2 Microchip Capillary Electrophoresis Analysis

1. Visually inspect the electrophoresis channel under a microscope for any defects or particulates (*see* **Notes 5–8**).
2. Filter all solutions through a 0.2 μm filter immediately prior to loading the microchip. This helps to avoid issues in electrophoresis due to particulates inside the microchannel.
3. Condition the microchip by filling the separation and cross channels first with 0.1 M NaOH (10 min), then with water (10 min), and, finally, with separation buffer (10 min).
4. It is strongly recommended that both a blank and a known standard are analyzed at the beginning of each day. A suggested standard is a mixture of thiols (20–50 μM each labeled with 2–4 times PBM) diluted to 500 nM prior to analysis.
5. Fill the channel with separation buffer.
6. Fill all wells except sample with 40–50 μL separation buffer and fill the sample well with phosphate/SDS buffer.
7. Place platinum electrodes in the wells. Make sure they do not touch each other or any other metallic surfaces. Ideally, place the wire in the well but away from the channel inlet. Also make sure there are no fluidic connections (aside from the microchannel) between the liquid in the wells. Apply potentials to acquire a blank electropherogram with the conditions described in Table 1.
8. Empty the sample well and add a labeled standard. Make sure the volume in all the reservoirs is approximately the same to avoid undesired pressure-driven flows, which can lead to low resolution and reproducibility issues.

Table 1
Potentials for separation of thiols in a commercial microchip (BF4-SC, Micralyne Inc., Edmonton, Canada)

Step	Time	Sample	Sample waste	Buffer	Waste
Injection	10 s	700	0	600	900
Separation	100–120 s	3,000	1,900	1,900	−3,000

The chips consist of a short channel (8.0 mm) bisected by a long channel (85.0 mm). Channels are approximately 50 μm wide and 20 μm deep

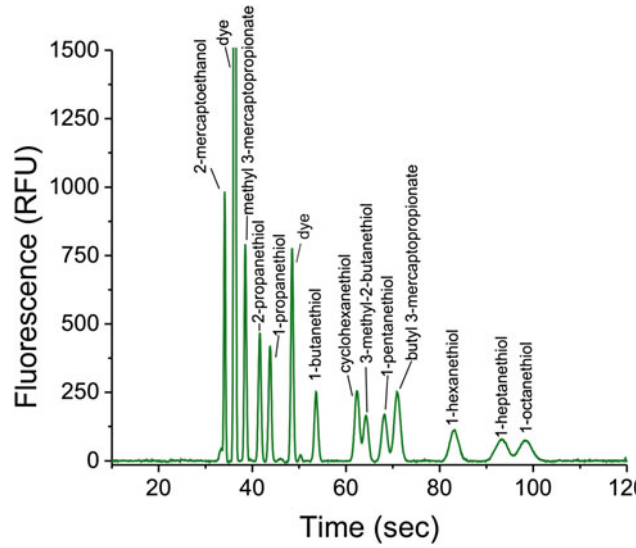

Fig. 2 Optimized separation of a 200 nM mixture of PBM-labeled thiols. Separation conditions: 15 mM tetraborate pH 9.2, 25 mM SDS. Reproduced with permission from Ref. 15

9. Apply potentials to acquire a standard electropherogram (*see* **Note 2**). An example of a separation of a standard mixture of 12 thiols is shown in Fig. 2.
10. Remove the standard sample from the microdevice, and then remove buffer from the remaining wells. Add new buffer to all wells except the sample well and add standard sample into the sample well. Acquire a second electropherogram by repeating **step 9** above.
11. Repeat **step 10** above a third time. Check that the reproducibility of the system is adequate.
12. Flush the channel with water and repeat **steps 5–11**, replacing the standard with the real sample.

3.3 Calibration Curve

1. Dilute stock solutions of thiols to concentrations ranging from 20 nM to 2 μM in labeling buffer.
2. Label these solutions with 60 μM PBM.
3. Analyze each concentration three times employing the protocol described above (Subheading 3.2).
4. Construct a calibration curve as S/N versus concentration of thiol. Fit the curve with a power law. These equations will be used to calculate the concentrations of thiols in the samples analyzed by this method. Examples of calibration curves for thiols employing this protocol are shown in Fig. 3.

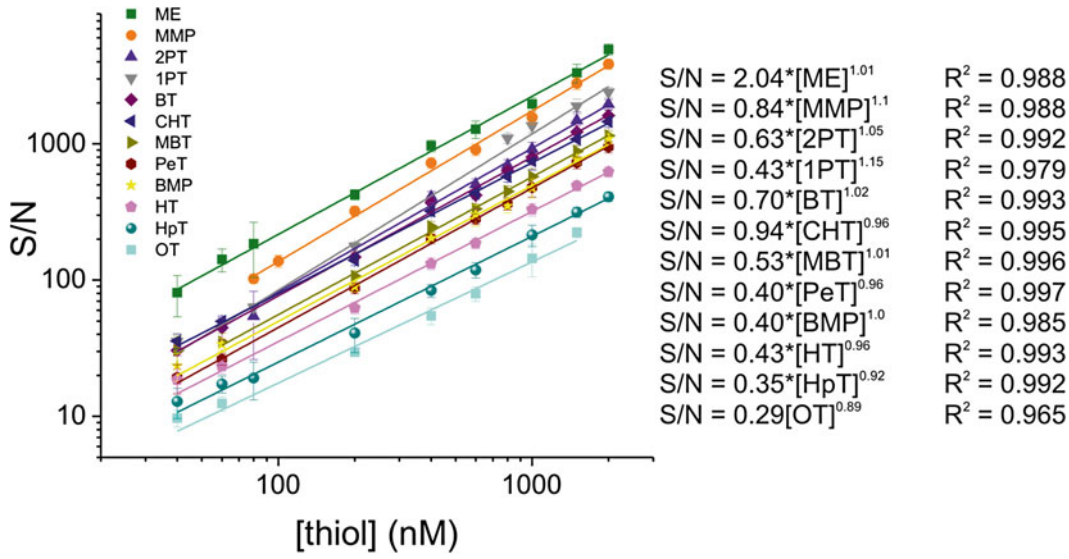

Fig. 3 Calibration curves for all thiols. Conditions: separation buffer 15 mM tetraborate buffer, SDS 25 mM pH = 9.2, samples in 25 mM phosphate, 25 mM SDS pH 7. V_{SEP} = 6 kV. Each concentration was measured in triplicate and error bars were calculated as the standard deviation of the three measurements. Reproduced with permission from Ref. 15

3.4 Real Sample Analysis

3.4.1 Sample Preparation

1. Dilute the real sample by half with dilution buffer and check that the pH is approximately 7. If it is not, add NaOH/HCl to adjust the pH to 7. Next, add excess PBM and let react for 1.5–2 h in sealed vials at room temperature. In case of unknown samples that might have low concentrations of thiols, it might be necessary to label with varying concentrations of dye in order to determine the appropriate quantity.
2. After pH adjustment, divide the sample into two aliquots.
3. Add a known thiol standard to one of the aliquots to serve as spiked sample.
4. Add PBM and let react as outlined in the above protocol.

3.4.2 Sample Analysis

1. Analyze both the sample and spiked sample employing the protocol described in Subheading 3.2.
2. Verify that the intensity for the internal standard is the expected value. This indicates that the labeling reaction and/or injection is not affected by the sample matrix. If the internal standard differs from the expected value by a small amount, calculate a correction factor based on that difference. If no signal is observed for the internal standard, dilute the sample further before labeling to mitigate the effects of the matrix.
3. Verify that there is a peak corresponding to unreacted dye. This corroborates that the dye was present in excess and

therefore that all thiols in the sample are completely labeled. If there is no significant amount of unreacted dye, repeat the labeling and analysis with a higher concentration of dye relative to the sample.

4. Verify that no peaks due to thiols of interest saturate the detector. If there is saturation, dilute the sample and repeat the analysis.
5. If there are peaks in the electropherogram for the sample, spike known concentrations of standards and reanalyze to verify that the peaks are due to the known compounds (*see* **Notes 4** and **5**).
6. Obtain the intensity of the peaks corresponding to thiols in the sample and use the equation from the calibration curves to calculate the concentration in the sample. If matrix effects were discovered in **step 2** above, apply that correction factor prior to this calculation.

4 Notes

1. Let solutions return to room temperature prior to use. Different storage conditions are indicated for various reagents, but all sample manipulation and all electrophoretic experiments are performed at room temperature.
2. Do not let the sample in the well for extended periods of time before applying potential. Sample diffusion will compromise the measured resolution.
3. If better sensitivity is required for a particular analyte, the running buffer can be modified to provide a higher signal for the thiol of interest (*see* Fig. 3).
4. If resolution is insufficient (this could vary with different microchips as the EOF varies), a higher concentration of tetraborate can be used (*see* Fig. 3).
5. Clean the microchips often. When using the same microchip for multiple analyses, clean and rinse the chip before and after each experiment. A vacuum pump can be used to repeatedly flush/refill wells. The frequent analysis of blank samples can assist in monitoring any potential sample carryover. The analysis of known standards helps verify the microchips are working properly.
6. Store microchips filled with filtered deionized water to prevent electrolytes from crystallizing inside the channels.
7. Always wipe glass microchips with lens paper to avoid any scratches.

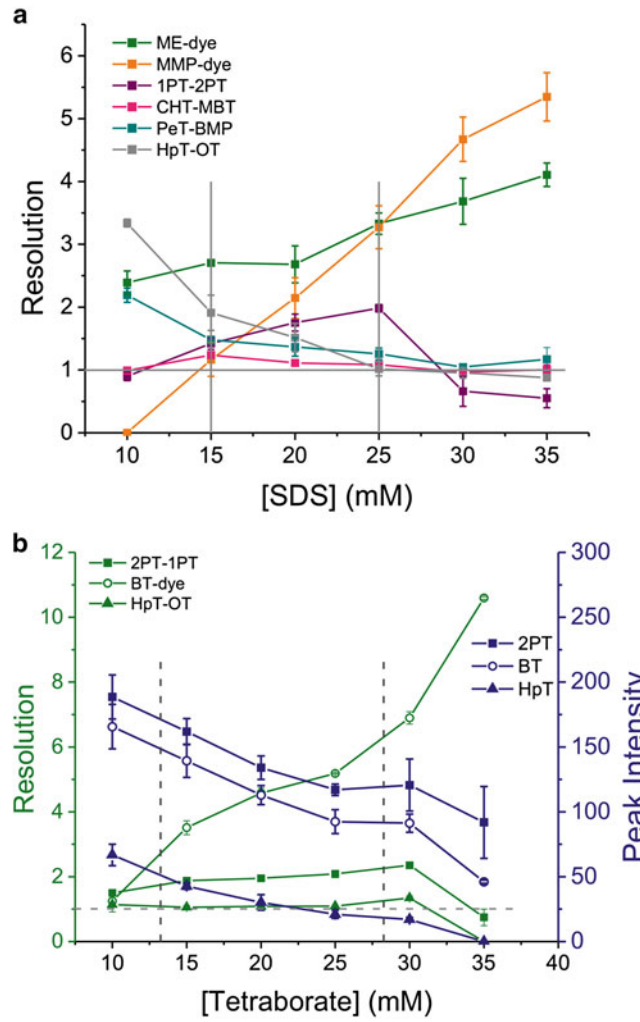

Fig. 4 (**a**) Resolution for neighboring peaks as function of [SDS]. Conditions: 100 nM each thiol, tetraborate buffer 20 mM, pH 9.2. (**b**) Effect of buffer concentration on the separation of the selected thiols. *Left axis*: resolution for neighboring peaks, (*filled green squares*) 2PT-1PT, (*open green circles*) BT-hydrolyzed dye, and (*filled green triangles*) HpT-OT. *Right axis*: peak intensities for 100 nM (*filled blue squares*) 2PT, (*open blue circles*) BT, and (*filled blue triangles*) HpT as function of buffer concentration. Conditions: 100 nM of each thiol, 25 mM SDS and buffer pH 9.2. Peak intensities and resolutions calculated as the average of at least three measurements. Error bars are calculated as the standard deviation. As the buffer concentration increases, the migration times of all analytes increase as well. A decrease in peak intensity is also observed for all the analytes with higher buffer concentrations. Because the resolution does not change significantly except for concentrations above 25, 15 mM was selected, as it provides good resolution with high peak intensity (and consequently better sensitivity). It is worth mentioning that in the case of complex samples, a higher concentration of buffer can be used to obtain better resolution. For very dilute samples, a lower concentration of buffer can be used to improve sensitivity. Reproduced with permission from Ref. 15

8. If a microdevice fails to give good results despite passing a visual inspection, the following various cleaning protocols are recommended:
   (a) Flush repeatedly NaOH solution, HCl solution, and H_2O.
   (b) Flush with 100 mM EDTA (especially if the last sample had high levels of dissolved polyvalent cations like Mg^{2+}, Ca^{2+}, Fe^{3+}, etc.).
   (c) Flush with piranha solution (1:1 H_2SO_4:H_2O_2) for a few minutes.

Acknowledgments

The research described here was carried out at the Jet Propulsion Laboratory, California Institute of Technology, under a contract with the National Aeronautics and Space Administration. Financial support for this project was provided by ASTID (Project #104320) and the NASA Postdoctoral Program (NPP) at the Jet Propulsion Laboratory, administered by Oak Ridge Associated Universities through a contract with NASA.

References

1. Pilcher CB (2003) Biosignatures of early earths. Astrobiology 3(3):471–486
2. Vance S, Christensen LE, Webster CR, Sung K (2011) Volatile organic sulfur compounds as biomarkers complementary to methane: Infrared absorption spectroscopy of CH_3SH enables in situ measurements on Earth and Mars. Planet Space Sci 59(2–3):299–303
3. Brown RH, Lebreton J-P, Waite JH (eds) (2009) Titan from Cassini-Huygens. Springer, New York
4. Toyo'oka T (2009) Recent advances in separation and detection methods for thiol compounds in biological samples. J Chromatogr B 877(28):3318–3330
5. Zhou J, O'Shea TJ, Lunte SM (1994) Simultaneous detection of thiols and disulfides by capillary electrophoresis-electrochemical detection using a mixed-valence ruthenium cyanide-modified microelectrode. J Chromatogr A 680(1):271–277
6. Inoue T, Kirchhoff JR (2000) Electrochemical detection of thiols with a coenzyme pyrroloquinoline quinone modified electrode. Anal Chem 72(23):5755–5760
7. Stenken JA, Puckett DL, Lunte SM, Lunte CE (1990) Detection of N-acetylcysteine, cysteine and their disulfides in urine by liquid chromatography with a dual-electrode amperometric detector. J Pharm Biomed Anal 8(1):85–89
8. Kuśmierek K, Chwatko G, Głowacki R, Bald E (2009) Determination of endogenous thiols and thiol drugs in urine by HPLC with ultraviolet detection. J Chromatogr B 877(28): 3300–3308
9. McDermott GP, Terry JM, Conlan XA, Barnett NW, Francis PS (2011) Direct detection of biologically significant thiols and disulfides with manganese(IV) chemiluminescence. Anal Chem 83(15):6034–6039
10. Seiwert B, Karst U (2007) Simultaneous LC/MS/MS determination of thiols and disulfides in urine samples based on differential labeling with ferrocene-based maleimides. Anal Chem 79(18):7131–7138
11. Mora MF, Greer F, Stockton AM, Bryant S, Willis PA (2011) Toward total automation of microfluidics for extraterrestrial in situ analysis. Anal Chem 83(22):8636–8641
12. Mora MF, Stockton AM, Willis PA (2012) Microchip capillary electrophoresis instrumentation for in situ analysis in the search for extraterrestrial life. Electrophoresis 33:2624–2638
13. Skelley AM, Scherer JR, Aubrey AD, Grover WH, Ivester RHC, Ehrenfreund P, Grunthaner FJ,

Bada JL, Mathies RA (2005) Development and evaluation of a microdevice for amino acid biomarker detection and analysis on Mars. Proc Natl Acad Sci U S A 102(4): 1041–1046

14. Benhabib M, Chiesl TN, Stockton AM, Scherer JR, Mathies RA (2010) Multichannel capillary electrophoresis microdevice and instrumentation for in situ planetary analysis of organic molecules and biomarkers. Anal Chem 82(6):2372–2379
15. Mora MF, Stockton AM, Willis PA (2013) Analysis of thiols by microchip capillary electrophoresis for in situ planetary investigations. Electrophoresis 34:309–316
16. Willis PA, Jiao H, Greer F, Fisher AM, Mora MF, Stockton AM, Cable ML (2012) The chemical laptop. U.S. Patent CIT-5905-P

Chapter 5

Analysis of Ofloxacin in Ofloxacin Ear Drops by Microfluidic Chip Coupled with Contactless Conductivity Detection

Bing Chen and Kaicheng Li

Abstract

A method using a microfluidic chip coupled with contactless conductivity detection (C^4D) is demonstrated for the determination of ofloxacin in Ofloxacin Ear Drops. Settings, optimizing procedures, electrophoresis conditions, regression equations, and the average recovery rate are discussed. Under optimum conditions, the determination of ofloxacin in standard solution is achieved within 1 min, which allows detection of ofloxacin in Ofloxacin Ear Drops. The demonstrated method is rapid, high efficient, sensitive, and economical.

Key words Microfluidic chip, Contactless conductivity detection, Fluoroquinolone, Ofloxacin, Ofloxacin ear drops

1 Introduction

The concept of microfluidic chip, or the so-called miniaturized total analysis system, or micro total analysis system (μTAS), or lab-on-chip (LOC), was first created in 1990 by Manz and Widmer et al. from Ciba-Geigy Co. Ltd., Switzerland [1]. As a replacement of conventional instruments in biological or chemical laboratories, microfluidic chips integrate basic operation units, such as sample preparation, chemical reaction, separation, and detection, onto a single chip of only several squares of centimeters (or even smaller). These different operation units connect with each other on the chip through the microchannels that are filled with fluids. In 1992, Harrison and Manz, using a well-known photolithographic technique (MEMS) for structures in the micrometer range [2], micromachining, successfully carved out microchannels on sheet glasses and developed the first instrument for microchip capillary electrophoresis (MCCE), with which they achieved the separation of fluorescence-labeled amino acids.

Ann Van Schepdael (ed.), *Microchip Capillary Electrophoresis Protocols*, Methods in Molecular Biology, vol. 1274,
DOI 10.1007/978-1-4939-2353-3_5,

In 1999, Hewlett-Packard Co., Ltd. (Agilent) and Caliper Life Sciences Co., Ltd. jointly launched the first commercial microfluidic instrument, known as the 2100 Electrophoresis Bioanalyzer, and the instrument was first applied to the field of bioanalytical and clinical analysis [3]. In the last decade, this method is favored by many researchers and rapidly developed because of its miniaturization, high integration, portability, economy, low loss, high efficiency, and rapidity.

Since the 1990s, the instrument has been gradually applied to other fields such as pharmaceutical analysis [4–8], biological analysis [9], and monitoring environmental pollutants [10].

Ofloxacin is a synthetic antibacterial agent belonging to the fluoroquinolone class. It has been used for restraining *Enterobacter* and both Gram-negative and Gram-positive bacteria in medical preparations [11]. As a preparation of ofloxacin, Ofloxacin Ear Drops are an effective treatment for diseases that are caused by sensitive bacteria, such as tympanitis, otitis externa, and myringitis. There are common methods for analyzing ofloxacin such as the chemical method [11], the spectrophotometric method [12], and high-performance liquid chromatography (HPLC) [13]. These methods require complex operations, long separation times, and large amounts of reagents. On the other hand, capillary electrophoresis (CE) has high efficiency, rapidity, sensitivity, and low reagent consumption. It has been shown that the determination of ofloxacin in tablets by CE can be finished within 5 min [14, 15].

It has been shown that microfluidic chips with C^4D [16–18] can also be applied to determine ofloxacin in Ofloxacin Ear Drops, and the separation and detection of ofloxacin are even more efficient and rapid, thus making microfluidic chips preferable to other methods including CE [11–15].

2 Materials

2.1 Instrument

1. CCD-08B model microchip capillary electrophoresis system that consists of a high-voltage power supply and a capacitively coupled contactless conductivity detector (C^4D, School of Pharmaceutical Sciences, Sun Yat-sen University, the People's Republic of China) [19–21].
2. Microchip of polymethyl methacrylate (PMMA), with an effective length of 43 mm (total length 44 mm) and a cross-shaped microchannel of 30 μm upper width, 100 μm lower width, and 30 μm depth (School of Pharmaceutical Sciences, Sun Yat-sen University, the People's Republic of China).

   Additionally, holes of 3 mm diameter, which serve as the buffer (Fig. 1a), sample (Fig. 1b), sample waste (Fig. 1c), and buffer waste reservoir (Fig. 1d), are drilled on the chip and connected with the corresponding microchannels. The buffer

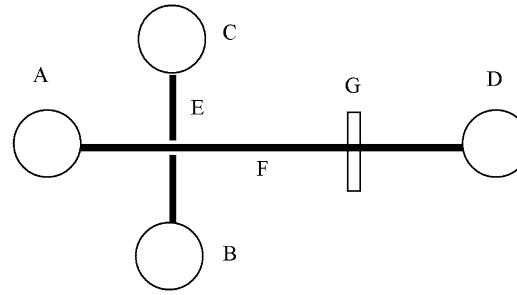

Fig. 1 A thin cover chip. (**a**) Buffer reservoir, (**b**) sample reservoir, (**c**) sample waste reservoir, (**d**) buffer waste reservoir, (**e**) injection channel, (**f**) separation channel, (**g**) check position

waste reservoir is also used as a detection cell, which settled the inconvenience of building another special cell for electrolysis. Each reservoir has a corresponding platinum wire inserted in it, acting as an electronic contact between the reservoir and the high-voltage power supply.

3. The high-voltage power supply is made of piezoelectric ceramics and provides a constant potential voltage of 0.1–0.5 kV for injection and a constant or pulsed potential voltage of 0.5–5 kV for separation.
4. The C^4D produces three waveforms (sine, square, and triangle) with an oscillation frequency of 0–300 kHz and an oscillation voltage of 0–0.3 kV (Vpp). An oscillation excitation frequency of 60 kHz and an oscillation excitation voltage of 22 V (Vpp) are selected in the experiments.
5. Experimental data are processed on the HW-2000 model chromatograph workstation, 2.18 edition (School of Pharmaceutical Sciences, Sun Yat-sen University, the People's Republic of China).

   The detector is connected to a personal computer through an A/D converter (model PCL-711B, EVOC, Taiwan).
6. The microchip is cleaned with a SHZ2D (III) model water ring vacuum pump (Gongyishi Yinyuyuhua instrument plant, the People's Republic of China).

2.2 Chemicals

Ofloxacin is purchased from the National Institute for the Control of Pharmaceutical and Biological Products (Beijing, the People's Republic of China). Ofloxacin Ear Drops (1030821, Shanxi Yellow River Traditional Chinese Medicine Co., Ltd., Chengdu, the People's Republic of China) is purchased from the Cunjin Branch of the Tianma Great Drugstore Chain Co., Ltd. (Zhanjiang, the People's Republic of China). All chemicals are of analytical reagent grade: L-histidine (His), 2-(N-morpholino)eth-

anesulfonic acid (MES), sodium tetraborate, ethanol, sodium hydroxide, and hydrochloric acid. Water is purified by quartz sub-boiling distillation.

2.3 Preparation of Stock Solutions

1. 0.1 M hydrochloric acid solution: measure 9 mL 36–38 % concentrated hydrochloric acid, dilute with quartz sub-boiling distilled water in a 50-mL beaker, cool down to room temperature, transfer to a 1,000-mL volumetric flask, set the volume to 1,000 mL, and store at 4 °C.
2. 1 M nitric acid solution: measure 6.25 mL 65 % concentrated nitric acid, dilute with quartz sub-boiling distilled water, set the volume to 100 mL, and store at 4 °C.
3. 1 M sodium hydroxide solution: weigh 4 g sodium hydroxide, dissolve in quartz sub-boiling distilled water, set the volume to 100 mL, and store at 4 °C.
4. 0.1 M trishydroxymethyl aminomethane (Tris) solution: weigh 1.2114 g Tris, dissolve in quartz sub-boiling distilled water, set the volume to 100 mL, and store at 4 °C.
5. 0.1 M (N-morpholino)ethanesulfonic acid monohydrate (MES) solution: weigh 2.132 g MES, dissolve in quartz sub-boiling distilled water, set the volume to 100 mL, and store at 4 °C.
6. 0.1 M L-histidine (His) solution: weigh 1.5516 g His, dissolve in quartz sub-boiling distilled water, set the volume to 100 mL, and store at 4 °C.
7. 0.1 M sodium dihydrogen phosphate solution: weigh 1.5601 g sodium dihydrogen phosphate dihydrate, dissolve in quartz sub-boiling distilled water, set the volume to 100 mL, and store at 4 °C.
8. 0.1 M disodium hydrogen phosphate solution: weigh 3.5822 g disodium hydrogen phosphate dodecahydrate, dissolve in quartz sub-boiling distilled water, set the volume to 100 mL, and store at 4 °C.
9. 1 M acetic acid solution: measure 0.6 mL 65 % glacial acetic acid, dilute with quartz sub-boiling distilled water, set the volume to 100 mL, and store at 4 °C.
10. 0.1 M sodium acetate solution: weigh 1.3609 g sodium acetate trihydrate, dissolve in quartz sub-boiling distilled water, set the volume to 100 mL, and store at 4 °C.
11. 0.1 M boric acid solution: weigh 0.6184 g of boric acid, dissolve in quartz sub-boiling distilled water, set the volume to 100 mL, and store at 4 °C.
12. 0.1 M sodium tetraborate solution: weigh 3.814 g of sodium tetraborate decahydrate, dissolve in quartz sub-boiling distilled water, set the volume to 100 mL, and store at 4 °C.

13. 0.1 M citric acid solution: weigh 2.101 g of citric acid monohydrate, dissolve in quartz sub-boiling distilled water, set the volume to 100 mL, and store at 4 °C.
14. 0.1 M sodium citrate solution: weigh 2.941 g of sodium citrate dihydrate, dissolve in quartz sub-boiling distilled water, set the volume to 100 mL, and store at 4 °C.
15. Other solutions with different concentrations are prepared from the above stock solutions with quartz sub-boiling distilled water.

2.4 Preparation of Standard Solutions

Stock solution of ofloxacin (approximately 1 mg/mL) is prepared by dissolving 10 mg of ofloxacin in 10 mL quartz sub-boiling distilled water. The stock solution is stored at 4 °C. Other solutions are prepared by diluting the stock solution with quartz sub-boiling distilled water.

2.5 Preparation of Sample Solution

Measure 1 mL Ofloxacin Ear Drops, transfer to a 10-mL volumetric flask, set the volume to 10 mL with quartz sub-boiling distilled water, and store at 4 °C.

3 Methods

3.1 Preparation of Running Buffer Solutions

1. Preparation of 1 mM MES and 1 mM His running buffer solution: measure 1 mL 0.1 M MES and 1 mL 0.1 M His, dilute with quartz sub-boiling distilled water, set volume to 100 mL, and store at 4 °C.
2. Preparation of 1 mM MES and 1 mM Tris running buffer solution: measure 1 mL 0.1 M MES and 1 mL 0.1 M Tris (*see* **Note 1**), dilute with quartz sub-boiling distilled water, set the volume to 100 mL with quartz sub-boiling distilled water, and store at 4 °C.
3. Preparation of 1 mM boric acid and 1 mM Tris running buffer solution: measure 1 mL 0.1 M boric acid and 1 mL 0.1 M Tris, dilute with quartz sub-boiling distilled water, set the volume to 100 mL, and store at 4 °C.
4. Preparation of 1 mM sodium dihydrogen phosphate and 1 mM disodium hydrogen phosphate running buffer solution: measure 1 mL 0.1 M sodium dihydrogen phosphate and 1 mL 0.1 M disodium hydrogen phosphate (*see* **Note 2**), dilute with quartz sub-boiling distilled water, set the volume to 100 mL with quartz sub-boiling distilled water, and store at 4 °C.
5. Preparation of 1 mM citric acid and 1 mM sodium citrate running buffer solution: measure 1 mL 0.1 M citric acid and 1 mL 0.1 M sodium citrate, dilute with quartz sub-boiling distilled water, set the volume to 100 mL with quartz sub-boiling distilled water, and store at 4 °C.

6. Preparation of 1 mM acetic acid and 1 mM sodium acetate running buffer solution: measure 1 mL 0.1 M acetic acid and 1 mL 0.1 M sodium acetate, dilute with quartz sub-boiling distilled water, set the volume to 100 mL with quartz sub-boiling distilled water, and store at 4 °C.
7. Preparation of 1 mM boric acid and 1 mM sodium tetraborate running buffer solution: measure 1 mL 0.1 M boric acid and 1 mL 0.1 M sodium tetraborate, dilute with quartz sub-boiling distilled water, set the volume to 100 mL with quartz sub-boiling distilled water, and store at 4 °C.

3.2 Activation and Treatment of a Microchip

1. A new chip is cleaned using the following procedures: the dust on the chip's surface is removed by an aurilave, and then the chip is rinsed several times with quartz sub-boiling distilled water and 50 % ethanol; after the chip has naturally dried, the chip is installed on the detector (*see* **Note 3**); then the chip is rinsed with 1 M nitric acid solution for 30 min, quartz sub-boiling distilled water for 10 min, 1 M sodium hydroxide solution for 30 min, and quartz sub-boiling distilled water for 10 min, respectively.
2. Cleaning the microchip before the operation: at the beginning of each day, the chip is rinsed with 0.1 M sodium hydroxide solution for 15 min, quartz sub-boiling distilled water for 10 min, and separation buffer for 15 min, respectively.
3. Cleaning the microchip during the operation: after six or seven separations have been performed, the chip channel is rinsed again with separation buffer for 15 min.
4. Cleaning the microchip after the operation: at the end of each day, the microfluidic chip's channels are washed with 1 M nitric acid solution for 10–15 min, quartz sub-boiling distilled water for 10–15 min, 1 M sodium hydroxide solution for 10–15 min, and quartz sub-boiling distilled water for 10–15 min, respectively, for two to three times.

3.3 Electrophoretic Operation

1. Turn on the high-voltage power supply for 30 min to preheat the instrument (*see* **Note 4**).
2. Clean the microchip (*see* Subheading 3.2) (*see* **Notes 5**–**7**).
3. Examine the working parameters of the instrument. Set the excitation voltage to 22 V (Vpp) and the excitation frequency to 60 kHz.
4. Sample injection is performed as follows: the running buffer is added into the chip reservoirs (Fig. 1a, c, d), the sample solution is added to the sample reservoir (Fig. 1b) (*see* **Note 8**), and the platinum electrodes are inserted into each reservoir.

   In order to inject samples into the sample channel, the high-voltage power supply is switched to the injection mode

with an injection voltage chosen between 0.10 and 0.50 kV. Usually, the first sample injection requires 20–30 s, and then the subsequent injections require 10–15 s. Depending on the specific samples detected, the injection time varies.

For example, sample A requires 20 s for the first injection and 10 s for the following injections, and sample B requires 25 s for the first injection and 15 s for the other injections.

5. Sample separation is performed as follows: the high-voltage power supply is switched to the separation mode with a separation voltage chosen between 0.50 and 5.00 kV. The separation time ranges between 0.5 and 5 min.
6. The experiment cleanup is performed as follows: the high-voltage power supply is turned off. The running buffer and sample solutions are removed from the reservoirs. The microchip is cleaned (*see* Subheading 3.2). The reservoirs are filled with quartz sub-boiling distilled water, and the microchip is covered with a watch glass to prevent dust pollution.

3.4 Data Recording and Storage

The detector outputs measurements to the data workstation on a personal computer through an A/D converter. The workstation interface displays the real-time signals. Experimental data are stored on the computer.

3.5 Determination of Separation Conditions

1. Effects of different injection times: the injection time is an important parameter for the microfluidic chip experiment. The effect of injection time on the migration time and the peak area is studied for injection times from 5 to 30 s. When the injection time is chosen at 5 s, the signal has a small peak area and a short migration time, but the peak of ofloxacin overlays with the EOF. An injection time of 10 s is determined to be the optimal because baseline separation is achieved and the peak area is maximized. The effect of injection times from 5 to 30 s on migration times and peak areas is presented in Fig. 2.
2. Effects of different separation voltages: the separation voltage is also an important parameter for the microfluidic chip experiment. The effect of separation voltages from 0.75 to 2.0 kV on migration time and peak area is studied. A voltage of 1.5 kV is chosen as the optimal separation voltage because the separation time is relatively minimized and the peak area is maximized (Fig. 3).
3. Effects of different buffer systems: the selection of the buffer system has a nontrivial influence on the separation. This experiment studies the effect of several different buffer systems on the separation and detection of ofloxacin. The investigated buffer systems include citric acid–sodium citrate, sodium dihydrogen phosphate–disodium hydrogen phosphate, Tris–sodium tetraborate, boric acid–Tris, MES–Tris, MES–His, and MES–sodium tetraborate.

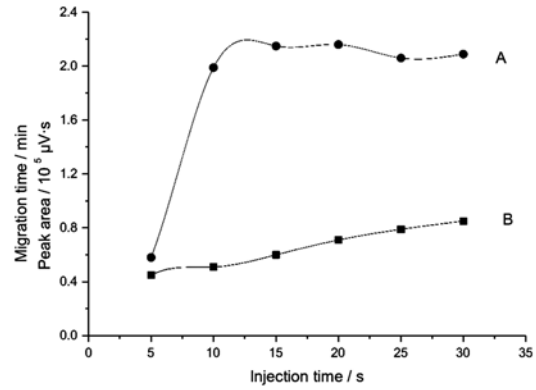

Fig. 2 Effect of injection time on migration time A and peak area B. Conditions: buffer, 1 mM His (pH 6.5) containing 1 mM MES; applied voltage, 1.5 kV; injection time, 5–30 s; temperature, 25 ± 0.5 °C; PMMA, with an effective length of 43 mm (total length 44 mm) and a cross-gallery microchannel of 30 μm upper width, 100 μm lower width, and 30 μm depth

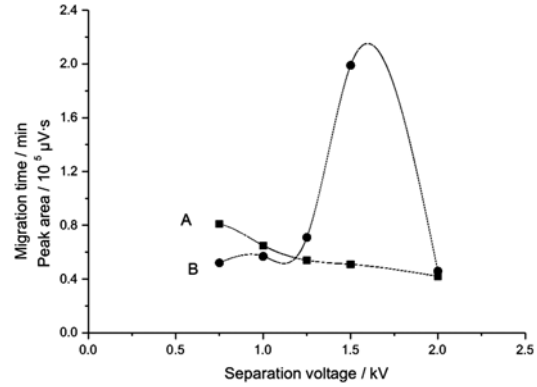

Fig. 3 Effect of separation voltage on migration time A and peak area B. Conditions: buffer, 1 mM His (pH 6.5) containing 1 mM MES; applied voltage, 0.5–2 kV; injection time, 10 s; other conditions as in Fig. 2

The MES–His buffer system is selected as the optimum buffer system because in this system the electrophoresis current is small, the baseline is stable, the peak shape is sharp, and the peak area is large.

4. Effects of different concentration ratios of the buffer system: the component concentration ratios of the buffer system influence the separation and detection of ofloxacin. This experiment explores the effects of MES–His concentration ratio on the separation and detection of ofloxacin. The result shows that as the concentration ratio of MES–His increases, the current increases, the ofloxacin migration time stays fairly constant regardless of the concentration ratio, and the peak area increases

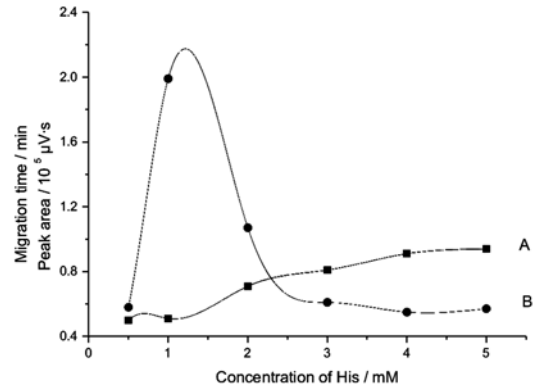

Fig. 4 Effect of concentration of His on migration time A and peak area B. Conditions: buffer, 1 mM MES containing 0.5–2 mM His; applied voltage, 1.5 kV; injection time, 10 s with a voltage of 0.5 kV; other conditions as in Fig. 2

at first then decreases. When the MES–His ratio is chosen at 1:1, the sample peak height and the peak area are maximized, and the sample peak is separated from the electroosmotic flow (EOF) and other peaks. Therefore, 1 mM His–1 mM MES is selected as the buffer system.

5. Effects of different His concentrations: the experiment explores the effect of His concentration on the separation and detection of ofloxacin. The results show that when the His concentration is set at 1 mM, the sample peak height and the peak area are maximized, and the sample peak is separated from the EOF and background noise. Therefore, 1 mM His concentration is selected for the buffer system (Fig. 4).
6. Effects of different MES concentrations: the experiment explores the effect of MES concentration on the separation and detection of ofloxacin (Fig. 5). When the concentration of MES is chosen at 1 mM in the buffer containing 1 mM His (pH 6.5), baseline separation of ofloxacin is achieved and the peak area of ofloxacin is maximized. Therefore, a MES concentration of 1 mM is selected as the optimal condition.
7. Linearity experiments: the optimum buffer is determined to be 1 mM His (pH 6.5) and 1 mM MES. The optimum applied voltage is determined to be 1.5 kV and the optimum injection time is determined to be 10 s. Under these optimum conditions, baseline separation of ofloxacin is achieved within 1 min. A typical electropherogram of the standard solution is presented in Fig. 6.

   Working standard solutions at concentrations (x, mg/mL) of 0.1, 0.2, 0.3, 0.4, 0.5, 0.6, 0.7, 0.8, 0.9, and 1.0 mg/mL are prepared. The data of each working standard solution are collected through six repeated runs. The peak area (y, μV·s) of

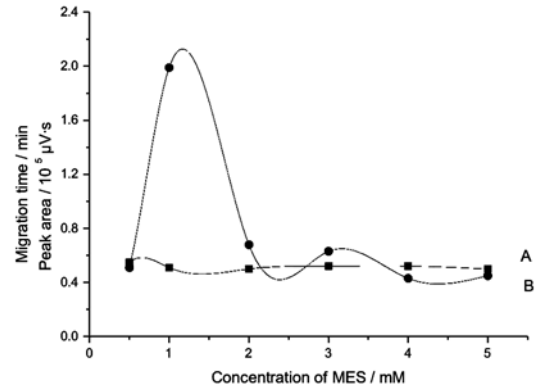

Fig. 5 Effect of concentration of MES on migration time A and peak area B. Conditions: buffer, 1 mM His (pH 6.5) containing 0.5–5 mM MES; other conditions as in Fig. 2

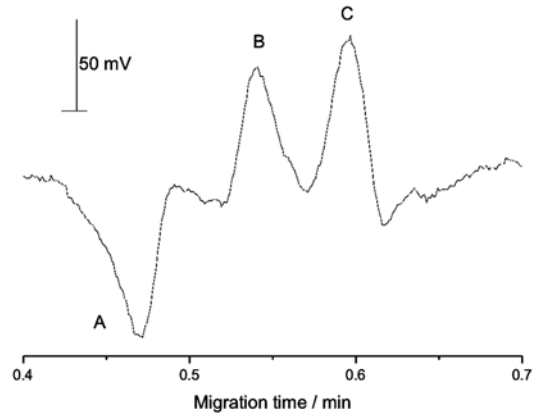

Fig. 6 Electropherogram of ofloxacin standard solution. Conditions: buffer, 1 mM His (pH 6.5) containing 1 mM MES; other conditions as in Fig. 2. Peaks: A = H_2O, B = ofloxacin, C = EOF

each working standard solution is obtained from the data workstation (*see* Subheading 3.4).

An *x*–*y* standard curve is made by plotting the mean peak area versus concentration with origin 9.0. The regression equation and the square of correlation coefficient (r^2) are obtained from the linear fitting applied to the plot. The r^2 should be between 0.999 and 0.9999.

8. Repeatability experiments: 1 mL 1 mg/mL ofloxacin standard solution is diluted ten times with quartz sub-boiling distilled water. Under optimum conditions, repeat the experiment six times, and find the relative standard deviations (RSD) of the migration time and peak area, which is lower than 5 %.
9. Sample analysis: 1 mL 1 mg/mL Ofloxacin Ear Drops is diluted ten times with quartz sub-boiling distilled water. Under

optimum conditions, repeat the experiment six times. Using the regression equation and the measured peak area values, the mass concentration of ofloxacin is calculated as 3 ± 0.15 mg/mL, 100 ± 5 % of the labeled amount.

10. The recovery test: three volumes of 1 mL 0.3 mg/mL Ofloxacin Ear Drops solution are placed in three 10-mL volumetric flasks, respectively, and 1.4, 1.0, and 0.6 mL 1 mg/mL ofloxacin standard solution are added to each flask, respectively, diluted with quartz sub-boiling distilled water, and the volume is set to 10 mL with quartz sub-boiling distilled water. These three solutions correspond to high, medium, and low concentrations. Each solution is measured six times, and the average peak area is obtained from the collected data. Using the regression equation and average peak area values, the total ofloxacin mass in each solution is calculated. Subtracting the real sample ofloxacin mass from the total ofloxacin mass yields the calculated standard ofloxacin mass. Dividing the calculated standard ofloxacin mass by the real standard ofloxacin mass yields the recovery rate. The recovery rates range from 98 % to 102 %.

4 Notes

1. Tightly screw the cap of the bottle that stores Tris solution because the Tris solution can absorb carbon dioxide from the air.
2. Sodium dihydrogen phosphate solution is easy to mold and will crystallize at temperatures below 10 °C.
3. Make sure the microchip clings to the detector.
4. The temperature is held at 25 ± 0.5 °C and the humidity is held at 60 %.
5. The microchip must be cleaned carefully.
6. Timely cleaning of the microfluidic chip ensures smooth flows in the microchannel. Failure to clean the microfluidic chip in a timely manner leads to channel blockage.
7. The microchip and its surroundings must be dry and clean. A strong electric field around the microchip might influence sample detection and instrument protection.
8. All solutions should be filtered through a 0.22-μm membrane filter before sample injection.

Acknowledgments

This work is supported by the Capillary electrophoresis—Laser Lab of Lingnan Normal University of the People's Republic of China.

References

1. Manz A, Graber N, Widmer HM (1990) Miniaturized total chemical analysis system: a novel concept for chemical sensing. Sens Actuators B 1:244–248
2. Manz A, Harrison DJ, Verpoorte EMJ, Fettinger JC, Paulus A, Lüdi H, Widmer HMJ (1992) Planar chips technology for miniaturization and integration of separation techniques into monitoring systems: capillary electrophoresis on a chip. J Chromatogr A 593:253–258
3. Janasek D, Franzke J, Manz A (2006) Scaling and the design of miniaturized chemical-analysis systems. Nature 442(27):374–380
4. Chen B, Mai QH, Chen QM (2014) Determination of ofloxacin in ofloxacin ear drops by microfluidic chip with contactless conductivity detection. J Liq Chromatogr Relat Technol 37:1513–1523
5. Shin D, Tryk DA, Fujishima A, Muck A Jr, Chen G, Wang J (2004) Microchip capillary electrophoresis with a boron-doped diamond electrochemical detector for analysis of aromatic amines. Electrophoresis 25:3017–3023
6. Yang XJ, Li OL, Chen ZG, Liu C, Lan Y, Zhao S (2008) Determination of pseudoephedrine hydrochloride and dextromethorphan hydrobromide in cold tablet by microfluidic chip. Chin J Anal Chem 36:673–677
7. Cañada-Cañada F, de la Peña AM, Espinosa-Mansilla A (2009) Analysis of antibiotics in fish samples. Anal Bioanal Chem 395:987–1008
8. Li XC, Pan JB, Yang F, Feng J, Mo JY, Chen ZG (2011) Simple amperometric detector for microchip capillary electrophoresis, and its application to the analysis of dopamine and catechol. Microchim Acta 174:123–130
9. Fiorini GS, Chiu DT (2005) Disposable microfluidic devices: fabrication, function, and application. Biotechniques 38:429–446
10. Chen G, Lin YH, Wang J (2006) Monitoring environmental pollutants by microchip capillary electrophoresis with electrochemical detection. Talanta 68:497–503
11. The Pharmacopoeia Commission of the People's Republic of China (2010) Pharmacopoeia of the People's Republic of China. Chemical Industry Press, Beijing, pp 824–825
12. Amin AS (2000) Quantitation of some recently introduced antibacterial drugs using Sudan III as chromogenic reagent. Mikrochim Acta 134: 89–94
13. Espinosa-Mansilla A, de la Peña AM, Gómez DG, Salinas F (2005) HPLC determination of enoxacin, ciprofloxacin, norfloxacin and ofloxacin with photoinduced fluorimetric (PIF) detection and multiemission scanning application to urine and serum. J Chromatogr B 822:185–193
14. See KY, Elbashir AA, Saad B, Ali ASM, Aboul-Enein HY (2009) Simultaneous determination of ofloxacin and ornidazole in pharmaceutical preparations by capillary zone electrophoresis. Biomed Chromatogr 23:1283–1290
15. Elbashir AA, Saad B, Ali ASM, Saleh MI, Aboul-Enein HY (2008) Development and validation of a capillary zone electrophoresis method for the determination of ofloxacin in tablets. J Liq Chromatogr Relat Technol 31:2771–2783
16. Zhang SF, Wang LS, Chen ZG, Dang Z, Chen HQ, Deng XR (2006) Fabrication method based on marginal reinforcing and improved high-voltage contactless conductivity detector for poly(dimethylsiloxane)/ glass microchips. Chin J Anal Chem 34:1501–1506
17. Chen ZG, Li QW, Li QL, Zhou X, Lan Y, Wei YF, Mo JY (2007) A thin cover glass chip for contactless conductivity detection in microchip capillary electrophoresis. Talanta 71:1944–1950
18. Li OL, Tong YL, Chen ZG, Liu C, Zhao S, Mo JY (2008) A glass/PDMS hybrid microfluidic chip embedded with integrated electrodes for contactless conductivity detection. Chromatographia 68:1039–1044
19. Ruecha N, Siangproh W, Chailapakul O (2011) A fast and highly sensitive detection of cholesterol using polymer microfluidic devices and amperometric system. Talanta 84:1323–1328
20. Pumera M, Wang J, Grushka E, Lev O (2007) Organically modified sols as pseudostationary phases for microchip electrophoresis. Talanta 72:711–715
21. Wang J, Chen G, Chatrathi MP, Wang M, Rinehart R, Muck A (2008) Screen-printed contactless conductivity detector for microchip capillary electrophoresis. Electroanalysis 20(22):2416–2421

Part III

Microchip Capillary Electrophoresis of Nucleic Acids, Proteins, Peptides, Pathogens

Chapter 6

Microchip Capillary Electrophoresis: Quantum Dots and Paramagnetic Particles for Bacteria Immunoseparation

Rapid Superparamagnetic-Beads-Based Automated Immunoseparation of Zn-Proteins from Staphylococcus aureus with Nanogram Yield

Sona Krizkova, Hoai Viet Nguyen, Maja Stanisavljevic, Pavel Kopel, Marketa Vaculovicova, Vojtech Adam, and Rene Kizek

Abstract

The emergence of drug-resistant bacteria and new or changing infectious pathogens is an important public health problem as well as a serious socioeconomic concern. Immunomagnetic separation-based methods create new possibilities for rapidly recognizing many of these pathogens. Nanomaterial-based techniques including fluorescent labeling by quantum dots as well as immunoextraction by magnetic particles are excellent tools for such purposes. Moreover, the combination with capillary electrophoresis in miniaturized microchip arrangement brings numerous benefits such as fast and rapid analysis, low sample consumption, very sensitive electrochemical and fluorescent detection, portable miniaturized instrumentation, and rapid and inexpensive device fabrication.

Here the use of superparamagnetic particle-based fully automated instrumentation to isolate pathogen *Staphylococcus aureus* and its Zn(II)-containing proteins (Zn-proteins) is reported using a robotic pipetting system speeding up the sample preparation and enabling to analyze 48 real samples within 6 h. Cell lysis and Zn-protein extractions were obtained from a minimum of 100 cells with the sufficient yield for SDS-PAGE (several tens ng of proteins).

Key words Magnetic particles, Immunoseparation, *Staphylococcus aureus*, Zn-protein

1 Introduction

1.1 Quantum Dots and Magnetic Particles

Nanoparticles are nanomaterials, which attract a lot of attention in science due to their specific physical and chemical characteristics as well as due to their small size and size-dependent characteristics. Aforementioned characteristics refer to excellent electrical, optical, magnetic, and catalytic properties.

Ann Van Schepdael (ed.), *Microchip Capillary Electrophoresis Protocols*, Methods in Molecular Biology, vol. 1274,
DOI 10.1007/978-1-4939-2353-3_6,

Quantum dots are semiconductor nanoparticles known for very good electrical and optical properties as a result of their small size, usually from 1 to 10 nm. They have specific characteristics such as wide absorption spectra and narrow emission spectra, high quantum yield, photostability, and resistance to chemical degradation. Quantum dots are usually used for labeling biomolecules [1–3], and they have wide applications in imaging of live cells [4]. In vivo targeting of tumor cells using QD-peptide was firstly reported by Akerman et al. [5]. Quantum dots besides their very wide application in medicine also have some other applications such as detection of bacteria in our environment [6–8], plant's tissue, proteins and organelles observation [9, 10], and other non-biological applications such as food industry [8, 11, 12]. Magnetic nanoparticles belong to another important group of nanoparticles. Like for all nanoparticles in this case, size and shape are directly connected to their properties as well. Decreasing magnetic nanoparticles to the small size induces their superparamagnetic characteristics, which means they exhibit better magnetic characteristics than paramagnetic ones. Typically they are produced at 10–20 nm size, and in this size each nanoparticle behaves as a single magnet with superparamagnetic characteristics in the magnetic field. After stabilization they are biodegradable and biocompatible for biological application [13]. Excellent magnetic characteristics of magnetic particles are used for easier and faster isolation of biomolecules. They are used for detection of microorganisms, and very early in the 1990s, isolation of cell organelles has been reported [14]. Today, with appropriate modification of magnetic particles, it is possible to modify them with targeted cellular proteins which can be used as a detection model [15] or for isolation or purification of biomolecules of interest such as enzymes, proteins [15–17], DNA [18–20], or other biologically important molecules. Nanoparticles used in processes of isolation or detection have shortened the time of processes as well as enabled their miniaturization due to the particles' size. Nanoparticles in combination with modern, precise instrumental techniques have a great potential, and further researches in this field could bring us excellent and useful results.

1.2 Nanoparticle-Based Immunoanalysis

A rapid detection of bacteria is extremely critical for an effective prevention and treatment of many microbial infections, pathogenic diseases, and foodborne illnesses. Several methods such as colony counting [21–23], the polymerase chain reaction (PCR) [24–27], and the enzyme-linked immunosorbent assay (ELISA) [28–31] are typically used for determining the presence and quantity of pathogens. However, the complexity of the biological matrix often requires application of an immunomagnetic separation technique prior to the analysis itself utilizing antibody-coated magnetic beads. Especially due to their large surface-to-volume ratio, magnetic particles are, with sizes ranging from few hundred nanometers to

several microns, useful for rapid immunomagnetic separation even in a dilute sample containing various background materials [32]. Among that wide variety of nanomaterials, mainly carbon nanotubes (CNTs) and gold nanoparticles (AuNPs) are gaining popularity as a label because of their chemical, electrical, and optical properties. A number of immunoassays based on CNTs have been suggested by using CNT itself [33, 34] or CNTs in combination with enzymes [35–37], polymers [34, 38], and/or metal particles [39–41]. Quantum dots can also be utilized as labels [42–44] and/or medium for indirect fluorescent determination of the immunocomplexes [45].

1.2.1 Magnetic Particles in Microchip CE

Advantages and Disadvantages of Chip CE Over the Conventional Capillary Electrophoresis

In the last 10 years, microchip capillary electrophoresis (MCE) has appeared as a result of the combination of chemical analysis and microfabrication techniques from the integrated circuit world. Capillary electrophoresis (CE) proved to be an excellent match for microchip technologies because it easily manipulates volumes at the nanoliter scale; provides fast, high-resolution separations; and requires no moving parts. The advantages of CE on chips over conventional separation techniques are small reagent and sample requirements, short analysis time, and high resolution. MCE has the potential to simultaneously analyze hundreds of samples in a matter of minutes or less. Microchips typically require only picoliters of samples. Furthermore, a microchip with both sample preparation and separation functionalities increases the possibility of integrating sample preparation and analysis on a single device [46]. However, in order to become one of the most powerful techniques, CE on chip has to face with many challenges. In microchip capillary electrophoresis, it is necessary to achieve high sensitivity detection due to the small sample size. One of the most critical aspects of CE and MCE analysis is the detection. Optical detection has traditionally been the most commonly used detection method in CE and MCE. The small sample injection volume and short path length available for optical measurements limit the detection schemes of MCE even more than in traditional CE [47]. Electrochemical detection is an attractive alternative for detection in CE and MCE.

MPs Reactors in Chip Separations

The first concept of micro total analysis system appeared in 1990 [48]. Since then, lab-on-a-chip or miniaturized analysis systems have rapidly developed. Microfluidics is a powerful technology, which has already been applied in many fields, such as point-of-care diagnosis [49], analytical chemistry [50], food safety [51, 52], single-nucleotide polymorphism [53], and drug delivery [54]. Parallel to the boom of microfluidic systems, magnetic particles (or magnetic beads) have attracted the attention of many researchers. Magnetic particles, which were widely applied to improve the selectivity and sensitivity of analysis methods, are a powerful tool with many characters. Magnetic particles display a well-controlled

surface, easy manipulation by the magnet, flexible functionalization, and large surface-to-volume ratio [55]. The magnetic particles were successfully applied in DNA hybridization [56, 57], protein analysis [58], virus detection [59], cell sorting [60], and immunoassay [61].

Magnetic separation and deposition of bacterial cells are widely used in food technology, industrial water, and environmental problems. Living *E. coli* in soil and food samples was separated by a microfluidic system using magnetic particles in some studies [62–64]. A microsystem for extraction, capture, and detection of pathogenic bacteria such as *E. coli* O157:H7 in soil sample was presented [62]. The assay protocol considered enzyme-linked immunosorbent assay, with each bacterium sandwiched between a magnetic bead and a horseradish peroxidase (HRP) enzyme. The system employed three different chips, the soil extraction and mixing chip, retention and reaction chip, and the detection chip. The extractor chip extracted bacterial solution directly from soil sample and mixed it with magnetic beads. The retention chip trapped bacteria attached to beads in a microfluidic chamber using a bar magnet. Subsequently, bacteria were bound to HRP which finally reacts with substrate solution to generate a fluorophore. The detection chip relied on a microfluidic flow cell and a pair of fibers to measure fluorescence due to the fluorophore that was related to the concentration of bacteria in the soil sample. Variation of fluorescence with concentration of bacteria in the sample was studied. Besides, the multitarget magnetic activated cell sorter, which makes use of microfluidics technology to achieve simultaneous spatially addressable sorting of multiple target cell types in a continuous-flow manner, was introduced [65]. This technique was used for sorting multiple bacterial strains by using 3 distinct subtypes of *Escherichia coli* MC1061 cells. In another work, typical Gram-positive- and Gram-negative bacteria such as *Salmonella* and *Staphylococcus* were separated by using magnetic particles in microfluidic systems [66]. This paper described an immunomagnetic separation of target bacterial cells from others by using magnetic beads. The bead surface was coated with antibodies which can capture specific organisms. The binding efficiency of immunomagnetic beads (IMB) capturing target bacterial cells was higher than 98 % when the concentrations of target and interfering bacterial cells were at the same level. The concentration of bacteria was determined indirectly by detecting adenosine 5′-triphosphate (ATP) employing the bioluminescence (BL) reaction of firefly luciferin–ATP. Benzalkonium chloride (BAC) was used as an ATP extract from living bacterial cells. The result showed that BAC could enhance the light emission when the concentration of BAC was less than 5.3×10^{-2} % (*w*/*v*) and the BL intensity reached its maximum at a BAC concentration of 2.7×10^{-2} %, which was tenfold stronger than that without BAC. A microfluidic chip combined with immunofluorescence assay for separating and detecting bacteria simultaneously was also developed. The IMBs were magnetically

fixed in the bead beds of chip channels with a 3 mm diameter NdFeB permanent magnet. The target bacterial cells could be captured magnetically and observed by a fluorescent microscope.

2 Materials

2.1 MNPs Separation of Zinc Proteins from S. aureus

1. Dynabeads MyOne™ Tosylactivated (Invitrogen, Norway).
2. Microfiltration device, such as Amicon Ultra 0.5 with cutoff 50 K (Millipore, USA). (*See* **Note 1**.)
3. Dynal magnet (Invitrogen, Norway). (*See* **Note 2**.)
4. Phosphate buffered saline (PBS) pH 7.4.
   Weigh 0.26 g $NaH_2PO_4 \cdot H_2O$ (MW 137.99), 1.44 g $Na_2HPO_4 \cdot 2H_2O$ (MW 177.99), and 8.78 g NaCl, dissolve in 0.9 L of ultrapure water, and adjust pH, if necessary. Adjust volume to 1 L with ultrapure water.
5. Coating buffer: 0.1 M sodium borate buffer pH 9.5.
   Weigh 6.183 g H_3BO_3 (MW 61.83). Dissolve in 800 mL of ultrapure water. Adjust pH to 9.5 using 5 M NaOH, and then adjust volume to 1,000 mL with ultrapure water. (*See* **Note 3**.)
6. Stock solution (3 M ammonium sulfate).
   Preparation and handling shall be performed in a fume hood. Weigh 39.6 g $(NH_4)_2SO_4$ (MW 132.1). Dissolve in 0.1 M sodium borate buffer (pH 9.5), control/adjust pH, and adjust volume to 100 mL.
7. Blocking buffer: PBS pH 7.4, 0.5 % BSA, 0.05 % Tween®20.
   Weigh 0.5 g of bovine serum albumin (BSA), sprinkle it on the surface of 90 mL of PBS pH 7.4, wait until BSA dissolves, add 5 μL of Tween®20, and adjust volume to 100 mL.
8. Washing/storage buffer: PBS pH 7.4, 0.1 % BSA, 0.05 % Tween®20.
   Weigh 0.1 g of BSA, sprinkle it on the surface of 90 mL of PBS pH 7.4, wait until BSA dissolves, add 5 μL of Tween®20, and adjust volume to 100 mL.
   To prepare storage buffer, add 0.02 % (w/v) NaN_3: add 2 mg of NaN_3 to 10 mL of washing buffer.

2.2 Isolation of Bacteria

1. Liquid broth: meat peptone 5 g/L, NaCl 5 g/L, beef extract 1.5 g/L, yeast extract 1.5 g/L, pH = 7.4 ± 0.2. Cultivation medium for staphylococci.
2. Dynal magnet. (*See* **Note 4**.)

2.3 Immuno-extraction of Zinc-Binding Proteins

1. PBS pH 4.5.
   Adjust pH of PBS pH 7.4 with HCl to the value of pH 4.5.

2. Elution buffer: 0.1 M citrate pH 3.0.
   Weigh 2.941 g of sodium citrate dihydrate (MW 294.1), dissolve in 80 mL of ultrapure water, and adjust pH to 3.0 by addition of HCl.
3. Dynal magnet. (*See* **Note 4**.)

3 Methods

3.1 Covalent Immobilization of IgG and IgY to the Paramagnetic Beads Surface

This protocol is derived from the manufacturer's manual for Dynabeads MyOne™ Tosylactivated (Invitrogen, Norway). Immunoglobulins are immobilized to the beads surface covalently via the N-terminal domain and the tosyl group. (*See* **Note 5**.) This immobilization protocol requires a relatively big amount of antibodies, but it is usable also for IgY, which lack a C-terminal protein G-binding domain. For IgG, which are used for isolation of staphylococci and G-group streptococci, this immobilization is preferable as the C-terminal domain binds the G- or A-protein on the bacterial membrane (*see* Fig. 1).

3.2 Immobilization Process

1. Resuspend the stock solution of the beads by leaving the vial on a mixing device for minimally 30 min. During this time prepare antibodies for binding.
2. Use 1,000 μg of immunoglobulins per 25 mg of beads. Calculate the appropriate volume to be pipetted from the stock solution of immunoglobulins.
3. Remove NaN_3 from the stock solution using Amicon Ultra 0.5 with cutoff 50K (Millipore, USA). Follow the instructions of the manufacturer. (1) Insert filter device into the collection tube, and pipette the calculated volume of immunoglobulins

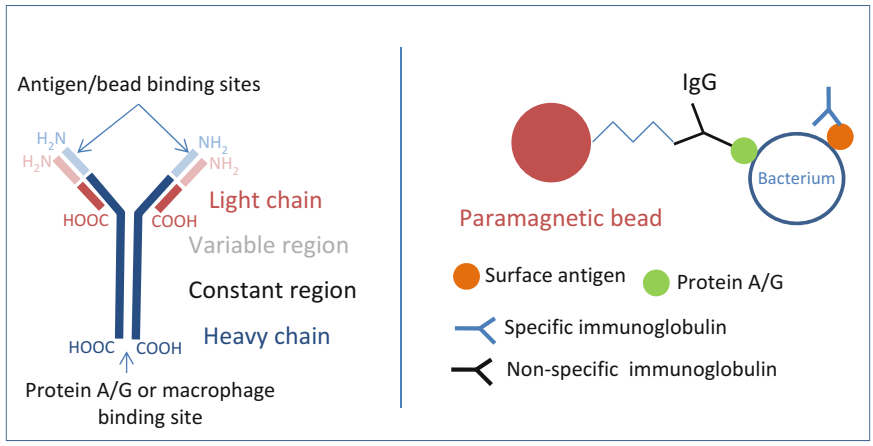

Fig. 1 Structure of immunoglobulins (*left*), binding of IgG-modified bead to the staphylococcal, or G-group streptococcal cell (*right*)

into the filter device and close the lid. (2) Spin the device at 14,000 × *g* for 10 min. (3) Pipette the same volume of PBS pH 7.4 as calculated in **step 1** into the filter device. (4) Spin the device at 14,000 × *g* for 10 min. (5) Discard the flow through. (6) Measure the new volume of immunoglobulins by pipetting. (*See* **Note 6**.)

4. To decrease pH to 2.5, add 0.2 μL of HCl (1 M) per 100 μL of immunoglobulins. Calculate the volume of HCl to be added from the new volume obtained after NaN_3 removal. Incubate for 15 min at laboratory temperature (approx. 22 °C). (*See* **Note 7**.)
5. (1) Pipette the acidified antibodies into the filter device, insert it to the collection tube, and close the lid. (2) Spin the device at 14,000 × *g* for 10 min. (3) Pipette the same volume of PBS pH 7.4 as measured prior acidification into the filter device. (4) Spin the device at 14,000 × *g* for 10 min. (5) Discard the flow through. (6) Measure the new volume of immunoglobulins by pipetting.
6. Transfer the appropriate volume of the beads corresponding to 25 mg from the stock solution into a 2 mL test tube. (*See* **Note 8**.)
7. Place the tube on a magnet (Dynal MPC) for 2 min or until the beads migrate to the side of the test tube and the liquid is clear.
8. Pipette off the supernatant carefully leaving the beads intact.
9. Remove the test tube from the magnet and add 1 mL of coating buffer.
10. Repeat **steps 7–8**.
11. Resuspend the beads in 100 μL of coating buffer.
12. To the bead pellet, pipette in this order the following volumes of coating buffer, immunoglobulins, and ammonium sulfate stock solution:

Total volume (μL)	625
Bead pellet	100
Coating buffer	$317.5 - x$
Immunoglobulins	x
3 M ammonium sulfate stock solution	207.5

13. Incubate the tube in horizontal position for 16–24 h at 37 °C with slow tilt rotation. (*See* **Note 9**.)
14. After incubation place the tube on a magnet, allow the beads to settle for approx. 2 min, until the solution is clear, and remove the liquid.

15. Add 625 μL of blocking solution and incubate the beads overnight under the same condition as in **step 12**.
16. Wash three times with 1 mL of washing buffer and resuspend in 625 μL of storage buffer.
17. Coated beads may be stored at 2–8 °C for several months.

3.3 Isolation of Bacteria

1. Resuspend the beads leaving the test tube on a mixing device for minimally 10 min.
2. Transfer 10 μL of the IgG-modified beads per sample to a new test tube.
3. Place the tube on a magnet (Dynal MPC) for 2 min or until the beads migrate to the side of the test tube and the liquid is clear.
4. Pipette off the supernatant carefully leaving the beads intact.
5. Remove the test tube from the magnet and add 1 mL of the cultivation medium.
6. Repeat **steps 3–5**.
7. Resuspend the beads in the original volume of medium. (*See* **Note 10**.)
8. Aliquot 10 μL of the beads to 2 mL test tubes.
9. Add 500 μL of the bacterial culture.
10. Incubate the test tubes for 1 h using a rotating programmable rotator mixer (Biosan, Latvia) in 2 mL microtubes.
11. Place the tube on a magnet (Dynal MPC) for 2 min or until the beads migrate to the side of the test tube and the liquid is clear.
12. Pipette off the supernatant carefully leaving the beads intact.
13. Resuspend the beads in 250 μL of the cultivation medium.
14. Place the tube on a magnet (Dynal MPC) for 2 min or until the beads migrate to the side of the test tube and the liquid is clear.
15. Resuspend the beads in 250 μL of the cultivation medium.
16. Cultivate the beads with bacteria for 3 h at 37 °C (optional, if very low bacterial content is expected).
17. Lyse the cells with ultrasound for 2 min at a frequency of 450 Hz.

3.4 Immunoextraction of Zinc-Binding Proteins

1. Resuspend the beads leaving the test tube on a mixing device for minimally 10 min.
2. Transfer 10 μL of the IgY anti-zinc-modified beads per sample to a new test tube.
3. Place the tube on a magnet (Dynal MPC) for 2 min or until the beads migrate to the side of the test tube and the liquid is clear.

4. Pipette off the supernatant carefully leaving the beads intact.
5. Remove the test tube from the magnet and add 1 mL of PBS pH 4.5.
6. Repeat **steps 3–5**.
7. Resuspend the beads in the original volume of PBS pH 4.5. (*See* **Note 11**.)
8. Aliquot 5 μL of the beads to the test tubes.
9. Place the tubes on a magnet, remove supernatant, and add 100 μL of the bacterial lysate.
10. Incubate the tubes for 30 min at 25 °C with spin shaking. Using a microcentrifuge, combine 25 cycles of medium vortex for 20 s and spinning at 1,500 × *g* for 15 s.
11. Place the tubes on a magnet, remove the supernatant, and wash the beads with 1 mL of PBS pH 7.4. (*See* **Note 12**.)
12. Resuspend the beads in 100 μL PBS pH 4.5.
13. Incubate the tubes for 30 min at 25 °C with spin shaking. Using a microcentrifuge, combine 25 cycles of medium vortex for 20 s and spinning at 1,500 × *g* for 15 s. (*See* **Notes 13–15**.)
14. Place the tubes on a magnet and transfer the supernatants to new test tubes.

4 Notes

1. It is possible to use any microfiltration device with the same properties.
2. It is possible to use any magnetic device for (super)paramagnetic particles handling.
3. The coating buffer is used for prewashing and coating of Dynabeads® MyOne™ Tosylactivated. Do not add any sugar and protein (apart from your ligand), i.e., to this buffer.
4. It is possible to use any magnetic device for (super)paramagnetic particles handling.
5. When handling uncoated Dynabeads® MyOne™ Tosylactivated, do not use any buffer containing protein or amino groups (glycine, Tris, etc.).
6. Sodium azide removal is necessary, because NaN_3 binds to tosyl groups of the beads.
7. Acidification of the antibodies for 15 min at room temperature or 1 h at 4 °C and then raising pH to approx. neutral prior addition to the beads generally increase binding and function of the antibodies.

8. Always check the bead concentration. For Dynabeads MyOne™ Tosylactivated (#655.01, Invitrogen, Norway), the appropriate volume is 250 μL.
9. During the incubation, don't allow the beads to settle, but don't shake the beads thoroughly.
10. Washing of the beads is necessary to remove bactericidal NaN_3.
11. This step is necessary to elute bound zinc from buffers, which reduces the binding capacity of the beads.
12. This step is necessary to remove unspecifically bound proteins.
13. In this step the proteins are eluted from the beads.
14. Depending on your sample type, the elution buffer composition may be modified; generally, the Zn-binding proteins are eluted by decreasing pH below 5, but the IgY molecule becomes unstable when pH decreases below 2.
15. The most effective is elution to a reducing SDS-PAGE sample buffer, but IgY fragments are co-eluted with the sample proteins.

Acknowledgment

The author M.V. wishes to express her thanks to project CZ.1.07/2.3.00/30.0039 for financial support.

References

1. Drbohlavova J, Adam V, Kizek R, Hubalek J (2009) Quantum dots—characterization, preparation and usage in biological systems. Int J Mol Sci 10:656–673
2. Ryvolova M, Chomoucka J, Janu L, Drbohlavova J, Adam V, Hubalek J, Kizek R (2011) Biotin-modified glutathione as a functionalized coating for bioconjugation of CdTe based quantum dots. Electrophoresis 32: 1619–1622
3. Stanisavljevic M, Janu L, Smerkova K, Krizkova S, Pizurova N, Ryvolova M, Adam V, Hubalek J, Kizek R (2013) Study of streptavidin-modified quantum dots by capillary electrophoresis. Chromatographia 76:335–343
4. Trojan V, Chomoucka J, Krystofova O, Hubalek J, Babula P, Kizek R, Havel L (2010) Quantum dots (CdSe) modified by glutathione and their localization of tobacco BY-2 cells. J Biotechnol 150:S479
5. Akerman ME, Chan WCW, Laakkonen P, Bhatia SN, Ruoslahti E (2002) Nanocrystal targeting in vivo. Proc Natl Acad Sci U S A 99:12617–12621
6. Lee LY, Ong SL, Hu JY, Ng WJ, Feng YY, Tan XL, Wong SW (2004) Use of semiconductor quantum dots for photostable immunofluorescence labeling of Cryptosporidium parvum. Appl Environ Microbiol 70:5732–5736
7. Shanehsaz M, Mohsenifar A, Hasannia S, Pirooznia N, Samaei Y, Shamsipur M (2013) Detection of Helicobacter pylori with a nanobiosensor based on fluorescence resonance energy transfer using CdTe quantum dots. Microchim Acta 180:195–202
8. Wang LX, Wu CS, Fan XD, Mustapha A (2012) Detection of Escherichia coli O157:H7 and Salmonella in ground beef by a bead-free quantum dot-facilitated isolation method. Int J Food Microbiol 156:83–87
9. Chen T, Wang XH, von Wangenheim D, Zheng MZ, Samaj J, Ji WQ, Lin JX (2012) Probing and tracking organelles in living plant cells. Protoplasma 249:157–167
10. Ravindran S, Kim S, Martin R, Lord EM, Ozkan CS (2005) Quantum dots as bio-labels for the localization of a small plant adhesion protein. Nanotechnology 16:1–4

11. Carrillo-Carrion C, Simonet BM, Valcarcel M (2011) Rapid fluorescence determination of diquat herbicide in food grains using quantum dots as new reducing agent. Anal Chim Acta 692:103–108
12. Guo DS, Chen GH, Tong MZ, Wu CQ, Fang R, Yi LX (2012) Determination of five preservatives in food by capillary electrophoresis with quantum dot indirect laser induced fluorescence. Chin J Anal Chem 40:1379–1384
13. Drbohlavova J, Hrdy R, Adam V, Kizek R, Schneeweiss O, Hubalek J (2009) Preparation and properties of various magnetic nanoparticles. Sensors 9:2352–2362
14. Kausch AP, Owen TP, Narayanswami S, Bruce BD (1999) Organelle isolation by magnetic immunoabsorption. Biotechniques 26:336–343
15. Krejcova L, Dospivova D, Ryvolova M, Kopel P, Hynek D, Krizkova S, Hubalek J, Adam V, Kizek R (2012) Paramagnetic particles coupled with an automated flow injection analysis as a tool for influenza viral protein detection. Electrophoresis 33:3195–3204
16. Krizkova S, Jilkova E, Krejcova L, Cernei N, Hynek D, Ruttkay-Nedecky B, Sochor J, Kynicky J, Adam V, Kizek R (2013) Rapid superparamagnetic-beads-based automated immunoseparation of Zn-proteins from Staphylococcus aureus with nanogram yield. Electrophoresis 34:224–234
17. Krizkova S, Ryvolova M, Hynek D, Eckschlager T, Hodek P, Masarik M, Adam V, Kizek R (2012) Immunoextraction of zinc proteins from human plasma using chicken yolk antibodies immobilized onto paramagnetic particles and their electrophoretic analysis. Electrophoresis 33:1824–1832
18. Masarik M, Huska D, Adam V, Hubalek J, Provaznik I, Trnkova L, Kizek R (2010) Automated pipetting system coupled with micro- and nanoparticles as a new tool for study of nucleic acids. Int J Mol Med 26:S46
19. Huska D, Ryvolova M, Chomoucka J, Drbohlavova J, Adam V, Trnkova L, Provaznik I, Hubalek J, Kizek R (2010) Determination of viral nucleic acids by electrochemical detection array using paramagnetic nanoparticles. J Biochem Techol 2:S74–S75
20. Adam V, Huska D, Hubalek J, Kizek R (2010) Easy to use and rapid isolation and detection of a viral nucleic acid by using of paramagnetic microparticles and carbon nanotubes-based screen-printed electrodes. Microfluid Nanofluid 8:329–339
21. Aungst M, King J, Steele A, Gordon M (2004) Low colony counts of asymptomatic group B streptococcus bacterium: a survey of practice patterns. Am J Perinatol 21:403–407
22. Paulsen P, Schopf E, Smulders FJM (2006) Enumeration of total aerobic bacteria and Escherichia coli in minced meat and on carcass surface samples with an automated most-probable-number method compared with colony count protocols. J Food Prot 69: 2500–2503
23. Wang XD, Yamaguchi N, Someya T, Nasu M (2007) Rapid and automated enumeration of viable bacteria in compost using a microcolony auto counting system. J Microbiol Methods 71:1–6
24. Landete JM, de las Rivas B, Marcobal A, Munoz R (2011) PCR methods for the detection of biogenic amine-producing bacteria on wine. Ann Microbiol 61:159–166
25. Kemp M, Jensen KH, Dargis R, Christensen JJ (2010) Routine ribosomal PCR and DNA sequencing for detection and identification of bacteria. Future Microbiol 5:1101–1107
26. Malorny B, Lofstrom C, Wagner M, Kramer N, Hoorfar J (2008) Enumeration of Salmonella bacteria in food and feed samples by real-time PCR for quantitative microbial risk assessment. Appl Environ Microbiol 74: 1299–1304
27. Yamamoto Y (2002) PCR in diagnosis of infection: detection of bacteria in cerebrospinal fluids. Clin Diagn Lab Immunol 9: 508–514
28. Adawi A, Neville LF (2012) Colony to colorimetry in 6 h: ELISA detection of a surface-expressed Pseudomonas aeruginosa virulence factor using immobilized bacteria. Diagn Microbiol Infect Dis 74:84–87
29. Fach P, Perelle S, Grout J, Dilasser F (2003) Comparison of different PCR tests for detecting Shiga toxin-producing Escherichia coli O157 and development of an ELISA-PCR assay for specific identification of the bacteria. J Microbiol Methods 55:383–392
30. Gutierrez R, Garcia T, Gonzalez I, Sanz B, Hernandez PE, Martin R (1997) A quantitative PCR-ELISA for the rapid enumeration of bacteria in refrigerated raw milk. J Appl Microbiol 83:518–523
31. Gutierrez R, Garcia T, Gonzalez I, Sanz B, Hernandez PE, Martin R (1998) Quantitative detection of meat spoilage bacteria by using the polymerase chain reaction (PCR) and an enzyme linked immunosorbent assay (ELISA). Lett Appl Microbiol 26:372–376
32. Sung YJ, Suk HJ, Sung HY, Li T, Poo H, Kim MG (2013) Novel antibody/gold nanoparticle/magnetic nanoparticle nanocomposites for immunomagnetic separation and rapid colorimetric detection of Staphylococcus aureus in milk. Biosens Bioelectron 43:432–439

33. Lee DJ, Chander Y, Goyal SM, Cui TH (2011) Carbon nanotube electric immunoassay for the detection of swine influenza virus H1N1. Biosens Bioelectron 26:3482–3487
34. Villamizar RA, Maroto A, Rius FX, Inza I, Figueras MJ (2008) Fast detection of Salmonella Infantis with carbon nanotube field effect transistors. Biosens Bioelectron 24:279–283
35. Bi S, Zhou H, Zhang SS (2009) Multilayers enzyme-coated carbon nanotubes as biolabel for ultrasensitive chemiluminescence immunoassay of cancer biomarker. Biosens Bioelectron 24:2961–2966
36. Chunglok W, Wuragil DK, Oaew S, Somasundrum M, Surareungchai W (2011) Immunoassay based on carbon nanotubes-enhanced ELISA for Salmonella enterica serovar Typhimurium. Biosens Bioelectron 26:3584–3589
37. Piao Y, Jin Z, Lee D, Lee HJ, Na HB, Hyeon T, Oh MK, Kim J, Kim HS (2011) Sensitive and high-fidelity electrochemical immunoassay using carbon nanotubes coated with enzymes and magnetic nanoparticles. Biosens Bioelectron 26:3192–3199
38. Wang J (2005) Carbon-nanotube based electrochemical biosensors: a review. Electroanalysis 17:7–14
39. Lerner MB, Goldsmith BR, McMillon R, Dailey J, Pillai S, Singh SR, Johnson ATC (2011) A carbon nanotube immunosensor for Salmonella. AIP Adv 1:1–8
40. Zarei H, Ghourchian H, Eskandari K, Zeinali M (2012) Magnetic nanocomposite of anti-human IgG/COOH-multiwalled carbon nanotubes/Fe3O4 as a platform for electrochemical immunoassay. Anal Biochem 421: 446–453
41. Amaro M, Oaew S, Surareungchai W (2012) Scano-magneto immunoassay based on carbon nanotubes/gold nanoparticles nanocomposite for Salmonella enterica serovar Typhimurium detection. Biosens Bioelectron 38:157–162
42. Beckman EM, Kawaguchi T, Chandler GT, Decho AW (2008) Development of a microplate-based fluorescence immunoassay using quantum dot streptavidin conjugates for enumeration of putative marine bacteria, Alteromonas sp., associated with a benthic harpacticoid copepod. J Microbiol Methods 75:441–444
43. Zhu XS (2009) ANYL 94—optical immunoassay for pathogenic bacteria using quantum-dot labeling and dissociation of immunocomplexes. Abstr Pap Am Chem Soc 238:1
44. Dudak FC, Boyaci IH (2008) ANYL 148—multiplexed bacteria detection by coupling immunomagnetic separation with quantum dot labeling. Abstr Pap Am Chem Soc 235:1
45. Decho AW, Beckman EM, Chandler GT, Kawaguchi T (2008) Application of photostable quantum dots for indirect immunofluorescent detection of specific bacterial serotypes on small marine animals. Nanotechnology 19:1–6
46. Dolnik V, Liu SR, Jovanovich S (2000) Capillary electrophoresis on microchip. Electrophoresis 21:41–54
47. Gong MJ, Wehmeyer KR, Limbach PA, Arias F, Heineman WR (2006) On-line sample preconcentration using field-amplified stacking injection in microchip capillary electrophoresis. Anal Chem 78:3730–3737
48. Manz A, Graber N, Widmer HM (1990) Miniaturized total chemical-analysis systems—a novel concept for chemical sensing. Sens Actuator B-Chem 1:244–248
49. Srinivasan V, Pamula VK, Fair RB (2004) An integrated digital microfluidic lab-on-a-chip for clinical diagnostics on human physiological fluids. Lab Chip 4:310–315
50. Yan JL, Du Y, Liu JF, Cao WD, Sun SH, Zhou WH, Yang XR, Wang EK (2003) Fabrication of integrated microelectrodes for electrochemical detection on electrophoresis microchip by electroless deposition and micromolding in capillary technique. Anal Chem 75:5406–5412
51. Jin SQ, Yin BC, Ye BC (2009) Multiplexed bead-based mesofluidic system for detection of food-borne pathogenic bacteria. Appl Environ Microbiol 75:6647–6654
52. Zhang CS, Wang HY, Xing D (2011) Multichannel oscillatory-flow multiplex PCR microfluidics for high-throughput and fast detection of foodborne bacterial pathogens. Biomed Microdevices 13:885–897
53. Chen L, Manz A, Day PJR (2007) Total nucleic acid analysis integrated on microfluidic devices. Lab Chip 7:1413–1423
54. Fiering J, Mescher MJ, Swan EEL, Holmboe ME, Murphy BA, Chen Z, Peppi M, Sewell WF, McKenna MJ, Kujawa SG, Borenstein JT (2009) Local drug delivery with a self-contained, programmable, microfluidic system. Biomed Microdevices 11:571–578
55. Yu X, Xia HS, Sun ZD, Lin Y, Wang K, Yu J, Tang H, Pang DW, Zhang ZL (2013) On-chip dual detection of cancer biomarkers directly in serum based on self-assembled magnetic bead patterns and quantum dots. Biosens Bioelectron 41:129–136
56. Cai S, Lau CW, Lu JZ (2010) Sequence-specific detection of short-length DNA via template-dependent surface-hybridization events. Anal Chem 82:7178–7184
57. Li HG, He ZK (2009) Magnetic bead-based DNA hybridization assay with chemiluminescence and chemiluminescent imaging detection. Analyst 134:800–804

58. Centi S, Tombelli S, Minunni M, Mascini M (2007) Aptamer-based detection of plasma proteins by an electrochemical assay coupled to magnetic beads. Anal Chem 79:1466–1473
59. Zhao W, Zhang WP, Zhang ZL, He RL, Lin Y, Xie M, Wang HZ, Pang DW (2012) Robust and highly sensitive fluorescence approach for point-of-care virus detection based on immunomagnetic separation. Anal Chem 84:2358–2365
60. Smith JE, Medley CD, Tang ZW, Shangguan D, Lofton C, Tan WH (2007) Aptamer-conjugated nanoparticles for the collection and detection of multiple cancer cells. Anal Chem 79:3075–3082
61. Dungchai W, Siangproh W, Lin JM, Chailapakul O, Lin S, Ying XT (2007) Development of a sensitive micro-magnetic chemiluminescence enzyme immunoassay for the determination of carcinoembryonic antigen. Anal Bioanal Chem 387:1965–1971
62. Sen A, Harvey T, Clausen J (2011) A microsystem for extraction, capture and detection of E-coli O157:H7. Biomed Microdevices 13: 705–715
63. Varshney M, Li Y, Srinivasan B, Tung S, Erf G, Slavik MF, Ying Y, Fang W (2006) A microfluidic filter biochip-based chemiluminescence biosensing method for detection of Escherichia coli O157:H7. Trans ASABE 49:2061–2068
64. Varshney M, Li YB, Srinivasan B, Tung S (2007) A label-free, microfluidics and interdigitated array microelectrode-based impedance biosensor in combination with nanoparticles immunoseparation for detection of Escherichia coli O157:H7 in food samples. Sensor Actuator B Chem 128:99–107
65. Adams JD, Kim U, Soh HT (2008) Multitarget magnetic activated cell sorter. Proc Natl Acad Sci U S A 105:18165–18170
66. Qiu JM, Zhou Y, Chen H, Lin JM (2009) Immunomagnetic separation and rapid detection of bacteria using bioluminescence and microfluidics. Talanta 79:787–795

Chapter 7

Fast High-Throughput Screening of H1N1 Virus by Parallel Detection with Multichannel Microchip Electrophoresis

Peng Zhang, He Nan, Seungah Lee, and Seong Ho Kang

Abstract

Influenza is one of the acute respiratory diseases of human caused by the influenza A (H1N1) virus and accounted for major public health concerns worldwide. The polymerase chain reaction (PCR) methods are the most popular tools for clinical diagnosis of influenza A virus. Microchip electrophoresis is a widely used method for DNA molecules separation. Herein, we describe the fast and high-throughput separation of hemagglutinin (HA) and nucleocapsid protein (NP) gene PCR products (116 bp and 195 bp, respectively) by parallel detection with multichannel microchip electrophoresis and programmed step electric field strength (PSEFS).

Key words *Influenza A* (H1N1) virus, Multichannel microchip electrophoresis, High-throughput separation

1 Introduction

Influenza is one of the most common infectious respiratory diseases of human caused by the influenza *A* (H1N1) virus [1]. It tends to occur most frequently in the elderly and children causing significant morbidity and mortality, and due to the high infectiousness, it can spread worldwide rapidly and become a major public health menace [2]. Recently, various protein- and gene-based detection methods have been used in clinical and laboratory diagnosis of the H1N1 virus [3–8]. For instance, the widely used rapid influenza A virus diagnostic test (RIDT) is based on the immunochromatographic lateral flow tests and uses monoclonal antibodies directly against the nucleocapsid protein (NP) of influenza virus [3]. However, the RIDT assay is still limited by its low accuracy (<70 %) [4, 5]. On the contrary, the gene detection methods based on polymerase chain reaction (PCR) assays are able to detect influenza virus with 97 % accuracy [6–8]. However, current PCR methods continue to rely heavily on slab gel electrophoresis (SGE) analysis; they take a few hours to obtain results, which is both time and labor expensive [9].

Ann Van Schepdael (ed.), *Microchip Capillary Electrophoresis Protocols*, Methods in Molecular Biology, vol. 1274,
DOI 10.1007/978-1-4939-2353-3_7,

Microchip electrophoresis (ME), due to its high-performance separation capacities for a variety of biomolecules, has become a powerful separation method which can reduce chemical consumption and the cost of analysis [10, 11]. On the other hand, integrating many separation channels onto a single wafer to form a multichannel microchip electrophoresis (MCME) system can provide a much more stable, precise, and user-friendly technique with extremely high throughput [12].

In this study, we developed a fast, high-throughput, and precise MCME separation method using programmed step electric field strength (PSEFS) with a laser-induced fluorescence (LIF) detector to analyze influenza A virus DNA PCR products [13]. The electric field strength, DNA molecular size, migration times, and peak areas were discussed for fast and high-throughput detection without loss of resolution.

2 Materials

All the buffers and solutions were prepared using ultrapure water (18.3 MΩ·cm at 25 °C) prepared by Human® water purification system (Human power I+, Human, Seoul, Korea) and analytical or higher grade reagents. All the reagents were prepared and stored at room temperature unless indicated otherwise. The waste materials were treated following all waste disposal regulations strictly.

2.1 Buffers

1. 1× TBE buffer: 0.089 M Tris, 0.089 M borate, 0.002 M EDTA, pH 8.4 (*see* **Note 1**).
2. 1× TAE buffer: 0.04 M Tris-acetate, 0.001 M EDTA, pH 8.4 (*see* **Note 1**).
3. ME running buffer: 1× TBE buffer, 0.5 ppm ethidium bromide (EtBr) (*see* **Note 2**).

2.2 H1N1 Virus DNA PCR Components

1. PalmTaq™ High-Speed PCR kit (Ahram Biosystems Inc., Seoul, Korea) containing PalmTaq™ 5× HS buffer solution (1.5 mM $MgCl_2$ final concentration), dNTP mixture (10 mM each dNTP), and PalmTaq™ High-Speed DNA polymerase (5 units/μL) (*see* **Note 3**).
2. To amplify the hemagglutinin (HA) and nucleocapsid protein (NP) gene, primers for HA (forward, 5′-GTG CTA TAA ACA CCA GCC TCC CA-3′, and reverse, 5′-CGG GAT ATT CCT CAA TCC TGT GGC-3′) and NP (forward, 5′-GCA CGG TCA GCA CTT ATT CTA AG-3′, and reverse, 5′-GTG AGC TGG GTT TTC ATT TGG TC-3′) were used.
3. Palm PCR F1-12 device (Ahram Biosystems Inc.).

4. H1N1 virus DNA samples (Ahram Biosystems Inc.).
5. Clinical H1N1 virus DNA sample (National Culture Collection for Pathogens, NCCP, Osong-eup, Korea).

2.3 Slab Gel Electrophoresis

1. 2.0 % agarose gel (Sigma, St. Louis, MO, USA).
2. 100-bp DNA ladder (14.4 ng/μL, Genepia, Seoul, Korea).
3. Video documentation system (MC2000, CoreBio, Seoul, Korea).

2.4 Multichannel Microchip Preparation

1. Lab-built multichannel microchip: The glass-based multichannel microchip was designed as a two-layer structure with three separation channels (50 μm wide and 10 μm deep, 6.5 cm long) and 10 reservoirs (*see* Fig. 1 and **Note 4**). Each channel is a typical double-T type with 150 μm split and both reservoirs have the same size (2.0 mm in diameter and 0.7 mm in depth). The interspace between the three channels (parallel part) was 150 μm.

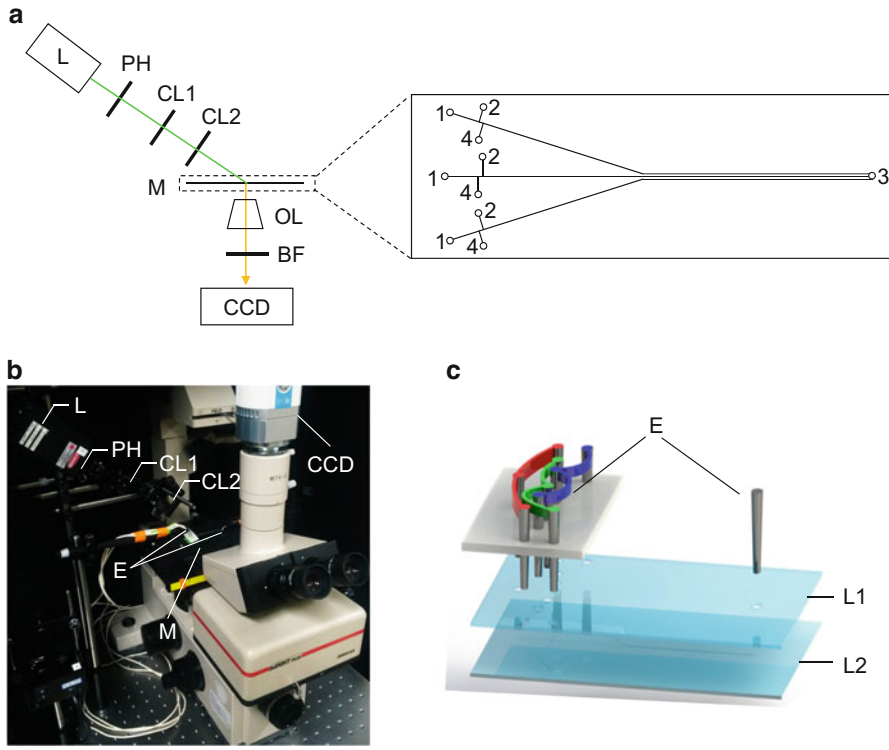

Fig. 1 Multichannel ME with a laser-induced fluorescence (LIF) detection system. (**a**) Schematic diagram of the LIF detection system and multichannel microchip. (**b**) Physical layout of the MCME system. (**c**) Two-layer structure of the multichannel microchip and setup of the electrodes. Indication: *L* laser, *PH* pin hole, *CL*1 first cylindrical lens, *CL*2 second cylindrical lens, *M* multichannel microchip, *OL* objective lens, *BF* band-pass filter, *CCD* charge-coupled device, *E* electrodes, *L*1 layer 1, *L*2 layer 2, *reservoir* 1 buffer inlet, *reservoir* 2 sample outlet, *reservoir* 3 buffer waste, and *reservoir* 4 sample inlet (reproduced from [13] with permission from Korean Chemical Society)

2.5 Multichannel Microchip Electrophoresis (MCME)

1. ME coating gel: 0.050 g poly(vinylpyrrolidone) (PVP, $M_r = 1{,}000{,}000$) (Polysciences, Warrington, England) was dissolved in 5.0 mL ME running buffer with the final concentration 1.0 % w/v. The solution was shaken ~5 min to dissolve PVP completely and then left to stand for 2 h to remove any bubbles (*see* **Note 5**).
2. ME sieving gel: 0.015 g poly(ethylene oxide) (PEO, $M_r = 8{,}000{,}000$) (Sigma) was dissolved in 5.0 mL ME running buffer with the final concentration 0.3 % w/v. The PEO solution was stirred overnight to dissolve the polymer and to remove any bubbles (*see* **Note 6**).
3. Vacuum pump (EYELA A-3s vacuum aspirator, Tokyo Rikakikai Co., Ltd, Tokyo, Japan).

2.6 MCME System with Laser-Induced Fluorescence (LIF) Detection

1. A microscope (IMT-2, Olympus, Tokyo, Japan) with an objective lens (10×/0.25 N.A., Olympus, Tokyo, Japan) was used to collect and transmit the fluorescence signal from the analyte to the detector.
2. A diode-pumped solid-state laser (excitation at 532 nm, Shanghai Laser & Optics Century, Shanghai, China) was used as an excitation source (*see* **Note 7**).
3. Two cylindrical lenses were used to focus the laser beam on the central part of the detection area of the multichannel microchip (*see* **Note 8**).
4. A charge-coupled device (CCD) (01-EXI-BLU-R-F-M-14-C, QImaging, Surrey, Canada) was used as the detector.
5. A band-pass filter (35-5081, 600 ± 8 nm, Ealing Catalog, Rocklin, CA, USA) was placed in front of the CCD camera to filter out irrelevant wavelengths.
6. Image-Pro Plus (IPP, Version 7.0, Media Cybernetics, Bethesda, MD, USA) program was used to acquire and analyze the fluorescent images of the detection region in the microchip.
7. Platinum wires (0.4 mm in diameter) were inserted into the reservoirs as electrodes (*see* **Note 9**).
8. The high-voltage power supply (DBHV-100, NanoEntek, Seoul, Korea) was controlled by DBMA-100 program.

3 Methods

Carry out all procedures at room temperature unless specified otherwise.

3.1 H1N1 Virus DNA PCR

1. 20 μL of PalmTaq™ 5× HS buffer solution (1.5 mM $MgCl_2$ final concentration) was added to 62.6 μL of sterilized distilled water, followed by 5 μL each of forward primer (10 μM),

reverse primer (10 μM), and template DNA (≤200 mg). Following the addition of 2 μL of dNTP mixture (10 mM each dNTP) and 0.4 μL of PalmTaq™ High-Speed DNA polymerase (5 units/μL), the total amount of the reaction mixture was divided into five sample tubes (*see* **Note 10**).

2. The following protocols programmed in the Palm PCR F1-12 device were performed: denaturation temperature of 98 °C and annealing temperature of 58 °C; the number of amplification cycles was set as 30 (*see* **Note 11**).
3. The final PCR products of HA and NP were mixed to confirm the separation of the mixture sample (HA:NP = 1:1).
4. The clinical sample of H1N1 virus DNA was amplified in the same way.

3.2 Slab Gel Electrophoresis

Amplified DNA molecules were identified by SGE in 2.0 % agarose gel using a 1× TAE buffer, stained with EtBr, and then photographed using a still video documentation system. The sizes of the DNA products were determined relative to a 100-bp DNA ladder (*see* Fig. 2).

3.3 100-bp DNA Ladder Separation by MCME

1. Multichannel microchip washing: The microchannel was rinsed with water followed by running buffer for 10 min each (*see* **Note 12**).
2. Surface coating of microchannel: The 1.0 % PVP dynamic coating was filled hydrodynamically using a vacuum pump for 5 min (*see* **Note 13**).

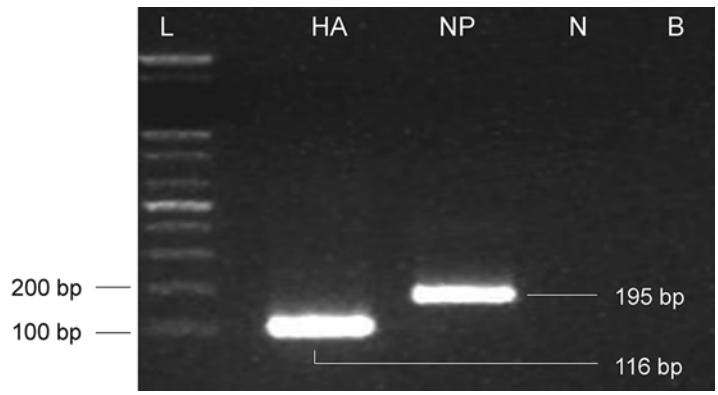

Fig. 2 Representative slab gel electrophoresis of amplified PCR products for the H1N1 virus. SGE conditions: 2.0 % agarose gel matrix in 1× TAE buffer (pH 8.4); applied voltage, 150 V for 50 min; temperature, ambient. *L* DNA ladder, *HA* hemagglutinin gene PCR product (116 bp), *NP* nucleocapsid protein gene PCR product (195 bp), *N* negative control, and *B* blank (reproduced from [13] with permission from Korean Chemical Society)

3. Filling of the microchannel with sieving gel: The 0.3 % PEO sieving matrix was filled hydrodynamically using a vacuum pump for 5 min (*see* **Note 13**).
4. Sample injection: 2.0 μL 100-bp DNA ladder was injected into the sample inlet reservoirs (reservoir 4 in Fig. 1). Then the multichannel microchip was placed and fixed on the stage of the microscope. The injection potential was set as 480 V at the sample outlet reservoir 2 followed by grounding the sample inlet reservoir 4 for 60 s after inserting the electrodes.
5. Effective length setting: Use the stage control of the microscope to set the effective length as 3.0 cm (*see* **Note 14**).
6. Applying constant electric field strength: A constant electric field strength in the range of 100–700 V/cm was used to separate all the DNA molecules of the DNA ladder (*see* Fig. 3).
7. Fluorescent signal acquisition and analysis: 2,000-frame fluorescent images of the separation channels were acquired and analyzed by the IPP program with 79 ms exposure time and 100 ms time interval (*see* **Note 15**).

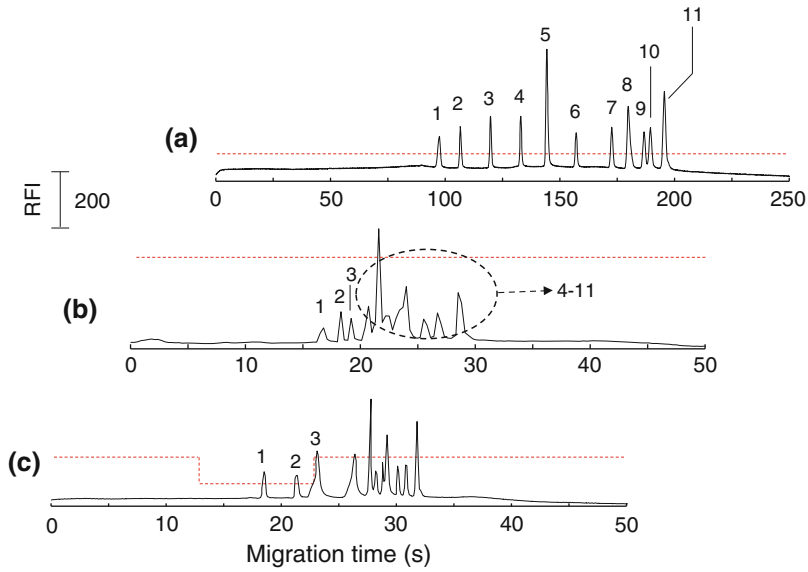

Fig. 3 Electropherograms of the 100-bp DNA ladder in the MCME system. (**a**) Low constant electric field strength (LCEFS) for separation, (**b**) high constant electric field strength (HCEFS), and (**c**) programmed step electric field strength (PSEFS) for separation. Separation conditions: running buffer, 1× TBE buffer (pH 8.4) with 0.5 ppm EtBr; coating matrix, 1.0 % PVP (M_r = 1,000,000); sieving matrix, 0.3 % PEO (M_r = 8,000,000); DNA ladder concentration, 14.4 ng/μL; applied separation electric field, (**a**) 138 V/cm, (**b**) 615 V/cm, and (**c**) 615 V/cm from 0 to 13 s, 300 V/cm from 13 to 23 s, 615 V/cm from 23 to 50 s. Peaks: 1 = 100 bp, 2 = 200 bp, 3 = 300 bp, 4 = 400 bp, 5 = 500 bp, 6 = 600 bp, 7 = 800 bp, 8 = 1,000 bp, 9 = 1,500 bp, 10 = 2,000 bp, 11 = 3,000 bp. *RFI* relative fluorescence intensity (reproduced from [13] with permission from Korean Chemical Society)

8. After the separation, the determination of whether PSEFS or constant electric field strength provided the best results was established (*see* **Note 16**).
9. If PSEFS was chosen, we eliminated or decreased the portions of the gradient prior to the first DNA peak (100 bp) and following the last DNA peak (200 bp) (*see* **Note 17**).
10. If PSEFS was acceptable, the gradient time was optimized to reduce the separation time (*see* **Note 18**).
11. After optimization, the best PSEFS conditions for the fast separation of 100-bp and 200-bp DNA molecules were determined at 615 V/cm from 0 s to 13 s, 300 V/cm from 13 s to 23 s, and 615 V/cm from 23 s to 50 s (*see* Fig. 3 and **Note 18**).

3.4 H1N1 Virus DNA PCR Products Fast Separation by MCME

1. The multichannel microchip was washed, surface coated, and filled with sieving gel as previously demonstrated.
2. 2.0 μL H1N1 virus DNA PCR products (HA, 116 bp, and NP, 195 bp) and 100-bp DNA ladder were injected into each of the three separation channels, respectively, as previously demonstrated.
3. Apply the previously optimized PSEFS (615 V/cm from 0 s to 13 s, 300 V/cm from 13 s to 23 s, and 615 V/cm from 23 s to 50 s).
4. Acquire and analyze the fluorescent signal as previously mentioned.
5. Finally, the HA and NP PCR products are detected at 19.5 s and 20.9 s, respectively (*see* Fig. 4 and Table 1).

3.5 H1N1 Virus DNA PCR Products Fast and High-Throughput Separation by MCME

1. The multichannel microchip was washed, surface coated, and filled with sieving gel as previously demonstrated.
2. The mixture of H1N1 virus DNA PCR products (HA:NP = 1:1) was injected into the three separation channels as previously demonstrated.
3. Apply the previously optimized PSEFS (615 V/cm from 0 s to 13 s, 300 V/cm from 13 s to 23 s, and 615 V/cm from 23 s to 50 s), and then acquire and analyze the fluorescent signal as previously mentioned.
4. Finally, the HA and NP PCR products are separated and detected at 19.5 s and 20.9 s, respectively (*see* Fig. 5 and Table 1).

3.6 H1N1 Virus Clinical DNA PCR Products Fast and High-Throughput Separation by MCME

1. The multichannel microchip was washed, surface coated, and filled with sieving gel as previously demonstrated.
2. The H1N1 virus clinical DNA products were injected into the three separation channels as previously demonstrated.
3. Apply the previously optimized PSEFS (615 V/cm from 0 s to 13 s, 300 V/cm from 13 s to 23 s, and 615 V/cm from 23 s

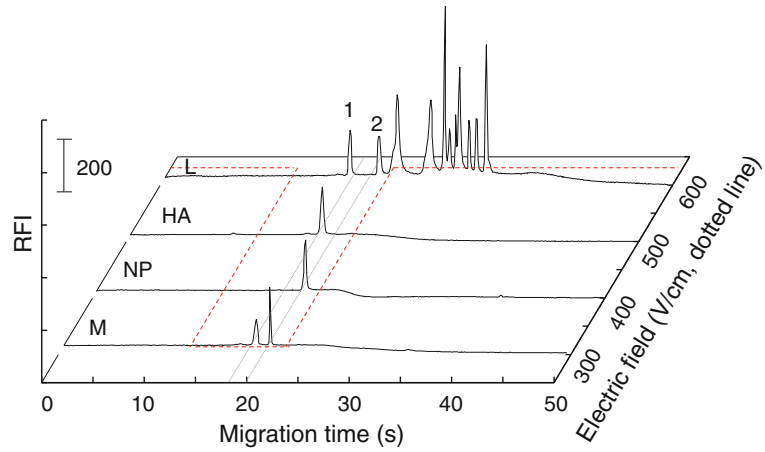

Fig. 4 Representative amplified PCR products for the H1N1 virus using PSEFS in MCME. MCME/PSEFS condition, running buffer, 1× TBE buffer (pH 8.4) with 0.5 ppm EtBr; coating matrix, 1.0 % PVP (M_r = 1,000,000); sieving matrix, 0.3 % PEO (M_r = 8,000,000); PSEFS, 615 V/cm from 0 to 13 s, 300 V/cm from 13 to 23 s, 615 V/cm from 23 to 50 s. *L* DNA ladder, *HA* hemagglutinin gene PCR product (116 bp), *NP* nucleocapsid protein gene PCR product (195 bp), *M* mixture of HA and NP PCR products. Peaks: 1 = 100 bp, 2 = 200 bp. *RFI* relative fluorescence intensity (reproduced from [13] with permission from Korean Chemical Society)

Table 1
Comparison of migration time and peak area of specific DNA molecules and PCR products of the H1N1 virus by the multichannel microchip electrophoresis method with a programmed step electric field strength (reproduced from [13] with permission from Korean Chemical Society)

Sample	Migration time (s)	Peak area
100 bp	19.20 ± 0.20	67.00 ± 0.50
200 bp	20.98 ± 0.10	63.98 ± 0.40
HA (116 bp)	20.05 ± 0.30	329.60 ± 3.80
NP (195 bp)	20.75 ± 0.40	226.30 ± 3.80

The data are presented as mean ± standard deviation (n = 3)

to 50 s), and then acquire and analyze the fluorescent signal as previously mentioned.

4. The PCR products of the clinical samples were detected at the same migration times of the HA and NP PCR products and diagnosed within 21 s (*see* Fig. 6).

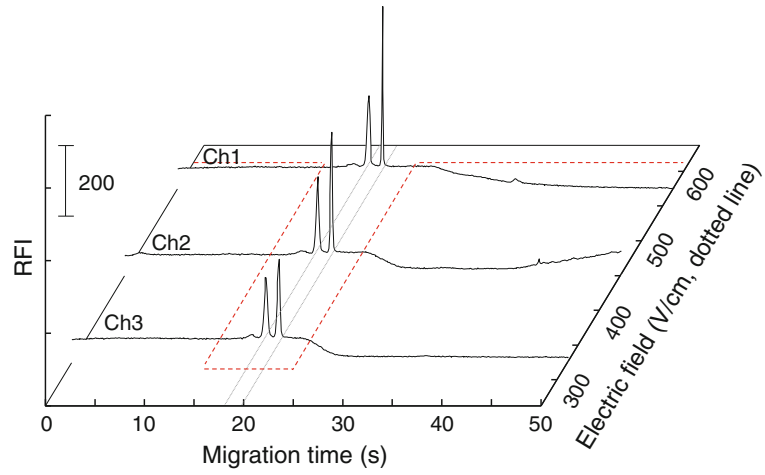

Fig. 5 High-throughput performance of the MCME/PSEFS method with amplified PCR products for the H1N1 virus from infected humans. MCME/PSEFS conditions, running buffer, 1× TBE buffer (pH 8.4) with 0.5 ppm EtBr; coating matrix, 1.0 % PVP (M_r = 1,000,000); sieving matrix, 0.3 % PEO (M_r = 8,000,000); PSEFS, 615 V/cm from 0 to 13 s, 300 V/cm from 13 to 23 s, 615 V/cm from 23 to 50 s. Ch1 = channel 1, Ch2 = channel 2, Ch3 = channel 3, *HA* hemagglutinin gene PCR product (116 bp), *NP* nucleocapsid protein gene PCR product (195 bp). *RFI* relative fluorescence intensity (reproduced from [13] with permission from Korean Chemical Society)

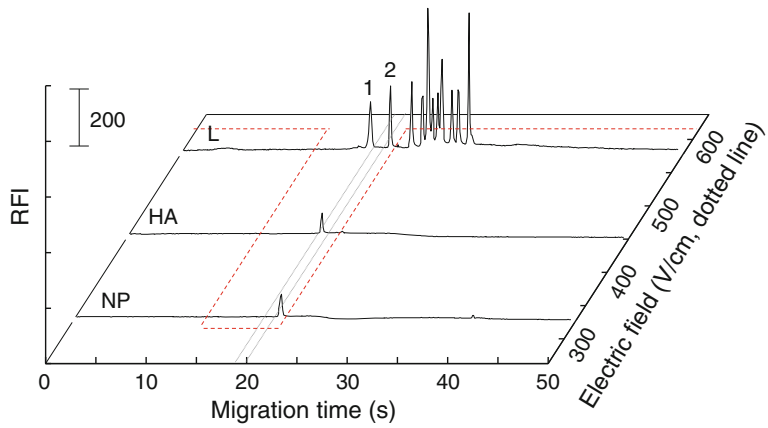

Fig. 6 Representative electropherograms of the H1N1 clinical sample after using PSEFS in MCME. MCME/PSEFS condition, running buffer, 1× TBE buffer (pH 8.4) with 0.5 ppm EtBr; coating matrix, 1.0 % PVP (M_r = 1,000,000); sieving matrix, 0.3 % PEO (M_r = 8,000,000); PSEFS, 615 V/cm from 0 to 13 s, 300 V/cm from 13 to 23 s, 615 V/cm from 23 to 50 s. *L* DNA ladder, *HA* hemagglutinin clinical sample, *NP* nucleocapsid protein clinical sample, Peaks: 1 = 100 bp, 2 = 200 bp. *RFI* relative fluorescence intensity (reproduced from [13] with permission from Korean Chemical Society)

4 Notes

1. The pH value of 1× TBE buffer and 1× TAE buffer can be adjusted by 0.1 M NaOH solution and 0.1 M HCl solution. The 1× TBE and 1× TAE buffers were prepared by dissolving a premixed powder (Amresco, Solon, OH, USA) in ultrapure water.
2. EtBr should be stored at 4 °C and protected from light.
3. The DNA ladder and PCR kit should be stored at −20 °C.
4. The design of the multichannel microchip allows to keep the parallel separation of samples and avoid the fluorescent signal cross talk of each channel.
5. Bubbles in the separation channel will cause serious problems during the separation such as current interruption and baseline noise. Therefore, all the bubbles should be removed from running buffer and gels.
6. To dissolve the PEO and avoid bubbles, the stirring rate should be controlled carefully. Meanwhile, any reasons which will disturb steady rotation of the stirring bar should be avoided.
7. To get a steady baseline, the laser should warm up for ~5 min.
8. The cylindrical lenses were used to transfer the cylindrical shape laser beam to a linear shape which can induce the fluorescent signal of three parallel channels simultaneously. To get the strongest signal, the laser beam should be aligned and focused on the center of the separation channel.
9. To keep the system steady, the electrodes were welded together and integrated onto a Teflon plate. In addition, the electrodes should be cleaned with HPLC grade methanol before each use.
10. Before the mixed sample solution was incubated, the sample tubes were centrifuged for 1 min at 5,000–6,000 rpm (8,000–9,600 × *g*) to remove any bubbles.
11. More amplification cycles will produce a higher concentration of the final PCR products but need a longer time. Here, 30 cycles are enough to produce the PCR products for detection.
12. Microscope observation is an easy way to check the condition of the channels. However, it cannot identify these transparent contaminants in channels. The other effective method to check the channel condition is the water-level observation. Fill the reservoirs (reservoirs 1, 2, and 4) with water and apply vacuum at the buffer waste reservoir (reservoir 3), and check the water level after 1 min. The same water level in each reservoir represents the same flow rate in each channel which indicates the clean and expedite condition of the separation channel.
13. The gel filling should be performed very carefully to avoid introducing any bubbles into the separation channel.

14. Due to the design of the multichannel microchip, 3.0 cm is the minimum distance from the double-T region to the parallel section of the microchannel.
15. The exposure time of the CCD detector should be set carefully. A long exposure time can provide high signal intensity and low temporal resolution, while a short exposure time can provide low signal intensity and high temporal resolution. This trade-off between signal intensity and temporal resolution should be considered carefully. Herein, the 100 ms time interval of each frame equals the 79 ms exposure time of the CCD camera plus 21 ms of time between frames.
16. Depending on the basic electrophoretic separation theory, the electrophoretic mobility of a DNA molecule directly relies on the applied electric field [11]:

$$\nu_{ep} = \mu_{ep} \times E$$

where ν_{ep} is the electrophoretic velocity, μ_{ep} is the electrophoretic mobility, and E is the applied electric field. Hence, increasing the applied electric field strength is a way to significantly increase electrophoretic velocity and decrease separation time. However, due to Ohm's law, the higher applied electric field will induce a higher current and more Joule heating, which will decrease the resolution of the analytes. Additionally, at high applied electric field conditions, the electrophoretic properties of the DNA molecules become electric field dependent ($\mu_{ep} \sim E$), especially for large DNA molecules.
17. Since the sizes of target DNA molecules (HA, 116 bp, and NP, 195 bp) are between 100 bp and 200 bp, the 100 bp and 200 bp DNA molecules in 100-bp DNA ladder can be used as the control.
18. The conditions for PSEFS were optimized as follows. First, we determined the low constant electric field strength required for the separation of all DNA molecules. Second, we applied a high-strength constant electric field. Next, we decreased the electric field strength at specific domains. Finally, if the separation achieved during the third step was deemed acceptable, we reduced the gradient time.

Acknowledgment

This research was supported by the Basic Science Research Program through the National Research Foundation of Korea (NRF) funded by the Ministry of Education, Science and Technology (2012R1A2A2A01013466).

References

1. Castillo-Salgado C (2010) Trends and directions of global public health surveillance. Epidemiol Rev 32:93–109
2. Ghebremedhin B, Engelmann I, Konig W et al (2009) Comparison of the performance of the rapid antigen detection actim Influenza A&B test and RT-PCR in different respiratory specimens. J Med Microbiol 58:365–370
3. Taylor J, McPhie K, Druce J et al (2009) Evaluation of twenty rapid antigen tests for the detection of human influenza A H5N1, H3N2, H1N1, and B viruses. J Med Virol 81: 1918–1922
4. Kwon D, Shin K, Kwon M et al (2011) Development and evaluation of a rapid influenza diagnostic test for the pandemic (H1N1) 2009 influenza virus. J Clin Microbiol 49: 437–438
5. Tsao KC, Kuo YB, Huang CG et al (2011) Performance of rapid-test kits for the detection of the pandemic influenza A/H1N1 virus. J Virol Methods 173:387–389
6. Wenzel JJ, Walch H, Bollwein M et al (2009) Library of prefabricated locked nucleic acid hydrolysis probes facilitates rapid development of reverse-transcription quantitative real-time PCR assays for detection of novel influenza A/H1N1/09 virus. Clin Chem 55:2218–2222
7. Bose ME, Beck ET, Ledeboer N et al (2009) Rapid semiautomated subtyping of influenza virus species during the 2009 swine origin influenza A H1N1 virus epidemic in Milwaukee, Wisconsin. J Clin Microbiol 47: 2779–2786
8. He J, Bose ME, Beck ET et al (2009) Rapid multiplex reverse transcription-PCR typing of influenza A and B virus, and subtyping of influenza A virus into H1, 2, 3, 5, 7, 9, N1 (human), N1 (animal), N2, and N7, including typing of novel swine origin influenza A (H1N1) virus, during the 2009 outbreak in Milwaukee, Wisconsin. J Clin Microbiol 47: 2772–2778
9. Amano Y, Cheng Q (2005) Detection of influenza virus: traditional approaches and development of biosensors. Anal Bioanal Chem 381:156–164
10. Sackmann EK, Fulton AL, Beebe DJ (2014) The present and future role of microfluidics in biomedical research. Nature 507:181–189
11. Zhang P, Nan H, Lee MJ et al (2013) Ultrafast separation of infectious disease-related small DNA molecules by single- and multichannel microchip electrophoresis. Talanta 106:388–393
12. Nan H, Lee SW, Kang SH (2012) Fast screening of rice knockout mutants by multi-channel microchip electrophoresis. Talanta 97: 249–255
13. Zhang P, Park G, Kang SH (2014) Fast high-throughput screening of the H1N1 virus by parallel detection with multi-channel microchip electrophoresis. Bull Korean Chem Soc 35:1082–1086

Chapter 8

Sex Identification of Ancient DNA Samples Using a Microfluidic Device

Kirsty J. Shaw, Keri A. Brown, Terence A. Brown, and Stephen J. Haswell

Abstract

Ancient DNA is the name given to the degraded, fragmented, and chemically damaged biomolecules that can be recovered from archaeological remains of plants, animals, and humans. Where ancient human DNA has survived at archaeological sites, it can give valuable information and is especially useful for its potential to identify kinship, population affinities, pathogens, and biological sex. Here, we describe the operation of a microfluidic device for the sex identification of ancient DNA samples using an efficient sample handling process. DNA is extracted from powdered bone samples and abasic sites labeled with biotin. Streptavidin-coated superparamagnetic particles are used to isolate the labeled DNA prior to amplification of the Amelogenin sex marker.

Key words Ancient DNA, DNA extraction, Lab-on-a-Chip, Polymerase chain reaction, Sex identification

1 Introduction

Ancient human DNA analysis is not routinely applied in archaeology because of three major problems: contamination with modern human DNA, costs associated with specialist facilities, and a limited range of suitable analytical methods and complex bioinformatic analysis [1]. The use of a lab-on-a-chip (LOC) system aims to overcome some of these limitations by combining DNA extraction and amplification techniques on a single device to which powdered bone samples can be added directly and then the system sealed to minimize contamination.

Due to its nature, ancient DNA is often damaged and can contain many abasic sites [2]. These abasic sites can be exploited to selectively enrich populations of damaged DNA by reacting them with an aldehyde-reactive probe (ARP) which is labeled with biotin. ARP undergoes a Schiff's base reaction resulting in biotin labeling of any abasic sites present within the DNA structure [3]. By using streptavidin-coated paramagnetic beads, the labeled DNA

Ann Van Schepdael (ed.), *Microchip Capillary Electrophoresis Protocols*, Methods in Molecular Biology, vol. 1274,
DOI 10.1007/978-1-4939-2353-3_8,

can be isolated and purified to ensure it is free of contaminants prior to amplification. In order to enable sex identification, the PCR target was the Amelogenin gene, which is present on the X and Y chromosomes. A 6 bp deletion within the amplified region of the X version of the gene means that the sizes of the PCR products indicate which chromosomes are present, the X product being 104 bp and the Y version 110 bp [4].

Integration of purification and amplification techniques is not without its challenges, in particular those issues raised by confinement of the solid-phase matrix, chemical compatibility, and surface properties of the device required for the different stages [5]. The methodology presented here uses a combination of magnetic and electrokinetic pumping mechanisms to achieve movement of reagents. An external magnet is used to manipulate the position of the paramagnetic beads within the device, while electroosmotic flow (EOF) is used to drive the bulk flow of solutions. In EOF, an electrical double layer is generated at the glass surface due to an electrostatic attraction of cations to the deprotonated silanol groups. The more diffuse mobile layer is pulled toward the cathode, in the presence of an applied electric field, dragging with it the bulk solution. In the absence of a pressure difference across the length of the microfluidic channel, a flat flow profile is produced which means that all molecules exhibit the same velocity, except for those very close to the internal surface wall [6].

Here, we detail a method for efficient processing of powdered bone samples within a microfluidic system for DNA extraction and amplification, enabling sex identification in an environment which minimizes the potential of contamination with modern DNA.

2 Materials

Prepare all solutions using ultrapure water (prepared by purifying deionized water to attain a resistivity of 18 MΩ·cm at 25 °C). Diligently follow all waste disposal regulations when disposing waste materials.

2.1 Preparation of Microfluidic Device

1. Microfluidic device prepared using standard photolithography and wet etching techniques to produce the design shown in Fig. 1.
2. Silanization solution: 150 mM trichloro(1*H*,1*H*,2*H*,2*H*-perfluorooctyl)silane in 2,2,4-trimethylpentane (Fisher Scientific, UK) (*see* **Note 1**).

2.2 DNA Extraction

1. DNA extraction buffer: 0.5 M ethylenediaminetetraacetic acid (EDTA) pH 8.0, 0.5 % sodium dodecyl sulfate (SDS), 100 μg proteinase K in water (Sigma-Aldrich, UK) (*see* **Note 2**).

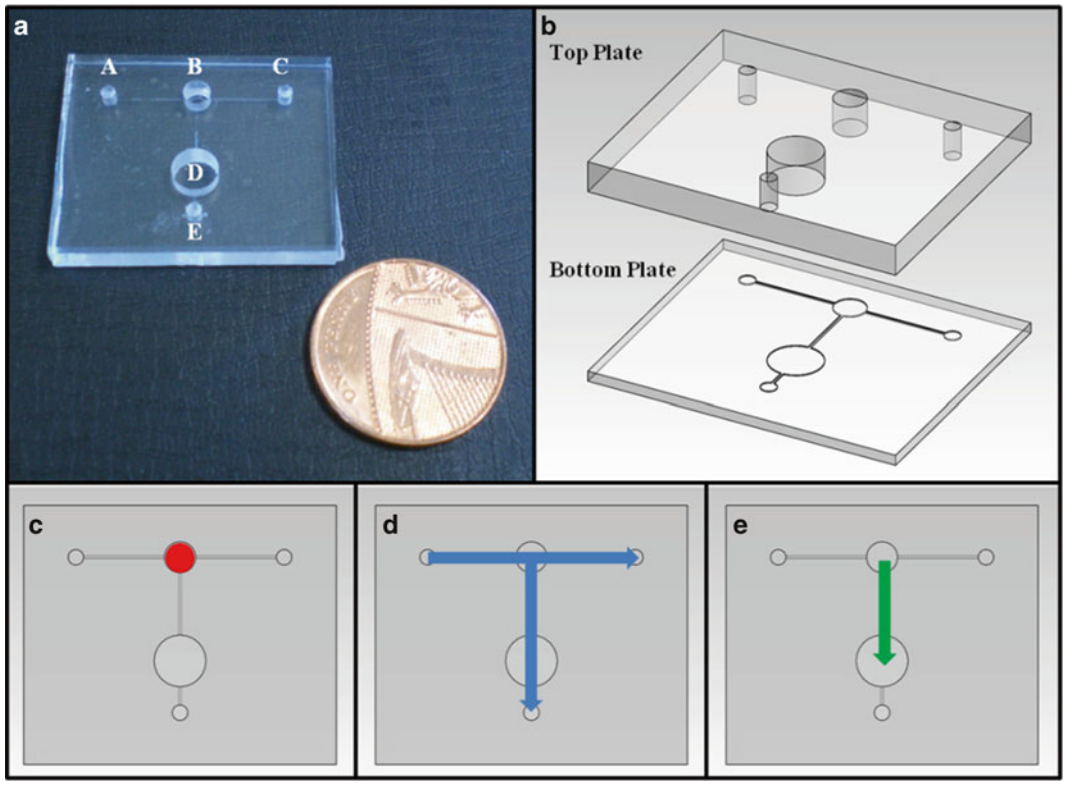

Fig. 1 (**a**) Photograph showing the microfluidic device used for integrated DNA extraction and amplification experiments, where A, C, and E are the 1 mm inlet/outlet holes for reagent/electrode addition; B is the DNA extraction chamber and D is the PCR chamber; (**b**) diagram showing the composition of the two-layer microfluidic device where the bottom plate was etched to a depth of 100 μm; schematic overviewing the operation of the microfluidic device for DNA extraction and amplification where (**c**) is the location for introduction of the sample and solid phase (DNA extraction chamber); (**d**) shows the flow path of the wash solutions (A–C and E) and (**e**) demonstrates the transfer of the magnetic particles into the PCR chamber for DNA amplification. Reproduced from Shaw et al., 2013, with kind permission from Elsevier [7]

2. Biotinylated aldehyde-reactive probe (ARP) (Invitrogen, UK).
3. Solid-phase matrix: 1 μm streptavidin-coated superparamagnetic polystyrene particles (Sigma-Aldrich, UK).
4. NdFeB permanent magnet (Magnet Sales, UK).
5. Paragon 3B Power Supply Unit (Kingfield Electronics, UK).

2.3 DNA Amplification

1. GoTaq® Hot Start DNA polymerase: 0.1 U/μL with 1× Colorless GoTaq® Flexi Buffer and 2 mM $MgCl_2$ (Promega, UK).
2. Deoxynucleotide triphosphate mix: 200 μM each (Bioline, UK).
3. Surface passivation mix: 0.2 μg/μL bovine serum albumin, 0.01 % (w/v) poly(vinylpyrrolidine), 0.1 % (v/v) Tween-20 (Sigma-Aldrich, UK).

4. Primer sequences for amplification of the Amelogenin locus: 0.5 μM forward primer, 5′-FAM-CCC TGG GCT CTG TAA AGA A-3′, and 0.5 μM reverse primer, 5′-ATC AGA GCT TAA ACT GGG AAG CTG-3′ (Eurofins MWG Operon, Germany) (*see* **Note 3**).
5. Peltier heating system (QuickOhm, Germany).

2.4 Capillary Gel Electrophoresis

1. Denaturing solution: 12 μL Hi-Di™ Formamide and 0.5 μL GeneScan™ 500 LIZ® Size Standard per sample (Applied Biosystems, UK).
2. 3500 Genetic Analyzer (Applied Biosystems, UK).

3 Methods

Carry out preparation of bone samples in laminar flow cabinet in an ultraclean room dedicated for ancient human DNA work. An overview of the design and operation of the microfluidic device is provided (Fig. 1).

3.1 Preparation of Microfluidic Device

1. Silanize the PCR chamber (D in Fig. 1a) in order to minimize DNA polymerase adsorption by adding the silanization solution to the chamber and incubating for 10 min at room temperature (*see* **Note 4**).
2. Wash with 2,2,4-trimethylpentane.
3. Wash with acetone.
4. Wash with distilled water and then place in a 100 °C oven to dry.

3.2 Preparation of Bone Samples

1. UV irradiate the outer surface of the bone to minimize contamination.
2. Use a dental pick to remove powdered bone from the spongy matrix within a broken end of the bone (*see* **Note 5**).
3. Add to the DNA extraction chamber (B in Fig. 1a) on the microfluidic device, and incubate with DNA extraction buffer for 24 h.

3.3 DNA Extraction

1. Add 5 mM of biotinylated ARP to the DNA extraction chamber and incubate for 1 h at room temperature.
2. Add 5 μL streptavidin-coated superparamagnetic polystyrene particles to the DNA extraction chamber and allow to incubate for an hour at room temperature.
3. Immobilize the magnetic particles in the DNA extraction chamber by placing a NdFeB permanent magnet underneath the extraction chamber (*see* **Note 6**).
4. Wash the particles using PCR-grade (DNase/RNase-free) water to remove potential contaminants. Place platinum wire electrodes within inlets A, C, and E (*see* Fig. 1), and connect to

an external Power Supply Unit. Apply a voltage of 100 V/cm between both electrodes A to C and A to E to facilitate EOF (*see* **Notes 7** and **8**).

5. Transfer the washed magnetic particles into the PCR chamber by manual movement of the NdFeB permanent magnet in the direction shown in Fig. 1e (*see* **Note 9**).

3.4 DNA Amplification

1. Add PCR reagent solution containing GoTaq® Hot Start DNA polymerase, deoxynucleotide triphosphate mix, surface passivation mix, and primer sequences for amplification of the Amelogenin locus solution to the PCR chamber.
2. Carry out thermal cycling using the following heat program: 4 min at 94 °C; followed by 44 cycles of 1 min at 55 °C, 1 min at 72 °C, and 1 min at 94 °C; followed by 1 min at 55 °C and 10 min at 72 °C (*see* **Notes 10** and **11**).

3.5 Capillary Gel Electrophoresis

1. Use a pipette to remove the PCR product from the microfluidic device and store in a 200 μL sterile tube until required.
2. Add 1 μL of PCR product to 12.5 μL of denaturing solution and denature for 5 min at 95 °C before snap-cooling on ice.
3. Load onto 3500 Genetic Analyzer following manufacturer protocols.
4. Following electrophoresis run, analyze data to identify the sex of the bone sample, where the X product is 104 bp and the Y product is 110 bp indicating male (XY) or female (XX).

4 Notes

1. The silanization solution has a limited shelf-life and should be prepared immediately prior to use. Avoid exposure of the reagents to water by storing the stock reagents with molecular sieve and drying all glassware prior to use in an oven.
2. SDS can precipitate and so the solution may need warming prior to use.
3. The forward primer has been labeled with FAM to facilitate fluorescence detection during capillary gel electrophoresis, but different labels could be used.
4. As well as the glassware to be used in the preparation of silanization solution, it is also advisable to wash the microfluidic device with 100 % ethanol and then place in a 100 °C oven to ensure that it is completely dry prior to use. Remove from the oven and place in a desiccator to maintain a moisture-free environment prior to addition of silanization solution.
5. Using a toothpick to remove bone powder rather than a drill prevents heating caused by friction which can potentially damage the DNA.

6. An ideal sized NdFeB permanent magnet is $5 \times 3 \times 3$ mm.
7. To ensure optimal functioning of the platinum electrodes, clean in between runs using very fine sandpaper and then wash in ethanol.
8. While carrying out electrokinetic movement, cool the microfluidic device to 4 °C, using the thermoelectric Peltier element, in order to reduce Joule heating and minimize sample evaporation.
9. Movement of the external magnet needs to be performed in a controlled manner and monitored to ensure that all the magnetic beads are transferred into the PCR chamber.
10. When carrying out DNA amplification on a microfluidic system using a thermoelectric Peltier element, ensure that the desired temperature settings are those which occur inside the DNA amplification chamber on the device, which may require setting of higher temperatures on the Peltier element to achieve the desired temperature within the device.
11. Cover all inlets with a drop of mineral oil to prevent evaporation during the thermal cycling process and minimize contamination.

References

1. Brown TA, Brown KA (2011) Biomolecular archaeology: an introduction. Wiley-Blackwell, Chichester, West Sussex, UK
2. Pääbo S, Poinar H, Serre D, Jaenicke-Després V, Hebler J, Rohland N, Kuch M, Krause J, Vigilant L, Hofreiter M (2004) Genetic analyses from ancient DNA. Annu Rev Genet 38:645–679
3. Fundador E, Rusling J (2007) Detection of labeled abasic sites in damaged DNA by capillary electrophoresis with laser-induced fluorescence. Anal Bioanal Chem 387:1883–1890
4. Sullivan KM, Mannucci A, Kimpton CP, Gill P (1993) A rapid and quantitative DNA sex test: fluorescence-based PCR analysis of X-Y homologous gene amelogenin. Biotechniques 15:636–641
5. Ferrance JP, Wu QR, Giordano B, Hernandez C, Kwok Y, Snow K, Thibodeau S, Landers JP (2003) Developments toward a complete micro-total analysis system for Duchenne muscular dystrophy diagnosis. Anal Chim Acta 500:223–236
6. Taylor JA, Yeung ES (1993) Imaging of hydrodynamic and electrokinetic flow profiles in capillaries. Anal Chem 65:2928–2932
7. Parton J, Abu-Mandil HN, Brown TA, Haswell SJ, Brown KA, Shaw KJ (2013) Sex identification of ancient DNA samples using a microfluidic device. J Archaeol Sci 40:705–711

Chapter 9

Fast and Continuous-Flow Detection and Separation of DNA Complexes and DNA in Nanofluidic Chip Format

Martina Viefhues, Jan Regtmeier, and Dario Anselmetti

Abstract

Fast separation of DNA and detection of protein/DNA complexes are important in many state-of-the-art molecular medicine technologies, like the production of gene vaccines or medical diagnostics. Here, we describe a nanofluidic chip-based technique for fast, efficient, and virtually label-free detection and separation of protein/DNA and drug/DNA complexes and topological DNA variants. The mechanism is based on a continuous-flow dielectrophoresis at a nanoslit and allows efficient separation of small DNA fragments (<7,000 base pairs) and fast detection of DNA complexes within 1 min.

Key words Nanofluidics, Continuous flow, Separation, Detection, Dielectrophoresis, DNA complexes

1 Introduction

The standard method for separating DNA compounds is gel electrophoresis, in either a slab gel or capillary format, or the different types of affinity chromatography. Although widespread and used in many laboratories, some intrinsic (systematic) disadvantages are obvious and remain unsolved: (1) preparation and separation take at least 2 h [1]; (2) the parameters of the separation cannot be adapted or optimized during the separation; (3) considerable shear force effects during separation may affect analyte integrity and functionality (topology); (4) sample elution and postprocessing are difficult and often rely on the use of toxic and mutagenic reagents. Nevertheless, capillary electrophoresis and electrophoretic mobility shift assays (EMSA) are standard analytical techniques for the purification of small and large DNA fragments along plasmid vaccine production, for the determination of binding affinities of new cytostatic drugs and rational drug design [2], and for protein-DNA interaction screenings [3–5] like screening for specific antibody-DNA complexes. Consequently, there is a huge need of novel tools that allow fast processing with low analyte volumes in low-cost devices suitable for real-time process control. Those new tools

Ann Van Schepdael (ed.), *Microchip Capillary Electrophoresis Protocols*, Methods in Molecular Biology, vol. 1274,
DOI 10.1007/978-1-4939-2353-3_9,

have to keep track with the advances in rational drug design and latest developments in molecular sciences.

Here, we present a new chip-based method for fast, continuous-flow detection and separation of DNA complexes and topological DNA variants. The detection and separation mechanism is based on electrodeless dielectrophoresis at a nanoslit. Dielectrophoresis (DEP) refers to the migration of polarizable objects within an inhomogeneous electric field [6]. Advantages of DEP are that it is noninvasive, label-free, and allows separation due to inherent molecular characteristics, namely, the electric polarizability.

For the studies, we applied ac and dc electric fields to a channel system consisting of a cross injector and a bowed ridge that generates a nanoslit (*see* Fig. 1). At the ridge, selective dielectrophoretic forces can be adjusted via the applied electric fields [7]. These selective forces effect two possible pathways at the nanoslit: either the molecule passes the nanoslit unaffected or it is deflected until it reaches the opposite channel wall (cf. Fig. 1). The respective pathway that a molecule follows depends on the ratio of the electrophoretic and dielectrophoretic forces [8].

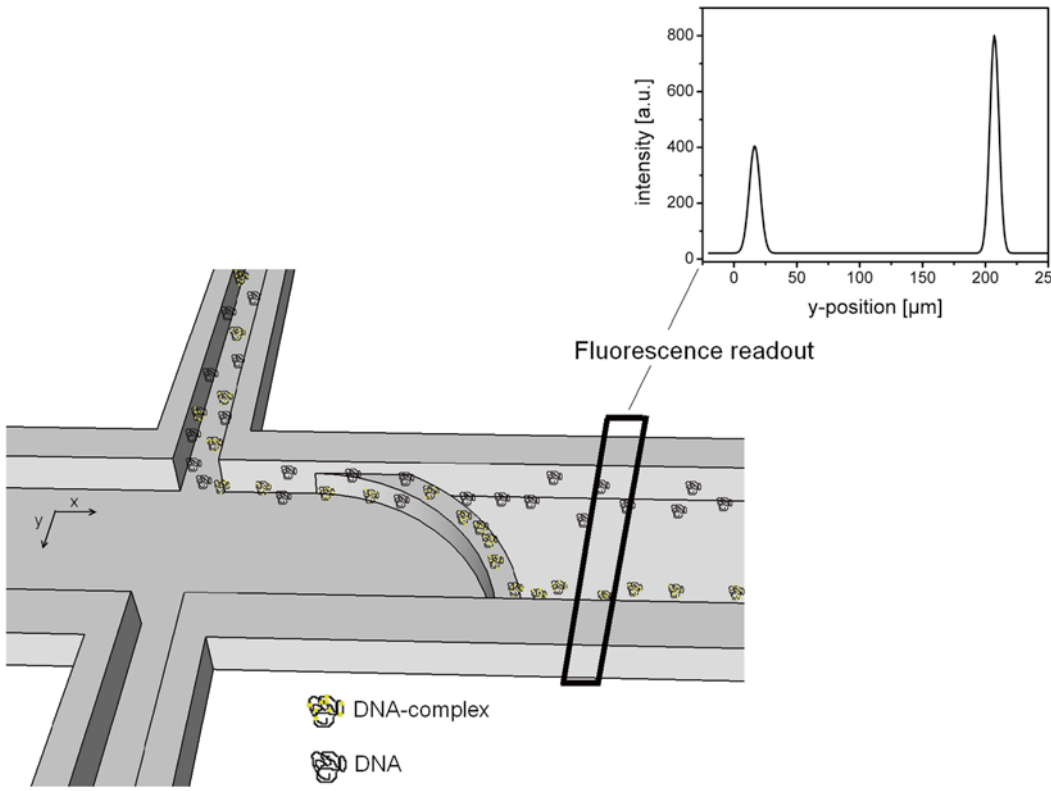

Fig. 1 Scheme of the continuous-flow separation and analysis. The analyte is injected toward the ridge as a narrow stream. At the ridge, one species is deflected; the second species passes the ridge unaffected. Downstream of the ridge, the response is monitored by fluorescence intensity distributions

DNA follows the second pathway, i.e., it is deflected at the ridge, if the dielectrophoretic potential $W_{\mathrm{DEP}} = \frac{1}{2}\alpha \vec{E}^2$, with α the polarizability, is larger than the potential energy of the electrophoretic motion. For the separation of two DNA species, e.g., reference DNA and DNA complex, it was exploited that α differs significantly between the species [7] resulting in two distinct streams of separated molecules (*see* Fig. 1).

A monolithic fabrication of the microfluidic device via soft lithography [9] allows an easy fabrication in most biology-focused laboratories, as no clean room is required, once a master wafer, the original negative relief of the actual fluidic network, was fabricated. A clean bench is sufficient for chip assembly. For detection, fluorescence microscopy was chosen, since this method is most often available. As a power supply, a cost-effective high-voltage amplifier is sufficient.

With the chip-based method, we could detect complex formation of DNA and actinomycin D in varying concentrations and complex formation of DNA and *Escherichia coli* RNA polymerase core enzymes within 1 min. For this purpose, only 0.9 ng DNA (about 10 pM) were necessary. Additionally, fast separation of topological DNA variants was performed within 1 min in a continuous-flow process with the application in in-production quality control of gene vaccines.

2 Materials

Prepare all solutions using deionized water and analytical grade reagents. Store all pure reagents as suppliers recommend. Working buffer and incubated DNA are stored at 7 °C. Diligently follow all waste disposal regulations when disposing waste materials.

2.1 Production of Master wafer

1. 4″ silicon wafer.
2. Wafer tweezers.
3. 1 L glasses.
4. Caro acid: one part hydrogen peroxide and two parts sulfuric acid.
5. SU8 photoresist and its thinner and developer.
6. 200 ml vials.
7. Waterproof marker.
8. Programmable hot plate.
9. Centrifuge (Ble-Laboratory Equipment GmbH, Germany).
10. Chromium photomasks (Delta Mask, Netherlands).
11. Mask aligner with UV light source (MJB3, Süss MicroTec, Germany).

12. Dektak profilometer 3030 (Stanford Nanofabrication Facility Equipment, USA).
13. Nitrogen gas and adapter with duster.
14. Acetone and isopropanol.
15. Adhesive tape.
16. Tridecafluor-1,1,2,2-tetra-hydrooctyl-trichlorsilane (TTTS).
17. Hourglass.
18. Exsiccator.

2.2 Chip Fabrication

1. Vinylmethylsiloxane-dimethylsiloxane trimethylsiloxy terminated copolymer, platinum-divinyltetramethyldisiloxane complex, 2,4,6,8-tetramethyl-2,4,6,8-tetravinylcycltetrasiloxane, and (25–35 % methylhydrosiloxane)-dimethylsiloxane copolymer.
2. Poly(dimethylsiloxane) Sylgard 184 and its linker.
3. Sharp tweezers and a bowed metal plate (15 × 30 cm) for peeling off the Poly(dimethylsiloxane) PDMS from master wafer.
4. Scalpel.
5. Punching pattern according to channel dimensions.
6. Glass cover slips (24 × 60 mm thickness of 0.13–0.16 mm).
7. Ultrasonic bath.
8. Oxygen plasma chamber.
9. Working buffer: 1 mM phosphate buffer (pH 7.4, 0.2 mM NaCl), 1 mM ethylenediaminetetraacetic acid (EDTA), 2 mM 6-hydroxy-2,5,7,8-tetramethylchroman-2-carboxylic acid (Trolox), 0.25 % N-dodecyl-β-D-maltoside (DDM), 0.03 % methyl cellulose (MC) (*see* **Note 1**).

2.3 Sample Preparation

1. 11,1-(4,4,7,7-tetramethyl-4,7-diazaundecamethylene)-bis-4-[3-methyl-2,3-dihydro-(benzo-1,3-oxazol)-2-methylidene]-quinoliumtetraiodid (YOYO-1) was used for the fluorescent labeling of DNA.
2. Pipettes of 2 µl, 20 µl, and 100 µl.
3. 2 ml Eppendorf vessels.
4. Vortexer.
5. DNA of linear and circular conformation (lengths of 2.2–6.7 kbp).
6. Actinomycin D (ActD) and *Escherichia coli* RNA polymerase (RNAP) core enzymes to form DNA complexes.

2.4 Chip Experiments

1. Poly(methyl methacrylate) (PMMA) block with integrated reservoirs and electrodes corresponding to the chip layout.

2.5 Setup

1. Inverted fluorescence microscope with a motorized x/y stage.
2. 100× oil-immersion objective together with a mercury arc lamp and respective fluorescence filter sets (BP 450-490, BP 515-565, FT 510, Zeiss, Germany) and a gray filter (25 % transmittance).
3. CCD interline-transfer camera (Imager3LS, LaVision, Germany) with a corresponding grabber card and software (DaVis 6.2) (*see* **Note 2**).
4. The voltage signal was created via a LabView 6i program and function generator DS345 (Stanford Systems, USA).
5. High-voltage amplifier (AMT-1B60-L Matsusada, Japan) and three power supplies to deliver dc voltages (HCL 14-12500, FUG, Germany).

3 Methods

Diligently follow general safety instructions for handling acids and solvents. Carry out all procedures at room temperature. Whenever the material is heated up or cooled down, use a temperature ramp of about 20 °C per 5 min (unless indicated otherwise).

3.1 Production of Master wafer

1. The 4″ silicon wafer is cleaned in caro acid for 5 min twice and rinsed with water.
2. SU8 photoresist of 12 %, 17 %, and 52 % solid fractions is diluted from stock photoresist with thinner (*see* **Note 3**).
3. A first layer of SU8 photoresist (12 % or 17 % solid fraction, respectively) is spin coated at 1,000 rpm (12 % solid fraction) or 900 rpm (17 % solid fraction) for 30 s (*see* Fig. 2). After spin coating, the wafer is mounted onto a 65 °C warm hot plate for 1 min. Thereafter, the photoresist is exposed to UV light through a chromium mask in a mask aligner for 2 s (*see* **Note 4**). After postexposure bake at 95 °C for 3 min, the wafer is developed in a developer for 1 min. The developer is removed carefully (*see* **Note 5**) with acetone and isopropanol, successively, and dried with nitrogen. The height of the first layer is determined at several positioning structures on the wafer, 180 nm (12 % solid fraction) or 670 nm (17 % solid fraction), with a profilometer.
4. A second layer of SU8 (52 % solid fraction) is spin coated (3,000 rpm for 30 s) and baked at 95 °C for 1 min (*see* **Note 6**). The photoresist is exposed to UV light for 7 s in the mask aligner. The exact alignment of the photomask to the first structures is of very high importance (*see* **Note 7**). After postexposure bake at 95 °C for 3 min, the wafer is developed in the developer for 1 min. Again, the developer is removed carefully with acetone and isopropanol, successively, and dried with nitrogen.

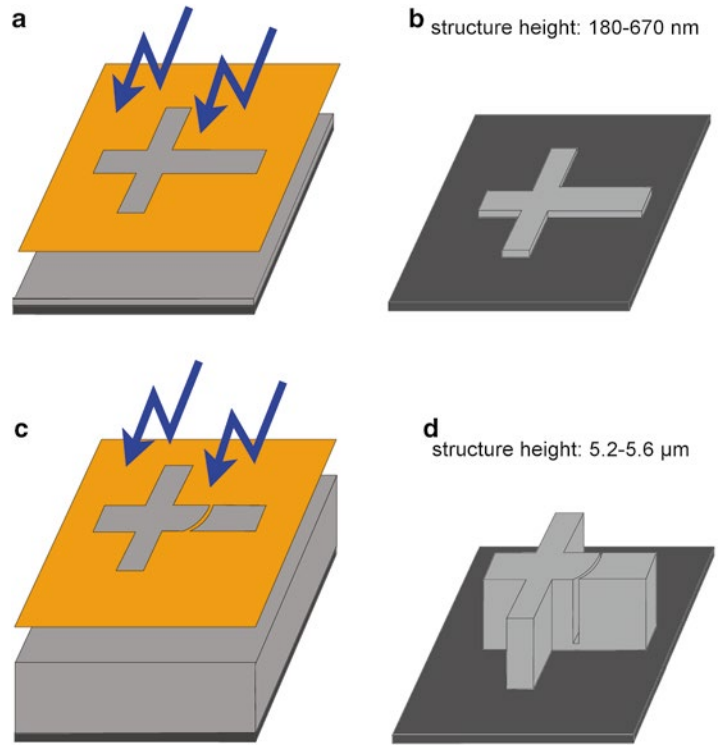

Fig. 2 Scheme of master wafer production. (**a**) A thin layer of photoresist (*dark gray*) is spin coated on a silicon wafer (*light gray*) and illuminated through a chromium mask (*orange*), defining the nanoslit height and the general channel layout. (**b**) Silicon wafer with the first layer of photoresist after developing. The structure height is from 180 to 670 nm corresponding to the parameters of photoresist and spin coating. (**c**) A second layer of photoresist is spin coated and illuminated through a chromium mask, defining the ridge shape and free channel height. (**d**) Master wafer, with negative relief structure, ready to be molded with PDMS

5. A terminal hardbake at 195 °C for 20 min is performed to close small cracks in the photoresist.
6. To prevent adhesion of the polymer to the photoresist structures, the wafer is silanized with TTTS in an exsiccator. Therefore, ten droplets of TTTS are given on an hourglass and placed at the bottom of the exsiccator. The wafer is placed on a perforated plate over the hourglass. The vacuum is set to 0.1 mbar for 1 h. Afterward, the exsiccator is slowly ventilated, and the wafer can be removed.

3.2 Chip Fabrication

1. A layer of h-PDMS (3.4 g vinylmethylsiloxane-dimethylsiloxane trimethylsiloxy terminated copolymer, 18 µl platinum-divinyltetramethyl-disiloxane complex, 1 droplet of 2,4,6,8-tetramethyl-2,4,6,8-tetravinylcyclotetrasiloxane, and 1 ml (25–35 % methylhydrosiloxane)-dimethylsiloxane copolymer) (*see* **Note 8**)

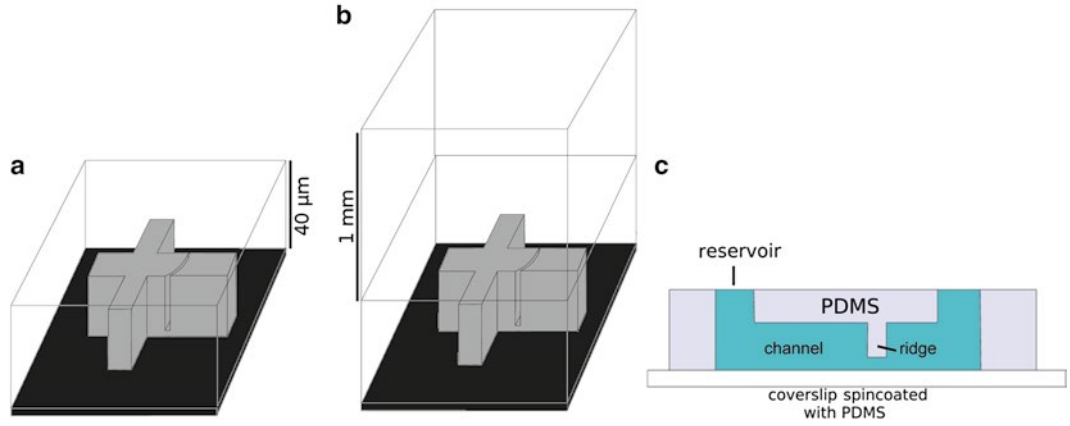

Fig. 3 Scheme of double-layer soft lithography. (**a**) First layer of h-PDMS 40 µm in height (*not to scale*), to stably mold the nanoslit. (**b**) Second layer of PDMS 1 mm (*not to scale*), for better handability. (**c**) Cross section of assembled chip with reservoirs and running buffer (*blue*)

is spin coated onto the wafer at 1,500 rpm for 10 s (*see* Fig. 3) (*see* **Note 9**). The h-PDMS is precured for 3 min on a hot plate at 65 °C (*see* **Note 10**).

2. A second layer of PDMS (6.5 g polydimethylsiloxane (PDMS) Sylgard 184 and 0.65 g silicone elastomer curing agent (PDMS-linker)) is poured on top of the h-PDMS and cured on a hot plate at 65 °C for 40 min.
3. The PDMS double layer is peeled off (*see* **Note 11**), and the microstructured part of the slab is cut out with a scalpel with at least 3 mm distance to the channel ends.
4. Reservoirs of 2 mm diameter are punched into the PDMS slab at the channel ends (*see* **Note 12**). Afterward, the PDMS slab is cleaned in acetone, ethanol, and deionized water 10 s each in an ultrasonic bath. PDMS (Sylgard 184) spin coated cover slips (*see* **Note 13**) are cleaned the same way. The coated cover slips and the PDMS slabs are oxidized in oxygen plasma for 30 s and assembled (*see* **Note 14**).
5. 30 min after chip assembly (*see* **Note 15**), the channels are filled with working buffer and incubated for at least 30 min [10].

3.3 Sample Preparation

1. The DNA is stained with YOYO-1, ratio YOYO-1 to DNA base pairs 1:10. Therefore, 1.6 µl of 10 µM YOYO-1 and 100 ng DNA are pipetted into an Eppendorf vessel and incubated on a vortexer for 2 h at the lowest shaking level.
2. For the DNA cytostatics complex, YOYO-1 and ActD (MW 384 kDa, 2 µl, 1 µl, or 0.5 µl of 0.3 mM solution) are added and incubated on a vortexer at the lowest shaking level for 2 h.
3. For the DNA polymerase complex, YOYO-1 and *RNAP* are added (100 ng DNA, 500 ng RNAP) and incubated on a vortexer at the lowest level for 2 h.

3.4 Chip Experiments

1. The working buffer is removed out of the reservoirs and the PMMA block is placed on top of the chip to enlarge the reservoirs and simplify handling.
2. 9 µl of working buffer is pipetted into every reservoir but reservoir 3 (*see* Fig. 1).
3. 9 µl of the DNA solution is pipetted into reservoir 3 of the prefilled chip (*see* **Note 16**).
4. The specific voltages for the separation experiments are chosen as follows. First, the dc voltages are set such that the DNA molecules continuously flow, parallel to the channel wall, toward the ridge (cf. Fig. 4) (*see* **Note 17**). It is assured that the inflowing molecules occupy less than a quarter of the total width of channel 2.
5. The ac voltage is switched on to reasonably small amplitudes (50 V), and its effect on the particle motion is observed while varying the frequency over an interval from 50 to 1,000 Hz. If no deflection is observed, the amplitude is increased, followed by varying the frequencies until a complete deflection of the DNA at the ridge is observed for the first time (*see* **Note 18**).

3.5 Image Acquisition and Processing

1. The channel is scanned over the whole width during running experiments with a constant speed of 10 µm/s along the y-direction at different x-positions of interest. Hence, the width of the injected molecules stream and the efficiency of the separation/detection can be determined, respectively. The y-position of the recorded images within the channel is determined from scanning speed and time.

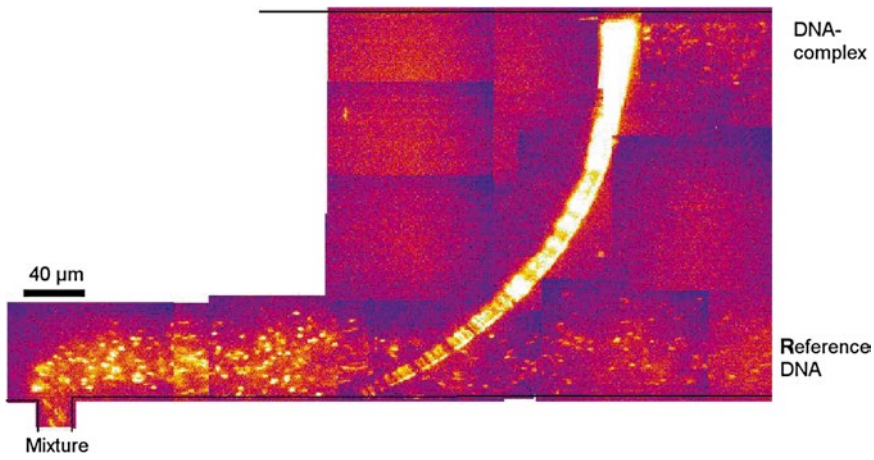

Fig. 4 Detection of complex formation and separation. Fluorescence images (collage) at the nanoslit. From the *left*, a mixture of DNA is continuously injected (*yellow spots* correspond to single DNA molecules). The reference DNA passes the nanoslit unhindered, whereas the DNA complexes are trapped on the ridge and migrate toward the opposite channel side before they escape due to Brownian motion. Evaluation of the separation resolutions reveals a clearly baseline-separated resolution

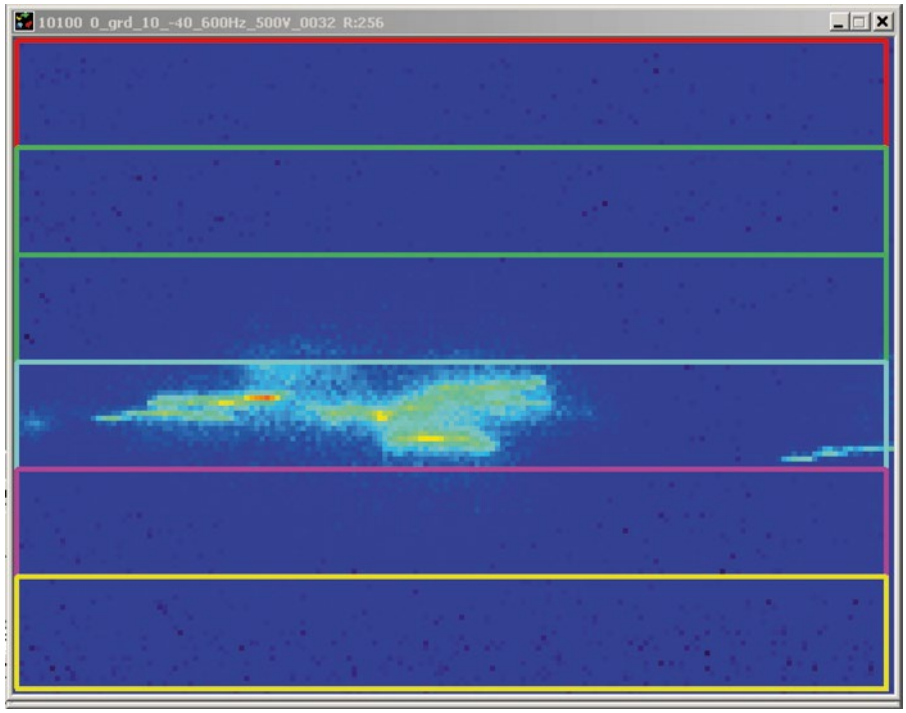

Fig. 5 The region of interest is partitioned in six slices, each with the height of 11 μm. To determine the analytes distribution, the fluorescence intensity is measured in each slice separately, along the scanning procedure, and averaged over up to six overlapping slices

2. To obtain the experiments result, the intensity distribution downstream of the ridge is evaluated. Therefore, a series of images are recorded during the scan in y-direction downstream of the nanoslit. Afterward, each image is partitioned in six slices of height 11.4 μm (in y-direction *see* Fig. 5), in order to reduce convolution effects. Then, the total fluorescence intensity within these slices is determined. Successively recorded images are shifted by 1 μm in y-direction, so that in every 11th image, those slices overlap within a precision of less than 1 μm.
3. The measured fluorescence intensity is averaged over up to six such overlapping slices and plotted as a function of the y-position. These data are fitted with Gaussian curves, and the resolution is calculated according to $\mathrm{Res} = \frac{x_2 - x_1}{2(\sigma_1 + \sigma_2)}$ with x_2, x_1 the position of each peak maximum and σ_1, σ_2 the corresponding peak width. Therefore, values of $\mathrm{Res} > 1$ indicate baseline separated resolution.

4 Notes

1. Surface coatings DDM and MC were added to reduce the adhesion of samples to the surfaces and for control and reproducibility of the electroosmotic flow.
2. By data acquisition with an 8 by 8 binning and 10 frames per second (fps), it was possible to detect single DNA molecules migration easily.
3. First, the respective amounts of photoresist (12 %, 23.21 ml; 18 %, 35.3 ml; and 52 %, 100 ml) are measured with water and filled into a vial. After the filling, heights are marked the respective amount of thinner (12 %, 100 ml; 18 %, 100 ml; 52 %, 32.7 ml) is measured with water and added into the vial, and the filling height is marked. Then the vials are cleaned with caro acid for 5 min, rinsed with water twice, and dried on a hot plate (180 °C for 30 min). After the vials are cooled to room temperature, photoresist and thinner are filled into the vials according to the respective marked filling heights and carefully mixed.
4. The wafer and the photomask are aligned such that the position can easily be reproduced along the second illumination. Thus, the time for alignment is minimized.
5. To prevent disturbance of the photoresist structures, the wafer is held horizontally and slowly flooded with acetone first until it is totally covered. Then the acetone is slowly replaced by isopropanol, which is gently removed with nitrogen.
6. It is important that the positioning crosses are covered with the adhesive tape before the second layer of photoresist is poured. The tape is removed the moment the hot plate reaches 65 °C. If tried at a lower temperature, the photoresist was found too sticky to be removed without damages. If tried at higher temperature, the adhesive became sticky due to the heat.
7. Even small malpositioning at the center of the wafer effects large displacement at the structures in the border area of the wafer. Thus, the positioning was checked at four positioning crosses to ensure perfect alignment of the second photomask to the first structures.
8. The 2,4,6,8-tetramethyl-2,4,6,8-tetravinylcycltetrasiloxane and 1 ml (25–35 % methylhydrosiloxane)-dimethylsiloxane copolymer was added and mixed up just before the h-PDMS was poured over the master wafer due to the fast polymerization after adding.

9. The first layer of h-PDMS had a thickness of about 40 μm and thus completely contained the microstructured channel formed by the master wafer.
10. The h-PDMS must be fully polymerized to ensure stable molding of the nanoslit. It was found that stable structures were formed if no imprint is visible when a tweezers is pressed onto the baked h-PDMS.
11. The h-PDMS is very brittle, although the double layer with PDMS allows better handability. To ensure that the h-PDMS does not crack during the removal, the wafer is mounted on a hot plate at 65 °C for 5 min. The following steps are performed with the wafer still on the hot plate. Pay attention not to be burnt!

    First, stickings are loosened by rounding the master wafer with a tweezer in between the h-PDMS and the master wafer. Then a bowed metal plate, which is warmed, too, is placed on top of the PDMS. When holding the PDMS double layer and the metal plate with a tweezers, the wafer is slowly peeled off, following the curvature of the metal plate.
12. To ensure a reproducible distance between the reservoirs, a punching pattern, consisting of blanks for all reservoirs, was used.
13. 1 ml PDMS is poured onto the cover slip and spin coated by 1,500 rpm for 10 s. If the PDMS layer is too thick, the DNA cannot be detected.
14. Due to the very small height of the structures, these are very sensible to pressures. To prevent a collapse of the nanostructures along assembly, the PDMS slab is gently laid onto the cover slip without bending the slab. If air is still in between the PDMS and the cover slip, the PDMS must not be pressed but softly swiped with a tweezer.
15. 30 min was found to ensure that covalent bonds were formed between the PDMS slab and the PDMS-coated cover slip. For shorter times, the channel system was leaky.
16. The DNA solution is filled in last. Otherwise, DNA would flood the other channels, which could prohibit controlled DNA injection as a narrow stream.
17. The dc voltages are set such that the velocity of the DNA molecules is about 30 μm/s. Otherwise, higher ac voltages would have to be applied.
18. If the applied parameters are close to appropriate parameters, the migration behavior of the DNA at the nanoslit alters. First, the DNA passes the nanoslit totally unaffected. When the parameters are close to the appropriate parameters, it looks like the DNA briefly stops before passing the nanoslit.

Acknowledgment

This work was supported by the German Research Foundation in the collaborative research center (SFB 613) project D2. We thank Anja Rischmüller and Martin Schleef from PlasmidFactory for the production and supply of *minicircle* DNA.

References

1. Hellman LM, Fried MG (2007) Electrophoretic mobility shift assay (EMSA) for detecting protein-nucleic acid interactions. Nat Protoc 2(8):1849–1861
2. Mandal S, Moudgil M, Mandal SK (2009) Rational drug design. Eur J Pharmacol 625(1–3):90–100
3. Hens K, Feuz J-D, Isakova A et al (2011) Automated protein-DNA interaction screening of drosophila regulatory elements. Nat Methods 8(12):1065–1070
4. Lalonde S, Ehrhardt DW, Loqu D et al (2008) Molecular and cellular approaches for the detection of protein-protein interactions: latest techniques and current limitations. Plant J 53(4):610–635
5. Yu L-P, Sun Y-Z, Zhao Z-X (2009) Biomolecule interactions studying on microfluidic chip. Curr Pharmaceut Anal 5:112–119
6. Regtmeier J, Eichhorn R, Viefhues M et al (2011) Electrodeless dielectrophoresis for bioanalysis: theory, devices and applications. Electrophoresis 32(17):2253–2273
7. Viefhues M, Regtmeier J, Anselmetti D (2013) Fast and continuous-flow separation of DNA-complexes and topological DNA variants in microfluidic chip format. Analyst 138:186–196
8. Viefhues M, Eichhorn R, Fredrich E et al (2012) Continuous and reversible mixing or demixing of nanoparticles by dielectrophoresis. Lab Chip 12(3):485–494
9. Xia Y, Whitesides G (1998) Soft lithography. Ann Rev Mater Sci 28:153–184
10. Viefhues M, Manchanda S, Chao T-C et al (2011) Physisorbed surface coatings for poly(dimethylsiloxane) and quartz microfluidic devices. Anal Bioanal Chem 401(7): 2113–2122

Chapter 10

Multidimensional Microchip-Capillary Electrophoresis Device for Determination of Functional Proteins in Infant Milk Formula

Ruige Wu, Zhiping Wang, and Ying Sing Fung

Abstract

Functional proteins have been found in infant milk formula as supplements, added by an increasing number of manufacturers. Their supplementations are expected to be controlled and monitored. Here, we describe a microchip-integrated CE method for the determination of these low levels of functional proteins in a protein-rich sample matrix. On-chip isoelectric focusing (IEF) is used to separate high-abundance proteins from low-abundance proteins instead of using some complicated time-consuming protein purification process. After that, transient isotachophoresis hyphenated capillary zone electrophoresis (t-ITP-CZE) can preconcentrate, separate, and analyze transferred functional proteins in the embedded capillary under UV detection.

Key words Isoelectric focusing, Isotachophoresis, Microchip-capillary electrophoresis device, Functional protein, Infant milk formula

1 Introduction

It is widely accepted that human milk provides the best nutrients for infants and babies because of its balanced proportions and high concentrations of several key functional proteins as compared to other types of milk [1, 2]. However, if babies cannot be breast-fed, infant milk formula provides the best alternative source of essential proteins. Although the manufacturers of infant milk formula have made their products to closely match to human milk, there are still significant differences in the composition of some key functional proteins, such as α-lactalbumin (α-LA), lactoferrin (LF), immunoglobulin G (IgG), and β-lactoglobulins (β-LgA and β-LgB), which can provide important sources of proteins needed for key functions such as immune system development. As an increasing number of manufactures have advertised elevated levels of functional proteins such as α-LA and IgG in their products, their supplementation is

Ann Van Schepdael (ed.), *Microchip Capillary Electrophoresis Protocols*, Methods in Molecular Biology, vol. 1274,
DOI 10.1007/978-1-4939-2353-3_10,

expected to be regulated shortly [3]. Thus, methods are needed for the determination of low levels of functional proteins in a protein-rich sample matrix for their control and monitoring.

Various methods have been reported in the literature for quantitative and semiquantitative determination of these functional proteins in dairy products, such as High-performance liquid chromatography (HPLC), Enzyme-linked immunosorbent assay (ELISA), surface plasmon resonance (SPR), and two-dimensional gel electrophoresis [4–7]. A time-consuming sample pretreatment procedure is performed to precipitate casein using acetic acid, one of the major milk proteins [6, 7]. However, loss of functional proteins due to coprecipitation with caseins has been reported [8]. Riechel et al. [9] reported a capillary electrophoresis (CE) procedure to separate spiked LF from whey proteins. However, it suffers from a relatively high detection limit of 10 mg/L and insufficient separation of major proteins from LF.

Here, we describe a microchip-CE device designed for the determination of functional proteins in infant milk formula sample. On-chip IEF is used to separate high-abundance proteins from low-abundance proteins instead of some complicated time-consuming protein purification process. After that, two steps of transient ITP (t-ITP) hyphenated capillary zone electrophoresis (CZE) can preconcentrate and separate transferred functional proteins in the embedded capillary under UV detection at 280 nm. The analysis of the functional proteins in an infant milk formula sample can be finished in less than 20 min.

2 Materials

2.1 Instrumentation and Apparatus

1. Octo-Channel high-voltage supply (0–4,500 V, Sutter Creek, CA, USA).
2. 24 kV constant voltage supply from Bertan, USA.
3. CO_2 laser engraver (10.6 μm, V-Series, Pinnacle, USA).
4. Hot press bonding machine (up to 500 °C and 1 MPa pressure, Guangju Machinery Company, China).
5. CCD microscope (40×, Olympus, Japan).
6. UV/Vis detector and data analysis system from CE Resources (UVV500, Singapore).
7. pH meter (Cole Palmer, 590002-02).
8. Poly(methyl methacrylate) (PMMA) plate: thickness 1.5 mm.
9. Capillary: outer diameter (350 μm), inner diameter (50 μm). Length: 111 mm.

2.2 Chemicals, Reagents, and Standards

Prepare all solutions at room temperature using deionized water (DI H_2O) and analytical grade reagent unless otherwise stated:

1. PEO stock solution: 10 g/L PEO. Add about 9 mL DI H_2O to a glass beaker. Weigh 0.1 g poly(ethylene oxide) (PEO, MW = 400,000) and transfer to the beaker and stir to dissolve it. Transfer the solution into a 10 mL cylinder. Make up to 10 mL with DI H_2O.
2. HEMC stock solution: 4 g/L HEMC. Weigh 0.4 g hydroxyethyl methyl cellulose (HEMC) and prepare a 10 mL solution as in previous step.
3. Anolyte: 0.05 M HAc, 0.1 g/L PEO, and 0.05 % HEMC.
4. Catholyte: 0.04 M NaOH, 0.1 g/L PEO, and 0.05 % HEMC.
5. Terminating electrolyte (TE): 0.05 M HAc, 0.1 g/L PEO, and 0.05 % HEMC.
6. Leading electrolyte (LE) and background electrolyte (BGE): same composition, including 0.05 M Tris–HCl, 0.1 g/L PEO, and 0.05 % HEMC.
7. IEF buffer solution: Add about 13 mL DI H_2O, 1 mL 36 % Pharmalyte (pH range 3–10), 180 μL Triton X100 (reduced form), 180 μL PEO stock solution, 2.25 mL HEMC stock solution, and 45 μL *N*,*N*,*N*′,*N*′-tetramethylethylenediamine (TEMED) to a cylinder, weigh 8.65 g Urea and transfer to the cylinder, and mix them. Make up to 18 mL with DI H_2O. Store at 4 °C.
8. Stock solution of standard proteins: 10 mg/mL. Prepare 10 mg/mL standard protein solutions using IEF buffer. Store at 4 °C.
9. Infant milk formula solution: 0.1 g infant milk formula sample is dissolved into 4 mL IEF buffer by over 30 min stirring, followed by centrifugation at 13.2 krpm for 10 min to remove insoluble matters.

3 Methods

All the following procedures are carried out at room temperature unless otherwise specified.

3.1 Fabrication of Microchip-CE Device

1. Prepare the design of the microchip-CE device using AutoCAD, SolidWorks, or other design software. The dimensions are indicated in Fig. 1. It consists of two pieces of 1.5 mm PMMA and one embedded capillary.
2. Laser ablation of PMMA device (*see* **Note 1**): Use a CO_2 laser to cut the PMMA plate to obtain two pieces with a dimension of 40 mm × 27 mm. Cut one piece (top layer) with 7 cut

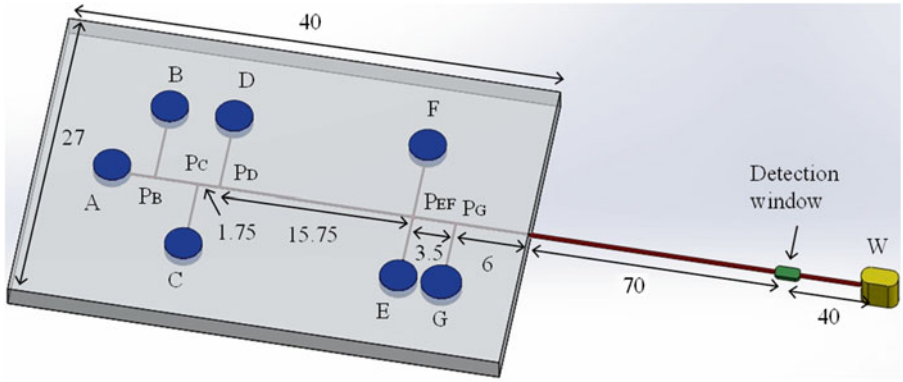

Fig. 1 Microchip-CE device used for determination of functional proteins in infant milk formula products. All dimensions shown are in mm. Vial (A), anolyte; (F), catholyte; (B), sample; (E), waste; (G), background electrolyte; (W), leading electrolyte; (C) and (D), both terminating electrolytes

through holes with a dimension of 3 mm, as shown in Fig. 1. Cut the microchannels with dimensions 120 μm wide and 110 μm deep on the other piece (bottom layer).

3. Bonding of microchip-CE device: Align the two plates of PMMA as shown in Fig. 1. Put the capillary between the two pieces of PMMA with 1 mm embedded length. Put the aligned PMMA parts and capillary on the hot press bonding machine, and bond them together under a pressure of 0.6 MPa at 95 °C for 25 min (*see* **Note 2**).
4. Seal the interface between the capillary and PMMA chip: Use an epoxy adhesive to seal the interface between the capillary and PMMA chip to prevent leakage and eliminate dead volume (*see* **Note 3**).
5. Burn the detection window on the capillary. Burn the protective coating of the capillary to form the detection window. The detection window is located 40 mm from the end of the capillary, as shown in Fig. 1 (*see* **Note 4**).

3.2 Operation of Microchip-CE Device

The loading of buffer and sample can be monitored by a 40× microscope:

1. Fill all channels with a terminating electrolyte (TE) by a syringe pump from the open end of the embedded capillary (*see* **Note 5**).
2. Seal the open end of the capillary and vials A, C, D, F, and G by silicone plugs.
3. Apply vacuum suction to vial E to draw sample solution from vial B to completely replace the TE in the channels between B and E (*see* **Note 6**).

4. Seal vials A, B, C, D, E, and F with silicone plugs; fill in BGE (identical to LE) from W to G by a syringe pump.
5. Add anolyte and catholyte to vials A and F, respectively.
6. Add TE to vials C and D.
7. Add BGE to vial G.
8. On-chip IEF of proteins (1D IEF): Apply 1,120 V at vial A, ground (0 V) at vial F, and all other vials "floating" (i.e., no voltage added), holding for 2 min. This step is to remove major milk proteins and separate other low-abundance functional proteins into different segments (*see* **Note 7**).
9. 2D t-ITP: Apply high voltages to eight vials for 1 min as follows, vials A, B, and C (4,060 V), vial D (4,160 V), vials E and F (3,580 V), vial G (3,480 V), and vial W (0 V). This step is to stack the proteins focused at the P_D–P_{EF} segment (such as LF and IgG) by isotachophoresis (ITP) (*see* **Note 7**).
10. 2D CZE: Apply high voltages to eight vials for 7 min as follows, vials A, B, C, D, E, and F (4,060 V) and vial W (0 V). This step is to separate the stacked proteins from step 2D t-ITP based on their mass to charge ratio (m/z) in the embedded capillary (*see* **Note 7**).
11. 3D t-ITP: Apply high voltages to eight vials for 1 min as follows, vials A and B (4,110 V), vial C (4,210 V), vial D (4,060 V), vials E and F (3,580 V), vial G (3,480 V), and vial W (0 V). This step is to stack the proteins focused at the P_C–P_D segment (such as α-LA, β-LgA, and β-LgB) by isotachophoresis.
12. 3D CZE: Apply high voltages to 8 vials for 7 min as follows, vials A, B, C, D, E and F (4,060 V) and vial W (0 V). This step is to separate the stacked proteins from **step 11** by CZE in the embedded capillary (*see* **Note 7**).
13. Record the electropherogram of protein samples by the UV/Vis detector at 280 nm.

3.3 Determination of Functional Proteins in Infant Milk Formula Sample

1. Dilute stock solution of proteins using IEF buffer to prepare different concentrations of standard proteins to establish standard curves, as shown in Table 1.
2. Obtain the electropherogram of standard proteins according to the operation of the microchip-CE device described under Subheading 3.2 (*see* **Note 5**).
3. Plot the calibration curve of each standard protein. Plot the peak area of each standard protein versus its concentration. Obtain the regression equation (Table 1) for each standard protein (*see* **Note 8**).
4. Obtain the electropherogram of the infant milk formula sample according to the operation of the microchip-CE device previously described under Subheading 3.2 (Fig. 2).

Table 1
Calibration curves of standard proteins obtained using the microchip-CE device

Standard proteins	Concentration (mg/mL)	Regression equation[a]
LF	0.005, 0.01, 0.05, 0.1, 0.5	$Y = 0.0447X + 0.00220$
IgG	0.005, 0.01, 0.05, 0.1, 0.5	$Y = 0.0831X + 0.00119$
α-LA	0.01, 0.05, 0.1, 0.5, 2	$Y = 0.00805X + 0.000155$
β-LgA	0.01, 0.05, 0.1, 0.5, 2	$Y = 0.00286X + 0.000451$
β-LgB	0.01, 0.05, 0.1, 0.5, 2	$Y = 0.00737X + 0.000338$

[a]Regression equation may be different using a different microchip-CE device. The equation shown here obtained in our previous results [10] is just for reference

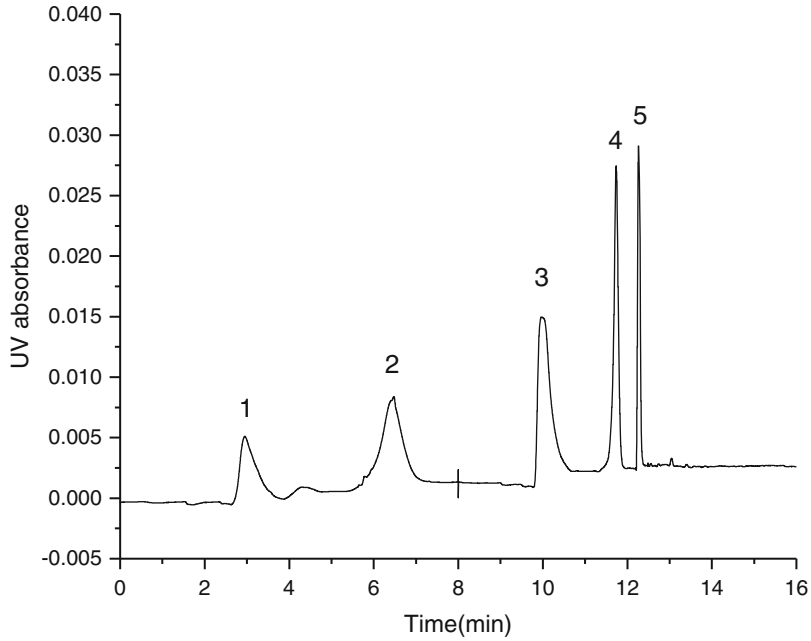

Fig. 2 The electropherogram obtained for an infant milk formula using the microchip-CE device. Peak identification: 1, LF; 2, IgG; 3, α-LA; 4, β-LgB; 5, β-LgA

Identification of functional proteins is completed by spiking individual and mixtures of proteins to infant milk formula sample to check their recovery (*see* **Note 8**).

5. Calculate the concentration of functional proteins in infant milk formula sample. Use the regression equation and the peak area of functional proteins obtained in the electropherogram of infant milk formula for this calculation.

4 Notes

1. The laser for microchip fabrication is isolated in an enclosed box with exhaust to pump off potentially harmful vapors generated during laser action.
2. Wear protective gloves when transferring the microchip-CE device to and from the hot press bonding machine.
3. Use clamps to hold the PMMA chip and embedded capillary vertically, with the capillary above the PMMA chip. Apply one drop of epoxy adhesive to the interface of the capillary and the PMMA chip. The epoxy adhesive will move in and occupy the gap between them by capillary and gravity force. After curing for some time, the epoxy adhesive will solidify and no leakage should be found in the interface.
4. Once the protective coating is removed, the capillary is very fragile and may easily be broken. Therefore, the detection window of the capillary should only be burnt just before the capillary is assembled onto the UV/Vis detector.
5. It is also preferred to rinse the microchip-CE device with DI H_2O, 0.1 M NaOH, DI H_2O consecutively before using and reusing the device. The same rinsing process should also be performed after using the microchip-CE device, which can remove the possible adsorption of test samples and reagents to the device and prevent precipitation of salts in the device.
6. The actual sample used for the test is less than 0.5 μL (from vial B to vial F). However, since there is TE prefilled in the channel, more sample (10 μL) is applied to thoroughly flush out TE buffer and replace this channel with sample to be tested.
7. All high-voltage contacts are isolated during operation with the electric power turned off automatically by safety switches when the protective cover is opened.
8. Determination of standard proteins and functional proteins in infant milk formula should be repeated at least 3 times. Using the average of these repeated tests can give more accurate results.

References

1. Fox PF, McSweeney PLH (1998) Milk proteins. In: Fox PF, McSweeney PLH (eds) Dairy chemistry and biochemistry. Blackie Academic, London, pp 146–238
2. Lien EL (2003) Infant formulas with increased concentrations of alpha-lactalbumin. Am J Clin Nutr 77:1555S–1558S
3. GB 14880-2012, Food safety national standards for the usage of nutrition enrichment, China
4. Palmano KP, Elgar DF (2002) Detection and quantitation of lactoferrin in bovine whey samples by reversed-phase high-performance liquid chromatography on polystyrene–divinylbenzene. J Chromatogr A 947:307–311
5. Hurley IP, Coleman RC, Ireland HE et al (2006) Use of sandwich IgG ELISA for the detection and quantification of adulteration of milk and soft cheese. Int Dairy J 16:805–812

6. Billakanti JM, Fee CJ, Lane FR et al (2010) Simultaneous, quantitative detection of five whey proteins in multiple samples by surface plasmon resonance. Int Dairy J 20:96–105
7. Yamada M, Murakami K, Wallingford JC et al (2002) Identification of low-abundance proteins of bovine colostral and mature milk using two-dimensional electrophoresis followed by microsequencing and mass spectrometry. Electrophoresis 23:1153–1160
8. Dalgleish DG (1990) Denaturation and aggregation of serum proteins and caseins in heated milk. J Agric Food Chem 38: 1995–1999
9. Riechel P, Weiss T, Ulber R et al (1998) Analysis of bovine lactoferrin in whey using capillary electrophoresis (CE) and micellar electrokinetic chromatography (MEKC). Adv Exp Med Biol 443:33–39
10. Wu RG, Wang ZP, Zhao WF et al (2013) Multi-dimension microchip-capillary electrophoresis device for determination of functional proteins in infant milk formula. J Chromatogr A 1304:220–226

Chapter 11

Fast Assembly of Anti-Voltage Photonic Crystals in Microfluidic Channels for Ultrafast Separation of Amino Acids and Peptides

Yi Chen, Tao Liao, and Can Hu

Abstract

Photonic crystals (PCs) with periodically ordered particle beds are ideal media for high-performance separation but hard to be stably and crack-freely assembled in various microfluidic channels. Here we describe a facile method to fast assemble crack-free and high-voltage-sustainable PCs into the micro channels. The key is to speed up an evaporation-induced assembly by heating up (at 70 °C) and blowing away the solvent vapor from one end of a channel and supplying silica suspension at the other end. Crack-free PCs can be prepared at a speed of 0.2 cm/min. The heat also accelerates the silica particles to gel with solvent water and in turn to form a particle network by linking each other through their gelled surface. PCs with two pieces of particle network at their ends are capable of resistance to electrical fields up to 2,000 V/cm. Ultrafast separation of amino acids can be achieved along a 2.5-mm PC in 4 s and peptides along a 10-mm PC in 12 s.

Key words Photonic crystals, Accelerated assembly, Micro channels, Ultrafast separation, Amino acids, Peptides

1 Introduction

Chromatography has tremendously advanced in recent years, but the advancement is far from completion [1]. With photonic crystals (PCs) that are periodically ordered bores [2–4] or particle beds [5, 6], efficient separation of DNA [7, 8] and proteins [7, 9] by their size is possible. PCs are also theoretically ideal media for high-performance chromatographic resolution of other analytes according to the chromatographic kinetic equation [10]:

$$H = 2\lambda d_{\mathrm{p}} + \frac{2\gamma D}{u} + f(k)\frac{d_{\mathrm{p}}^2}{D}u \qquad (1)$$

where H is the plate height, d_{p} the diameter of packed particles, λ a uniformity-dependent factor, γ a diffusion obstruction factor also depending on packing uniformity, D the molecular diffusion

Ann Van Schepdael (ed.), *Microchip Capillary Electrophoresis Protocols*, Methods in Molecular Biology, vol. 1274,
DOI 10.1007/978-1-4939-2353-3_11,

coefficient in mobile phase flowing at a linear velocity of u, and $f(k)$ a function of retention factor k. Equation 1 shows clearly that the packing uniformity governs the separation efficiency, being as critical as the particle size (decrease of which has resulted in the emergence of ultrahigh-performance liquid chromatography [11–13]).

Actually, PCs have been demonstrated to be suitable for efficient chromatographic separation of small molecules [14, 15] because the packed sub-microparticles can form nano-channel networks which are at present a hot research field [16–18]. The challenge which blocks the wide spread of PC-based separation methods lies in the difficulty to prepare a stable and crack-free PC in a required space such as in a column or in a micro channel.

There are in theory two basic strategies to create a PC bed in columns and/or micro channels, that is, by drilling holes through a cylindrical block [2–4] or by self-assembly of monodispersed particles into a column or channel [5, 6]. Drilling techniques allow the fabrication of some specially designed PCs but not as robust as self-assembling methods which are easy to manipulate in a normal laboratory. We have hence focused our efforts on the methods of assembly, especially evaporation-induced assembly.

Evaporation-induced assembly is the most convenient to use. It is cheap but has very slow assembling speed. It may take days to weeks to assemble a usable size of PCs. Extra treatments are also needed to stabilize the assembled PCs, for example, by sintering silica PCs at 900 °C [15]; by pressing plastics at 115 °C [14], in virtue of chemical reactions [8, 19]; or through a sandwiching approach [20]. These stabilizing processes are also not fast but take time.

In this chapter a fast assembling method is presented for filling PCs into microfluidic channels. The core idea is to assemble and fix silica PCs in glass channels simultaneously. The key points include (1) speedup of the solvent evaporation by heating up and blowing away the solvent vapor and (2) acceleration of the gelation of silica particles in aqueous suspension by heating it at 70 °C, which makes the packed particles link to each other to form a particle network after they cool down again, able to serve as a permeable stopper to block the PCs from slipping out of the channels. As a result, crack-free and stable (against at least 2,000 V/cm) PCs were assembled in micro channels at a speed of 0.2 cm/min and could be used for ultrafast resolution of amino acids and peptides in seconds [21].

2 Materials

Unless indicated otherwise, store all reagents and chemicals at room temperature. Diligently follow all waste disposal regulations when disposing waste.

2.1 Instruments, Chemicals, and Materials

1. A laboratory-built microchip separation system (*see* **Note 1**). All the PC-based separations were performed on a laboratory-built microchip system, with a chip laid on an inverted fluorescence microscope (IX71, Olympus, Japan; single-photon detector (Andor iXon DV885, Northern Ireland)), connected to four direct current high-voltage power supplies (0–5,000 V from Dongwen High-Voltage Power Supply Plant, Tianjing, China) through gold wire electrodes inserted in its four reservoirs as illustrated in Fig. 1. The power supplies were controlled using laboratory-edited software via a multichannel digital/analogue convert board (model AC6302 from wwlab, Beijing, China).
2. A commercial pH meter for monitoring pH whenever required.
3. A commercial ultrasonicator for degassing solutions or accelerating dissolution of chemicals.
4. A thermostatic water bath able to regulate temperature between 20 and 30 °C.
5. A water purification system for the production of ultrapure water with resistance >1.2 MΩ (e.g., a Milli-Q academic system, Millipore, Billerica, MA, USA).
6. A commercial UV exposure system (e.g., model URE-2000/35, from the Institute of Photoelectrics, Chinese Academy of Sciences, Chengdu, China).

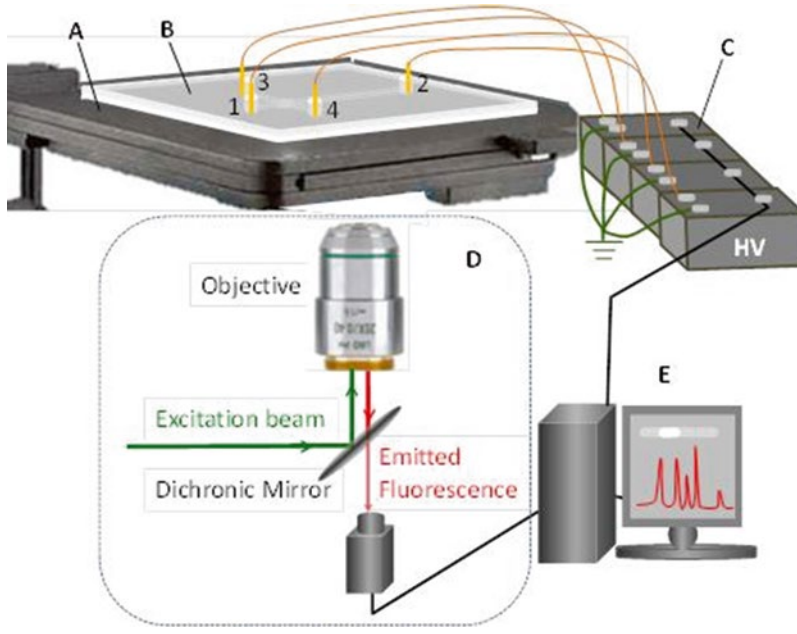

Fig. 1 A laboratory-built chip-based separation system with (**a**) purposely scaled-up stage (to view clearly) and (**b**) glass chip connected via gold electrodes to (**c**) four direct current high-voltage supplies and subject to (**d**) green light (470–495 nm) excitation to conduct fluorescent detection at 520 nm, all controlled by (**e**) a computer

7. A muffle furnace (e.g., a ceramic fiber muffle furnace, model MF-09129, from Hua Gang Tong Tech. Co. Ltd., Beijing, China).
8. Tetraethyl orthosilicate (TEOS, 98 %) (Alfa Aesar, Ward Hill, MA, USA).
9. 28 % (w/w) ammonium hydroxide ($NH_3 \cdot H_2O$).
10. Fluorescein isothiocyanate (FITC) isomer I.
11. Amino acids, e.g., phenylalanine (Phe), arginine (Arg), glutamic acid (Glu), glycine (Gly), and oligoglycine peptides, e.g., $(Gly)_4$, $(Gly)_5$, and $(Gly)_6$.
12. 30 % (w/w) hydrogen peroxide.
13. 65 % (w/w) nitric acid.
14. Borax ($Na_2B_4O_7 \cdot 10H_2O$).
15. Ceric ammonium nitrate.
16. NaOH.
17. 1.7-mm-thick glass plates with chromium and photoresist coating (e.g., SG4009 coated with 145 nm Cr and 570 nm S-1085 photoresist, from Shaoguang Microelectronics Corp., Changsha, China).

2.2 Solutions and Samples

Prepare all samples and buffer solutions with chemicals of analytical reagent grade in Milli-Q water, and unless specially indicated otherwise, store them at 4 °C:

1. 20 mM $Na_2B_4O_7$ buffer: weigh 381 mg $Na_2B_4O_7 \cdot 10H_2O$, and dissolve it in 50 ml water, adjusted to a required pH value by step addition of powdered NaOH and/or 6 M HCl.
2. 10 or 5 mM $Na_2B_4O_7$ buffer: dilute the original 20 mM $Na_2B_4O_7$ buffer with water at a volume ratio of 1:1 or 1:3, and adjust the pH to 9.2 if required.
3. Sample solutions:
   (a) FITC labeling solution (3.0×10^{-4} M): weigh 3.0 mg FITC, dissolve it in 25 ml acetone, and store the solution at –20 °C.
   (b) Individual amino acid and peptide solutions (1.00×10^{-3} M): weigh 1.74 mg Arg, 1.65 mg Phe, 0.750 mg Gly, 1.47 mg Glu, 2.46 mg $(Gly)_4$, 3.03 mg $(Gly)_5$, and 3.60 mg $(Gly)_6$, and dissolve them in 10 ml $Na_2B_4O_7$ buffer (5 mM, pH 9.2), separately.
4. 0.4 % (w/v) NaOH for photoresist development: weigh 0.40 g powdered NaOH and dissolve it in 100 ml water.
5. Chromium-removing solution: weigh 25 g ceric ammonium nitrate ($(NH_4)_2Ce(NO_3)_6$), and dissolve it in 117 ml water added with 4.5 ml glacial acetic acid (*see* **Note 2**).

6. Chemical etching solution: mix 20 volumes of concentrated HF with 14 volumes of HNO_3 and 66 volumes of water (*see* **Note 3**).
7. Piranha solution: prepare the solution just before use by slow addition of 30 % H_2O_2 into 98 % sulfuric acid at a volume ratio of 1:3 (*see* **Note 4**).

3 Methods

Carry out all procedures at room temperature unless otherwise specified.

3.1 Labeling of Samples

1. Mix 20 μl FITC labeling solution with 20 μl sample solution of an individual amino acid or peptide.
2. Keep the mixture in dark at room temperature for 12 h to complete the reaction.
3. Dilute the reacted mixture 100–1,000 times with 5 mM $Na_2B_4O_7$ buffer just before use.
4. Mix up the individual FITC-amino acid solutions or FITC-peptide solutions at an equal volume to form various mixed samples.
5. Dilute the mixed sample solution to the desired concentration with an appropriate volume of 5 mM $Na_2B_4O_7$ buffer.

3.2 Synthesis of Silica Nanoparticles [22]

1. Warm a round-bottomed flask in a water bath at 25 °C.
2. Add 73.8 ml ethanol, 10.8 ml water, and 9.8 ml ammonium hydroxide (28 %) into the flask via magnetic stirring.
3. Quickly pour 5.6 ml TEOS (98 %) into the mixture.
4. Stir the mixed solution for 12 h until uniform silica nanoparticle form.
5. Separate the particles from the suspension by centrifugation.
6. Wash the particles with pure ethanol 4 times.
7. Further clean the particles by washing them with water until pH 7.
8. Sinter the particles at 600 °C for 10 h 3 times [23].
9. Re-disperse the sintered silica particles in water at 10 % (w/v) for long-term storage.
10. Characterize the synthesized particles by scanning electron microscopy (SEM) to observe and measure the particle shape and size as shown in Fig. 2.

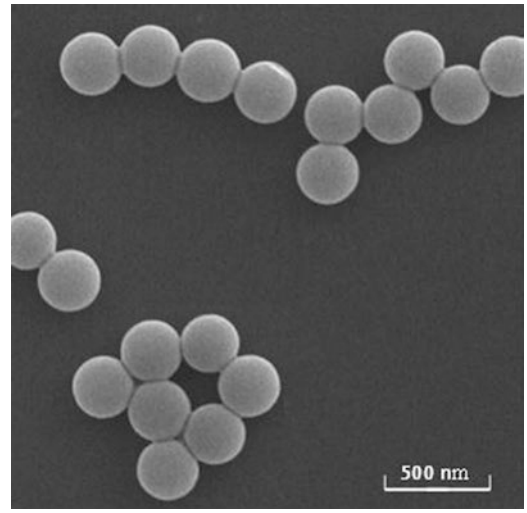

Fig. 2 SEM of a batch of laboratory-synthesized silica particles with expected diameter of 250 nm

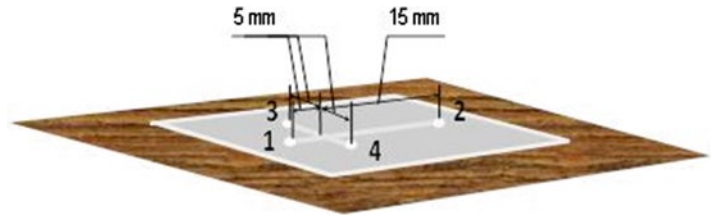

Fig. 3 A photomask patterned with two channels crossing at 5 mm to (1) inlet, (3) sample, and (4) waste reservoirs and 15 mm to (2) outlet reservoir

3.3 Fabrication of Glass Microchip

A simplified photolithographic technique (*see* **Note 5**) is adopted to fabricate a glass chip, with somewhat detailed steps as follows:

1. Select a photomask with two crossly patterned micro channels (50 μm wide) (*see* **Notes 1** and **6**) with the cross point set at 5 mm to the inlet (1), injection (3), and waste (4) reservoirs and 15 mm to the outlet reservoir (2) as shown in Fig. 3.
2. Align a 1.7-mm-thick glass wafer coated with chromium and photoresist under the photomask (*see* **Note 5**).
3. Expose the photoresist to UV light through the mask for about 15 s (*see* **Notes 5** and **7**).
4. Develop the on-photoresist channel pattern in 0.4 % NaOH for 10 s (*see* **Note 8**).
5. Etch the uncovered Cr layer in the chromium-removing solution for 10 s (*see* **Note 9**).
6. Further etch the pattern into the glass wafer in the chemical etching solution to a depth of ca. 30 μm and width of ca. 100 μm (for about 15 min in common) (*see* **Note 6**).

7. Drill holes through the wafer at each channel end with a diamond-tipped drill bit (e.g., 0.5, 1.0, and/or 2.0 mm diameter) (*see* **Note 10**).
8. Remove the photoresist coating in acetone by sonication for ca. 1 min (*see* **Note 11**), and wash the wafer with water, and dry the wafer by a compressed air flow.
9. Clear off the chromium layer in the chromium-removing solution until the glass becomes totally transparent (for ca. 1 min).
10. Wash the glass wafer with water, dry it with a compressed air stream, and further clean it in the piranha solution at 90 °C for about 30 min (*see* **Notes 4** and **12**).
11. Wash the glass wafer with water 3 times and blow it to dryness with a compressed air flow.
12. Thermally bond the cleaned glass wafer with another cleaned glass wafer (130 μm thick) (*see* **Note 13**).
13. Store the bonded chips in a clean box set in a safe place.

3.4 Assembly of Silica PCs in Microfluidic Channels

1. Select a glass chip with two cross channels and four reservoirs as shown in Fig. 1 (*see* **Notes 1** and **14**).
2. Rinse the channels with 0.1 M HNO_3 and water three times each.
3. Degas silica particle suspension by sonication for about 30 min.
4. Fill 5 μl degassed suspension into the reservoir 2 and in turn into the channels (Fig. 4a) by making use of the surface tension or capillary force (*see* **Note 15**).
5. Fill the left reservoirs 1, 3, and 4 with the same suspension once all the channels are completely filled (*see* **Note 15**).
6. Blow the reservoirs 1, 3, and 4 all together with a hot airflow at 70 °C, while reservoir 2 is kept at room temperature and continuously supplied with the particle suspension (Fig. 4b) (*see* **Notes 16** and **17**).
7. Stop blowing reservoirs 1, 3, and 4 once the PC reaches a desired length or reaches the reservoir 2.
8. Fill reservoirs 1, 3, and 4 with 5 μl water each, and blow the channel end at reservoir 2 with the 70 °C hot air flow (Fig. 4c) until reservoir 2 is dried (ca. 3 min) to fix the silica PC in the end (*see* **Note 17**).
9. Remove the deposited silica particles in all the reservoirs and clean them with water.
10. Fill the reservoirs with water, and seal the reservoirs with soft PDMS (Fig. 4d) to prevent the water from evaporating during storage (*see* **Notes 18** and **19**).

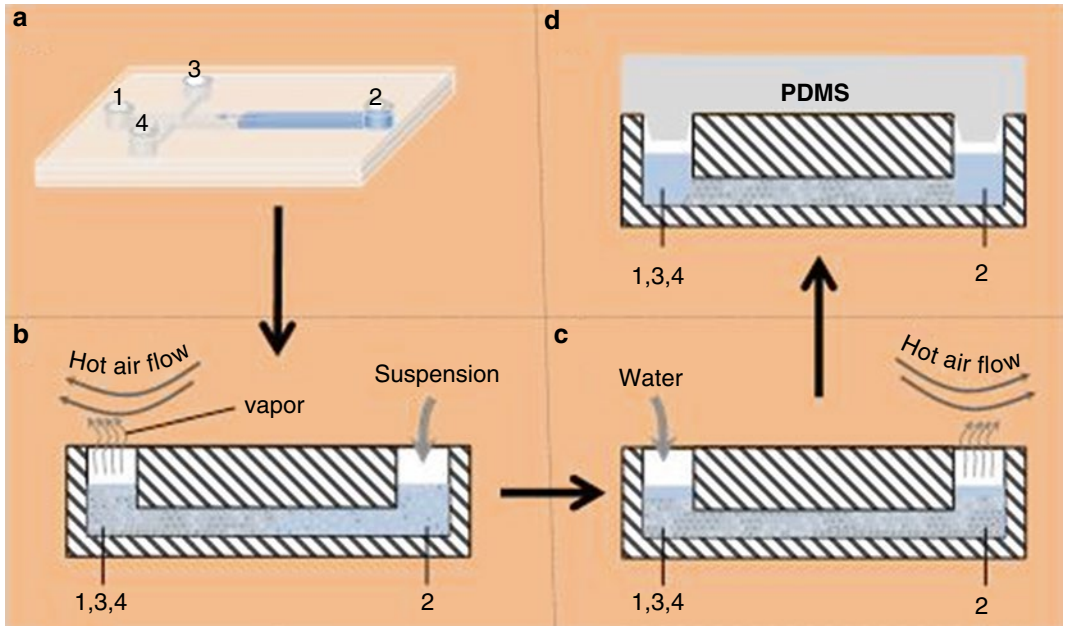

Fig. 4 Key steps to fast assembly of silica particles in glass chip channels by heat-accelerated evaporation. (**a**) Fill the particle suspension into the channels via reservoir 2; (**b**) blow a hot air flow at 70 °C against the reservoirs 1, 3, and 4 all together; (**c**) blow the same hot air against only the reservoir 2 while the reservoirs 1, 3, and 4 were supplied with water; (**d**) fill all the reservoirs with water after the removal of the particles in the reservoirs, and seal the reservoirs with a piece of soft PDMS for safe storage of a long time

3.5 Separation of Samples on a PC-Filled Channel

1. Replace the water in the reservoirs with $Na_2B_4O_7$ buffer (*see* **Notes 20** and **23**), and equilibrate the channels at 100 V/cm until the current becomes stable. Repeat the replacement and equilibration three times (*see* **Note 21**).
2. Load reservoir 3 with a sample solution immediately after evacuation of its buffer.
3. Inject the sample solution into the channels by electric clip injection with application of 200 V, 200 V, 1,300 V, and 0 V (commonly grounded) potential at the reservoirs 1, 3, 2, and 4, respectively (*see* **Note 22**).
4. Drive the clipped section of sample into the separation channel between the reservoirs 1 and 2, and separate it by application of a voltage across the reservoirs 1 and 2, typically at 1,000 V/cm along the channel (*see* **Note 23**), with a "pull-back" voltage of 1,500 V applied to the reservoirs 3 and 4 to prevent the sample from leaking into the separation channel.
5. Detect the separated bands by a single-photon detector through collecting time-lapse intervals of 520-nm fluorescence images (excited at 470–495 nm) using a 10× objective lens with 0.3 numerical aperture (*see* **Note 24**).

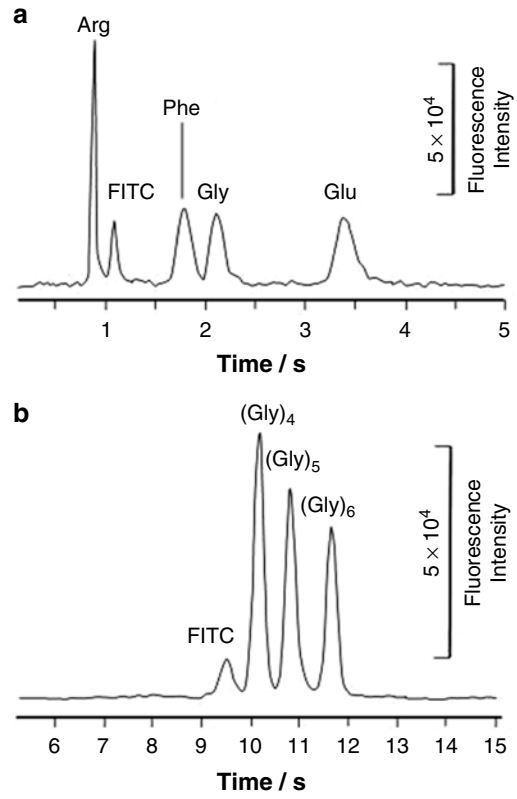

Fig. 5 Ultrafast separation of (**a**) FITC-labeled amino acids along a 2.5-mm silica PC bed at 1,200 V/cm and (**b**) FITC-peptides along a 10-mm silica PC bed at 1,000 V/cm using a running buffer of 20 mM $Na_2B_4O_7$ at pH 10.02

6. Analyze the imaging data with Andor SOLIS software (www.andor.com) by summation of the fluorescent intensity values over a region of 50 μm (along channel) × 100 μm (wide) on the sequential images (*see* **Note 24**).
7. Plot the electrochromatogram by the summed data versus time (Fig. 5) (*see* **Notes 25** and **26**).

4 Notes

1. A commercial chip instrument can be selected if available, but the chip channel format may vary. In common, a chip with cross channels is the basic element for fabrication of complex microfluidic chips and can easily adapt to different commercial instruments. If not, one should use a chip adaptable to the instrument.
2. Ceric ammonium nitrate is an oxidant. Store it in a ventilated place isolated from reducers. Always wear eyeglasses and latex gloves when using it, and prepare the solution in a hood with a sash between you and the solution.

3. The concentrations of HF and HNO_3 can be adjusted depending on the etching speed you need. Both HF and HNO_3 are harmful and have to be used with protection, for example, wear eyeglasses and latex gloves, and perform the mixing procedure in a hood with the sash between you and the solution.
4. Piranha solutions are extremely energetic and may result in explosion and/or skin burns. It should be handled with great care! Always wear gloves and eye protection while using it! Piranha will melt plastics, and the solution has to be prepared in glass (preferably Pyrex) containers in a hood with the sash between you and the solution. When preparing the piranha solution, always add the peroxide to the sulfuric acid, not inversely!
5. The basic etching procedure is schematically illustrated in Fig. 6.
6. In order to etch a channel of 30 μm in depth and 100 μm in width, a ca. 50-μm-wide channel has to be patterned on a mask because the wet etching engraves not only the bottom side but also both the lateral surfaces of a channel. The etching speed is commonly controlled at about 2 μm/min. But for smooth channels, the etching speed has to be lowered, preferably at ca. 0.5 μm/min. The etched channels can be observed under a microscope.
7. This operation transfers the channel pattern from the mask to the photoresist on the glass wafer. The exposure time depends on the photoresist and instrument you are using. Please refer to the related specifications and/or manuals of your own

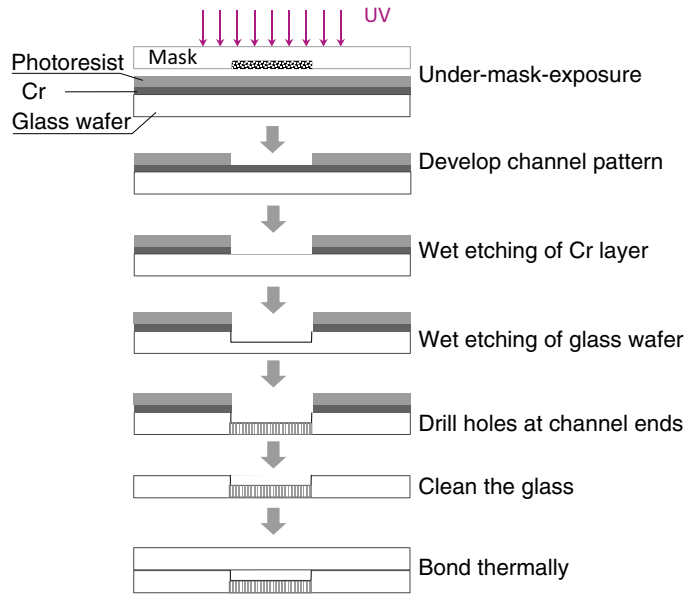

Fig. 6 Basic procedure for preparation of a glass chip by photolithography

instrument and photoresist. Commonly, a certain photoresist needs a fixed exposure dose, but the UV lamp mounted in the exposure instrument decreases its power gradually. The exposure time or lamp voltage thus needs to increase after use for a certain amount of time. It is better to measure the lamp illumination intensity with an exposure meter before calculation of your exposure time or adjusting your instrument.

8. The developed channels are clearly brightened and can be viewed by naked eyes. The on-photoresist channel traces are better observed under a microscope to check whether the development is perfectly complete or not. If not, supplementary development should be conducted for several extra seconds.
9. The developed channels may not easily be observed by the naked eye because the color of the developing solution is fairly intense (orange red). The observation can be realized after washing the wafer with water, by preference under a microscope. If the development is not complete, supplementary development has to be conducted for several extra seconds.
10. Glass can be drilled using a diamond-tipped drill bit, with water as a coolant dropped on the drilling position. The drilling edges may crack if glass is directly drilled, but cracks can be avoided by gluing? the glass to be drilled on another glass with melted colophony which will become solid again after cooling. After drilling, the solidified colophony can easily be cleaned with acetone followed by washing with water.
11. The color of the acetone will change to orange red.
12. The cleaning can also be performed at room temperature, but it takes ca. 12 h.
13. To thermally bond two pieces of glass wafers, they are aligned layer by layer and heated up to a near-melting point or softening point and then cooled down gradually after they were kept at the softening point for a certain time. A practical program is as follows: the aligned glasses are pressed with a heavy corundum brick and heated in a muffle furnace at 10 °C/min first to 100 °C (maintained for 30 min) and then to 550 °C (maintained for 30 min) and at 1 °C/min to 570 °C (maintained for 4 h). The temperature is then lowered to 300 °C in 2 h, followed by a natural cooling of the furnace to room temperature.
14. A single channel can also be used, but the inlet has to be tapered and made hydrophobic to inject picoliters' sample into the PC channel. More complicated channels are also usable depending on the chip instruments used.
15. For chips with only a single channel, the silica particle suspension is added into the non-tapered end. For more complicated channels, the suspension is better added into a reservoir far from others, so that, later assembling steps can be conducted

more conveniently. The left reservoirs have to be added with the suspension after all the channels are fully filled with the suspension. If a chip has already been filled with water, evacuation of the water is unnecessary, but the water in the reservoirs needs to be replaced with the particle suspension.

16. This will assemble a layer (ca. 100 μm) of silica particles on the bottom of the reservoirs 1, 3, and 4, followed by a formation of silica PC along the channels by drawing the suspension from the reservoir 2. The heating can simply be achieved using a hair dryer, but a thermostated gas flow is more preferred for repeatable preparation.
17. The heating helps to gel the silica particle surface with water. This will make the contacting particles connect into a particle network and fix them together after cooling. Thus, the heated part of the assembled silica PC at the channel ends will form a stable plug to block the inner PCs from moving out. This fixation is critical for efficient separation at high voltage. Figure 7a shows that, without any fixation, the PC will be unable to undergo an electric field even as low as 100 V/cm. For a PC fixed at only one end, it is stable if a positive voltage is applied at the fixed end, but it disbands quickly if the positive voltage is applied at the unfixed end (Fig. 7b). Completely different from the previous two cases, the PCs with two ends fixed can sustain high voltage, up to at least 2,000 V/cm, as illustrated by microscopic images in Fig. 7c, d. Furthermore, the relationship of current vs. electric field maintains an excellent linearity (Fig. 7e, f), implying that Ohm's law is well obeyed in this case.
18. The reservoirs have to be filled with water to avoid their drying out during storage, which can be achieved easily by always supplying the reservoirs with water or by sealing the reservoirs with soft PDMS. Alternatively, the filled chips can also be maintained wet for a long time by filling the reservoirs with water and storing in a sealed box which is pre-saturated with water vapor. In case some minor parts of the filled PCs are dried or contain bubbles, they may be recovered by filling the reservoirs with more water and subjecting to a low voltage between 100 and 300 V/cm for a certain time. It may be more effective to apply a gradient voltage across the channels, starting from 100 V/cm and ending at ca. 500 V/cm at a step increment of 20 V/cm every 30 min. Once the packed PCs are dried out largely and can never be recovered, they are detruded or evacuated for repacking (*see* **Note 21**).
19. The prepared PCs in micro channels can be characterized by viewing their iris colors under natural light (Fig. 8a), by imaging on scanning electric microscope or on laser-induced fluorescent confocal microscope (Fig. 8b), and by measuring their reflection or transmission spectrum (Fig. 8c). Compared with

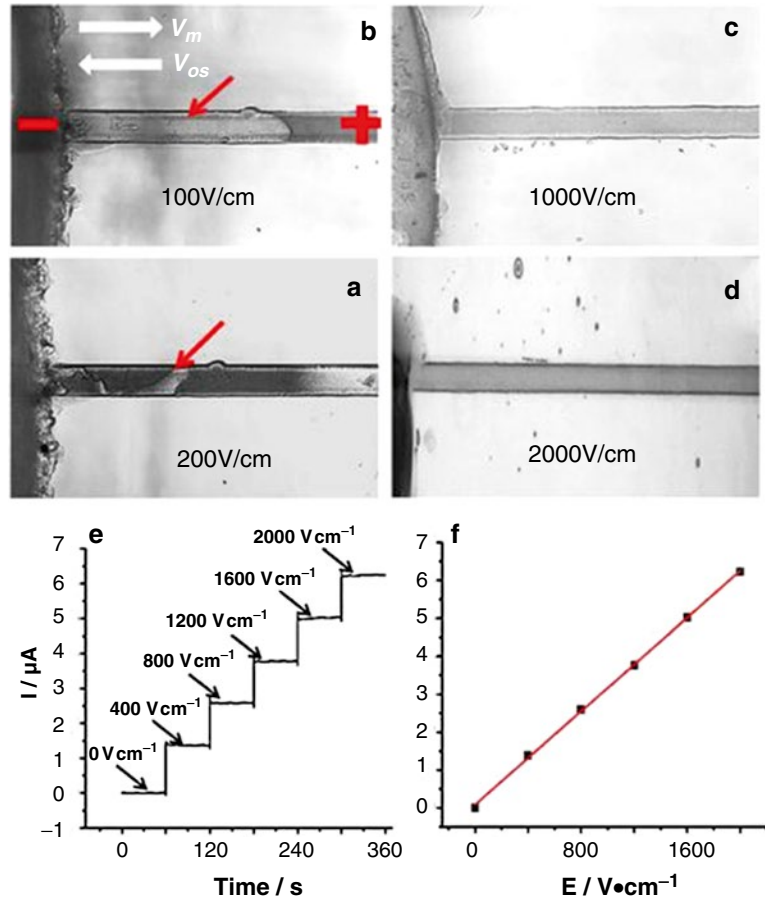

Fig. 7 The stability of assembled silica PCs illustrated by (**a**–**d**) microscopic images, (**e**) current stability, and (**f**) Ohm's law. (**a**) Without fixation; (**b**) one end fixed; (**c**)–(**f**) both ends fixed. The *red arrows* indicate the cracking positions (color figure online)

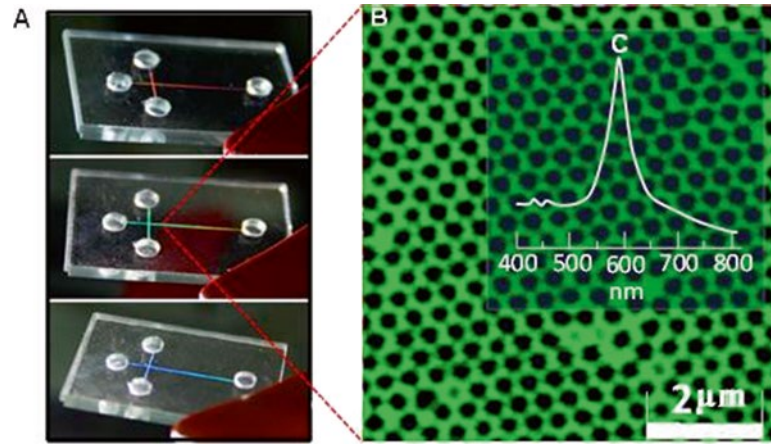

Fig. 8 A silica PC chip assembled from 266-nm silica particles having (**a**) various irised colors at different angles under the natural light, (**b**) well-ordered microstructure in laser-induced fluorescence confocal microscopic image, and (**c**) typical forbidden band at 584 nm in the reflection spectrum, agreeing well with theoretical calculation at an observation angle of 0° against the (111) face of PC

SEM, the fluorescent imaging is easy in manipulation, which is conducted with FITC solution as an indicator. Figure 8a illustrates that the PC-packed chip reflects different colors at different observation angles, agreeing well with theoretical expectation. Figure 8b confirms that the assembled silica particles are well ordered in the channels, and Fig. 8c further confirms that the ordered particle beds have a typical forbidden band in the reflection spectrum that a PC should have. All the data imply that the assembled silica particles in the micro channels have significant PC features.

20. The buffer should be selected according to the separation format adopted, which is dependent on the analytes to be separated. Commonly, to separate FITC-amino acids, a 5 mM or 10 mM $Na_2B_4O_7$ buffer works well.
21. The equilibration can be accelerated by application of a bit higher electric field, e.g., 200–500 V/cm, if the column is bubble-free. In case there are bubbles or the current is not stable, it is better to equilibrate the channels with the buffer by application of a gradient electric field between 100 and 300 V/cm (*see* **Note 18**). If the equilibration cannot be achieved, the PC-filled chips are not useful anymore and have to be reassembled. This can be achieved by evacuation of the channels and then reassembly with silica suspension as described in this chapter. The evacuation of the packed chip channels can be realized first by sonication to loosen the fixed PCs and then by application of a voltage across the chip channels to make the loosened particles migrate out of the channels.
22. The clipped sample solution flow can be imaged under a fluorescent microscope by using FITC as an indicator. It should be noted that FITC and its derivatives cannot be measured clearly at the first several injections, possibly due to their strong nonspecific adsorption. The quality of the detected signals will improve gradually after several injections of concentrated FITC solutions. With the indication of the fluorescent images, the clip injection can be optimized by adjusting the potential applied on each electrode. For only one channel chip, the injection can be achieved by contact of the tapered inlet with a sample solution by diffusion [24] or by electrokinetic injection.
23. The higher the electric field applied, the better the theoretical efficiency (Fig. 9) obtained and the higher the separation speed (Fig. 10). Figure 9 shows that the theoretical plate height decreases very fast at the very beginning phase and then slows down gradually after the migration speed reaches 0.5 mm/s. However, the electric field strength is better optimized. In fact, ultrafast separation of some analytes is not too difficult while using PC beds after some optimization of running buffer, injection approach, and especially the separation length of PC and voltage applied.

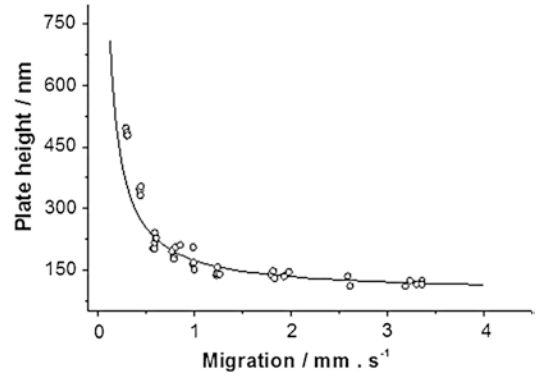

Fig. 9 Impact of migration speed (parallel to applied electric field strength) on the theoretical plate height measured at 200–2,000 V/cm by migration of a plug FITC along 2.4-mm PC using 5 mM $Na_2B_4O_7$ buffer at pH 9.20

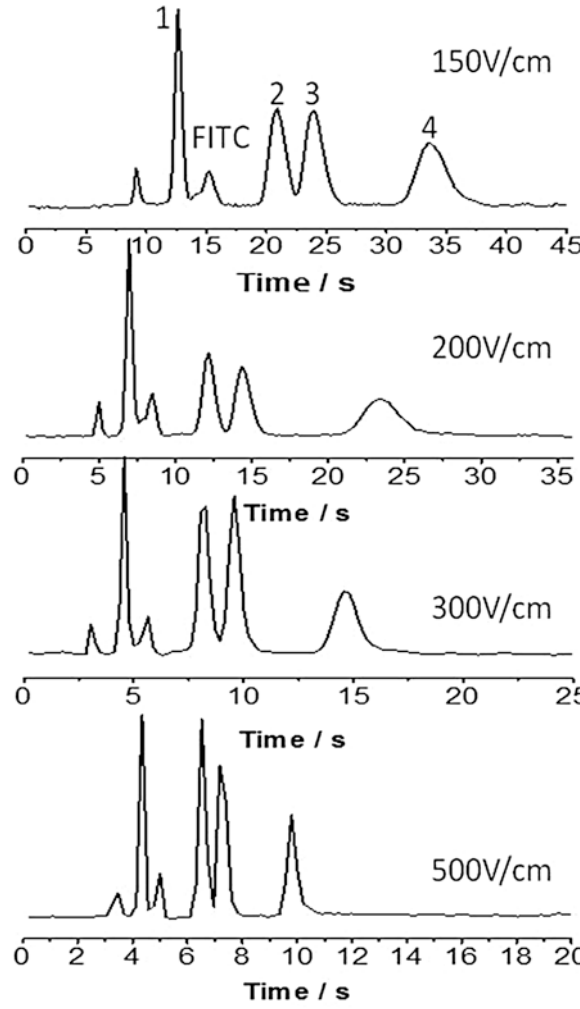

Fig. 10 Electrochromatogram measured on a glass chip assembled with 460-nm silica particles (pre-sintered at 600 °C before assembly). The separation was achieved along a 15-cm (3 mm effective) × 75-μm × 20-μm PC with a running buffer of 10 mM $Na_2B_4O_7$ at pH 9.2 at different electric fields as shown in the figures. Peak identity: (1) Arg, (2) Phe, (3) Gly, and (4) Glu

24. In order to save computer space, the collection size of the images should be reduced to a small region of 20×200–200×200 μm², which is enough to completely cover the channels. Commonly, narrowing the collection length along the channel will improve the speed and the peak resolution as well as reduce the signals. The speed and detection sensitivity have to be compromised, depending on different analytes. For fast separations, the digitalization of the fluorescent images should also be maintained at ~10–25 Hz by using the Andor software introduced in this chapter.
25. The electrochromatograms of amino acids and peptides shown in Fig. 5a, b, respectively, are typically ultrafast separation examples, where the baseline separation of the analytes is achieved at a level from seconds to tens of seconds. Ultrafast separation can be achieved after optimization of the separation conditions (*see* **Note 23**). If the resolution is very high, a very short PC will be enough to fully resolve some target analytes just as in the case of amino acids where only ca. 2-mm PC is sufficient to yield a baseline resolution. Shortening the injection length may further increase the separation efficiency.
26. The separation on PC beds is highly reproducible. The run-to-run standard deviation of migration time is less than 0.5 % measured by $(Gly)_5$, and chip-to-chip standard deviation of migration time is below 8 %, which is much better than many routine separation methods. Figure 11 shows two examples of repeatable separations.

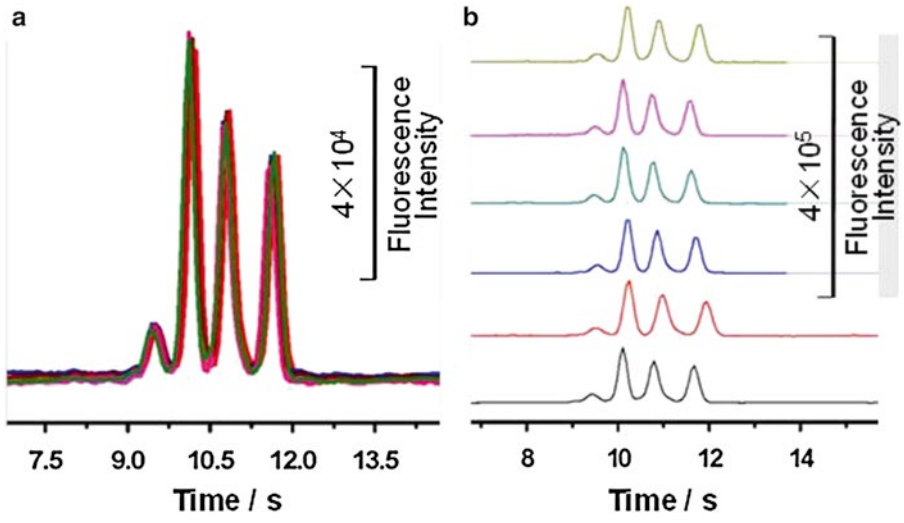

Fig. 11 Separation reproducibility of PC-filled chips measured from (**a**) a same PC and (**b**) different PCs

Acknowledgment

This research was financially supported by NSFC (Nos. 21475136, 21235007, and 91117010), MOST, and CAS.

References

1. Stachowiak TB, Svec F, Frechet JMJ (2004) Chip electrochromatography. J Chromatogr A 1044:97–111
2. Ostendorf A, Chichkov BN (2006) Two-photon polymerization: a new approach to micromachining. Photon Spectra 10:72–79
3. Leon-Saval SG, Birks TA, Joly NY, George AK, Wadsworth WJ, Kakarantzas G, St. Russell P (2005) Splice-free interfacing of photonic crystal fibers. Opt Lett 30:1629–1631
4. Noda S, Tomoda K, Yamamoto N, Chutinan A (2000) Full three-dimensional photonic bandgap crystals at near-infrared wavelengths. Science 289:604–606
5. Vlasov YA, Bo XZ, Sturm JC, Norris DJ (2001) On-chip natural assembly of silicon photonic bandgap crystals. Nature 414: 289–292
6. Miguez H, Yang SM, Tetreault N, Ozin GA (2002) Oriented free standing three-dimensional silicon inverted colloidal photonic crystal microfibers. Adv Mater 14:1805–1808
7. Zeng Y, Harrison DJ (2007) Self-assembled colloidal arrays as three-dimensional nanofluidic sieves for separation of biomolecules on microchips. Anal Chem 79:2289–2295
8. Zeng Y, He M, Harrison DJ (2008) Microfluidic self-patterning of large-scale crystalline nanoarrays for high-throughput continuous DNA fractionation. Angew Chem Int Ed 47:6388–6391
9. Wei BC, Malkin DS, Wirth MJ (2010) Plate heights below 50 nm for protein electrochromatography using silica colloidal crystals. Anal Chem 82:10216–10221
10. Billen J, Desmet G (2007) Understanding and design of existing and future chromatographic support formats. J Chromatogr A 1168: 73–99
11. Anspach JA, Maloney TD, Brice RW, Colon LA (2005) An injection valve for ultrahigh pressure liquid chromatography. Anal Chem 77:7489–7494
12. MacNair JE, Patel KD, Jorgenson JW (1999) Ultrahigh-pressure reversed-phase capillary liquid chromatography: isocratic and gradient elution using columns packed with 1.0-micron particles. Anal Chem 71:700–708
13. Mellors JS, Jorgenson JW (2004) Use of 1.5 μm porous ethyl-bridged hybrid particles as a stationary-phase support for reversed-phase ultrahigh-pressure liquid chromatography. Anal Chem 76:5441–5450
14. Park J, Lee D, Kim W, Horiike S, Nishimoto T, Lee SH, Ahn CH (2007) Fully packed capillary electrochromatographic microchip with self-assembly colloidal silica beads. Anal Chem 79:3214–3219
15. Zheng SP, Ross E, Legg MA, Wirth MJ (2006) High-speed electroseparations inside silica colloidal crystals. J Am Chem Soc 128: 9016–9017
16. Lee SK, Kim SH, Kang JH, Park SG, Jung WJ, Kim SH, Yi GR, Yang SM (2008) Optofluidics technology based on colloids and their assemblies. Microfluid Nanofluid 4:129–144
17. Ge J, Yin Y (2011) Responsive photonic crystals. Angew Chem Int Ed 50:1492–1522
18. Shamah SM, Cunningham BT (2011) Label-free cell-based assays using photonic crystal optical biosensors. Analyst 136:1090–1102
19. Malkin DS, Wei BC, Fogiel AJ, Staats SL, Wirth MJ (2010) Sub-micron plate heights for capillaries packed with silica colloidal crystals. Anal Chem 82:2175–2177
20. Gong MJ, Bohn PW, Sweedler JV (2009) Centrifugal sedimentation for selectively packing channels with silica microbeads in three-dimensional micro/nanofluidic devices. Anal Chem 81:2022–2026
21. Liao T, Guo Z, Li J, Liu M, Chen Y (2013) One-step packing of anti-voltage photonic crystals into microfluidic channels for ultra-fast separation of amino acids and peptides. Lab Chip 13:706–713
22. Stober W, Fink A, Bohn E (1968) Controlled growth of monodisperse silica spheres in the micron size range. J Colloid Interface Sci 26:62–69
23. Chabanov AA, Jun Y, Norris D (2004) Avoiding cracks in self-assembled photonic band-gap crystals. Appl Phys Lett 84: 3573–3575
24. Chen Y, Zhu A (1991) Diffusion injection for high performance capillary electrophoresis. Chinese J Chromatogr 9:353

Part IV

Nonaqueous Applications

Chapter 12

Rapid Determination of Catecholamines in Urine Samples by Nonaqueous Microchip Electrophoresis with LIF Detection

Hongmei Hu, Yuanming Guo, and Tiejun Li

Abstract

Nonaqueous microchip electrophoresis (NAMCE), which makes use of an organic medium instead of a conventional aqueous buffer solution, is a promising separation method for analytical chemistry due to the enhanced solubility of hydrophobic analytes and tailored selectivity of separation. Here, we describe an NAMCE with LIF detection combined with a pump-free negative pressure sampling device for rapid determination of catecholamines (CAs) in urine samples, and the whole analysis time (including sampling time and separation time) was less than 1 min.

Key words Catecholamines, Microchip electrophoresis, Nonaqueous, Pump-free negative pressure sampling device, Urine samples

1 Introduction

Since the pioneering work of Manz et al. [1] and Harrison et al. [2] in 1992, microchip electrophoresis (MCE), which sets capillary electrophoresis (CE) as core technique and microchip as platform, has generated considerable interest in a broad perspective application [3, 4]. Compared to CE, MCE has the advantage of higher degree of integration and portability, less consumption of solvent/reagent, higher performance and speed, and easier minimization [5].

Nonaqueous MCE (NAMCE), which uses organic solvents as background electrolytes, has been shown to offer several advantages compared with MCE, including enhanced solubility of hydrophobic analytes (i.e., extended application range), tailored selectivity of separation (via changes in solvation or acid-base properties of analytes), and relative absence of interferences [6–9]. The first use of a background electrolyte based on pure organic solvents was published when Walbroehl and Jorgensen reported the separation

Ann Van Schepdael (ed.), *Microchip Capillary Electrophoresis Protocols*, Methods in Molecular Biology, vol. 1274,
DOI 10.1007/978-1-4939-2353-3_12,

of quinoline derivatives in acetonitrile containing a tetraethylammonium perchlorate/hydrochloric acid electrolyte system [10]. In recent years, NAMCE has been successfully applied in the separation of lipid mixtures [11], aliphatic amines [12], toxic metal ions [13], trinitroaromatic explosives [14], rhodamine dyes [15], etc.

It is well known that sample injection is crucial because it determines the quality and the shape of a sample plug, both of which are closely related to separation [16]. Our research group has proposed some bias-free negative pressure sampling devices in which negative pressure is generated by a syringe pump [17], a microvacuum pump [18], or a pipet bulb [19], which only need 0.5–2 s for sampling and are much shorter than the electrokinetically pinched injection [20, 21]. It has been reported that long sampling times, typically 10–150 s, are required for sampling with the electrokinetically pinched scheme, which restricts the analytical speed [22].

Because of the advantages of NAMCE over MCE and the superiority of negative pressure sampling discussed above, we have determined catecholamines (CAs) (norepinephrine (NE), epinephrine (E), and dopamine (DA)) in urine samples in less than 1 min by NAMCE with LIF detection combined with a pump-free negative pressure sampling device. In this analytical system, the sample loading and NAMCE separation can be easily controlled by switching a three-way valve with satisfactory sample throughput, analytical precision, and high sensitivity.

2 Materials

Prepare solutions using organic reagents or ultrapure water (prepared by purifying deionized water to attain a resistivity of 18 MΩ·cm at 25 °C) and analytical grade chemicals and reagents. Prepare and store all reagents at room temperature (unless indicated otherwise). Diligently follow all waste disposal regulations when disposing waste materials.

2.1 Standard Solutions, Derivatization Solution, and Derivatization Buffer

1. Diluent for standards: 2.5 mM HCl in methanol (*see* **Note 1**). Add 10 μL HCl to a 50 mL volumetric flask. Make up to 50 mL with methanol. Store at 4 °C.
2. Standard stock solution: 200 mg/L NE, 200 mg/L E, 200 mg/L DA. Weigh 2.0 mg NE, E, and DA, dissolve them with diluent for standards, and transfer to a 10 mL volumetric flask, respectively. Make up to 10 mL with diluent for standards. Store in the dark at 4 °C (*see* **Note 2**).
3. Mixed standard solution: 80 mg/L NE, 40 mg/L E, 80 mg/L DA. Add 4 mL standard stock solution of NE, 2 mL standard stock solution of E, and 4 mL standard stock solution of DA to a 10 mL volumetric flask. Mix and make up to 10 mL with diluent for standards. Store in the dark at 4 °C.

4. Stock solution of 4-chloro-7-nitro-1,2,3-benzoxadiazole (NBD-Cl): 100 mM NBD-Cl in acetonitrile (ACN). Weigh 0.04 g NBD-Cl, dissolve it with ACN, and transfer to a 2 mL brown volumetric flask. Make up to 2 mL with ACN. Store in the dark at 4 °C (*see* **Note 3**).
5. Derivatization solution: 30 mM NBD-Cl in ACN. Add 0.3 mL stock solution of NBD-Cl to a 1 mL brown volumetric flask. Make up to 1 mL with ACN. Prepare it fresh before use and store in the dark at 4 °C (*see* **Note 4**).
6. Stock solution of ammonium acetate: 200 mM ammonium acetate in DMSO. Weigh 0.1542 g ammonium acetate, dissolve it with DMSO, and transfer to a 10 mL volumetric flask. Make up to 10 mL with DMSO.
7. Derivatization buffer: 20 mM ammonium acetate in ACN/DMSO (3:2, v/v). Add 0.5 mL stock solution of ammonium acetate, 3 mL ACN, and 1.5 mL DMSO to a 5 mL volumetric flask. Prepare it fresh (*see* **Note 5**), filter it through a 0.45 μm polyvinylidene fluoride membrane, and degas it in an ultrasonic bath prior to use (*see* **Note 6**).
8. Stock solution of sodium tetraborate: 100 mM sodium tetraborate in methanol. Weigh 0.9534 g sodium tetraborate, dissolve it with methanol, and transfer to a 25 mL volumetric flask. Make up to 25 mL with methanol.
9. Running buffer: 20 mM sodium tetraborate, 20 mM SDS, 20 % ACN (v/v), 0.1 % glacial acetic acid (v/v) in methanol. Weigh 0.5758 g SDS; dissolve it with 20 mL stock solution of sodium tetraborate, 20 mL ACN, 0.1 mL glacial acetic acid, and 50 mL methanol; and transfer it to a 100 mL volumetric flask. Make up to 100 mL with methanol. Prepare it fresh (*see* **Note 7**), filter it through a 0.45 μm polyvinylidene fluoride membrane, and degas it in an ultrasonic bath prior to use (*see* **Note 8**).

2.2 Developer Solution, Chromium Etchant, Glass Etchant, Glass Substrate, and Polishing Glass Cover Plate

1. Developer solution: 0.5 % NaOH. Weigh 0.5 g NaOH; dissolve it with 100 mL ultrapure water.
2. Chromium etchant: weigh 25 g ammonium cerium nitrate; dissolve it with 6.45 mL perchloric acid and 110 mL ultrapure water.
3. Glass etchant: 2 M HF/2 M NH_4F/3 M HNO_3 (2:1:1, v/v). Add 8 mL HF and 92 mL ultrapure water to a Teflon bottle and mix to obtain 2 M HF. Weigh 7.4 g NH_4F; dissolve it with 100 mL ultrapure water to obtain 2 M NH_4F. Add 20 mL HNO_3 and 82 mL ultrapure water to a glass bottle and mix to obtain 3 M HNO_3. Take 100 mL 2 M HF, 50 mL 2 M NH_4F, and 50 mL 3 M HNO_3, mix, and transfer to a Teflon bottle.

4. Glass substrate (size: 63 mm × 63 mm × 1.7 mm, SG 2506, Shaoguang Microelectronics Corp., China) coated uniformly with 145 nm thick chromium and 570 nm thick Az-1805 positive photoresist. Store in the dark at 4 °C.
5. Polishing glass cover plate (size: 63 mm × 63 mm × 1.7 mm, SG 2506, Shaoguang Microelectronics Corp., China).
6. NaOH solution: 2 M NaOH. Weigh 4 g NaOH; dissolve it with 50 mL ultrapure water.

3 Methods

Carry out all procedures at room temperature unless otherwise specified.

3.1 Microchip Fabrication

1. Design film photomasks with CorelDRAW 9.0 (Fig. 1).
2. Make film photomasks with a high-resolution laser phototypesetter.
3. Transfer the profile of designed film photomasks by ultraviolet exposure lithography onto the glass substrate (Fig. 1). Exposure time is 45 s (*see* **Note 9**).
4. Develop the photoresist in a developer solution for 30–40 s (*see* **Note 10**), wash with tap water, and then hard bake for about 10 min at 110 °C.
5. Eliminate the exposed chromium channel on the glass substrate with chromium etchant for about 30 s (*see* **Note 11**), wash with tap water, and then cover the reverse side and exposed edges of the glass substrate with tape (*see* **Note 12**).
6. Etch the channels in a well-stirred bath containing glass etchant at 40 °C for 20 min (*see* **Note 13**), wash with tap water, and remove the tape.

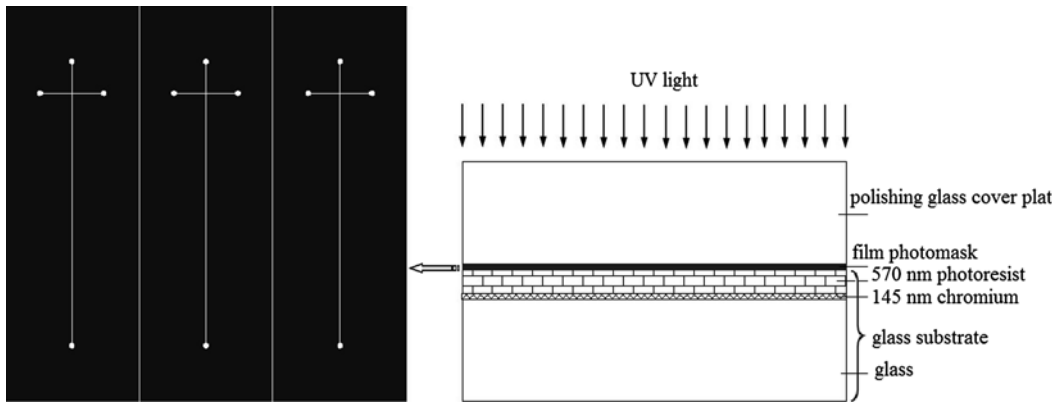

Fig. 1 Top view of the film photomask (*left*) and the profile of the designed film photomask transferred by ultraviolet exposure lithography onto the glass substrate (*right*)

7. Incise both the etched glass substrate and polishing glass cover plate to the size needed and drill holes at each main channel terminal on the etched glass substrate with a 1.2 mm diameter diamond-tipped drill bit.
8. Eliminate the photoresist with ethanol and wash with tap water (*see* **Note 14**).
9. Eliminate the exposed chromium out of the channels with chromium etchant and wash with tap water.
10. Scrub the polishing glass cover plate with absolute ethanol, and dip the glass substrate and cover plate into a boiling NaOH solution for 15 min (*see* **Note 15**).
11. Scrub both the glass substrate and cover plate with high-speed tap water and ultrapure water, in turn.
12. Bond the glass substrate and cover plate in ultrapure water (*see* **Note 16**), and clamp them with clips.
13. Hard bake the microchip for about 30 min at 60 °C and then hard bake for 1 h at 110 °C.
14. Put the microchip into the muffle. Bond it for 2 h at 100 °C, then raise the temperature to 200 °C at 10 °C/min (hold 10 min), then heat to 300 °C at 10 °C/min (hold 10 min), and finally, heat to 500 °C at 20 °C/min (hold 2 h).
15. Turn off the muffle, and let the bonded microchip cool to room temperature naturally.
16. Join four 5 mm inner diameter and 30 mm tall micropipette tips on the microchip surface surrounding the four holes using epoxy resin.

3.2 Sample Preparation

1. Collect urine samples from the volunteers.
2. Filter the urine samples with a 0.45 μm filter to remove solid material.
3. Add 0.4 mL urine sample and 0.8 mL ethanol to a 1.5 mL polypropylene tube, mix, and centrifuge at 6,000 rpm ($3824 \times g$) for 5 min.
4. Transfer the supernatant liquid to another 1.5 mL polypropylene tube and evaporate to dryness with a stream of nitrogen.
5. Dissolve the residue with 20 μL diluent for standards.

3.3 Derivatization

1. Add 20 μL mixed standard solution or treated urine sample, 100 μL derivatization buffer, and 100 μL derivatization solution to a 500 μL microcentrifuge tube, and mix them thoroughly.
2. Conduct the derivatization reaction at 60 °C for 20 min in a water bath in the dark.
3. Add 180 μL derivatization buffer to the reaction vial.

3.4 Nonaqueous Microchip Electrophoresis

1. Connect the pipet bulb (30 mL) to terminal c of the 3-way electromagnetic valve through a PTFE tubing of 0.8 mm id and 1.8 mm od, and seal the small gap between the hole and the PTFE tubing with epoxy glue (Fig. 2).
2. Connect a PTFE tube to terminal b of the 3-way electromagnetic valve, and insert the other end of the PTFE tube to an interfacing plug (10 mm length of silicone tubing of 1.6 mm id and 4.1 mm od).
3. Switch the 3-way electromagnetic valve to connect terminal b to terminal c, and press out the air in the pipet bulb by hand via terminal b to create a subatmospheric pressure in the pipet bulb.
4. Switch the 3-way electromagnetic valve to connect terminals b and a.
5. Add 150 μL, 150 μL, and 15 μL running buffer to buffer reservoir (B), buffer waste reservoir (BW), and sample waste reservoir (SW), respectively. Add 30 μL sample solution to sample reservoir (S).
6. Push fit the interfacing plug into SW, and keep the end of the PTFE tubing about 3 mm above the liquid level.
7. Apply a constant voltage of 1,500 V to B with BW grounded and S and SW floating in the whole analysis process (Fig. 2).
8. Switch the 3-way electromagnetic valve to connect terminal b to c for 0.5 s.
9. Switch the 3-way electromagnetic valve to connect terminal b to a, and at the same time, the data acquisition and processing system record the electropherogram.

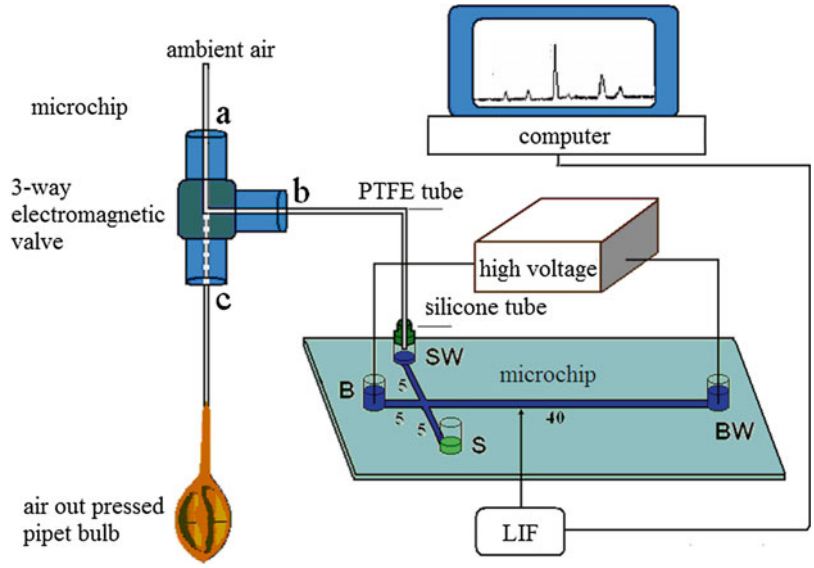

Fig. 2 Schematic diagram of the integrated NAMCE-LIF system (dimensions are given in millimeter)

4 Notes

1. E, NE, and DA will be oxidized and lose their activities in neutral or alkaline solution; hence, they should be prepared in acidic solution.
2. E, NE, and DA are sensitive to light.
3. NBD-Cl is sensitive to light.
4. We find that it is best to prepare this fresh each time.
5. We find that it is best to prepare this fresh each time.
6. The presence of gas will affect the derivatization as E, NE, and DA are sensitive to air.
7. We find that it is best to prepare this fresh each time.
8. The presence of gas will affect the derivatization as E, NE, and DA are sensitive to air.
9. 45 s is suitable.
10. 30–40 s for developing is suitable.
11. 30 s is suitable.
12. All surfaces except for the channels that will be exposed should be covered with tape to avoid being etched in the following step.
13. The length of etching time determines the channels' dimensions. In our experiment, the etching speed is 1 μm/min, and the depth of the channels is 20 μm, so 20 min is required.
14. After eliminating the photoresist with ethanol and before eliminating the exposed chromium out of the channels, it is necessary to wash the microchip with tap water; otherwise, the ethanol will affect the chromium etchant.
15. We find that the efficiency of boiling NaOH solution is best.
16. Bonding of the glass substrate and cover plate must be performed in ultrapure water; otherwise, diffraction fringes may occur.

Acknowledgment

This work was supported by the Test Analysis of Science and Technology Plan Project of Zhejiang Province (No. 2012C37022) and Major science and technology plan projects of Zhejiang Province (No. 2012F20026) and the Natural Science Foundation of Zhejiang province (No. LQ13C200004, LQ14B070002).

References

1. Manz A, Harrison DJ, Verpoorte EMJ et al (1992) Planar chips technology for miniaturization and integration of separation techniques into monitoring systems. J Chromatogr 593:253–258
2. Harrison DJ, Manz A, Fan Z et al (1992) Capillary electrophoresis and sample injection systems integrated on a planar glass chip. Anal Chem 64:1926–1932
3. Dolnik V, Liu SR (2005) Application of capillary electrophoresis on microchip. J Sep Sci 28:1994–2009
4. Arora A, Simone G, Salieb-Beugelaar G et al (2010) Latest developments in micro total analysis systems. Anal Chem 82:4830–4847
5. Kutter JP (2000) Current developments in electrophoretic and chromatographic separation methods on microfabricated devices. Trends Anal Chem 19:352–363
6. Sarmini K, Kenndler E (1997) Influence of organic solvents on the separation selectivity in capillary electrophoresis. J Chromatogr A 792:3–11
7. Steiner F, Hassel M (2000) Nonaqueous capillary electrophoresis: a versatile completion of electrophoretic separation techniques. Electrophoresis 21:3994–4016
8. Matysik FM (2002) Special aspects of detection methodology in nonaqueous capillary electrophoresis. Electrophoresis 23:400–407
9. Geiser L, Veuthey JL (2009) Non-aqueous capillary electrophoresis 2005–2008. Electrophoresis 30:36–49
10. Walbroehl Y, Jorgenson JW (1984) On-column UV absorption detector for open-tubular capillary zone electrophoresis. J Chromatogr 315:135–143
11. Gibson LR II, Bohn PW (2013) Non-aqueous microchip electrophoresis for characterization of lipid biomarkers. Interface Focus 3: 20120096
12. Wang J, Pumera M (2003) Nonaqueous electrophoresis microchip separations: conductivity detection in UV-absorbing solvents. Anal Chem 75:341–345
13. Deng G, Collins GE (2003) Nonaqueous based microchip separation of toxic metal ions using 2-(5-bromo-2-pyridylazo)-5-(N-propyl-N-sulfopropylamino) phenol. J Chromatogr A 989:311–316
14. Lu Q, Collins GE, Smith M et al (2002) Sensitive capillary electrophoresis microchip determination of trinitroaromatic explosives in nonaqueous electrolyte following solid phase extraction. Anal Chim Acta 469:253–260
15. Hu HM, Yin XF, Wang XZ et al (2013) A study on the system of nonaqueous microchip electrophoresis with on-line peroxyoxalate chemiluminescence detection. J Sep Sci 3: 713–720
16. Fu LM, Yang RJ, Lee GB (2003) Electrokinetic focusing injection methods on microfluidic devices. Anal Chem 75:1905–1910
17. Zhang L, Yin XF, Fang ZL (2006) Negative pressure pinched sample injection for microchip-based electrophoresis. Lab Chip 6: 258–264
18. Zhang L, Yin XF (2007) Parallel separation of multiple samples with negative pressure sample injection on a 3-D microfluidic array chip. Electrophoresis 28:1281–1288
19. Hu HM, Yin XF, Qi LY et al (2009) Pump-free and low-cost negative pressure sampling device for rapid sample loading in MCE. Electrophoresis 30:4213–4218
20. Jacobson SC, Hergenroder R, Koutny LB et al (1994) High-speed separations on a microchip. Anal Chem 66:1114–1118
21. Jacobson SC, Hergenroder R, Koutny LB et al (1994) Effects of injection schemes and column geometry on the performance of microchip electrophoresis devices. Anal Chem 66: 1107–1113
22. Zhang CX, Manz A (2001) Narrow sample channel injectors for capillary electrophoresis on microchips. Anal Chem 73:2656–2662

Part V

Capillary Electrochromatography on Microchips

Chapter 13

Carbon Nanotube-Based Separation Columns for Microchip Electrochromatography

K.B. Mogensen, B. Delacourt, and J.P. Kutter

Abstract

Fabrication of the stationary phase for microchip chromatography is most often done by packing of the individual separation channel after fabrication of the microfluidic chip, which is a very time-consuming and costly process (Kutter. J Chromatogr A 1221:72–82, 2012). Here, we describe in detail the fabrication and operation protocols for devices with microfabricated carbon nanotube stationary phases for reverse-phase chromatography. In this protocol, the lithographically defined stationary phase is fabricated in the channel before bonding of a lid, thereby circumventing the difficult packaging procedures used in more conventional protocols.

Key words Microchip electrochromatography, Carbon nanotubes, Nonaqueous separations, Microfabrication

1 Introduction

Carbon nanotubes (CNTs) are considered to be discovered as early as 1952 [1, 2] and gained widespread popularity as a research subject after the report of Iljima in 1991 [3] due to their unique mechanical, electrical, and chemical properties. Carbon nanotubes have a very high surface to volume ratio and sorptive properties that make them very useful for analytical chemistry, such as stationary phase additives for reverse-phase liquid chromatography [4–7]. In the vast majority of work relating to separation science, the carbon nanotubes have been purchased as a powder and, in various ways, immobilized on the column, which is a procedure that is typically not amenable to mass fabrication and inherently a stochastic process.

An additional advantage of carbon nanotubes is that they can be rapidly grown on a substrate by catalysis from, e.g., Fe or Ni nanoparticles in a furnace. This is exploited in the current method in order to take advantage of microfabrication techniques that allow parallel processing of many devices on a substrate with a very

Ann Van Schepdael (ed.), *Microchip Capillary Electrophoresis Protocols*, Methods in Molecular Biology, vol. 1274,
DOI 10.1007/978-1-4939-2353-3_13,

high uniformity [7]. In this work, the carbon nanotubes are grown in hexagonal regions that mimic porous beads in packed bed columns [8, 9].

Carbon nanotubes are furthermore a very versatile stationary phase material in the sense that they can be functionalized to possess a wide range of surface groups, e.g., upon oxidation or reduction, the isoelectric point can be controlled in a pH range spanning from around 4 to 10, making it possible to control the zeta potential, so that a cathodic as well as an anodic electroosmotic flow should be feasible without further modifications [7]. The carbon nanotubes can also readily be chemically functionalized if desired by coupling to, e.g., carboxylic acids on oxidized nanotubes or by pi-stacking interactions [10].

Here, the very high hydrophobicity of carbon nanotubes is exploited with the objective of performing nonaqueous separations of hydrophobic compounds. In this case, compounds can be separated with 90 % organic modifier contents in the buffer while showing no retention on a C18-functionalized column at 50 % organic modifier contents [8]. This is a clear indication of the very hydrophobic nature of the column.

To date, only very few groups have presented microfluidic devices with carbon nanotubes grown on the column comparable to what is described in this method [7–9, 11–14].

2 Materials

2.1 Microfabrication Materials

1. Silicon wafers (any brand), 500 μm thickness, single side polished.
2. Borosilicate wafers (Pyrex, SCHOTT), 500 μm thickness, double side polished.
3. Positive resist (e.g., AZ5214E, Clariant, Germany).
4. Developer (e.g., AZ 300 MIF for 60s).
5. Nitric acid (concentrated).
6. 5 % buffered hydrofluoric acid (BHF).
7. 40 % hydrofluoric acid.
8. a-Si etching solution: *see* **step 1** in Subheading 3.1.2.
9. Glass etching solution: three parts of 5 % BHF, one part of 40 % hydrofluoric acid.
10. Piranha solution: three parts of sulfuric acid (concentrated), one part of hydrogen peroxide (concentrated).
11. 10 mm thick Teflon plate.
12. 3.0 mm inner diameter/1.5 mm thickness o-rings (EP-70, M seals, Denmark).

2.2 Chip Separation Materials and Instrumentation

1. Separation buffer: 95 % acetonitrile, 5 % deionized water, 50 mM ammonium acetate (pH = 9.0).
2. Coumarin dyes C460 and C480 (*see* **Note 1**).
3. Diode laser (CNI Laser, Shanghai Dream Lasers, China, $P = 10$ mW, $\lambda = 377$ nm) (*see* **Note 2**).
4. Microscope equipped with a fluorescence high-pass filter ($\lambda = 420$ nm, NT46-426, Edmund Optics, USA) and a photomultiplier tube with I-V converter (e.g., Hamamatsu H10722, Japan).
5. High-voltage power supply (e.g., UltraVolt, USA).
6. LabJack U12 data acquisition card (LabJack Corporation, USA) and software.

3 Methods

3.1 Column Design and Microfabrication Procedure

1. Design the two photolithographic masks, where mask I contains the microfluidic channel layout in a standard cross-channel design for performing electrokinetic injections. Mask II is used for patterning of regions in the separation channel that are intended to contain the carbon nanotubes (Fig. 1) (*see* **Note 3**).
2. The starting material consists of 4 in. silicon wafers (500 μm thickness, single side polished) with a layer of around 10 μm pre-grown silicon dioxide (Fig. 2) (*see* **Note 4**).

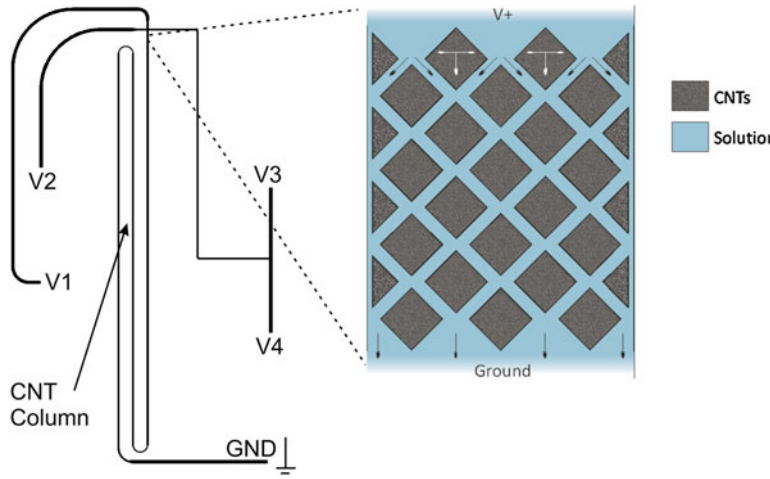

Fig. 1 (*Left*) Mask I, showing the microfluidic channel layout. (*Right*) Sketch seen from the top of the pillar design (mask II), where the Ni catalyst is positioned (*dark regions*). The length of the pillars (in the axial direction) is below 10 μm to avoid electrolysis of the aqueous buffer solution, while the inter-pillar distance is above 2.5 μm to avoid carbon nanotubes from different pillar regions to overlap [7]

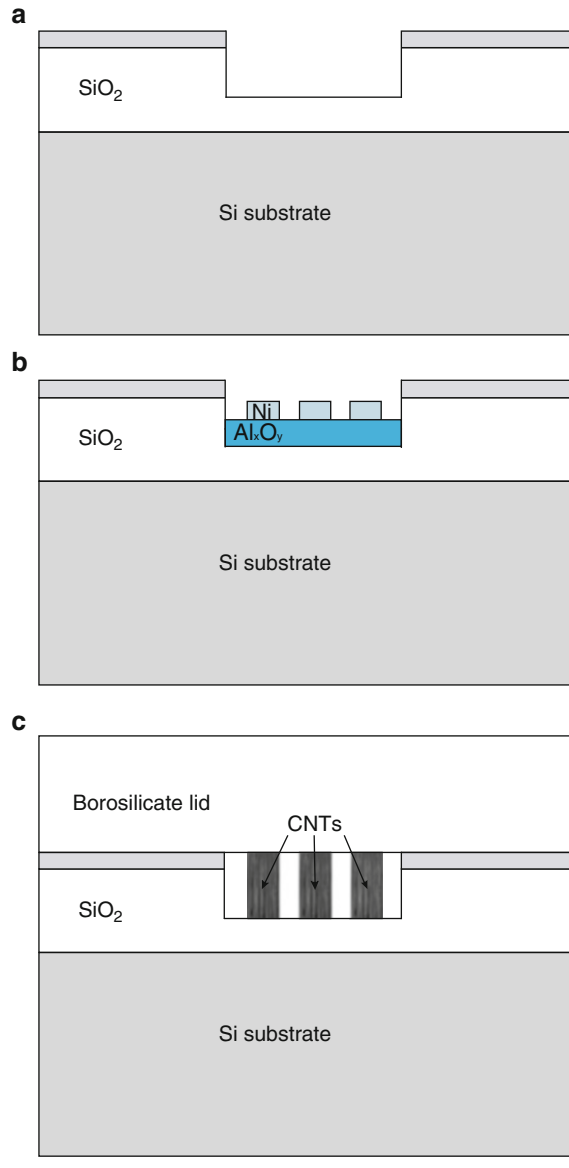

Fig. 2 Cross-sectional view of the fabrication procedure at different stages of completion for integration of carbon nanotubes in electrically insulated microfluidic channels. A thick silicon dioxide layer grown on the silicon wafer is used to allow high electrical fields for electroosmotic pumping of the liquid

3. Grow a 30–50 nm thick amorphous Si layer on the wafer for subsequent anodic bonding of a glass lid. This is done by, e.g., low pressure chemical vapor deposition or some other Si deposition process (*see* **Note 5**).

3.1.1 Photolithography Mask I: Microfluidic Channel Network

1. Treat the wafer with HMDS (hexamethyldisilazane).
2. Spin coat a 1.5 μm layer of positive resist and prebake at 90 °C for 2 min.

3. UV expose the wafer (e.g., using 14 mW/cm^2 for 11 s).
4. Dip the wafer in a suitable developer and rinse with water.

3.1.2 Wet Etching of Amorphous Si (a-Si) and Glass Channels

1. Prepare the chemicals for a-Si and glass etching:
   For the amorphous Si etch, mix the following in a plastic beaker: 1:1 deionized water (DIW)/nitric acid (concentrated). Let it cool down for 15–30 min, and then add 5 vol% of 5 % buffered hydrofluoric acid (BHF).

   For the glass etch, mix the following in a plastic beaker: 3:1 of 5 % BHF/40 % hydrofluoric acid to achieve ~14 % BHF (*see* **Note 6**).
2. Hard bake the wafer on a hot plate for 2 min at 90 °C to improve resist adhesion.
3. Apply a polymer lamination foil/tape on the back side and wafer edge to avoid etching of the backside a-Si (necessary for the anodic bonding of the lid later on in the process).
4. Immerse the wafer for ~10 s in 5 % BHF to remove the native oxide.
5. Transfer to a-Si etching solution for 30–60 s. A color change in the etched regions is an indication that the etch step is completed.
6. Dip the wafer in the SiO_2 (glass) etching solution for around 7 min in order to etch a 2.5–3.0 μm deep channel, then rinse in water for 2 min, and remove lamination foil.

3.1.3 Fabrication of Aluminum Oxide De-wetting Layer

1. Deposition of 5 nm aluminum by e-beam evaporation ($P = 2 \times 10^{-6}$ mbar).
2. Metal lift-off in acetone.
3. Clean in Piranha solution for 10 min to remove residual photoresist.
4. Oxidize aluminum at 550 °C for 8 h.

3.1.4 Photolithography Mask II: Patterning of Catalyst Regions in the Channels

1. Treat the wafer with HDMS (hexamethyldisilazane).
2. Spin coat a 1.5 μm layer of positive resist and prebake at 90 °C for 2 min.
3. UV expose the wafer (e.g., using 14 mW/cm^2 for 8 s using the $\lambda = 365$ nm line) (*see* **Note 7**).
4. Dip the wafer in a suitable developer and rinse with water.
5. Remove residual resist by a low power oxygen plasma process ($P = 200$ W, for 2 min, resist etch rate = 10–25 nm/min) (*see* **Note 8**).

3.1.5 Fabrication of Carbon Nanotubes

1. Deposit a 2 nm thick Ni metal catalyst layer using an evaporation rate of 1–2 Å/s ($P = 2 \times 10^{-6}$ mbar).
2. Lift off the resist by immersing the wafer in acetone. Gently use cleanroom paper to wipe the resist off the wafer, while it is immersed in the acetone. When the acetone becomes cloudy and/or polluted, move the wafer to a new petri dish with clean acetone and continue until all resist is lifted off. Rinse the wafer with isopropanol and subsequently water, before drying (*see* **Note 9**).
3. Grow a 1–2 μm thick carbon nanotube layer using thermal chemical vapor deposition. The best recipes are typically very dependent on the specific catalyst deposition conditions and on the furnace, which means that it needs to be optimized for each laboratory. Here, the following conditions were used (*see* **Note 10**).
4. Purge chamber three times with H_2 (60 sccm)/N_2 (40 sccm).
5. Anneal samples at 630 °C for 5 min in a H_2 (60 sccm)/N_2 (40 sccm) atmosphere in order to create the Ni catalyst nanoparticles.
6. Grow carbon nanotubes at 630 °C by adding acetylene, C_2H_2 (1.5 sccm), for 15 min. The pressure during annealing and CNT growth is 20 mbar.
7. Post anneal at 630 °C for 10 min in a H_2 (60 sccm)/N_2 (40 sccm) atmosphere for the removal of amorphous carbon, also at a $P = 20$ mbar.

3.1.6 Fabrication of Borosilicate Lid and Bonding

1. Apply lamination foil on both sides of 500 μm thick double side polished borosilicate wafers and mark 1.5 mm diameter holes in the foil by CO_2 laser machining. The machined foil serves as a mask for sand blasting of the access holes in the glass lid.
2. Sand blast holes in the glass using the lamination foil as a mask.
3. Rinse thoroughly in water.
4. Remove foil and sonicate in water for 15 min.
5. Clean glass lids for 10 min in a 4:1 H_2SO_4 (concentrated)/H_2O_2 (concentrated) solution (*see* **Note 11**).
6. Dry lids and assemble with the bottom substrate.
7. Align holes to the fluidic channels and anodically bond the substrates together. Anodic bonding occurs at 400 °C, 900 V for 15 min in a nitrogen atmosphere (*see* **Note 12**).
8. Oxidize the devices at 400 °C for 1 h in air (*see* **Note 13**).

3.2 Chip Operation Protocol

1. Mount chip in holder (Fig. 3) (*see* **Note 14**).
2. Prepare separation buffer by mixing 95:5 acetonitrile/deionized water with 50 mM ammonium acetate (pH = 9.0) (*see* **Note 15**).

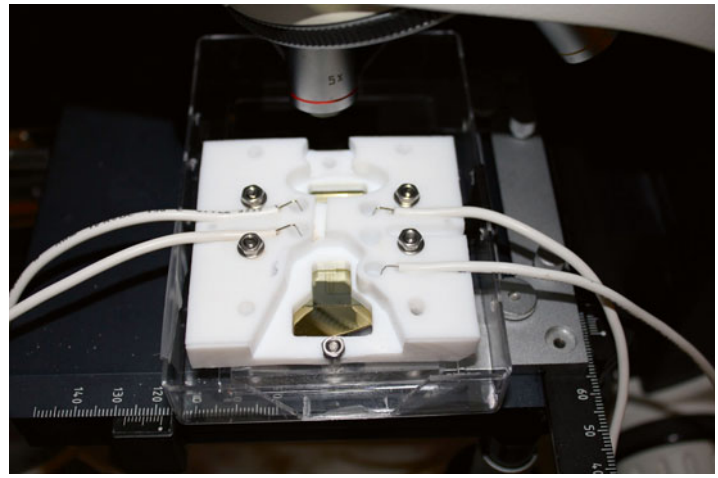

Fig. 3 Chip mounted in a micromilled Teflon holder. Five screws are holding the assembly together, and o-rings are used for leak-free connections to the fluidic reservoirs located in the 10 mm thick Teflon layer. Trenches are machined to hold the electrodes in place, and openings for optical detection with a microscope objective are included

3. Prepare test analytes, e.g., coumarin C460 in 10–100 μM concentration in order to test and verify the column performance.
4. Degas all analyte solutions under vacuum and ultrasonication for 5 min.
5. Add acetonitrile to one reservoir of the chip/holder assembly and wait until the chip is filled by capillary action.
6. Fill the rest of the reservoirs and remove the remaining air bubbles with suction or by applying pressure to the chip for around 10 min.
7. Mount chip/holder assembly under a microscope equipped with a PMT and emission filter for collection of the fluorescence signal.
8. Adjust voltages for gated injection (*see* **Note 16**).
9. After the experiment, rinse chip for at least 10 min in acetonitrile to remove the buffer salts and the analytes.
10. If the chip is not going to be used for a week or more, then completely empty the reservoirs of all liquids and store it dry.
11. In case the chip is used again within a couple of days, store the chip wet. Fill reservoirs and cover with Parafilm. Store in the fridge at 5 °C for delayed solvent evaporation (*see* **Note 17**).

4 Notes

1. These analytes can be used for testing of the chromatographic column performance because they are neutral (non-charged) and highly fluorescent upon excitation around $\lambda = 375$ nm.
2. A $\lambda = 405$ nm laser diode can also be used, since it is much cheaper and more easily available. The overlap with the absorption band of the coumarin dyes is, however, not as good as with the $\lambda = 375$ nm diode laser.
3. The column layout with respect to design of the pillar regions generally takes into account that keeping the length of the pillars (in the axial direction) below 10 μm allows the use of an electrical field strength of up to $E = 1$ kV/cm without risking bubble formation due to electrolysis of the aqueous buffer solution. The necessary inter-pillar distance depends on the length of the carbon nanotubes and should be large enough to avoid overlap between the CNTs of adjacent regions.
4. Anodic bonding is used for the devices due to the high yield of this process and because it can be done without treating the carbon nanotube wafers (by, e.g., immersion in a Piranha solution), thereby maintaining the as-grown structural and chemical properties of the CNTs in the final devices. This limits the substrates to materials that can be anodically bonded, such as borosilicate glass and silicon. Since the current carbon nanotube growth process takes place at 640 °C, only silicon can be used as a substrate for the CNTs in our case. If a low temperature CNT process is used (<550 °C), then borosilicate glass can also be used as a bottom substrate. Since electroosmotic flow is used in the devices, an electrically insulating oxide layer of around 10 μm is grown on the silicon substrate as the first step. This takes around 2 weeks at 1,150 °C; however, a furnace can be loaded with more than 150 wafers at the same time in order to have these substrates on stock.
5. This process was initially developed [15] in order to fabricate electrically insulated channels in silicon with the use of anodic bonding. If the amorphous Si layer is thinner than around 30 nm, then the yield of the process starts to decrease. When the a-Si layer is thicker than around 50 nm, it starts to become too conducting and will influence the electrical field distribution across the electrolyte solution and may eventually result in gas bubble formation due to electrolysis of water. There are thus opposing requirements on the electrical properties of the a-Si layer. For the anodic bonding to work, it needs to have a high enough conductivity for the electrical potential from the bottom electrode to reach in between the two wafers. On the other hand, during operation of the devices (using electroos-

motic flow), the conductivity of the a-Si layer needs to be low, in order not to affect the electrokinetics. Luckily, the a-Si layer is oxidized during bonding with a resulting increase in electrical resistance (anodic oxidation), which means that there is a window in terms of a-Si thickness, where these seemingly opposing requirements can be met.

Bonding with, e.g., PDMS is not desirable for this application, due to its tendency to absorb neutral hydrophobic compounds.

6. The etching rate is too low in 5 % buffered hydrofluoric acid in order to reach the desired channel depth before the resist starts to delaminate and fall off the wafer. Therefore, 40 % HF is added to increase the etching rate.
7. A shorter exposure time (in this case 8 s) is used for the second mask layer compared to the first mask, the reason being that overexposure in the second mask layer makes it hard to reproduce the hexagonal pillars that are spaced 2.5–3.0 μm apart, while this is noncritical for the first layer.
8. This step may not be necessary.
9. This step is one of the most critical, the reason being that ultrasonication, which is normally used for metal lift-off, tends to also remove the very thin catalyst layer and can therefore not be applied. If a thicker catalyst layer can be used, e.g., 7–10 nm (if plasma-enhanced chemical vapor deposition is used for the growth of the carbon nanotubes [9]), then ultrasonication may give acceptable results.
10. A cheap in-house built chemical vapor deposition system was put together that simply consists of a vacuum chamber equipped with a pump and mass flow controllers for control of the nitrogen, hydrogen, and acetylene flow rates. The heating is achieved using a graphite block with drilled holes in the sides for insertion of two light bulbs, which makes it possible to reach around 900 °C in 5 min. Low-voltage DC bulbs were used to avoid sparking in the system; hence, an 800 VA transformer (with rectifier and capacitors) was assembled for conversion of the voltage to DC. The voltage to the lamps was controlled manually by using an AC variable 220 V transformer, before conversion of the power to DC. Here, 160 V AC gave a temperature of 630 °C.
11. The bottom substrate containing the carbon nanotubes is not treated with Piranha cleaning solution, because this would disrupt the nanotubes.
12. The devices are bonded by ramping up the voltage manually until just before electrical breakdown occurs. It is important to leave the wafers at the maximum voltage that can be applied (without breakdown) for about 15 min. This ensures that as

much as possible of the amorphous Si layer is oxidized during the bonding. Otherwise, gas bubble formation due to electrolysis of the water in the channels can occur if the conductance of the Si layer is too high.

13. Oxidation of the carbon nanotubes moves the isoelectric point to lower pH, so the acidic oxygen groups are deprotonated, when using a standard buffer solution in the pH range 7–10. This ensures that the carbon nanotubes have a negative zeta potential for generation of a cathodic electroosmotic flow.
14. Initially, glass reservoirs were glued onto the lid of the devices over the access holes. The reservoirs, however, tended to fall off after a couple of hours due to dissolution of the glue in the acetonitrile-based buffer solution. Therefore, a Teflon holder with fluidic reservoirs micromilled into the Teflon was made, which overcame this problem and made the chip operation much more convenient.
15. Ammonium acetate can be chosen as the buffer salt for non-aqueous separations due to its high solubility in acetonitrile compared to other commonly used salts. It, however, still has a low solubility at the 100 % acetonitrile level, which is why at least 5 % water needs to be added to the buffer. The elution strength of the buffer can be further increased, if desired, by adding tetrahydrofuran (THF) to a 95:5 acetonitrile/water mixture. With such a low water content, the current through the column is at least one order of magnitude lower (<100 nA) than typically encountered with standard aqueous buffers, which means that a much higher electrical field strength can be applied before being limited by band broadening due to Joule heating.
16. The gated injection scheme is described in, e.g., ref. 16.
17. Traditional chromatography columns are typically stored wet, when not in use. The reason for this is that repeated drying of the column may affect the integrity of the stationary phase material, which is also the case for microfluidic columns. In traditional columns, end caps can be screwed on, which is not possible with typical CEC microfluidic holder designs; therefore, the terminal openings are simply covered with Parafilm, and the chip is stored in the fridge. Even slower solvent evaporation can be obtained by filling the major part of the reservoirs with water. In this case, water should not be sucked into the channel network of the chip, but only be filled into the fluidic reservoirs in the holder. The high hydrophobicity of the column material prevents the bulk part of the water from entering the column by capillary forces.

Acknowledgment

This work was partly supported by the Danish National Advanced Technology Foundation via the project "Multiplex Blood Culture Test."

References

1. Radushkevich LV, Lukyanovich VM (1952) O strukture ugleroda, obrazujucegosja pri termiceskom razlozenii okisi ugleroda na zeleznom kontakte (About the structure of carbon formed by thermal decomposition of carbon monoxide on iron substrate). Zurn Fisic Chim 26:85–95
2. Monthioux M (2006) Who should be given the credit for the discovery of carbon nanotubes? Carbon 44:1621–1623
3. Iijima S (1991) Helical microtubules of graphitic carbon. Nature 354:56–58
4. Asensio-Ramos M, Herrera-Herrera A, Rodríguez-Delgado MA, Hernández-Borges J, Fanali S (2013) Carbon nanotubes: applications in chromatography and sample preparation. LCGC Europe 1:196–203
5. Valcarcel M, Cardenas S, Simonet BM (2007) Role of carbon nanotubes in analytical sciences. Anal Chem 79:4788–4797
6. Herrera-Herrera AV, González-Curbelo MA, Hernández-Borges J, Rodríguez-Delgado MA (2012) Carbon nanotubes applications in separation science: a review. Anal Chim Acta 734:1–30
7. Mogensen KB, Kutter JP (2012) Carbon nanotube based stationary phases for microchip chromatography. Lab Chip 12:1951–1958
8. Mogensen KB, Miaoxiang C, Molhave K, Boggild P, Kutter JP (2011) Carbon nanotube based separation columns for high electrical field strengths in microchip electrochromatography. Lab Chip 11:2116–2118
9. Mogensen KB, Gangloff L, Bøggild P, Teo KBK, Milne WI, Kutter JP (2009) Carbon nanotubes integrated in electrically insulated channels for lab-on-a-chip applications. Nanotechnology 20(9):095503
10. Sun YP, Fu K, Lin Y, Huang W (2002) Functionalized carbon nanotubes: properties and applications. Acc Chem Res 35(12): 1096–1104
11. Stadermann M, Dick B, Noy A, Bakajin O, McBrady AD, Reid V, Vanessa R, Synovec RE (2006) Ultrafast gas chromatography on single-wall carbon nanotube stationary phases in microfabricated channels. Anal Chem 78(16):5639–5644
12. Fonverne A, Ricoul F, Demesmay C, Delattre C, Fournier A, Dijon J, Vinet F (2008) In situ synthesized carbon nanotubes as a new nanostructured stationary phase for microfabricated liquid chromatographic column. Sens Actuators B 129:510–517
13. Goswami S, Bajwa N, Asuri P, Ci L, Ajayan P, Cramer SM (2009) Aligned carbon nanotube stationary phases for electrochromatographic chip separations. Chromatographia 69(5, 6): 473–480
14. Wu R, Yang C, Wang P, Tseng F (2009) Nanostructured pillars based on vertically aligned carbon nanotubes as the stationary phase in micro-CEC. Electrophoresis 30: 2025–2031
15. Mogensen KB, Petersen NJ, Hübner J, Kutter JP (2001) Monolithic integration of optical waveguides for absorbance detection in microfabricated electrophoresis devices. Electrophoresis 22:3930–3938
16. Geschke O, Klank H, Telleman P (eds) (2003) Microsystem engineering of lab-on-a-chip devices. VCH-Wiley, Weinheim, Germany. ISBN 3-527-30733-8

Chapter 14

Electrochromatography on Acrylate-Based Monolith in Cyclic Olefin Copolymer Microchip: An Attractive Technology

Y. Ladner, G. Cretier, and K. Faure

Abstract

Electrochromatography (EC) on a porous monolithic stationary phase prepared within the channels of a microsystem is an attractive alternative for on-chip separation. It combines the separation mechanisms of electrophoresis and liquid chromatography. Moreover, the porous polymer monolithic materials have become popular as stationary phase due to the ease and rapidity of fabrication via free radical photopolymerization. Here, we describe a hexyl acrylate (HA)-based porous monolith which is simultaneously in situ synthesized and anchored to the inner walls of the channel of a cyclic olefin copolymer (COC) device in only 2 min. The baseline separation of a mixture of neurotransmitters including six amino acids and two catecholamines is realized.

Key words Acrylate-based monolith, COC microchip, Electrochromatography

1 Introduction

On the spur of the incredible number of applications developed in microfluidic devices, such as extraction, microreaction, separation, and sample preparation [1], the implementation of porous solid supports becomes a requisite in the development of lab-on-chips [2]. Acrylate- or methacrylate-based monoliths are among the most popular materials used as stationary phase for electrochromatography (EC) in capillary format and microchip [3]. The main advantages of these monolithic supports are the ease and rapidity of preparation and the non-requirement of frits [4–6]. These porous solids are prepared via free radical photopolymerization which allows localization of the monolith in a specific separation area [7].

Electrochromatography (EC) on a monolith support prepared within the channels of the microsystem is an attractive on-chip separation technique. It combines the separation mechanisms of electrophoresis (differences in electrophoretic mobility for ionized analytes) and liquid chromatography (differences in specific

Ann Van Schepdael (ed.), *Microchip Capillary Electrophoresis Protocols*, Methods in Molecular Biology, vol. 1274,
DOI 10.1007/978-1-4939-2353-3_14,

interactions between solute and stationary phase). This technique also allows the implementation of both injection and separation within the same device. Moreover, the driving force is generated by two electrodes and a power supply, which is easily portable. This chip-EC approach has been previously developed in glass microfluidic devices [8, 9]. Recently, cyclic olefin copolymer (COC) emerged as substrate allowing the fabrication of cost-effective and solvent-resistant devices [10].

We previously showed that wall ruggedness was sufficient to hold a non-anchored monolith in a COC device used in EC without pressure, but separation efficiency remained poor (about 70,000 plates/m) [11]. Anchoring of acrylate monolith inside the COC microchip channel [12, 13] improves electrochromatographic efficiency (up to 120,000 plates/m). The achievement of efficiencies as high as the ones obtained in glass microchips for neutral solutes (e.g., 250,000 plates/m for PAH) requires furthermore the optimization of light intensity during photopolymerization [14].

Here, we describe an optimized hexyl acrylate (HA) monolith which is simultaneously in situ synthesized and anchored to the inner walls of the channel of a COC device in only 2 min.

2 Materials

Prepare all solutions using ultrapure water (prepared with a PURELAB UHQ II system (Elga, France) to attain a resistivity of 18 MΩ at 25 °C) and analytical grade reagents. Prepare all reagents at room temperature. Diligently follow waste disposal regulations when disposing waste materials.

2.1 Monolith Synthesis

1. Monomers: hexyl acrylate, (HA), 1,3-butanediol diacrylate (BDDA), and 2-acrylamido-2-methyl-1-propanesulfonic acid (AMPS). Store at 4 °C.
2. Photoinitiator: benzoin methyl ether (BME). Store at 4 °C.
3. Solvents: acetonitrile (ACN) and ethanol, HPLC grade.

2.2 Primary Amine Derivatization

1. NDA derivatization solutions: 2.5 mM of naphthalene-2,3-dicarboxaldehyde weekly prepared in ACN/water 50/50 v/v, 43 mM of sodium cyanide (NaCN) weekly prepared in water. Store at 4 °C.
2. 100 mM pH 9 borate solution weekly prepared by mixing 500 mM boric acid solution and 125 mM sodium tetraborate solution to obtain pH 9. Store at 4 °C.
3. Aqueous solution of neurotransmitters: catecholamines (noradrenaline and dopamine) and amino acids (arginine, α-aminobutyric acid (GABA), serine, glycine, glutamic acid, and aspartic acid) diluted in water. The concentration of each solute is 120 μM. Store at 4 °C.
4. Solvents: acetonitrile (ACN) was HPLC grade.

2.3 Mobile Phase

1. Ammonium phosphate ($NH_4H_2PO_4$), orthophosphoric acid (H_3PO_4), and lithium dodecyl sulfate (LiDS).
2. Acetonitrile (ACN) was HPLC grade.

2.4 Instrumentation

1. Microfluidic system: COC Topas 6013 microchips fabricated by microfluidic ChipShop (Germany) exhibit only one 81 mm long, 75 μm deep, and 75 μm wide channel.
2. Monolith synthesis system: a Bio-Link cross-linker (VWR International, France) equipped with five 8 W UV tubes for UV irradiation at 365 nm and a UV radiometer (Vilber Lourmat, Germany) for light intensity measurements.
3. Mobile phase preparation: a MeterLab pH meter (Radiometer, France) for pH value monitoring in the aqueous part.
4. Electric field application: μTK high power supply (Micralyne, Canada) to generate an electrical field that induces electroosmotic flow inside COC microchannels.
5. Electrochromatographic separation monitoring: IX-71 inverted fluorescence microscopic system (Olympus, France) equipped with XF02-2 100 W mercury lamp (Omega, USA) and an excitation filter of 405 nm (collection above 500 nm) for NDA-labeled solutes (amino acids and catecholamines). A CCD camera was combined with NI Vision software (Alliance Vision, France) for detection processing.

3 Methods

3.1 In Situ Synthesis of Monolith

1. Prepare the porogenic mixture by mixing 2.4 mL of ACN (54 % w/w), 800 μL of ethanol (23 % w/w), and 800 μL of water (23 % w/w).
2. Prepare the monomer mixture by mixing 1.243 g of HA (66.4 % w/w) and 0.63 g of BDDA (33.6 % w/w).
3. Mix the monomer mixture to the porogenic mixture with a monomer to porogen ratio equal to 34.5:65.5 w/w.
4. Add 9.3 mg of AMPS (0.5 % w/w of monomers) to the polymerization mixture (*see* **Note 1**).
5. Add 46.8 mg of BME (2.5 % w/w of monomers) to the polymerization mixture (*see* **Note 2**).
6. Sonicate for 15 min.
7. Introduce the polymerization mixture in the microchannel by pressure using a syringe.
8. Place the microchip in the 365 nm illumination system at 2.5 cm from the UV tubes. Control that the UV light intensity is 4.7 mW/cm^2 on the UV radiometer (*see* **Note 3**).
9. Apply a UV irradiation of 6 min (which corresponds to an energy of 1.9 J/cm^2 on the UV radiometer).

10. After irradiation, the monolith present in the reservoirs is scraped away.
11. Fill all the reservoirs with ACN/water 70:30 (v/v) +2 mM $NH_4H_2PO_4$ + 5 mM LiDS (*see* **Note 4**).
12. Apply an electric field of 620 V/cm for 30 min for rinsing purposes (*see* **Note 5**).
13. When not in use, immerse the HA-filled COC microchips in ethanol for conservation (*see* **Note 6**).

3.2 Derivatization Protocol of Primary Amines with NDA (See Note 7)

1. Mix 50 µL of 100 mM pH 9 borate solution, 50 µL of 43 mM NaCN solution, and 250 µL of 2.5 mM NDA solution in a 2 mL opaque plastic vial (*see* **Note 8**).
2. Add 100 µL of aqueous solution of neurotransmitters to the previous NDA derivatization mixture.
3. Shake rapidly the mixture to get NDA-labeled primary amines. Proceed at ambient temperature for 4 min before injection (*see* **Note 9**).

3.3 Electrochromatographic Separations

1. Introduce 2 µL of NDA-labeled primary amines in the inlet reservoir for the sampling step (*see* **Note 10**) (Fig. 1). Fill the outlet reservoirs with mobile phase (ACN/water 50:50 (v/v) + 2 mM $NH_4H_2PO_4$ + 5 mM LiDS, pH adjusted to 4 with H_3PO_4).

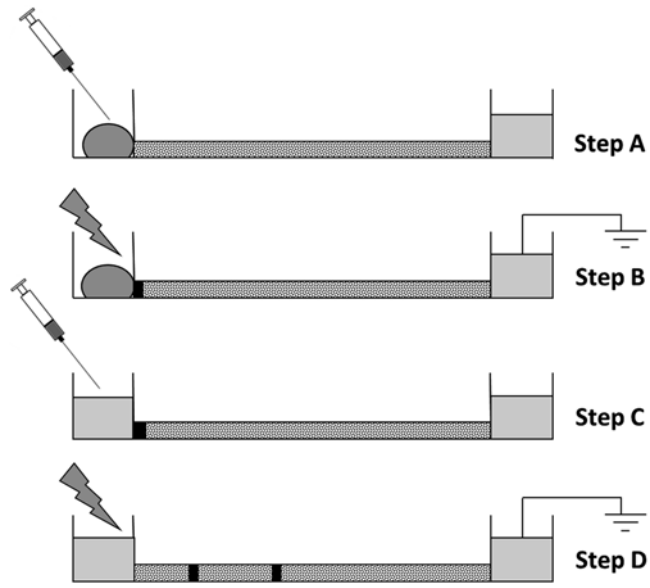

Fig. 1 Scheme of the simple direct injection. (A) Sampling step, (B) injection step, (C) rinsing step, and (D) separation step (reproduced from [11] with permission)

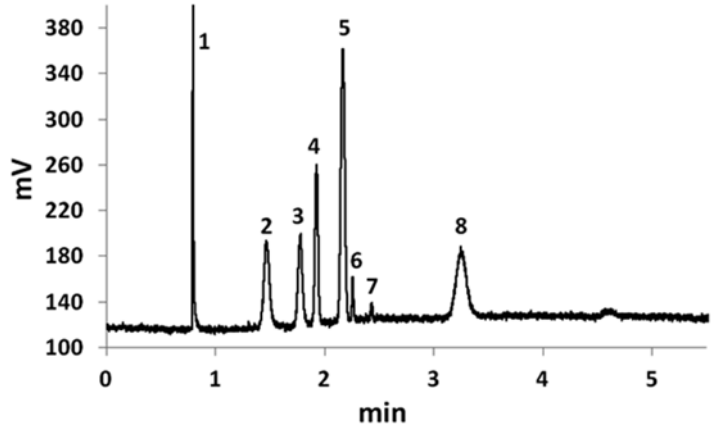

Fig. 2 Separation of eight neurotransmitters labeled with NDA in HA-filled COC microchip. Solutes: 1 = arginine, 2 = noradrenaline, 3 = GABA, 4 = serine, 5 = glycine, 6 = glutamic acid, 7 = aspartic acid, 8 = dopamine. Mobile phase: ACN/water 50:50 (v/v) + 2mM $NH_4H_2PO_4$ + 5 mM LiDS, pH adjusted to 4 with H_3PO_4. Separation length: 7 cm. Injected concentration of each solute: 120 μM. Injection time: 10 s

2. Apply an electric field of 125 V/cm for a 10 s injection time to introduce the solutes in the separation channel (step B).
3. Wash the inlet reservoir with the mobile phase (step C).
4. Apply an electric field of 620 V/cm for separation (step D) (*see* **Note 11**) (Fig. 2). The separation length is 7 cm.
5. After the separation of eight neurotransmitters, rinse the separation channel by application of 620 V/cm during 5 min.
6. When not in use, immerse the HA-filled COC microchips in ethanol for conservation.

4 Notes

1. The charged monomer AMPS is added to generate a stable electroosmotic flow (EOF).
2. The concentration of the photoinitiator BME is fixed at 2.5 % of monomers to allow the synthesis of organic monolith and its anchoring to the COC channel walls in one step [9].
3. In this position, the microchip is irradiated with a light intensity of 4.7 mW/cm^2, which is optimal for the chip used [14].
4. LiDS is systematically added to mobile phases to improve the wettability of HA monolith with mobile phase containing high content of water. Adsorption of the surfactant on the surface of the stationary phase decreases the surface tension at the interface solid-liquid, which avoids stationary phase drying and subsequent current instability. This mechanism was reported to make EC analysis on particle columns easier [15].

5. The rinsing step allows removing any remaining reagent present in the channels filled with the HA-based monolith. It should proceed until current is stable.
6. The microchip can be stored in ethanol during 3 months without degradation of electrochromatographic performances of HA monolith.
7. For fluorescence detection, the primary amine function of the different solutes was labeled off-line with NDA before injection.
8. The derivatization protocol is adapted from a previous work [16]. The storage in an opaque plastic vial prevents the degradation of NDA-labeled primary amines under the influence of light.
9. The stability of the NDA derivatization mixture is 2 h.
10. Sample injection in the separation channel is performed by using the simple direct injection procedure introduced in a previous publication [11].
11. At pH 4, the NDA-derivatized catecholamines with p*K*a of their catechol function of about 6–7 are undissociated and can be considered as neutral. Their migration in HA monolith entirely results from a chromatographic process. On the other hand, the carboxylic acid function of free alpha-amino acids is nearly totally dissociated (p*K*a = 2.1–2.4). So serine, glycine, glutamic acid, and aspartic acid are anionic, and interplay between electrophoretic and chromatographic processes controls their migration. Since the carboxylic function of GABA exhibits a p*K*a of 4.2, and the electrolyte is not buffered, its migration time can vary and special attention should be paid for the preparation and replenishment of fresh mobile phase. With a p*K*a of 12.5, the guanidinium group of arginine is positively charged, and NDA-derivatized arginine is globally neutral. But its high polarity results in a low retention on HA monolith. With no electrophoretic mobility and weak chromatographic retention, NDA-derivatized arginine almost migrates along the electroosmotic flow.

Acknowledgments

The present process is under French patent no. FR1156586. The authors wish to thank the French National Research Agency for funding project ANR-11-JS09-01701.

References

1. Arora A, Simone G, Salieb-Beugelaar GB, Kim JT, Manz A (2010) Latest developments in micro total analysis systems. Anal Chem 82(12):4830–4847. doi:10.1021/ac100969k
2. Peterson DS (2005) Solid supports for micro analytical systems. Lab Chip 5:132–139
3. Banholczer A, Pyell U (2000) Some considerations concerning the composition of the mobile phase in capillary electrochromatography. J Chromatogr A 869:363–374
4. Svec F (2009) CEC: selected developments that caught my eye since the year 2000. Electrophoresis 30(S1):S68–S82
5. Svec F (2006) Less common applications of monoliths: preconcentration and solid-phase extraction. J Chromatogr B 841(1–2): 52–64
6. Hilder EF, Svec F, Fréchet JMJ (2004) Development and application of polymeric monolithic stationary phases for capillary electrochromatography. J Chromatogr A 1044(1–2):3–22
7. Pumera M (2005) Microchip-based electrochromatography: designs and applications. Talanta 66(4):1048–1062
8. Proczek G, Augustin V, Descroix S, Hennion M-C (2009) Integrated microdevice for preconcentration and separation of a wide variety of compounds by electrochromatography. Electrophoresis 30(3):515–524
9. Augustin V, Proczek G, Dugay J, Descroix S, Hennion MC (2007) Online preconcentration using monoliths in electrochromatography capillary format and microchips. J Sep Sci 30(17):2858–2865
10. Nunes P, Ohlsson P, Ordeig O, Kutter J (2010) Cyclic olefin polymers: emerging materials for lab-on-a-chip applications. Microfluid Nanofluid 9(2):145–161
11. Ladner Y, Crétier G, Faure K (2010) Electrochromatography in cyclic olefin copolymer microchips: a step towards field portable analysis. J Chromatogr A 1217(51):8001–8008
12. Stachowiak T, Mair D, Holden T, Lee LJ, Svec F, Fréchet JMJ (2007) Hydrophilic surface modification of cyclic olefin copolymer microfluidic chips using sequential photografting. J Sep Sci 30(7):1088–1093
13. Ladner Y, Bruchet A, Cretier G, Dugas V, Randon J, Faure K (2012) New "one-step" method for the simultaneous synthesis and anchoring of organic monolith inside COC microchip channels. Lab Chip 12(9):1680–1685
14. Ladner Y, Crétier G, Faure K (2012) Fabrication of acrylate monolith using photopolymerization: effect of light intensity on electrochromatographic performance. J Sep Sci 35(15):1940–1944
15. Valette JC, Bizet AC, Demesmay C, Rocca JL, Verdon E (2004) Separation of basic compounds by capillary electrochromatography on an X-Terra RP18 stationary phase. J Chromatogr A 1049(1):171–181
16. Robert F, Bert L, Denoroy L, Renaud B (1995) Capillary zone electrophoresis with laser-induced fluorescence detection for the determination of nanomolar concentrations of noradrenaline and dopamine: application to brain microdialyzate analysis. Anal Chem 67(11):1838–1844

Part VI

Sample Preparation Approaches

Chapter 15

On-Chip Electromembrane Extraction for Monitoring Drug Metabolism in Real Time by Electrospray Ionization Mass Spectrometry

Nickolaj J. Petersen, Henrik Jensen, and Stig Pedersen-Bjergaard

Abstract

Sample preparation is an essential step in any bioanalytical procedure and very often the most challenging step in method development. Most of the currently used methods require a relatively large amount of sample and are time consuming. Here, we describe a new approach based on electromembrane extraction (EME) integrated in microfluidic polymer chips. This procedure is fast, requires only small amounts of sample, and may thus be used for monitoring drug metabolism and the formation of metabolites in real time.

Key words Electromembrane extraction, Drug metabolism, Mass spectrometry

1 Introduction

The choice of sample preparation method is dependent on the analyte, sample matrix, and requirements for sensitivity, specificity and speed. From a practical point of view, the ability to automate and integrate sample preparation with other parts of the analytical procedure is often an issue. The present chapter will focus on the coupling of electromembrane-based sample preparation in microfluidic systems. Electromembrane-based sample preparation has been utilized in larger systems [1–3]. The electromembrane extraction (EME) system is composed of a donor phase (metabolic reaction mixture), an acceptor phase compatible with MS detection (10 mM formic acid), and an organic solvent (oil)-filled porous membrane (typically polypropylene with immobilized 2-nitrophenyl octyl ether) separating the two aqueous phases. An electric field is applied across the membrane, which causes charged analytes to be transported from the donor to the acceptor phase across the membrane. The extraction efficiency of the analytes is dependent on the analyte charge, applied potential, and partition coefficient (Log *P*). Switching polarity of the applied potential will thus lead to

Ann Van Schepdael (ed.), *Microchip Capillary Electrophoresis Protocols*, Methods in Molecular Biology, vol. 1274,
DOI 10.1007/978-1-4939-2353-3_15,

extraction of analytes with an opposite charge. The magnitude of the applied potential also affects the partitioning of the analyte ions into the membrane and may thus be used to discriminate between analytes of similar charge [4].

Microfluidic systems have a number of key advantages compared to more established methods. In microfluidics, generally, nanoliter- to microliter-sized samples are analyzed which are several orders of magnitude smaller than the sample volume requirements using other methods. Furthermore, several steps of the analytical method may be integrated on the microchip, such as electrophoretic separation and detection. The integration of the entire analytical method on a single microchip enables a high level of automation to be achieved.

Many biochemical reactions take place in highly complex matrices and therefore require an effective sample preparation of small amounts of material for a successful analysis.

The main advantage of the microchip EME setup is that we obtain online sample pretreatment that removes both small ions and proteins of the biological samples that otherwise will cause problems with MS detection and with electrophoretic separations, and at the same time the setup concentrates our analytes of interest. The shallow microchannels are only 50 μm deep and therefore allow fast extraction kinetics due to the short diffusion distances, and the low volume also minimizes sample and reagent consumption. The enrichment of the drugs and metabolites is easily controlled by the acceptor/sample solution flow rate.

Being able to monitor drug metabolism in real time will reveal if transient toxic drug metabolites are formed. From a drug development point of view, there is for this reason an interest in new tools and technologies for monitoring drug metabolism and simultaneous quantification of drug metabolites.

Here, practical considerations on chip fabrication, on-chip integration of EME-based sample preparation, and hyphenation to mass spectrometry-based detection are described.

2 Materials

Prepare all solutions using deionized water (18 MΩ cm at 25 °C) and analytical grade reagents.

2.1 Buffer and Reagents Used for the Metabolic Reaction Mixture

1. 1.0 M potassium phosphate buffer, pH 7.4 (stock solution) (*see* **Note 1**).

   Weigh 34.2 g potassium dihydrogen phosphate (KH_2PO_4) in a 250 mL graduated cylinder or volumetric flask; add 190 mL water. Dissolve and adjust pH to 7.4 with 5 M KOH. Fill up with water to 250 mL.

2. 100 mM potassium phosphate buffer. Dilute the 1.0 M potassium phosphate buffer tenfold.
3. 100 mM $MgCl_2$ (stock solution). Weigh 5.08 g magnesium chloride hexahydrate ($MgCl_2 \cdot 6H_2O$) in a 250 mL graduated cylinder or volumetric flask. Dissolve in approximately 200 mL water. Fill to the mark with water and mix.
4. Acceptor solution: 10 mM formic acid. Fill approximately 200 mL water in a 250 mL graduated cylinder or volumetric flask. Add 94 μL of concentrated formic acid (98–100 %). Fill to the mark with water and mix.
5. 10 mM β-nicotinamide adenine dinucleotide 2′-phosphate reduced tetrasodium salt hydrate (NADPH) (stock solution). Weigh approximately 25 mg of NADPH; dissolve in 0.12 mL water per mg of NADPH measured (*see* **Note 2**).
6. 1.00 mg/mL (3.19 mM) stock solution of amitriptyline hydrochloride. In the reaction mixture, the final drug concentration is 1–10 μM (*see* **Note 3**). Weigh 25.0 mg amitriptyline hydrochloride (MW 313.86 g/mol) in a 25.0 mL volumetric flask, dissolve in 10 mM formic acid, and fill to the mark (*see* **Note 4**).
7. 35.0 μM stock solution of amitriptyline hydrochloride. From the 1.00 mg/mL drug solution, prepare a 35.0 μM stock solution in 100 mM phosphate buffer, pH 7.4. Add 1.5 mL of the 1.0 M potassium phosphate buffer, pH 7.4, to a 15 mL volumetric flask, add 165 μL of the 1.00 mg/mL amitriptyline hydrochloride stock solution, fill to the mark with water, and then mix.
8. Rat liver microsomes (RLM) (male Sprague-Dawley, pooled) 20 mg/mL, BD Biosciences (San Jose, CA, USA) (*see* **Note 5**).

2.2 Material for Chip Fabrication

1. Polymethyl methacrylate (PMMA) plates Plexiglas® XT klar (Nordisk Plast A/S, Randers, DK), approximately 2 mm thick and cut in squares of 5 cm × 5 cm (*see* **Note 6**).
2. Porous polypropylene membrane, 25 μm thick and having pore sizes of 0.21 × 0.05 μm and porosity of 55 % (Celgard 2500 microporous membrane, Celgard, Charlotte, NC, USA).
3. 2-Nitrophenyl octyl ether (NPOE) obtained from Fluka (Buchs, Switzerland) was used for the supported liquid membrane (SLM).
4. 1.5 cm platinum electrode, 76 μm OD (Sigma-Aldrich, St Louis, MO, USA).
5. CNC micro-milling machine (Folken M3400 E CNC mini mill, Folken Industries, Glendale, CA, USA).
6. Mill and drill bits (KYOCERA Corporation Cutting Tool Group, Kyoto, Japan, www.kyoceraMicroTools.com).

7. Vacuum sealer bag (FoodSaver® GameSaver® heat seal rolls, Jarden Corporation, Rye, NY, USA).
8. Vacuum sealing device (FoodSaver®).

2.3 Material for Setting Up the Device

1. Microsyringe pumps (KDS-100-CE syringe pump, KD Scientific, Holliston, MA, USA).
2. Variable DC power supply (EL302T Triple power supply, Thurlby Thandar Instruments Ltd, Camps, UK).
3. Overhead stirrer (IKA® EUROSTAR digital, IKA®-Werke GmbH & Co. KG, Staufen, Germany).

3 Methods

3.1 Chip Fabrication

3.1.1 Micro Milling

The chip consists of the 25 μm thick porous polypropylene membrane bonded in between two PMMA plates with channel structures facing the membrane. The channels in both the top and bottom substrates should be 2.0 mm wide and 6.0 mm long and approximately 50 μm deep (*see* **Note 7**):

1. The channels are milled using a CNC micro-milling machine (*see* **Note 8**).
2. For the fluidic connections, 1.60 mm holes are drilled at the ends of the 6 mm channels.
3. The access holes are then slightly tapered opposite to the channel structures using a 2 mm drill (*see* **Note 9**).

3.1.2 Bonding

Bonding of the PMMA substrates with the shallow (50 μm deep and 2.0 mm wide) channels is achieved by solvent-assisted bonding where the solvent (ethanol) slightly modifies the PMMA surface and allows bonding well below the glass transition temperature of PMMA (*see* **Note 10**). A clean environment is essential as particles and fingerprints will affect the bonding (*see* **Note 11**); hence, wear gloves:

1. Cut a piece of the porous polypropylene membrane (*see* **Note 12**).
2. To remove particles and debris, the PMMA substrates are cleaned under running deionized water, and then the surface is washed with ethanol.
3. Place the cleaned membrane and milled substrates in an LAF bench (laminar flow cabinet) (*see* **Note 11**).
4. Using a squirt bottle with ethanol, the plates are rinsed once again but now in the LAF bench to remove any leftover particles. Use compressed air to blow-dry the surface at a low angle to the surface.
5. Allow the substrates to dry on clean room wipes.

6. Cut a 1.5 cm piece of the 76 μm Pt wire and thread it through the 1.60 mm holes so that it lies in the milled microchannel (*see* **Note 13**).
7. Wet the membrane with ethanol and allow excess ethanol to drip off (*see* **Note 14**).
8. Place the moist membrane on top of the substrate having the platinum electrode placed in the channel and then sandwich the cover substrate on top also having channels facing the membrane.
9. Pull the two ends of the platinum electrode so that the electrode lies straight into the channel.
10. Press the sandwiched structure firmly together.
11. Hold the device in an upright position, and using compressed air, gently blow with a distance of a few cm toward one of the reservoirs. This airflow causes the ethanol to be pushed/dried out of the microchannel, while the membrane is left moist where bonding is required. Apply this procedure from both sides of the device (*see* **Note 14**).
12. Place the device in a vacuum sealer bag and vacuum seal. Press the device firmly together and inspect device visually through the transparent bag (*see* **Note 15**).
13. Place the sealed bag with the sandwiched structure in a 70 °C oven for 10–15 min.
14. Remove the bag from the oven and cut it open.

3.1.3 Reaction Chamber

1. The reaction chamber can be made from a 9 mm ID, polypropylene test tube (*see* **Note 16**).
2. The reaction chamber for the metabolic reaction is maintained at 37 °C by circulating water (*see* **Note 17**).

3.2 Setup

3.2.1 Setting Up the Device

1. Before connecting the reaction chamber and tubings to the extraction device, 0.2 μL NPOE is loaded directly onto the membrane from one of the reservoirs using a pipette. The NPOE will fill the nanoporous membrane in the extraction channel by capillary forces (*see* **Notes 18–20**).
2. Standard HPLC tubing (stainless steel or PEEK) with an OD of 1/16 in. can be used for the fluidic connections. The 1/16 in. OD tubing fits perfectly into the 1.60 mm ID access holes allowing almost zero dead volume in the connections (*see* **Notes 21** and **22**).
3. The inlet at the acceptor channel is connected using standard HPLC steel tubing. The steel tubing allows for easy application of the extraction voltage, Fig. 1 (*see* **Notes 23** and **24**).
4. The outlet of the acceptor channel is coupled with a nanospray capillary compatible with the electrospray ionization (ESI)

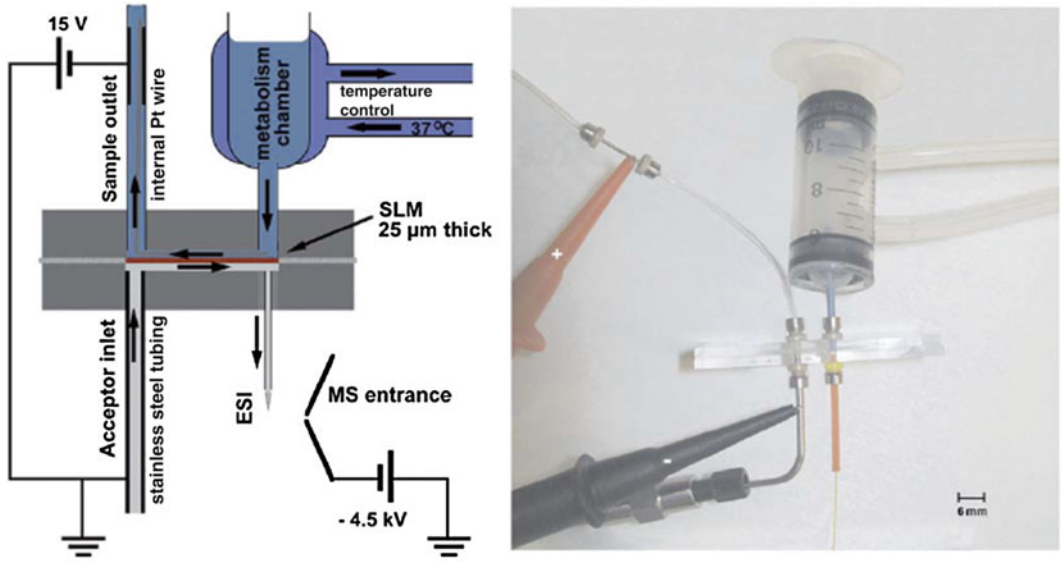

Fig. 1 Schematic illustration and photo of the on-chip system for real-time measurement of drug metabolism [5]. Reproduced with permission from the Royal Society of Chemistry

source of the MS (*see* **Note 21**). The setup can be used with basically all MS instruments having a grounded electrospray needle (*see* **Note 25**).

5. The tubing for the outlet channel of the sample side should preferably be a transparent tube to assure no leaks are present (*see* **Note 26**). Since electrical contact is applied at the sample outlet, the tubing should have an internal electrode (*see* **Notes 23** and **24**). Electrical contact can be applied at a steel union further down the tube (Fig. 1).
6. The flow to the device is delivered by two microsyringe pumps. It is important to have leak-tight connections (*see* **Note 22**). Pumping is optimal for the system but not suitable for the given application (*see* **Note 26**).
7. The electrodes are connected to a variable DC power supply. This power supply allows the cathode (acceptor side) to be connected to ground (*see* Fig. 1). +15 V is applied to the sample outlet (*see* **Note 27**).
8. Stirring in the reaction chamber is performed with an overhead stirrer (*see* **Note 28**).

3.2.2 Interfacing with an Autosampler

The setup may as well be coupled with an autosampler instead of the reaction chamber. This is desirable if one would like to obtain standard curves for the model analytes (*see* **Note 29**).

3.3 Metabolic Experiment

Prior to each metabolic experiment, the EME chip should be connected with tubings, and the tubing on the acceptor side is filled with 10 mM formic acid, while the one on the sample side is filled with 100 mM potassium phosphate buffer (*see* **Note 30**):

1. Turn on the circulating water (37 °C) for the reaction chamber. Make sure all connections are leak tight.
2. Fill 50 μL of 100 mM $MgCl_2$, 100 μL 1.0 M potassium phosphate buffer (pH 7.4), and 600 μL deionized water into the reaction chamber and initiate the stirring at 800 rpm.
3. Allow the system to temperature equilibrate (4 min).
4. Turn on the acceptor solution flow 3 μL/min (syringe pump) and suction of the acceptor solution 20 μL/min (syringe pump) (*see* **Note 31**).
5. Turn on the extraction voltage 15 V (*see* **Note 27**) and allow the MS signal to stabilize for a few minutes.
6. Add 100 μL of 35.0 μM drug substance to the reaction chamber and wait for the MS signal for the drug substance to stabilize, Fig. 2a.
7. Add 50 μL of 20 mg/mL rat liver microsomes to the reaction chamber (Fig 2b). Allow the MS signal for the drug substance to stabilize.

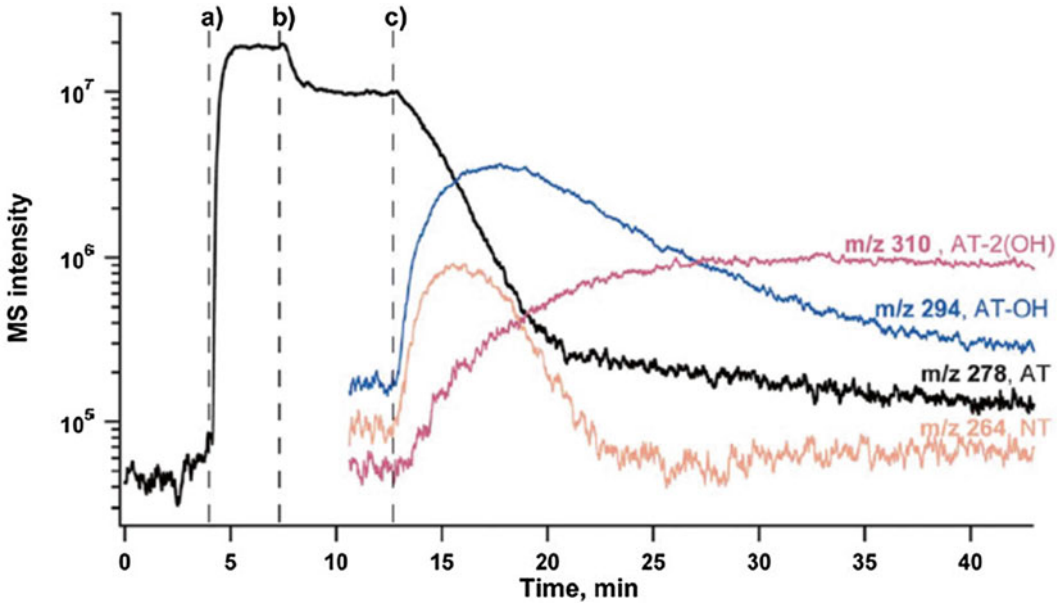

Fig. 2 MS signal versus time for in-vitro metabolism of 10 μM amitriptyline by rat liver microsomes. (a) $t = 4.0$ min: 100 μL solution of 100 μM amitriptyline added to the reaction chamber. (b) $t = 7.3$ min: 100 mL solution of rat liver microsomes (10 mg protein per mL) added. (c) $t = 12.7$ min: 100 μL solution of 10 μM NADPH added. Supported liquid membrane: NPOE, sample flow, 20 μL/min; acceptor phase, 20 μL/min of 10 mM HCOOH; extraction voltage, 15 V [5]. Reproduced with permission from the Royal Society of Chemistry

8. Add 100 μL of 10 mM NADPH as cofactor and the metabolic reaction is initiated (Fig 2c). During the next 30–60 min (*see* **Note 32**), operate the MS in the full scan mode to monitor both the parent drug and the metabolites extracted by the EME device.
9. The response time of the system can easily be observed from the time delay between changing the composition in the reaction chamber and the MS response. Part of this response time is the transport to the ESI after the extraction (*see* **Note 33**).

4 Notes

1. Cell-culturing buffers from major chemical suppliers at physiological pH can also be obtained. These buffers may in addition to the buffer salts also contain variable amounts of NaCl, KCl, $MgSO_4$, D-glucose, amino acids, and vitamins. Hanks' balanced salt solution (HBSS), Williams' medium E, and Dulbecco's Modified Eagle medium have all been tested with the microchip EME setup showing similar performance and without interfering ions in the MS signal [5].
2. NADPH is stored at −20 °C. The gumlike consistence of NADPH makes it difficult to weigh a required predetermined amount if using a volumetric flask. For this reason and since NADPH is relatively expensive, we recommend to weigh a small portion and dissolve in an appropriate amount of water to achieve the desired concentration. The prepared solution can be divided in several Eppendorf vials and stored at −90 °C until use (100 μL 10 mM NADPH is required for each experiment).
3. Other drug substances can be used in combination with the system, but may require optimization with regard to the organic liquid immobilized in the pores of the membrane and the extraction polarity and voltage [6].
4. Preparing the drug solution in formic acid both enhances the solubility of the alkaline drug substance and allows the standard to be injected directly into the MS to obtain a standard curve.
5. Rat liver microsomes are usually supplied in Eppendorf test tubes and stored at −90 °C. For each experiment, only 50 μL is needed, and to avoid unnecessary thawing and freezing of the RLM, the solution can be divided into individual test tubes and stored at −90 °C. After thawing and before dividing into the smaller volumes, the RLM is vortexed (using a vortex mixer) to get a homogeneous solution.
6. The glass transition temperature of PMMA varies from supplier to supplier (typically in the range from 85 to 160 °C), but this has no influence on our bonding method (*see* **Notes 10, 14,** and **15**).

7. Several parallel extraction channels can be micro-milled on the same substrate. This saves time during the fabrication since the time-consuming step is the cleaning of the substrates before bonding. We make five extraction channels separated 5.0 mm apart on each plate.
8. The CNC milling station is operated with 8,000 rpm and a scan speed of 2 mm/s. While milling, the drill tool and PMMA surface are wetted with detergent solution to dissipate the heat generated. The channels are milled using a 2.00 mm end mill, and the through holes for the connections are made with a 1.60 mm drill.
9. The through holes to the membrane were 1.60 mm ID and made a perfect fit for standard 1/16 in. OD tubing. The tapering allows easy insertion of the tubes or sleeves. The tapering can be done by rotating the drill bit between two fingers while inserted into the 1.60 mm hole (NB! The tapering should be done on the opposite side of the channel structures).
10. Heating the PMMA close to the glass transition temperature while the substrates are mechanically pressed together is typically used for bonding polymer devices (fusion bonding) with larger channel structures. For the current device, fusion bonding is not recommended since the 2 mm wide and only 50 μm deep channel may collapse.
11. The LAF bench will minimize the amount of particles in the air that otherwise will affect the bonding of the device.
12. Make a small cut at the edge of the membrane using scissors, and then one can easily tear the membrane to get a uniform width.
13. The platinum wire serves two purposes: firstly, it provides electrical contact for the EME extraction (donor side) and, secondly, it makes sure the flexible membrane does not block the flow when suction is applied (*see* **Note 26**).
14. Ethanol will facilitate the bonding by modifying the surface of the polymer. If ethanol is present in the channel, it may dissolve and redeposit PMMA in the channel which may both modify the channel geometry and lead to blocking of the channel.
15. The vacuum sealer bag serves three purposes: first of all, it works as a press holding the sandwiched structure in close contact, required for the bonding. The clamping force (1 bar) is uniform on the whole surface. Second, the transparent bag allows easy visualization if particles or craters are present in the device before the actual bonding. If the visual evaluation shows particles close to the extraction channel, then the device can be disassembled and cleaned once again. Third, it makes the vapors of ethanol stay longer in between the plates required for the solvent-assisted bonding (vapor-assisted bonding). Using liquid solvent-assisted bonding, the polymer may redeposit in the channels thereby modifying the channel dimensions or closing the channel, while the vapors have no such redeposit effect.

16. Polypropylene is the standard polymer for many laboratory vials and test tubes. It has the advantage of being slightly elastic and not being brittle. Drilling a 1.55 mm hole in the bottom and inserting a 1/16 in. OD PEEK tubing can provide a leak-tight connection that makes it possible to use a short connection tubing since no fittings are required. The short tubing will minimize the dead volume toward the SLM.
17. A simple water jacket for the temperature control can be made from a plastic 10 mL syringe (Fig. 1); ask your local workshop for help.
18. When filling the membrane with NPOE, the appearance of the porous membrane changes from white to transparent.
19. If a part of a the channel is not being filled, the applied NPOE can be forced further down the channel by gently blowing with compressed air.
20. The immobilized SLM can be used for many days if it is kept with aqueous solution on both sides of the membrane.
21. Upchurch Scientific (IDEX Corporation, Oak Harbor, WA, USA) supplies NanoTigth™ Teflon sleeves having 1/16 in. OD. These sleeves come with different IDs that can be used if special spray capillaries are used for the ESI.
22. Leak-tight connections can be made in several ways by fabricating a chip holder using commercial fittings. If no such holder is available, the simplest way is to glue the tubings to the device; however, in this case special care should be taken to the choice of the glue. Using NPOE as the SLM, we found that, even though the glue is not in direct contact with the SLM, components in the glue may modify the extraction performance. This is most probably due to the different solvents and initiators in the different types of glue. It is recommended to use a hot melt glue which shows no interference with the extraction performance [7].
23. The electrodes used for the electromembrane extraction should preferably be placed as close as possible to the SLM, to assure that the applied voltage drop mainly is applied across the membrane and not in the connection tubings.
24. As in any electric system, reduction/oxidation will take place at the electrodes. The amount is proportional to the current in the system. Analytes have the risk of being oxidized or reduced in the system, but in most cases the most predominant redox process will be from the oxidation/reduction of water. In the double flow system, the possibility of electrochemical degradation of the sample is eliminated by having the electrode for the EME in the outlet of the donor channel (*see* Fig. 1). At the inlet reservoir on the acceptor side, standard HPLC steel tubing is used for the connection. The suggested electrode configuration

will minimize problems of the analyte and metabolites being oxidized/reduced. If pronounced electrolysis takes place, the electrolysis may result in the formation of gas bubbles (H_2 and/or O_2), which could block electrical contact.

25. It is important that the spray needle for the MS is grounded for safety reasons so no high voltage can be delivered to the chip. The microchip EME setup has successfully been used in combination with Bruker Esquire LC-MS ion traps (model G1979A, Bruker Daltonics Inc., Billerica, MA) as well as Agilent. 1100 Series LC/MSD ion traps (G2445, Agilent Technologies, Santa Clara, CA, USA).
26. Accurate flow rates are easy to apply using microsyringe pumps, but for the metabolic reaction mixture, this will not be suitable since oxygen is used for the metabolic reaction. To allow access to air/oxygen, the reaction solution is delivered to the EME channel by suction at the outlet reservoir. When applying suction, it is very important to have leak-tight connections since air easily can get into the flow and modify the flow rate or disturb the electrical contact. Using transparent tubing at the outlet allows the user to observe if any bubbles are introduced in the system.
27. Different compounds may have different voltage selectivity. In this description, 15 V was the optimum for amitriptyline and its metabolites. Usually the extraction reaches a plateau where an increase in voltage will not increase the extraction performance. Preferably the voltage should be kept as low as possible since the current will increase with the applied voltage.
28. Since the reaction chamber is placed on top of the microfluidic EME chip, a traditional magnetic stirrer cannot be used since chamber and EME chip cannot be placed close to the magnet stirring bar.
29. In the given EME setup, the acceptor solution is grounded, and the sample side of the chip is connected to the DC power supply for enhancing the extraction. Care should be taken if coupling an autosampler to the sample setup since the configuration may modify the actual extraction voltage across the membrane. The autosampler and loop are normally grounded and may therefore modify the extraction voltage depending on the actual configuration. We have successfully coupled the autosampler to the system just by not grounding the autosampler (using a power cable without ground connection).
30. The same device can be used several days if the system is left wet with water in the channels. Care should be taken not to keep the extraction voltage on during storage since the steel tubing may corrode and block the tubing.

31. The ratio of the acceptor and sample flow will determine the possible concentration factor. The lower the acceptor flow, the higher the concentration of the extract. The spray stability and ionization efficiency also depend on the flow rate delivered to the given ESI source and spray capillary. To obtain the highest sensitivity, one may optimize the acceptor flow in the range of 3–20 μL/min while extracting the analyte and observing the MS signal.
32. The required analysis time is dependent on the speed of the metabolism; with a sample flow of 20 μL/min, one can study the metabolism for 50 min.
33. After the extraction, any further metabolism is prevented since microsomes, NADPH, and the physiological buffer solution are not able to pass the membrane. The time delay in the system at both the acceptor and donor sides can easily be estimated by the dimensions of the tubings, but may also be validated by the observed change in extraction current. When adding the drug to the acceptor reservoir, the extraction current will increase a few μA when the drug has reached the SLM. After this time delay, the time delay before the MS signal increases gives an indication of the delay on the acceptor side.

References

1. Pedersen-Bjergaard S, Rasmussen KE (2006) Electrokinetic migration across artificial liquid membranes—new concept for rapid sample preparation of biological fluids. J Chromatogr A 1109(2):183–190
2. Rezazadeh M, Yamini Y, Seidi S (2011) Electromembrane extraction of trace amounts of naltrexone and nalmefene from untreated biological fluids. J Chromatogr B Anal Technol Biomed Life Sci 879(15–16):1143–1148
3. Kuban P et al (2011) Electromembrane extraction of heavy metal cations followed by capillary electrophoresis with capacitively coupled contactless conductivity detection. Electrophoresis 32(9):1025–1032
4. Cabaleiro Dominguez N et al (2012) Selective electromembrane extraction at low voltages based on analyte polarity and charge. J Chromatogr A 1248:48–54
5. Petersen NJ et al (2012) On-chip electromembrane extraction for monitoring drug metabolism in real time by electrospray ionization mass spectrometry. Analyst 137(14):3321–3327
6. Gjelstad A, Pedersen-Bjergaard S (2011) Electromembrane extraction: a new technique for accelerating bioanalytical sample preparation. Bioanalysis 3(7):787–797
7. Petersen NJ et al (2010) On-chip electro membrane extraction. Microfluid Nanofluid 9(4): 881–888

Chapter 16

Sample Preparation for N-Glycosylation Analysis of Therapeutic Monoclonal Antibodies by Electrophoresis

Ákos Szekrényes, Jan Partyka, Csaba Varadi, Jana Krenkova, Frantisek Foret, and András Guttman

Abstract

There are a considerable number of biopharmaceuticals that have been approved for clinical use in the past decade. Over half of these new generation drugs are glycoproteins, such as monoclonal antibodies or other recombinant glycoproteins, which are mostly produced in mammalian cell lines. The linked carbohydrate moieties affect not only their physicochemical properties and thermal stability but also crucial features like receptor-binding activity, circulating half-life, as well as immunogenicity. The structural diversity of these attached glycans can be manifested in altered monosaccharide composition and linkages/positions among the monosaccharide building blocks. In addition, as more and more biosimilar products hit the market, understanding the effects of their glycosylation modification has become a recent target in efficacy and safety issues. To ensure consistent quality of these products, glycosylation profiles have to be monitored and controlled in all steps of the manufacturing process, i.e., from clone selection to lot release. In this paper, we describe some of the recently introduced and commonly used sample preparation techniques for capillary electrophoresis (CE)-based profiling and structural elucidation of N-glycans. The presented protocols include protein A affinity partitioning of monoclonal antibodies (mAbs), enzymatic release of the N-linked glycans, labeling of the liberated carbohydrates, reaction mixture purification techniques to remove the excess labeling reagent, and high-resolution and rapid capillary electrophoresis-laser-induced fluorescence (CE-LIF)-based profiling of the labeled and purified N-glycans.

Key words Biopharmaceuticals, Therapeutic monoclonal antibody, N-glycan analysis, Fluorophore labeling, Capillary electrophoresis

1 Introduction

Glycosylation is one of the most important and complex posttranslational modifications on the majority of new biotherapeutic drugs. Glycoproteins are typically produced as mixtures of different glycoforms having the same polypeptide backbone but differing in glycosylation site specificity (macroheterogeneity) and in the structures at a same site (microheterogeneity) [1]. It is well known that these attached carbohydrate chains are very important from the point of view of quality by design (QbD) in biopharmaceutical

Ann Van Schepdael (ed.), *Microchip Capillary Electrophoresis Protocols*, Methods in Molecular Biology, vol. 1274,
DOI 10.1007/978-1-4939-2353-3_16,

manufacturing because of their significant influence on activity and efficacy. Since glycan biosynthesis and processing are exquisitely responsive to the host cell type and growth environment, changes may occur in the glycosylation profile of different production batches of the innovative drug but also in their follow-up versions (biosimilars) [2]. Meanwhile, there have been reports of adverse events caused by nonhuman glycosylation moieties due to the presence of immunogenic residues, such as α-1,3-Gal or N-glycolylneuraminic acid [3]. Therefore, it is crucial to maintain the carbohydrate distribution profile of glycosylated biopharmaceuticals for efficient and safe use [4, 5]. Advances are continually being made in the biotechnology industry to minimize glycan heterogeneity and improve the sensitivity and specificity of the analytical assays used to identify and quantify possible glycosylation changes. In spite of the fact that several analytical techniques and assays have already been implemented and validated for the characterization of these complex molecules, rapid and comprehensive profiling and quantitation of all glycoforms are still a challenging task. One of the most powerful bioseparation techniques for detailed N-linked glycosylation analysis of biotherapeutics is capillary electrophoresis combined with laser-induced fluorescent (CE-LIF) detection [6–10]. Different CE-based assays can be used to characterize the drug during the manufacturing process, troubleshoot production problems, and demonstrate biosimilarity or comparability.

In this protocol, we introduce some of the most efficient sample preparation methods for CE-LIF analysis of complex carbohydrates. Usual protocols start with affinity partitioning of the formulated or crude monoclonal antibody product using protein A resins. This step is essential for the complete removal of all additives and formulation ingredients, which can affect glycan labeling or the consequent CE-LIF analysis. Next, we describe some of the commonly used in-solution N-glycan release method using peptide-N-glycosidase F (PNGase F). The affinity partitioning and glycan release steps are followed by fluorophore labeling of the liberated glycans and the removal of the excess labeling material. Finally, we describe the optimal capillary electrophoresis analysis parameters for the labeled N-linked glycans in respect to regular profiling (high resolution) and rapid screening (low resolution).

2 Materials

Always use HPLC grade or ultrapure water (18 MΩ cm at 25 °C) for all solutions and buffers in all procedures. In addition, all reagents should be microbiology or HPLC grade unless otherwise stated. The use of powder-free, nitrile gloves for all sample handling procedures is important too. Ensure that all glass, plasticware,

and solvents are free of glycosidases and possible environmental carbohydrate contaminations. All procedures should be performed using appropriate personal safety protection, laboratory coat, eyeglasses, and nitrile gloves. The labeling reactions should be performed in a fume hood.

2.1 Protein A Affinity Partitioning Using PhyTip 200+ Columns

1. Crude or formulated mAb sample.
2. 1× PBS buffer, pH 7.2.
3. 200+ PhyTip protein A columns with 5 μL bed volume (Phynexus Inc., San Jose, CA).

   All PhyTip protein A columns are supplied with buffers and reagents including:

   Capture buffer: provided for those situations where additional buffer is needed to supplement sample volume and ensure correct capture pH.

   Wash buffer I: phosphate buffer solution, pH 7.4.

   Wash buffer II: saline solution.

   Enrichment buffer: phosphate buffer solution, pH 2.5.

   Neutralization buffer: Tris buffer solution, pH 9.0.
4. Rainin PureSpeed (Rainin Instrument LLC, Oakland, CA, USA) electronic semiautomated multichannel pipette (8 or 12 channels).
5. 96-well plate, 0.5 mL/well capacity.
6. 0.2-mL flat cap PCR tubes.
7. 100 mM sodium carbonate buffer (pH 9.0) to replace the neutralization buffer.
8. 20 mM sodium carbonate buffer, pH 7.0.
9. 10 % acetic acid in water to replace the enrichment buffer.
10. 10 kDa cutoff spin filters (Nanosep 10k Omega, Pall, Port Washington, NY, USA).
11. Microcentrifuge equipped with a rotor suitable for 2.0-mL microfuge tubes and capable to provide 17,200 × *g*.
12. Centrifugal vacuum evaporator (e.g., SpeedVac).

2.2 In-Solution N-Glycan Release and APTS Labeling of N-Glycans

1. 50 mM dithiothreitol (DTT) in water.
2. 50 mM iodoacetamide (IAM) in water.
3. 20 mM $NaHCO_3$, pH 7.0.
4. Peptide-N-glycosidase F (ProZyme, Hayward, CA, USA).
5. 0.2-mL flat cap PCR tubes.
6. PCR thermocycler or other general microvial-based heating devices capable to provide stable 65 and 37 °C temperature.
7. 15 % acetic acid in water.

8. 8-Aminopyrene-1,3,6-trisulfonic acid (APTS) (Beckman Coulter, Brea, CA, USA).
9. 1 M sodium cyanoborohydride in tetrahydrofuran (THF).
10. 10 mg/mL APTS solution in 15 % acetic acid.
11. 10 kDa cutoff spin filters (Nanosep 10 k Omega, Pall, Port Washington, NY, USA).
12. Microcentrifuge equipped with a rotor suitable for 2.0-mL microfuge tubes and capable to provide 17,200 × *g*.
13. Centrifugal vacuum evaporator.
14. Vortex mixer.
15. Pipettors and disposable pipette tips (P5/P10, P200, and P1000).
16. Miscellaneous labware for buffers and dilutions.

2.3 APTS Cleanup Using 1000+ PhyTip with 20 μL Normal Phase Resin

1. 1000+ PhyTip normal phase columns with 20 μL bed volume.
2. Rainin multichannel 100–1000-μL pipettor (8 channels).
3. Acetonitrile (100 %, HPLC grade).
4. 20 % acetonitrile in water.
5. 95 % acetonitrile in water.
6. 96-deep-well plate 2 mL/well.
7. Centrifugal vacuum evaporator.
8. 0.2-mL flat cap PCR tubes.

2.4 Sample Preparation Using GlykoPrep Rapid N-Glycan Preparation Platform

1. GlykoPrep Digestion Module (ProZyme) includes:
   - Digestion (RX) cartridges (24 cartridges).
   - Immobilization reagent set.
   - Denaturation reagent.
   - Blocking reagent.
   - Digestion reagent set.
   - N-Glycanase.
   - 25× digestion buffer.
   - Finishing reagent.
   - Aluminum sealing film.
2. GlykoPrep APTS Cleanup Module (ProZyme) includes:
   - 5× APTS sample loading buffer.
   - Cleanup (CU) cartridges (24 cartridges).
3. Acetonitrile (HPLC grade).
4. Microcentrifuge (capable of 50–1,000 × *g*) and rotor suitable for 1.5-/2.0-mL microcentrifuge vials.
5. Heater and heating block accommodating 0.2-mL PCR tubes.
6. Centrifugal vacuum evaporator.

7. Vortex mixer.
8. Pipettors and disposable pipette tips (P5/P10, P200, and P1000).
9. Miscellaneous labware for buffers and dilutions.

2.5 CE-LIF Analysis of APTS-Labeled N-Glycans

1. Beckman Coulter PA 800 *plus* Pharmaceutical Analysis System, equipped with LIF detection (solid-state 488-nm laser) and 32 Karat software v.8.0 or higher.
2. Carbohydrate separation buffer (Beckman Coulter).
3. N–CHO-coated capillary, 50 μm ID (Beckman Coulter).
4. Sample vials.
5. 2.0-mL plastic vials.
6. Vial caps.
7. Capillary cartridge equipped with N–CHO-coated capillary with a total length of 60.2 cm (effective length 50.2 cm).

3 Methods

3.1 Protein A Affinity Partitioning of mAbs

1. Dilute the crude or formulated mAb sample to 2 mg/mL using the PBS buffer, pH 7.2 (*see* **Note 1**).
2. Transfer 220 μL of capture buffer to the first row of the 96-well plate.
3. Transfer 100 μL of diluted mAb sample and 120 μL of *capture buffer* to each well in the second row. Mix the sample gently by pipetting.
4. Fill up the wells in the third row with 220 μL of *wash buffer I*.
5. Fill up the wells in the fourth row with 220 μL of *wash buffer II*.
6. Fill up the wells in the fifth row with 25 μL of 10 % acetic acid.
7. Conditioning (first row): 200 μL of capture buffer over the resin bed for one cycle at a flow rate of 250 μL/min.
8. Capture (second row): capture the IgG by passing 200 μL of sample solution through the resin bed in four cycles at a flow rate of 100 μL/min.
9. Purification (third and fourth row): pass 100 μL of protein A wash buffer I through the resin bed in one cycle at a flow rate of 250 μL/min followed by a second wash with 200 μL wash buffer II, passing through the resin bed in one cycle at a flow rate of 250 μL/min. It is essential to use wash buffer II as it exchanges the pH 7.4 buffer of wash buffer I and in doing so ensures effective low pH elution during the enrichment step.
10. Enrichment (fifth row): elute the captured IgG with 15 μL 10 % acetic acid solution (pH ~2.5) passed through the resin bed in four cycles at a flow rate of 100 μL/min. Neutralize the sample by the addition of 175 μL of 100 mM sodium carbonate buffer (pH 9.0).

11. Wash the membrane of the 10 kDa cutoff spin filter with 250 µL of water for 15 min at 17,200 × *g*.
12. Pipette the sample onto the membrane and centrifuge for 15 min at 17,200 × *g*.
13. The sample is washed three times with 250 µL of water by spinning for 15 min at 17,200 × *g* (*see* **Note 2**).
14. The desalted proteins are recovered from the membrane by inversion of the cartridge—to a new tube—and centrifugation at 1,320 × *g* for 4 min (*see* **Note 3**).
15. To increase the recovery, invert the cartridge again—back to the original position—pipette 50 µL of water onto the membrane, vortex it for 1 min, invert the cartridge, and centrifuge at 1,320 × *g* for 4 min. Repeat this step two times (*see* **Note 4**).
16. After the desalting step, dry the recovered mAb sample in the centrifugal vacuum evaporator (heat setting turned to the off position) using continuous vacuum.

3.2 In-Solution N-Glycan Release

1. Dissolve the dry protein samples in 45 µL of 20 mM sodium carbonate buffer, pH 7.0.
2. Add 5 µL of 50 mM dithiothreitol (DTT) to the sample and incubate at 65 °C for 15 min.
3. After the incubation step, add 5 µL of 50 mM iodoacetamide (IAM) to the sample and keep in the dark for 10 min at room temperature (RT).
4. Add 2 µL 2.5 U/mL of N-glycanase solution to the sample and incubate for 2 h to overnight at 37 °C.
5. Wash the membrane of the 10 kDa cutoff spin filter with 250 µL of water for 15 min at 17,200 × *g*.
6. Pipette the sample onto the membrane and centrifuge for 15 min at 17,200 × *g* (*see* **Note 5**).
7. Wash the membrane again with 50 µL of water for 15 min at 17,200 × *g*.
8. Collect the flow through and transfer it to a 0.2-mL clean PCR tube.
9. Dry the clean released glycans in a centrifugal vacuum evaporator (heat setting turned to off position).

3.3 N-Glycan Release Using GlykoPrep Digestion (RX) Cartridges

1. Dissolve the dry protein sample in 50 µL of 20 mM sodium carbonate buffer, pH 7.0.
2. Add 50 µL of denaturation reagent to the protein solution. Mix well by pipetting up and down several times.
3. Incubate at room temperature for at least 5 min.
4. Nest the cartridge in a 0.5-mL screw cap microtube.

5. Pipette 50 μL of 100 % acetonitrile into the sample cup of the RX cartridge.
6. Place the tube in a centrifuge and spin at 300 × *g* for 3 min.
7. Pipette 150 μL of denaturation reagent into the sample cup of each cartridge.
8. Spin at 1,000 × *g* for 2 min.
9. Empty the flow through by lifting each RX cartridge and removing the liquid collected in the microtube below. Dispose off this liquid and return the cartridge to the tube.
10. Load 100 μL of the denatured mAb sample into the sample cup of each RX cartridge.
11. Spin at 50 × *g* until all sample cups are empty (~15 min).
12. Empty the flow through as described in **step 9**.
13. Pipette 50 μL of blocking reagent into the sample cup of each RX cartridge.
14. Spin at 300 × *g* for 3 min.
15. Pipette 50 μL of digestion buffer (1× concentrated) into the sample cup of each RX cartridge.
16. Spin at 300 × *g* for 3 min.
17. Prepare the digestion and elution assembly by nesting each PCR tube into 0.5-mL tubes and nesting that within a 2.0-mL microcentrifuge tube.
18. Transfer the RX cartridge into the corresponding digestion and elution assemblies and return to the centrifuge. Dispose the microtubes and the flow through.
19. Pipette 10 μL of enzyme solution (2.5 μL of N-glycanase and 7.5 μL of 1× digestion buffer) into the sample cup of the RX cartridge.
20. Spin at 300 × *g* for 3 min; *do not* discard the flow through.
21. Transfer the PCR tubes with the RX cartridges to a 45 °C PCR heat block and incubate for 30 min.
22. Remove the PCR tubes with RX cartridges from the heat block and return to the digestion and elution assembly.
23. Pipette 15 μL of finishing reagent into the sample cup of each RX cartridge.
24. Spin at 300 × *g* for 3 min.
25. Remove RX cartridge from the PCR tube. The eluted N-glycans are now in the PCR tubes; *do not discard*.
26. Open the PCR tubes, return them to the digestion assembly (minus the RX cartridge), and dry the N-glycans in a centrifugal vacuum evaporator (heat setting turned to the off position) for 30 min or until fully dry.

3.4 APTS Labeling of the Released N-Glycans

1. Add 4 μL of 10 mg/mL APTS (in 15 % acetic acid) to the dried sugars.
2. Add 2 μL of 1 M $NaBH_3CN$ (in THF) to the sample (*see* **Note 6**).
3. Incubate the reaction mixture at 37 °C overnight. For nonsialylated glycoproteins, incubation at 55 °C for 2 h is sufficient.

3.5 Removal of Excess APTS Using Normal Phase Columns

1. Add 100 μL of water to the labeled samples and mix it by pipetting up and down several times. Transfer the mixture to the third row of the plate (Fig. 1) and add 900 μL acetonitrile to it. Mix the sample well again.
2. Prepare the elution (20 % acetonitrile in water) and the washing solutions (95 % acetonitrile in water) and fill up the 96-deep-well plate as shown in Fig. 1 (*see* **Note 7**).
3. Insert the 1000+ DPA-6S normal phase PhyTip columns (20 μL bed volume) to the multichannel pipettor.
4. Perform conditioning in the first row (Fig. 1) by passing 900 μL of elution solution through the resin bed four times.
5. Equilibrate the columns by passing 900 μL of washing solution over the resin bed for four times in the second row in Fig. 1.

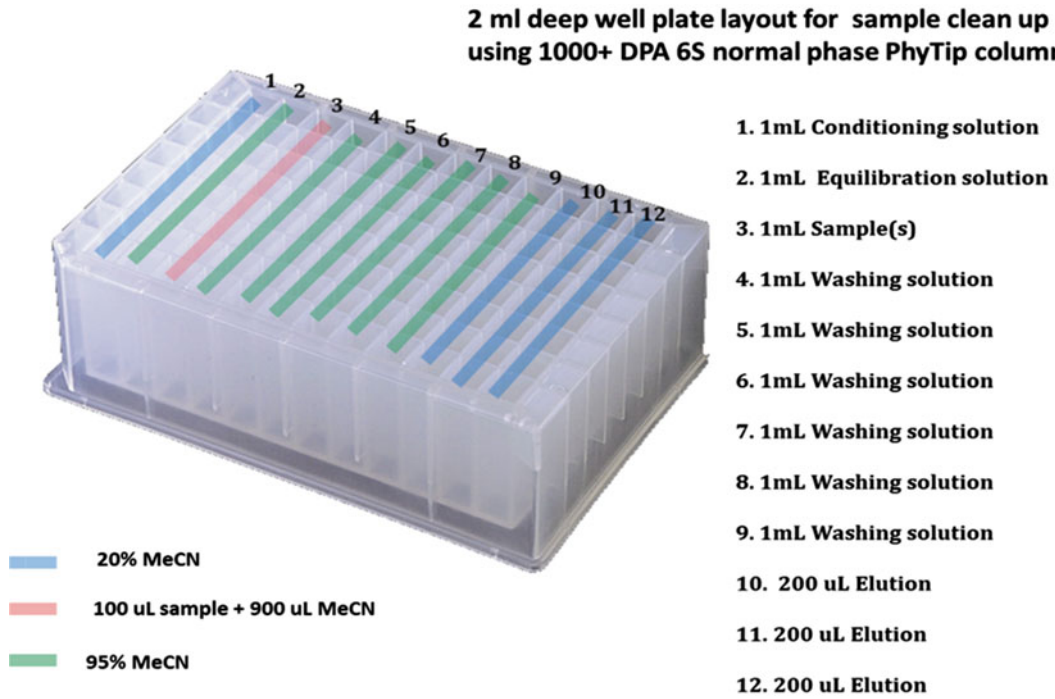

Fig. 1 Reagent distribution in a deep-well plate for labeling reagent cleanup

6. Load the labeled glycans to the columns by pipetting 900 µL of sample mixture through the resin bed ten times (Fig. 1, third row).
7. Wash off the salts and excess labeling reagent by pipetting 900 µL of washing solution through the resin bed ten times. Repeat this step six times, always using fresh solution in a new row (Fig. 1, fourth to ninth row).
8. Elute the APTS-labeled glycans by passing 180 µL elution solution through the resin bed three times. Repeat this step in the next two rows (Fig. 1, 10th to 12th row).
9. Collect the eluted sample from the elution positions to a 2.0-mL tube and dry it in a centrifugal vacuum evaporator (heat setting turned to the off position).
10. Dissolve the dried samples in 25 µL HPCE grade water and proceed to capillary electrophoresis analysis.

3.6 Cleanup of the Fluorophore-Labeled Glycans by APTS Cleanup Modules

1. Prepare 5 mL of APTS sample load buffer by adding 1 mL of 5× APTS sample load buffer to a small, glass graduated cylinder. Bring the volume up to 5 mL with 100 % acetonitrile.
2. Dissolve the dried and labeled glycan samples in 200 µL of APTS sample load buffer. Pipette it up and down a couple of times to mix well.
3. Add 200 µL of APTS sample load buffer to each N-glycan sample in the PCR tubes. Pipette up and down to mix.
4. Transfer each N-glycan sample into the sample cup of a CU cartridge. Place the CU cartridge into a 0.5-mL tube by nesting within a 2.0-mL microcentrifuge tube.
5. Spin at 300 × *g* for 3 min or until the sample cup of each CU cartridge is empty.
6. Discard the flow through and spin at 300 × *g* for 3 min again.
7. Pipette 200 µL of APTS sample load buffer into the sample cup of each CU cartridge.
8. Spin at 300 × *g* for 3 min.
9. Discard the flow through and repeat **steps 6** and **7** again.
10. Place the CU cartridge to a clean 0.2-mL PCR tube and nest this back to the 2.0-mL microcentrifuge tube, which is already containing the 0.5-mL tube.
11. Pipette 25–50 µL of ultrapure water into the sample cup of each CU cartridge.
12. Spin at 1,000 × *g* for 3 min. The PCR tube now contains the purified labeled N-glycans; *do not discard*.
13. N-Glycan samples are now ready for capillary electrophoresis analysis. If not analyzed immediately, store sealed at –20 °C in the dark.

3.7 CE-LIF Analysis of APTS-Labeled N-Glycans

3.7.1 Preparing the Glucose Ladder Standard (G20)

1. Weigh and dissolve 5 mg of glucose ladder standard (G20, supplied with the N–CHO Carbohydrate Kit) in 80 μL deionized water in 1.5-mL microcentrifuge tube. Sonicate if necessary.
2. Aliquot at least ten 2 μL portions of the glucose ladder standard solution to 0.5-mL microcentrifuge vials and dry them in a centrifugal vacuum evaporator. The dried glucose ladder can be stored at room temperature or used immediately.
3. Label the ladder standard as described under Subheading 3.4 and proceed with sample cleanup.
4. Transfer the APTS-labeled samples and standards to a 0.2-mL sample tube (Beckman Coulter), nest the tubes to 2-mL plastic vials, and cap them tight. Place the sample vials to the sample tray and record their actual positions in the methods timetable.
5. Fill the appropriate reagents into vials as follows:
   - 1.5 mL of ultrapure water into H2O vial (four vials).
   - 1.5 mL of carbohydrate separation buffer into Gel-R vial (one vial).
   - 1.3 mL of carbohydrate separation buffer into Gel-S vial (two vials).
   - 0.8 mL of ultrapure water into waste vial (one vial).

   Place the vials in the buffer tray and set up their actual positions in the methods timetable.
6. Set up the initial detection and separation parameters as follows:
   - Detection: laser-induced fluorescence.
   - Wavelength excitation, 488 nm; emission, 520 nm.
   - Data rate: 4 Hz.
   - Dynamic range: 100 RFU (relative fluorescence units).
   - Filter setting: normal.
   - Peak width: 16–25.

3.7.2 Performing the High-Resolution CE-LIF Analysis

1. Rinse the capillary with buffer for 3 min at 30 psi from gel buffer (Gel-R vial for rinse) vial to waste vial.
2. Inject the sample at 0.5 psi for 5 s from sample vial to buffer vial (Gel-S vial for separation).
3. Wait for 0.2 min with vials filled with ultrapure water. This step dips the capillary in water to protect against sample carryover. Change the rinse water vials if they are contaminated.
4. Separation step: 20 min from gel buffer vial to gel buffer vial (Gel-S vial for separation). The applied voltage should be 30 kV, with REVERSED polarity (anode at the detection side) with 0.17 min ramp time.

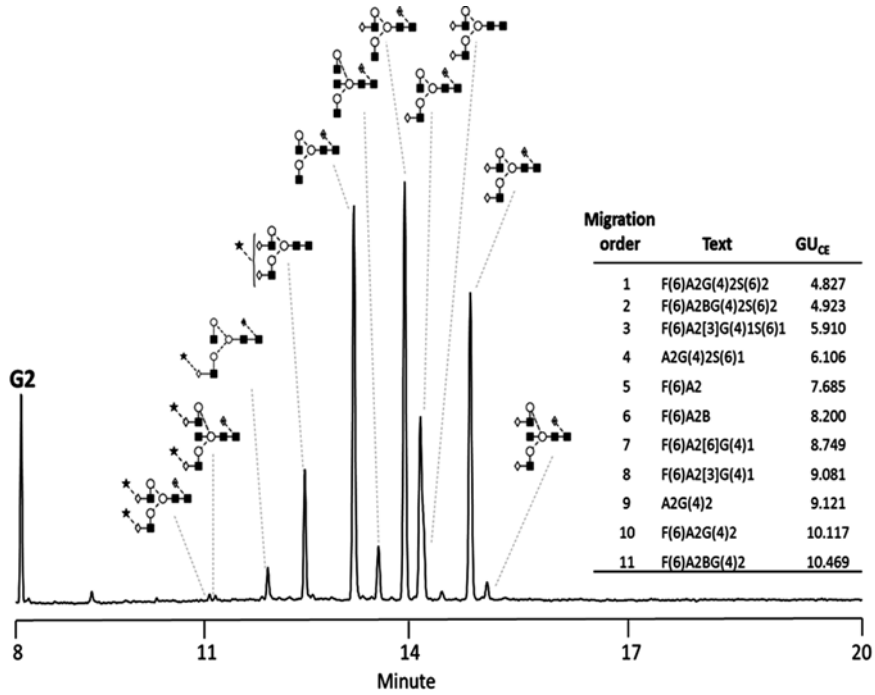

Fig. 2 High-resolution capillary electrophoresis profiling of IgG N-glycans. Conditions: capillary, N–CHO neutral-coated capillary (effective length, 50 cm; total length, 60 cm); separation buffer, N–CHO carbohydrate separation buffer; applied electric field, 500 V/cm; separation temperature, 25 °C; pressure injection, 6.89 kPa for 5 s. The different glycans have been represented with cartoons based on the Oxford symbol notation with embedded linkage information [11]

5. Autozero at 1.0 min.
6. End at 20.0 min.
7. An example of a high-resolution CE-LIF analysis of APTS-labeled IgG N-glycans performed on 50 cm separation length is shown in Fig. 2 with the corresponding glycan structures of the peaks.

3.7.3 Performing the Rapid CE-LIF Analysis for High-Throughput Screening

1. Rinse the capillary with buffer for 3 min at 30 psi from gel buffer (Gel-R vial for rinse) vial to waste vial.
2. Inject the sample at 0.5 psi for 5 s from sample vial to buffer vial (Gel-S vial for separation). When injecting from the 10 cm effective length side of the capillary, make sure that the tray layout has changed accordingly.
3. Wait for 0.2 min with vials filled with ultrapure water. This step dips the capillary in water to protect against sample carryover. Change the rinse water vials if they are contaminated.
4. Separation step: 5 min from gel buffer vial to gel buffer vial (Gel-S vial for separation). The applied voltage should be 30 kV, with NORMAL polarity (cathode at the detection side) with 0.17 min ramp time.

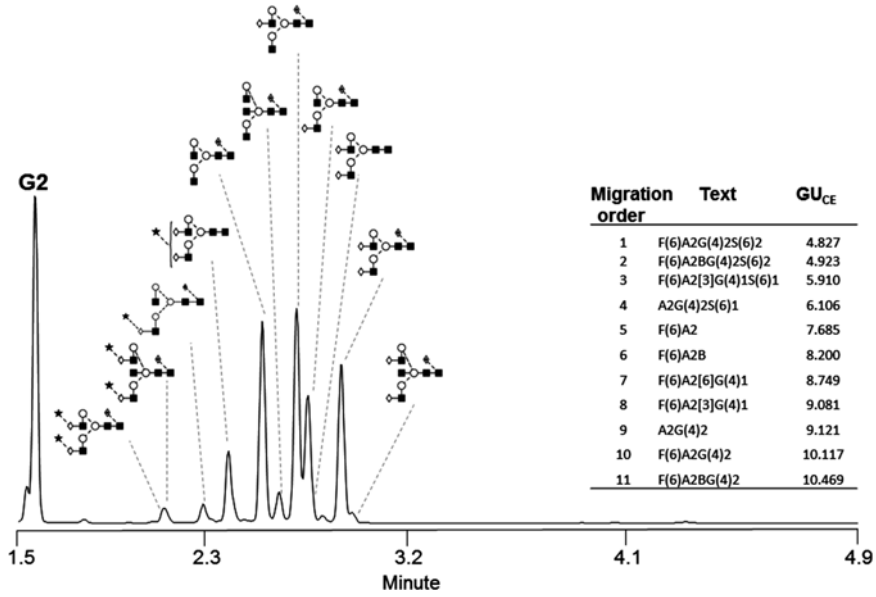

Migration order	Text	GU_{CE}
1	F(6)A2G(4)2S(6)2	4.827
2	F(6)A2BG(4)2S(6)2	4.923
3	F(6)A2[3]G(4)1S(6)1	5.910
4	A2G(4)2S(6)1	6.106
5	F(6)A2	7.685
6	F(6)A2B	8.200
7	F(6)A2[6]G(4)1	8.749
8	F(6)A2[3]G(4)1	9.081
9	A2G(4)2	9.121
10	F(6)A2G(4)2	10.117
11	F(6)A2BG(4)2	10.469

Fig. 3 Rapid capillary electrophoresis profiling of IgG N-glycans. Conditions: same as in Fig. 2 with the effective separation length of 10 cm

5. Autozero at 1.0 min.
6. End at 5.0 min.
7. An example of a rapid CE-LIF analysis of APTS-labeled IgG N-glycans performed on 10 cm separation length is shown in Fig. 3 with the corresponding glycan structures of the peaks.

4 Notes

1. If the sample concentration is less than 2 mg/mL, pre-concentrate before starting the procedure.
2. Make sure that all the liquid passed through the membrane after the last step. If not, spin it again.
3. Never use higher *g*-forces for the inverted cartridge as it can destroy the membrane.
4. When vortexing, always hold the filtration device vertically.
5. *Do not* discard the flow through because it contains the released N-glycans.
6. Always work with $NaBH_3CN$ in the fume hood!
7. Always prepare fresh acetonitrile solutions.

Acknowledgments

The authors acknowledge the kind support of Beckman Coulter, Inc., PhyNexus, Inc., and ProZyme, Inc. This work was supported by the Fulbright Research Scholarship #I-174444, the OTKA Grant #K-81839 of the Hungarian Research Council, the MTA-PE Translational Glycomics program (#97101) of the Hungarian Academy of Sciences, the P301-11-2055 of the Grant Agency of the Czech Republic, and IACH institutional research plan RVO: 68081715.

References

1. Marino K et al (2010) A systematic approach to protein glycosylation analysis: a path through the maze. Nat Chem Biol 6(10): 713–723
2. Brinks V et al (2011) Quality of original and biosimilar epoetin products. Pharm Res 28(2):386–393
3. Chung CH et al (2008) Cetuximab-induced anaphylaxis and IgE specific for galactose-alpha-1,3-galactose. N Engl J Med 358(11): 1109–1117
4. Endo T (2009) New era of glycoscience: intrinsic and extrinsic functions performed by glycans. Foreword. Biol Pharm Bull 32(5): 765–766
5. Jelkmann W (2010) Biosimilar epoetins and other "follow-on" biologics: update on the European experiences. Am J Hematol 85(10): 771–780
6. Kamoda S, Kakehi K (2006) Capillary electrophoresis for the analysis of glycoprotein pharmaceuticals. Electrophoresis 27(12): 2495–2504
7. Guttman A (1996) Capillary gel electrophoresis. Methods Mol Biol 52:157–169
8. Oefner PJ, Chiesa C (1994) Capillary electrophoresis of carbohydrates. Glycobiology 4(4):397–412
9. Volpi N, Maccari F, Linhardt RJ (2008) Capillary electrophoresis of complex natural polysaccharides. Electrophoresis 29(15):3095–3106
10. Laroy W, Contreras R, Callewaert N (2006) Glycome mapping on DNA sequencing equipment. Nat Protoc 1(1):397–405
11. Harvey DJ et al (2009) Proposal for a standard system for drawing structural diagrams of N- and O-linked carbohydrates and related compounds. Proteomics 9(15):3796–3801

Index

Ann Van Schepdael (ed.), *Microchip Capillary Electrophoresis Protocols*, Methods in Molecular Biology, vol. 1274,
DOI 10.1007/978-1-4939-2353-3, © Springer Science+Business Media New York 2015

E

F

G

H

I

L

M

N

O

P

Q

R

S

T

U

V

W

Y

Z